PhD

3rd CYCLE

FCUP
2025

Integrating comparative tools and mechanistic niche models to understand the effects of size variation on species' phenotypic diversification, coexistence and vulnerability to global change

Carolina Reyes-Puig

FACULDADE DE CIÊNCIAS UNIVERSIDADE DO PORTO

Ciências ULisboa Faculdade de Ciências da Universidade de Lisboa

Integrating comparative tools and mechanistic niche models to understand the effects of size variation on species' phenotypic diversification, coexistence and vulnerability to global change

Carolina Reyes-Puig

PhD Thesis presented to the
Faculty of Sciences of the University of Porto and Faculty of Sciences of the University of Lisboa
Doctoral Program in Biodiversity, Genetics and Evolution
2025

Integrating comparative tools and mechanistic niche models to understand the effects of size variation on species' phenotypic diversification, coexistence and vulnerability to global change

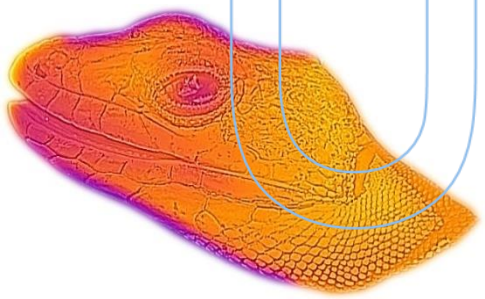

Carolina Pilar Reyes Puig
Doctoral Program in Biodiversity, Genetics and Evolution
Department of Biology, Faculty of Sciences of the University of Porto
2025

Supervisor
Antigoni Kaliontzopoulou, Ramón y Cajal Researcher,
BEECA, Faculty of Biology, University of Barcelona,
IRBio, Institut de Recerca de la Biodiversitat

Co-supervisors
Urtzi Enriquez-Urzelai, Postdoc researcher,
Czech Academy of Sciences, Institute of Vertebrate Biology

Neftalí Sillero, Principal researcher,
CICGE - Research Centre on Geo-Spatial Sciences,
Faculty of Science of the University of Porto


U.PORTO
FACULDADE DE CIÊNCIAS
UNIVERSIDADE DO PORTO

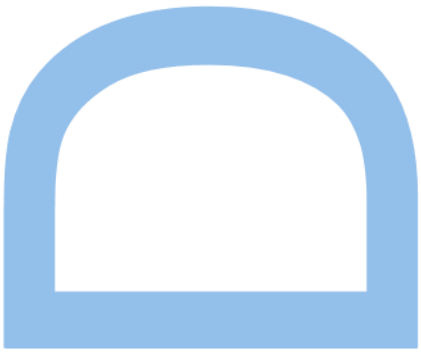

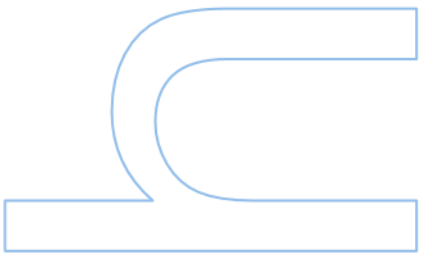

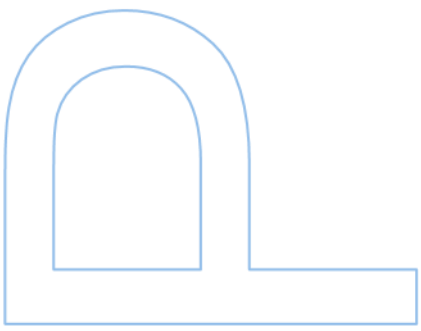

Dedicated to Ankalli, my deepest love

Declaration of Honour

I, Carolina Pilar Reyes-Puig, born in Ecuador, residing in Quito with telephone number +593983469871, Ecuadorian national, holder of passport number 1718010760, enrolled in the Doctoral Program in Biodiversity, Genetics and Evolution at the Faculty of Sciences of the University of Porto declare, under the terms of article 14 a) of the U. Porto Code of Ethics for Academic Conduct, that the content of this thesis reflects the perspectives, research work and my interpretations at the time of submission. This thesis includes two published articles authored by me, which are reproduced in accordance with their respective publication licenses, ensuring proper attribution and citation.

By submitting this thesis, I also declare that it is the result of my own research work and contains original contributions that have not previously been used in other work submitted to this or any other institution.

I further declare that all references to other authors scrupulously respect the rules of attribution and are duly cited in the body of the text and identified in the bibliographical references section.

I am aware that the practice of plagiarism and self-plagiarism constitutes an academic offence.

Firmado electrónicamente por:
CAROLINA PILAR
REYES PUIG

Carolina Reyes-Puig

9th February 2025

Foreword

Two scientific articles were published in indexed, peer-reviewed international journals as a result of the work developed within the scope of this thesis. Additionally, one article has been submitted to a specialised journal, and another is in preparation for submission. As these works were carried out in collaboration with other authors, the candidate clarifies that they actively participated in all stages, mainly in methods, analysis, discussion of the results, and reviewing the final versions of the articles. The articles in question are:

- Reyes-Puig, C., Adams, D. C., Enriquez-Urzelai, U., and Kaliontzopoulou, A. (2023). Rensch's rule: linking intraspecific to evolutionary allometry. *Evolution*, *77*(12), 2576– 2589. https://doi.org/10.1093/evolut/qpad172. This article has been reproduced for Chapter 3 of this thesis, respecting copyright laws, with permission from Oxford University Press (License Number: 5957140265468).

- Reyes-Puig, C., Enriquez-Urzelai, U., Carretero, M. A., and Kaliontzopoulou, A. (2024). Is it all about size? Dismantling the integrated phenotype to understand species coexistence and niche segregation. *Functional Ecology*, *38*(11), 2350-2368. https://doi.org/10.1111/1365-2435.14646. This article has been reproduced for Chapter 4 of this thesis, respecting copyright laws, with permission from John Wiley & Sons (License Number: 5957131066512)

- Reyes-Puig, C., Enriquez-Urzelai, U., Sillero, N., and Kaliontzopoulou, A. (2025). Niche differentiation in coexisting species: ecological insights into the role of activity patterns, space use and environmental preferences. *Oecologia*, *in revision.*

- Reyes-Puig, C., Kaliontzopoulou, A., Sillero, N., and Enriquez-Urzelai, U. (2025). Microhabitats mediate the thermal and hydric challenges under climate change: a mechanistic perspective on similar yet distinct lizard species. *In preparation*.

This thesis was developed at BIOPOLIS-CIBIO/InBIO – Research Centre in Biodiversity and Genetic Resources, Vairão, Portugal. And supported by the Department of Biology, Faculdade de Ciências, Universidade do Porto, Porto, Portugal; Instituto de Biodiversidad Tropical IBIOTROP, Museo de Zoología, Colegio de Ciencias Biológicas y Ambientales COCIBA, Universidad San Francisco de Quito, Quito, Ecuador; Department of Evolutionary Biology, Ecology and Environmental Sciences, and

Biodiversity Research Institute (IRBio), Universitat de Barcelona, Barcelona, Spain; Czech Academy of Sciences, Institute of Vertebrate Biology, Brno, Czech Republic; CICGE-Centro de Investigação em Ciências Geo-Espaciais, Faculdade de Ciências da Universidade do Porto, Vila Nova de Gaia, Portugal. Furthermore, this research benefited from the collaboration of the Russell E. Train Education for Nature Program of WWF (World Wildlife Fund for Nature) and the Asociación Española de Ecología Terrestre (AEET).

The candidate's work was supervised by Dr. Antigoni Kaliontzopoulou (Department of Evolutionary Biology, Ecology and Environmental Sciences, and Biodiversity Research Institute (IRBio), Universitat de Barcelona, Barcelona), co-supervised by Dr. Urtzi Enriquez-Urzelai (Czech Academy of Sciences, Institute of Vertebrate Biology, Brno, Czech Republic), and co-supervised by Dr. Neftalí Sillero (CICGE-Centro de Investigação em Ciências Geo-Espaciais, Faculdade de Ciências da Universidade do Porto, Vila Nova de Gaia, Portugal).

The candidate was financially supported by Russell E. Train Education for Nature Program of WWF; Instituto de Biodiversidad Tropical IBIOTROP, Museo de Zoología, Colegio de Ciencias Biológicas y Ambientales COCIBA, Universidad San Francisco de Quito, Quito, Ecuado; BIOPOLIS-CIBIO/InBIO – Research Centre in Biodiversity and Genetic Resources, Vairão, Portugal; and Asociación Española de Ecología Terrestre (AEET).

Preferred Citation

Reyes-Puig C. 2025. Integrating comparative tools and mechanistic niche models to understand the effects of size variation on species' phenotypic diversification, coexistence and vulnerability to global change. Ph.D. Thesis, Faculdade de Ciências da Universidade do Porto, Portugal.

Acknowledgements

I would like to express my gratitude to my supervisors, Antigoni Kaliontzopoulou, Urtzi Enriquez-Urzelai, and Neftalí Sillero. Their support throughout all stages of this long journey has been indispensable in completing this phase. I am especially grateful to Antigoni for placing her trust in me and my abilities, and for giving me the opportunity to carry out such enriching work. I deeply appreciate Urtzi, who always took the time to respond to my messages, meet with me regardless of time and time differences, and dedicate time to long meetings to resolve coding issues. To Neftalí, I am grateful for his assistance in sourcing the geographic information required for certain chapters of this research and for his general comments.

I would also like to thank Dean C. Adams for his collaboration on the third chapter of this thesis, which focused on allometry and sexual dimorphism. I am thankful to Miguel Carretero for his openness and for providing access to his laboratory of ecophysiology, and for his collaboration in the fourth chapter related to physiological laboratory experiments.

I would like to extend my gratitude to the authorities of the Universidad San Francisco de Quito (USFQ), who supported me throughout this research process and enabled my prolonged research stays in Portugal. Additionally, I am deeply grateful to WWF for their EFN (Education for Nature) programme, which provided essential support for my postgraduate studies.

I am also deeply grateful to Katerina Sioumpoura, Frederico Barroso, Pablo Vincent, Verónica Gomes, Duarte Oliveira, Inês Freitas, Fernando Martínez-Freiría, David Brito-Zapata, Gorki Ríos-Alvear, and Ankalli Ríos-Reyes, who assisted at various stages of the laboratory experiments or field work. Finally, I extend my deepest thanks to my family for their unwavering support from my beginnings in biology until now (my parents, brothers, sister, husband, mother-in-law, and son). I also wish to thank those who have supported me in one way or another during these years, including Diego F. Cisneros-Heredia and Emilia Peñaherrera-Romero.

Resumo

O tamanho corporal é uma característica fenotípica que influencia diretamente múltiplos aspectos da biologia de um organismo, desde a sua fisiologia até interações ecológicas mais complexas. Em ectotérmicos, o tamanho corporal é particularmente relevante devido à sua relação com os processos de equilíbrio térmico e hídrico, que são altamente dependentes das condições climáticas circundantes. Com o aumento das temperaturas globais e a maior frequência de eventos climáticos extremos, é essencial compreender como o tamanho corporal influencia outras características fenotípicas nas dimensões morfológica, funcional, fisiológica e ecológica. Esta compreensão é crucial para explorar como a integração de várias características determina a vulnerabilidade dos ectotérmicos às mudanças climáticas. Esta tese tem como objetivo explorar o papel do tamanho corporal na diversificação fenotípica, na coexistência de espécies e na sua vulnerabilidade às mudanças climáticas, utilizando ferramentas comparativas e modelos mecanicistas de nicho. Para isso, lagartos verdes dos géneros *Lacerta* e *Timon* foram utilizados como sistema modelo num contexto macroevolutivo e ecológico, integrando dados empíricos, experimentais, de simulação e de modelação mecanicista. As metodologias incluíram o uso de simulações computacionais e métodos filogenéticos comparativos para avaliar padrões alométricos de diferenciação sexual relacionados com o tamanho corporal e outras características morfológicas dentro e entre espécies. Dados morfológicos, de desempenho funcional, ecológicos e fisiológicos foram recolhidos através de trabalho de campo e medições experimentais, sendo posteriormente analisados com técnicas multivariadas para avaliar o impacto do tamanho corporal nestas características e o seu papel na segregação de nichos. Observações detalhadas de campo registaram padrões de atividade diferenciados e utilização do espaço, ligando esses comportamentos a variáveis ambientais como temperatura e humidade. Adicionalmente, modelos mecanicistas de nicho foram usados para simular respostas fisiológicas e comportamentais em diferentes cenários climáticos, integrando dados de microhabitats e as características térmicas e hídricas das espécies. Os resultados gerais desta tese mostram que o tamanho corporal é o principal motor da variabilidade na maioria das características fenotípicas. A combinação de simulações computacionais e um exemplo empírico com lagartos verdes demonstra que padrões consistentes com a Regra de Rensch podem ser observados no tamanho corporal e em outras características no mesmo organismo, assim como o padrão inverso. Adicionalmente, análises do efeito da alometria intraespecífica sobre a alometria evolutiva mostram que a pendente alométrica estática é o principal parâmetro

que influencia a Regra de Rensch. Esta pesquisa confirmou que o tamanho corporal influencia a maioria das características estudadas e molda principalmente a morfologia e a ecofisiologia, em vez do desempenho. O seu papel multidimensional vai além de características individuais, integrando adaptações ecológicas e funcionais num quadro multidimensional abrangente. Em relação à segregação de nichos, esta tese reflete que o tamanho corporal é um dos principais fatores que influenciam a segregação de nichos nas espécies coexistentes *T. lepidus* e *L. schreiberi*. No entanto, não é o único fator, pois outros aspetos chave independentes do tamanho corporal, principalmente relacionados com o comprimento dos membros, equilíbrio hídrico, padrões de atividade e uso diferenciado do espaço em microhabitats específicos, também contribuem para a segregação de nichos entre as duas espécies. Modelos mecanicistas de nicho mostraram que, em cenários de aumento de temperatura (+2 °C e +4 °C), as taxas de perda de água aumentarão em ambas as espécies, mas serão particularmente elevadas em *L. schreiberi*, especialmente quando a perda de água corrigida pelo tamanho é considerada. Da mesma forma, os requisitos para sombra selecionada também aumentarão significativamente em *L. schreiberi*, devido à sua preferência por áreas húmidas e sombreadas. Os tempos de forrageamento e aquecimento aumentarão para ambas as espécies e, portanto, devido às suas exigências fisiológicas e de uso do espaço, *L. schreiberi* enfrentará maiores desafios para lidar com as mudanças climáticas. A abordagem mecanicista destaca os microhabitats e as suas propriedades do terreno, como inclinação e aspeto, como características-chave da paisagem que atuam como potenciais amortecedores térmicos, permitindo que as espécies mantenham condições fisiológicas ótimas em cenários climáticos presentes e futuros. Finalmente, os resultados desta tese sublinham a importância do tamanho corporal como um eixo central nos processos macroevolutivos, fenotípicos e ecológicos, incluindo a evolução do dimorfismo sexual no tamanho corporal, a compreensão da coexistência de espécies e a capacidade dos ectotérmicos de se adaptarem às mudanças ambientais, fornecendo informações essenciais para estratégias de conservação no contexto das mudanças globais.

Palavras-chave: ectotérmicos, fenótipo, alometria, macroevolução, ecologia, fisiologia, mudanças climáticas.

Abstract

Body size is a phenotypic trait that directly influences multiple aspects of an organism's biology, from its physiology to more complex ecological interactions. In ectotherms, body size is particularly relevant due to its relationship with thermal and hydric balance processes, which are highly dependent on the surrounding climatic conditions. As global temperatures rise and extreme climatic events become more frequent, it is essential to understand how body size influences other phenotypic traits across morphological, functional, physiological, and ecological dimensions. This understanding is crucial for exploring how the integration of several traits determines the vulnerability of ectotherms to climate change. This thesis aims to explore the role of body size in phenotypic diversification, species coexistence, and their vulnerability to climate change, using comparative tools and mechanistic niche models. To this end, green lizards of the genera *Lacerta* and *Timon* were used as a model system within a macroevolutionary and ecological context, integrating empirical, simulation experimental, and mechanistic modelling data. The methodologies included the use of computational simulations and comparative phylogenetic methods to evaluate allometric patterns of sexual differentiation related to body size and other morphological traits within and between species. Morphological, functional performance, ecological, and physiological data were collected through fieldwork and experimental measurements, then analysed with multivariate techniques to assess the impact of body size on these traits and its role in niche segregation. Detailed field observations captured differential activity patterns and space use, linking these behaviours to environmental variables like temperature and humidity. Additionally, mechanistic niche models were used to simulate physiological and behavioural responses under different climate scenarios, integrating microhabitat data and the thermal and hydric features of the species. The general results of this thesis show that body size is the main driver of variability in most phenotypic traits. The combination of computational simulations and an empirical green lizard example demonstrate that patterns consistent with Rensch's Rule may be observed in body size and other traits within the same organism, as well as the converse pattern. Additionally, analyses of the effect of intraspecific allometry on evolutionary allometry show that the static allometric slope is the main parameter influencing Rensch's Rule. This research confirmed that body size influences most of the studied traits and primarily shapes morphology and ecophysiology rather than performance. Its multidimensional role extends beyond individual traits, integrating ecological and functional adaptations into a comprehensive multidimensional framework. Regarding niche segregation, this thesis

reflects that body size is one of the main factors influencing niche segregation in the coexisting species *T. lepidus* and *L. schreiberi*. However, it is not the only factor, as other key aspects independent of body size, primarily related to limb length, hydric balance, activity patterns, and differentiated space use within specific microhabitats also contribute to niche segregation between the two species. Mechanistic niche models show that, under scenarios of increased temperature (+2 °C and +4 °C), rates of water loss will increase in both species, but will be particularly high for *L. schreiberi*, especially when size-corrected water loss is considered. Likewise, the requirements for selected shade will also significantly increase for *L. schreiberi*, due to its preference for humid and shaded areas. Foraging and basking times will increase for both species, and, therefore, due to their physiological and space-use requirements, *L. schreiberi* would face greater challenges in coping with climate change. The mechanistic approach highlights microhabitats and their terrain properties, such as slope and aspect, as key landscape features that act as potential thermal buffers, enabling species to maintain optimal physiological conditions under both present and future climatic scenarios. Finally, the findings of this thesis underscore the importance of body size as a central axis in macroevolutionary, phenotypic, and ecological processes, including the evolution of sexual size dimorphism, the understanding of species coexistence, and the capacity of ectotherms to adapt to environmental changes, thereby providing key insights for conservation strategies in the context of global change.

Keywords: ectotherms, phenotype, allometry, macroevolution, Ecology, physiology, climate change

Table of Contents

List of Tables

List of Figures

List of Abbreviations

FCUP	FACULTY OF SCIENCES OF THE UNIVERSITY OF PORTO
UP	UNIVERSITY OF PORTO
RR	RENSCH'S RULE
MNMS	MECHANISTIC NICHE MODELS
SD	SEXUAL DIMORPHISM
SSD	SEXUAL SIZE DIMORPHISM
ID	INTERCEPT DIFFERENCE
PGLS	PHYLOGENETIC GENERALIZED LEAST-SQUARES REGRESSION
SLD	SLOPE DIFFERENCE
SVL	SNOUT TO VENT LENGTH
TRL	TRUNK LENGTH
HL	HEAD LENGTH
HW	HEAD WIDTH
HH	HEAD HEIGHT
FLL	FORELIMB LENGTH
HLL	HINDLIMB LENGTH
HS	HEAD SIZE
GLMS	GENERAL LINEAR MODELS
MASL	METERS ABOVE SEA LEVEL
MAXSPR	MAXIMUM SPRINT SPEED
MNV	MANOEUVRABILITY
RES.MAXSPR	RESIDUALS OF MAXIMUM SPRINT SPEED
BF	BITE FORCE
RES.BF	RESIDUALS OF BITE FORCE
TPREF	PREFERRED (MEAN) TEMPERATURE
TPREFV	TEMPERATURE VARIANCE
RH	RELATIVE HUMIDITY
EWL	EVAPORATIVE WATER LOSS
P_WET	PROPORTION OF SURFACE AREA THAT IS WET
RES.EWL	RESIDUAL OF EVAPORATIVE WATER LOSS
RES.P_WET	RESIDUAL OF PROPORTION OF SURFACE AREA THAT IS WET
MORPH	MORPHOLOGY

PERFORM	FUNCTIONAL PERFORMANCE
ECOPHY	ECOPHYSIOLOGY
RES.MORPH	RESIDUAL OF MORPHOLOGY
RES.PERFORM	RESIDUAL OF FUNCTIONAL PERFORMANCE
RES.ECOPHY	RESIDUAL OF ECOPHYSIOLOGY
PCA	PRINCIPAL COMPONENT ANALYSIS
MANCOVA	MULTIVARIATE ANALYSIS OF COVARIANCE
FDA	FLEXIBLE DISCRIMINANT ANALYSIS
PLS	PARTIAL LEAST SQUARES REGRESSION
TA	MAXIMUM TRUNK ANGLE BENDING
HA	MAXIMUM HEAD ANGLE BENDING
SP	SPECIES
DF	DEGREES OF FREEDOM
ROY	ROY'S MAXIMUM ROOT
RMSE	ROOT MEAN SQUARE ERROR
MCMC	MARKOV CHAIN-BASED MONTE CARLO
LB	LOWER BOUND
UP	UPPER BOUND
DIC	DEVIANCE INFORMATION CRITERION
WAIC	WATANABE-AKAIKE INFORMATION CRITERION
KDE	KERNEL DENSITY ESTIMATION
SVM	SUPPORT VECTOR MACHINES
RUF	ROUGHNESS HEIGHT
SLE	SUSBTRATE LONGWAVE IR EMISSIVITY
DENSITY	SOIL MINERAL DENSITY
THCOND	SOIL MINERAL THERMAN CONDUCTIVITY\
MAXSHADE	MAXIMUM AVAILABLE SHADE
WW_G	WET BODY WEIGHT
PCT_WET	SKIN PERCENTAGE THAT IS WET
T_F_MIN	MINIMUM ACTIVITY TEMPERATURE
T_F_MAX	MAXIMUM TEMPERATURE FOR FORCED ACTIVITY
MINSHADE	MINIMUM AVAILABLE SHADE
T_RB_MIN	MINIMUM BODY TEMPERATURE TO LEAVE REFUGE
T_B_MIN	MINUMUM BODY TEMPERATURE FOR BASKING
IPCC	INTERGOVERNMENTAL PANEL ON CLIMATE CHANGE

C3S	COPERNICUS CLIMATE CHANGE SERVICE
VH	HERBACEOUS VEGETATION
GRO/ROCK	ROCKY SUBSTRATE AND BARE SOIL
CARP	CARPOBROTUS VEGETATION
WK	WALKWAY

Chapter 1

General Introduction

Body size is a fundamental node linking phenotypic and ecological traits in organisms, influencing their biotic and abiotic interactions. The pervasive influence of body size on morphological, functional, physiological, and behavioural processes demonstrates its central role in understanding patterns ranging from the organismal level to macroevolutionary dynamics (Maurer et al., 1992; White et al., 2007; Woodward et al., 2005). The importance of body size becomes even more critical in the face of current biodiversity challenges, such as species coexistence and vulnerability to climate change, particularly in ectotherms (Huey et al., 2012). Understanding how body size and other phenotypic traits shape organisms' responses to external conditions requires the integration of experimental processes, extensive field work studies, and mechanistic modelling. This introduction delves into the fundamental concepts of body size, allometry, species coexistence, and vulnerability to climate change in ectotherms. Thus, providing insights into the ecological and evolutionary effects of body size variation.

1.1. The role of body size in phenotypic and ecological traits

Body size is one of the most influential traits in the biology of organisms (Well et al., 2023; Woodward et al., 2005). It has a major role in almost every aspect of their physiology, morphology and functional ecology (Angilletta Jr., 2009; Deeming, 2022; Woodward et al., 2005). Effects of body size range from size-dependent energetic requirements to locomotor capabilities and even interactions between the species and the environment (Boukal et al., 2019; Gomes et al., 2016; Kleiber, 1947). Body size can influence the distribution and abundance of species depending on their mobility (Rocha et al., 2018). Larger organisms can disperse more efficiently and surpass biogeographic barriers more frequently, which facilitates colonization and diversification in distinct habitats (Jenkins et al., 2007; Woodward et al., 2005). On the other hand, smaller organisms often benefit from lower energetic costs and higher reproductive rates, allowing them to adapt to environments with limited resources and exploit ecological niches that may be inaccessible to larger organisms (Brown et al., 2004; Kleiber, 1947).

There is extensive information on the predictable relationship between body size and morphological, physiological and ecological traits (Angilletta Jr., 2009; Gayon 2000; Kleiber, 1947). This association is known as allometry, introduced as a concept by Julian Huxley (1924) and later revised, coined and formally defined by Huxley and Teisser

(1936) as the proportional growth of two linked traits. This proportional growth would produce a pattern of covariation following a power law. Thus, in the context of body size, allometry explains how changes in overall size influence the proportions of other traits (Figure 1.1; Gayon, 2000). Allometry follows three main patterns: positive allometry, in which a trait increases in greater proportion than body size; isometry, where traits scale proportionally to body size; and negative allometry, where traits grow at a slower rate relative to body size, due to functional or ecological constraints (Gayon, 2000; Mirth et al., 2016). Allometric relationships can be examined at three levels: ontogenetic allometry inspects trait scaling during organism's growth; static allometry explores trait scaling in individuals of the same species at a given life stage; and evolutionary allometry examines trait scaling across species (Eberhard et al., 2018; Freidline et al., 2015; Gayon, 2000; Pélabon et al., 2013)

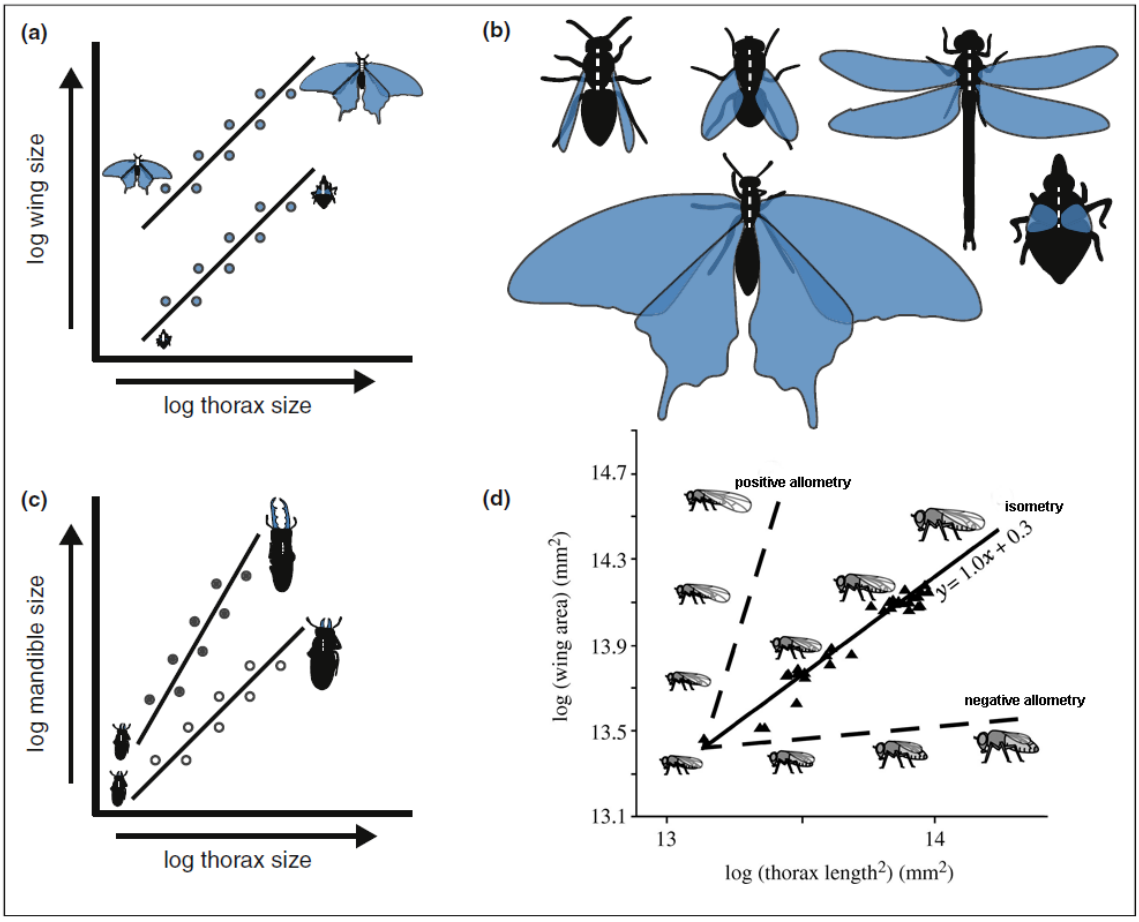

Figure 1.1 Example of allometry in insects. (a) In butterflies and planthoppers, wing size scales proportionally with to thorax size (isometry), maintaining consistent shape across all body sizes. (b) morphological diversity among insect orders, highlighting variations in wing size relative to body size. (c) In stag beetles, males exhibit positive allometry, with mandibles growing disproportionately larger relative to thorax size, altering shape as size increases. Conversely, females display isometry, with mandibles scaling proportionally to thorax size, preserving shape across body sizes (extracted from Mirth et al., 2016). (d) Relationship between thorax length and wing area in a log-log scale, illustrating different growth patterns (positive allometry, isometry, negative allometry) in *Drosophila melanogaster* (modified from Shingleton et al., 2008).

A well established example of functional allometry is the association between body size and bite force. Larger organisms, with larger heads tend to show stronger bite force, which enhances their ability to manipulate prey (Deeming, 2022; Verwaijen et al., 2002). Another example is allometric limb proportions, directly related to locomotor performance (Herrel et al., 2001; Huyghe et al., 2005). Larger limbs are linked with higher sprint speed and jumping ability (Kohlsdorf and Navas, 2012; Losos 1990). Since muscle strength is positively correlated to size and mass (Irschick et al., 2008), locomotor and other performance traits are also connected to intraspecific and interspecific interactions, such as combat and resource competition (Anderson et al., 2008; Kohlsdorf and Navas, 2012). In addition, body size plays a key role in sexual selection, driving allometric trends in selected traits such as head size, limb length or head ornamentation (Fairbairn, 1997; Gayon, 2000; Gomes et al., 2020; Mirth et al., 2016). In several organisms, males have relatively larger heads, limbs or mandibles than females, these adaptations may optimise performance in combat and territorial defence (Deeming, 2022; Kohlsdorf and Navas, 2012; Mirth et al., 2016). Consequently, the influence of body size on functional performance extends beyond trophic and environmental interactions, significantly impacting territorial defence and mating through direct interference (Huyghe et al., 2005; Husak et al., 2006).

In the physiological context, and due to the surface area-to-volume ratio, larger organisms generally exhibit higher absolute metabolic demands and water loss, but lower relative values of these traits per unit of mass. Conversely, smaller individuals exhibit lower absolute metabolic demands and water loss, but proportionally higher metabolic rates and water loss relative to their size (Chown and Klok, 2003; Kleiber, 1947). Furthermore, thermal physiology and body size are closely interconnected, through heterothermic capacity (Baudier et al., 2018; Streinzer et al., 2016; Webber et al., 2022). For instance, larger ectotherms tend to experience smaller fluctuations in body temperature, maintaining more stable daily thermal conditions. This stability is attributed to higher thermal inertia, which provides a buffering effect against environmental temperature changes (Angilletta Jr., 2009; Lutterschmidt and Reinert, 2012). Thus, allometric relationships not only provide a framework to better understand trait covariation but also reveal how size-dependent thermal dynamics influence ecological strategies, habitat use and the ability of organisms to cope with extreme environments (Kearney, 2013; Kearney and Porter, 2009; Lutterschmidt and Reinert, 2012).

1.2. Body size as a central axis in ecology and macroevolution

Through its influence on individual traits, body size is fundamental in determining the ecological processes that shape overall patterns of global biodiversity (Well et al., 2023; Woodward et al., 2005). As such, several macroecological and biogeographical patterns are related to variation in body size and other body traits. For example, Bergmann's rule predicts that larger body sizes are distributed in colder climates, in contrast to warmer climates (Bergmann, 1847). Allen's rule states that the body appendages of organisms in cold climate conditions are shorter than those of animals in warm environments (Allen, 1877). Both patterns are related to physiological allometric relationships, such as energy dynamics to avoid heat loss and save energy by optimising metabolic rate and heat balance (Angilletta Jr. et al., 2003; Mousseau, 1997). And although these patterns were initially proposed for endothermic vertebrates, several investigations have also tested them in ectotherms, finding congruent or contradictory results (Angilletta Jr. et al., 2003; Arnett and Gotelli, 1999; Ashton, 2002; Bidau and Martí, 2008; Porter and Hawkins, 2001). Body size is thus fundamental to metabolism, serving as a key factor in an organism's ability to adapt to its environment. It shapes not only energy efficiency but also survival and reproductive success under different climatic conditions (Angilletta Jr., 2009; Kleiber, 1947). Ecological networks depend on the body size of organisms in communities and ecosystems. It is well established that larger species live at lower densities (Damuth's rule), so the relationship between size and abundance sheds light on resource use and niche partitioning (Peters, 1983; White et al., 2007). Body size acts as a central axis linking individual physiology to community dynamics and global patterns of biodiversity, highlighting its importance as one of the most influential traits in an ecological framework (Woodward et al., 2005).

In addition, body size is pivotal in macroevolutionary patterns, moulding phenotypic diversification and adaptations through evolutionary timescales (LaBarbera, 1989; Maurer et al., 1992; Mirth et al., 2016). Body size evolution responds to micro- and macroevolutionary pathways, including environmental pressures, underlying genetic variation and ontogenetic constraints (Maurer et al., 1992). Microevolutionary forces may act on fitness traits, favouring body sizes that enhance survival and reproductive rates. Meanwhile, macroevolutionary trajectories across separately evolving lineages may confer advantages to distinct body sizes (LaBarbera 1989; Maurer et al., 1992). Macroevolutionary trends related to body size, such as Cope's rule, suggest that lineages tend to increase in body size over evolutionary time (Cope, 1887, 1896).

Conversely, island ecosystems provide well-documented examples of both gigantism and dwarfism (Benitez-López et al., 2021). Of particular relevance to this thesis is the relationship between body size and sexual dimorphism, which offers a valuable framework for examining macroevolutionary patterns, particularly, exploring sexual size dimorphism (i.e., differences in phenotypic traits between sexes within a taxon) through the lens of Rensch's Rule (RR). This rule highlights that sexual dimorphism in size tends to increase in groups where males are larger than females, applying not only to body size but also to other traits (Rensch, 1950; 1959). Thus, allometric relationships between males and females can serve to elucidate patterns of sexual selection and ecological divergence at the intra- and interspecific level (Dale et al., 2007; Fairbairn, 2005). Consequently, incorporating empirical studies that test Rensch's Rule is essential for gaining a deeper understanding of sexual size dimorphism, allowing to explore the selective pressures driving the evolution of sexually dimorphic traits.

Finally, the evolution of body size is closely tied to resource acquisition and competitive behaviour. Its interaction with evolutionary pressures highlights the mechanisms through which selection operates, from the individual level to the species level over evolutionary time (Maurer et al., 1992; Rensch, 1959, Woodward et al., 2005). Natural selection shapes body size within populations (microevolution), while macroevolution acts at the ancestor-descendant level, both processes are intricately linked to environmental conditions and ecological interactions (Maurer et al., 1992). Consequently, macroevolutionary patterns emphasise the integrative role of body size in connecting individual adaptations to broader evolutionary trends, directly influencing biodiversity and enhancing our understanding of evolution and ecology (Diniz-Filho, 2023; Maurer et al., 1992).

1.3. Phenotypic diversification and its link to species coexistence and niche segregation

The phenotype is best understood as a whole, combining morphological, physiological, functional performance, and behavioural traits that enable the organism to function as a unit (Bloom et al., 2012; Murren, 2012). Phenotypic traits do not act in isolation but rather work together synergistically to tackle environmental and genetic pressures (Murren, 2012; Wojczynski and Tiwari, 2008). Thus, phenotypic diversification allows organisms to exploit various dimensions of the ecological niche (Murren, 2012).

The ecological niche is known as a property of species that enables them to interact with the environment and other organisms, ensuring their survival, reproduction, and persistence (Colwell and Rangel, 2009; Hutchinson, 1978; Sales et al., 2021). It can be conceptualised as an n-dimensional hypervolume, where every point represents a state of the environment that permits the species to exist indefinitely (Hutchinson, 1957). By definition, both the phenotype and the ecological niche are multidimensional (Bloom et al., 2012; Hutchinson, 1957; Murren, 2012; Sales et al., 2021). Therefore, the exploration of phenotype and niche in multidimensional space is key to understanding how species exploit resources, distribute and coexist.

Particular attention has been dedicated to species coexistence, defined as the capacity of species to occur in the same area without displacing one another (Gravel et al., 2011; Valladares et al., 2015). Consequently, multidimensionality has emerged as an important aspect to consider when exploring species coexistence (Damas-Moreira et al., 2020; Lu et al., 2011). Phenotypic traits adapt to environmental changes, expanding the possibilities for specialisation in several niche dimensions (Layman et al., 2015; Smart and Gee, 1979). One mechanism by which species can coexist is niche segregation (Gravel et al., 2011; Tokeshi, 2009). Niche segregation mediates and facilitates species coexistence by optimising resource use and significantly reducing direct competition through differences in niche differentiation (Figure 1.2; Pianka and Huey, 1978; Valladares et al., 2015). Phenotypic variability, based on genetic variation, responds to biotic and abiotic conditions that limit processes such as dispersal, migration or even extinction (Valladares et al., 2015).

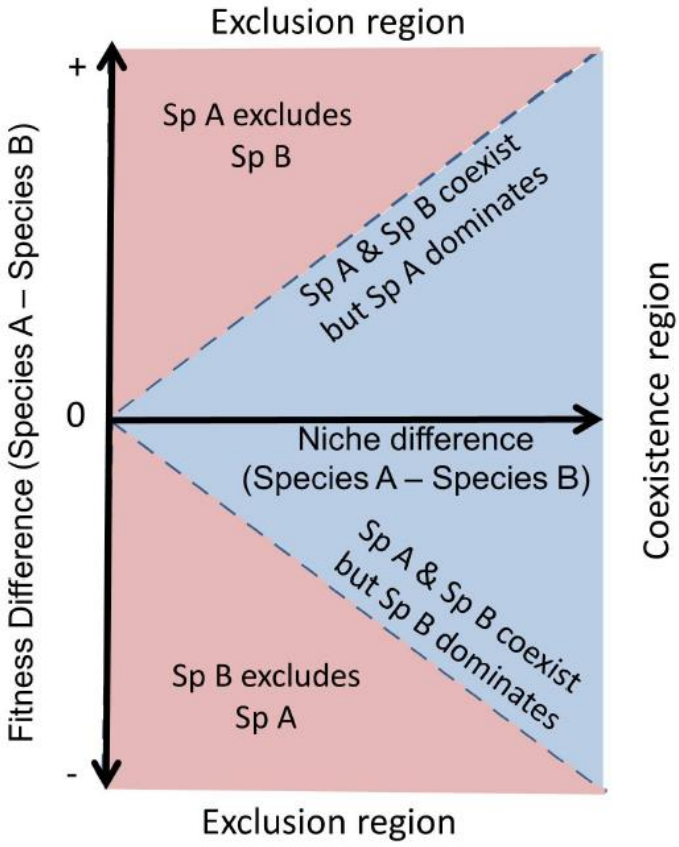

Figure 1.2 Theoretical framework of coexistence between two species. Stable coexistence occurs when niche differences exceed fitness asymmetries (blue region). In contrast, competitive exclusion arises when fitness differences outweigh niche differences (red region) (extracted from Valladares et al., 2015).

Niche segregation in coexisting species may occur across both spatial and temporal axes (Hart et al., 2017; Pita et al., 2011; Valladares et al., 2015). Spatial heterogeneity facilitates species segregation by promoting specialization in space use, including spatial patterns associated with the physical properties of habitats (e.g., substrates, vegetation, terrain, and water bodies). In this way, species can exhibit substantial niche overlap while selecting unique resources that promote coexistence (Darmon et al., 2012). Spatial scale and environmental variability play a crucial role in understanding niche segregation, as differences in physiological tolerance allow species to occupy distinct microhabitats, even within small areas, thus avoiding competitive exclusion (Hart et al., 2017). Moreover, at smaller spatial scales, niche differentiation becomes more pronounced, while at landscape scales, niche overlap tends to increase (Pita et al., 2011). Importantly, body size influences how species perceive and utilize habitat space and how they access resources within it (Pita et al., 2011; Woodward et al., 2005). Thus, body size emerges once again as a major factor in ecology influencing species coexistence and niche segregation. On the other hand, temporal segregation is

a mechanism through which species achieve coexistence by differing in their activity patterns and utilizing distinct resources at different times (Castro-Arellano and Lacher Jr, 2009; Loreau, 1989). Likewise, temporal segregation may depend on seasonality in species life-history traits and ecology, such as mating periods, where differences in foraging and thermoregulatory activities further enhance coexistence (Martínez-Freiría et al., 2010; Navarro et al., 2013).

To better understand how phenotypic diversification influences niche segregation, it is essential to combine empirical field observations and experimental data that integrate niche dimensions and environmental variables. Incorporating body size alongside size-independent traits is also central, as their combined effects provide a more comprehensive understanding of how organisms partition resources and adapt to their environments. Furthermore, integrating both spatial and temporal segregation provides deeper insights into species coexistence (Navarro et al., 2013; Valladares et al., 2015). An approach that combines perspectives from morphology, physiology, and habitat features, improves our ability to predict organismal responses to global changes within a broader ecological context.

1.4. Vulnerability of ectotherms to climate change

Ectotherms are particularly vulnerable to changes in environmental features due to their dependence on climatic conditions (Angilletta Jr., 2009; Rohr and Palmer, 2013). Over the past twenty years, there has been a consistent increase in global temperatures, drawing attention to the emerging climate change crisis that threatens biodiversity, with ectotherms being particularly threatened (Masson-Delmotte et al., 2023). Global temperatures have risen approximately 1.1 °C since pre-industrial times, significantly affecting many organisms (C3S, 2024; IPCC, 2023). Particularly ectotherms have shown more pronounced responses compared to endotherms, primarily through shifts in altitudinal and latitudinal distributions (Nunez et al., 2019; Ramalho et al., 2023). The physiological and ecological consequences of climate change for ectotherms extend beyond critical thermal limits. Exposure to less than lethal temperatures, and the disruption of underlying processes such as fertility and alterations in energy balance are increasingly recognized as factors in the vulnerability of organisms to climate change (Parratt et al., 2021; Van Heerwaarden and Sgrò, 2021; Walsh et al., 2019). When these limits are exceeded, metabolic performance deteriorates, often leading to increased

mortality (Huey et al., 2012; Rohr and Palmer, 2013). Although some ectotherms exhibit physiological plasticity to enhance their adaptation to climate change, certain species remain more vulnerable than others (Kearney, 2013; Seebacher et al., 2015). Even phenotypic variability does not always compensate for the long-term impacts of rising temperatures (Gunderson and Leal, 2016; Seebacher et al., 2015). Other significant effects include reductions in body size, increased physiological rates (e.g., metabolic and water loss), and alterations in organismal activity (Gunderson and Leal, 2016; Kearney, 2013; Rohr and Palmer, 2013).

Microhabitats and microclimates can provide suitable local conditions that shelter and buffer ectotherms from extreme temperatures (Dobrowski, 2011). However, the ability of microhabitats to mitigate these effects is increasingly challenged by additional stressors such as habitat loss, invasive species, and emerging diseases, which amplify the negative impacts of climate change on ectotherms (Rohr and Palmer, 2013). Despite these challenges, microhabitats remain critical in reducing heat stress during climatic extremes (Dobrowski, 2011; Scheffers et al., 2014). Additionally, microhabitats have historically played an important role in enabling species to persist through climatic events over time (Dobrowski, 2011). Topographical features of the terrain directly influence the amount of solar radiation received, which in turn affects microhabitat climatic conditions and species' micro-distributions (Sillero and Gonçalves-Seco, 2014). Factors such as slope and aspect are related to vegetation cover and soil properties, influencing vegetation composition and, in turn, helping to buffer the impacts of climate change by altering microhabitat conditions (Bennie et al., 2018; Singh, 2018). The microclimates derived from the physical structure of microhabitats serve as critical thermoregulatory resources for ectotherms, enabling them to balance their internal temperatures by seeking shade or moving to cooler areas (Kearney and Porter, 2009). Consequently, ectotherms can adjust their behaviour to cope with extreme temperatures, thereby reducing the energetic costs of adapting to climate warming (Kearney and Porter, 2009; Kearney et al., 2014). As such, microhabitats serve as natural buffers that mitigate local climatic conditions, reducing extinction risks for species dependent on restricted thermal and hydric niches (Bennie et al., 2018; Dobrowski, 2011; Kearney and Porter, 2009; Scheffers et al., 2014).

1.5. Integrating mechanistic approaches to understanding ectotherms' challenges to climate change

Understanding the complex interplay between climate change and ectotherm responses requires finely tuned models that account for detailed factors such as physiology, behaviour, and environmental conditions. Mechanistic niche models (MNMs) provide critical insights into how ectotherms cope with extreme climatic changes (Kearney and Porter, 2009; Kearney et al., 2014). Unlike correlative approaches, MNMs explicitly integrate the physiological traits of organisms, enabling the simulation of microclimatic conditions and physiological responses, such as heat and water exchange. This allows researchers to predict microhabitat use and physiological performance under future scenarios without the risk of inaccurate extrapolation (Kearney, 2006; Kearney and Porter, 2017). MNMs incorporate key dimensions like thermal and water balance, thermoregulatory behaviour and energetics, providing information of processes such as resource use, fitness, and life history traits (Kearney, 2013; Kearney et al., 2014; Kearney and Enriquez-Urzelai, 2023).

A core strength of MNMs lies in their ability to link detailed data on organismal traits—such as body size, shape, physiology and thermoregulatory behaviours—with environmental variables, including temperature, humidity, and solar radiation at temporal and spatial scales (Figure 1.3). This integration allows the prediction of physiological and ecological patterns, which can then be extrapolated to generate maps of organismal responses across landscapes (Figure 1.3) (Kearney and Porter, 2009). An essential component of these models is the incorporation of mass balance equations from biophysical ecology (Porter and Tracy, 1983). These equations describe energy exchange through conduction, convection, and radiation, as well as heat and mass exchange via evaporation (i.e., water loss) and metabolism (Kearney and Porter, 2009; Kearney et al., 2021). As highlighted earlier, body size a pivotal trait in physiology, directly influences body temperature (heat budget) and water loss rates (water balance and exchange), making it critically relevant in the context of climate change (Gardner et al., 2011; Olhberger, 2013). Rising temperatures and increasing variability in water availability amplify the physiological challenges faced by organisms, underscoring the importance of MNMs (Kearney and Porter, 2009; Kearney, 2013).

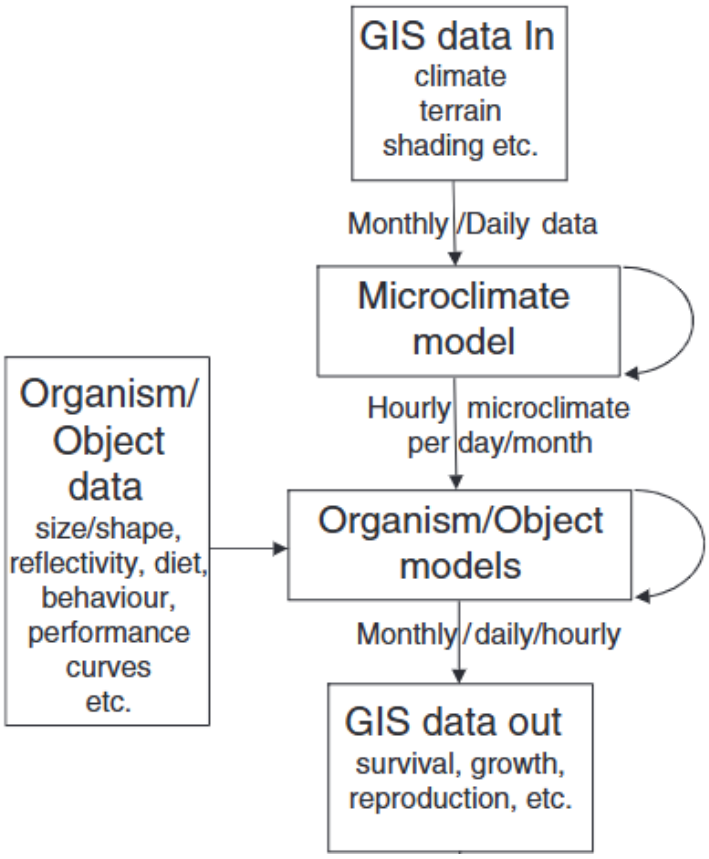

Figure 1.3 Diagram illustrating mechanistic modelling approach to link physiological, behavioural, and fitness traits with environmental variables, enabling predictions of organismal responses across geographical and environmental gradients (adapted from Kearney and Porter, 2009).

Mechanistic niche models (MNMs) incorporate GIS data on the physical configuration of habitats with microclimatic information to simulate hourly and daily conditions at microscales. Then, these models integrate microclimatic conditions with organisms' functional traits (i.e. physiological, behavioural, and morphological traits), and with that they are able to accurately predict organismal fitness (i.e. survival, growth, reproduction, and activity windows (Fig. 1.3). MNMs operate under two main frameworks: steady-state and transient-state models. Steady-state models assume that ectothermic organisms achieve thermal equilibrium at a stable body temperature at each time step (e.g. one hour), providing predictions without considering heat storage (Kearney and Porter, 2009; Kearney et al., 2021). In contrast, transient-state models account for thermal and hydric dynamics over time, simulating how climatic fluctuations affect organismal responses throughout the day (Kearney and Porter, 2009). The advantage of MNMs lies in their ability to incorporate heat and water budgets, offering a holistic framework to explore how ectotherms balance hydric and thermoregulatory

dynamics to cope with current and future environmental conditions (Enriquez-Urzelai and Gvoždík, 2024; Kearney and Enriquez-Urzelai, 2023). This approach is crucial for understanding the effects of climate change on temperature-dependent groups.

References

Allen, J. A. (1877). The influence of physical conditions in the genesis of species. *Radical review, 1*, 108-140.

Anderson, R. A., McBrayer, L. D., and Herrel, A. (2008). Bite force in vertebrates: opportunities and caveats for use of a nonpareil whole-animal performance measure. *Biological Journal of the Linnean Society, 93*(4), 709–720. https://doi.org/10.1111/j.1095-8312.2007.00905.x

Angilletta Jr., M. J. (2009). *Thermal adaptation: a theoretical and empirical synthesis.* Oxford University Press.

Angilletta Jr., M. J., and Dunham, A. E. (2003). The temperature–size rule in ectotherms: simple evolutionary explanations may not be general. *The American Naturalist, 162*(3), 332–342. https://doi.org/10.1086/377187

Arnett, A. E., and Gotelli, N. J. (1999). Geographic variation in life history traits of the ant lion, *Myrmeleon immaculatus*: evolutionary implications of Bergmann's rule. *Evolution, 53*(5), 1180–1188. https://doi.org/10.1111/j.1558-5646.1999.tb04531.x

Ashton, K. G. (2002). Do amphibians follow Bergmann's rule? *Canadian Journal of Zoology, 80*(5), 708–716.

Baudier, K., and O'Donnell, S. (2018). Complex body size differences in thermal tolerance among army ant workers (*Eciton burchellii parvispinum*). *Journal of Thermal Biology, 78*, 277–280. https://doi.org/10.1016/j.jtherbio.2018.10.011

Benítez-López, A., Santini, L., Gallego-Zamorano, J., Milá, B., Walkden, P., Huijbregts, M. A., and Tobias, J. A. (2021). The island rule explains consistent patterns of body size evolution in terrestrial vertebrates. *Nature Ecology & Evolution, 5*(6), 768–786.

Bennie, J., Huntley, B., Wiltshire, A., Hill, M. O., and Baxter, R. (2008). Slope, aspect and climate: Spatially explicit and implicit models of topographic microclimate in chalk grassland. *Ecological Modelling, 216*(1), 47–59. https://doi.org/10.1016/j.ecolmodel.2008.04.010

Bergmann, C. (1847). Ueber die verhältnisse der wärmeökonomie der thiere zu ihrer grösse. *Gottinger Studien, 3*, 595–708.

Bidau, C. J., and Martí, D. A. (2008). A test of Allen's rule in ectotherms: the case of two South American melanopline grasshoppers (Orthoptera: Acrididae) with partially overlapping geographic ranges. *Neotropical Entomology, 37*(4), 370–380. https://doi.org/10.1590/S1519-566X2008000400004

Bloom, A. J., Hastings, A., and Gross, L. (2012). Integrated whole organism physiology. In A. Hastings & L. Gross (Eds.), *Encyclopedia of Theoretical Ecology* (pp. 376–381). University of California Press.

Boukal, D. S., Bideault, A., Carreira, B. M., and Sentis, A. (2019). Species interactions under climate change: connecting kinetic effects of temperature on individuals to community dynamics. *Current Opinion in Insect Science, 35*, 88–95. https://doi.org/10.1016/j.cois.2019.06.014

Brown, J. H., Gillooly, J. F., Allen, A. P., Savage, V. M., and West, G. B. (2004). Toward a metabolic theory of ecology. *Ecology*, *85*(7), 1771-1789. https://doi.org/10.1890/03-9000

Castro-Arellano, I., and Lacher Jr, T. E. (2009). Temporal niche segregation in two rodent assemblages of subtropical Mexico. *Journal of Tropical Ecology, 25*(6), 593–603. https://doi.org/10.1017/S0266467409990186

Champy, C. (1929). La croissance dysharmonique des caractères sexuels accessoires. *Archives des Sciences Physiques et Naturelles*, Zoologie, 193–244.

Chown, S. L., and Klok, C. J. (2003). Water-balance characteristics respond to changes in body size in subantarctic weevils. *Physiological and Biochemical Zoology, 76*(5), 634–643. https://doi.org/10.1086/376919

Colwell, R. K., and Rangel, T. F. (2009). Hutchinson's duality: The once and future niche. *Proceedings of the National Academy of Sciences of the United States of America, 106*(Supplement_2), 19651–19658. https://doi.org/10.1073/pnas.0901650106

Cope, E. D. (1887). *The origin of the fittest: Essays on evolution.* D. Appleton and Co.

Cope, E. D. (1896). *The primary factors of organic evolution.* Open Court Publications Co.

Copernicus Climate Change Service (C3S). (2024). Copernicus: June 2024 marks the 12th month with global temperature reaching 1.5°C above pre-industrial levels. Retrieved November 27, 2024, from https://climate.copernicus.eu/copernicus-june-2024-marks-12th-month-global-temperature-reaching-15degc-above-pre-industrial

Dale, J., Dunn, P. O., Figuerola, J., Lislevand, T., Székely, T., and Whittingham, L. A. (2007). Sexual selection explains Rensch's rule of allometry for sexual size dimorphism. *Proceedings of the Royal Society B: Biological Sciences, 274*(1628), 2971–2979. https://doi.org/10.1098/rspb.2007.1043

Damas-Moreira, I., Riley, J. L., Carretero, M. A., Harris, D. J., and Whiting, M. J. (2020). Getting ahead: Exploitative competition by an invasive lizard. *Behavioral Ecology and Sociobiology, 74*, 117. https://doi.org/10.1007/s00265-020-02893-2

Damuth, J. (1981). Population density and body size in mammals. *Nature, 290*, 699–700.

Darmon, G., Calenge, C., Loison, A., Jullien, J. M., Maillard, D., and Lopez, J. F. (2012). Spatial distribution and habitat selection in coexisting species of mountain ungulates. *Ecography, 35*(1), 44–53. https://doi.org/10.1111/j.1600-0587.2011.06664.x

Deeming, D. C. (2022). Inter-relationships among body mass, body dimensions, jaw musculature and bite force in reptiles. *Journal of Zoology, 318*(1), 23–33. https://doi.org/10.1111/jzo.12981

Diniz-Filho, J. A. F. (2023). Patterns in Body Size. In The Macroecological Perspective: Theories, Models and Methods (pp. 293-338). Cham: Springer International Publishing.

Dobrowski, S. Z. (2011). A climatic basis for microrefugia: the influence of terrain on climate. *Global Change Biology, 17*(2), 1022–1035. https://doi.org/10.1111/j.1365-2486.2010.02263.x

Eberhard, W. G., Rodríguez, R. L., Huber, B. A., Speck, B., Miller, H., Buzatto, B. A., and Machado, G. (2018). Sexual selection and static allometry: The importance of function. *The Quarterly Review of Biology, 93*(3), 207–250. https://doi.org/10.1086/699410

Enriquez-Urzelai, U., and Gvoždík, L. (2024). Impacts of behaviour and acclimation of metabolic rate on energetics in sheltered ectotherms: a climate change perspective. *Proceedings of the Royal Society B, 291*(2017), 20232152. https://doi.org/10.1098/rspb.2023.2152

Enriquez-Urzelai, U., Tingley, R., Kearney, M. R., Sacco, M., Palacio, A. S., Tejedo, M., and Nicieza, A. G. (2020). The roles of acclimation and behaviour in buffering climate change impacts along elevational gradients. *Journal of Animal Ecology, 89*(7), 1722–1734. https://doi.org/10.1111/1365-2656.13222

Fairbairn, D. J. (1997). Allometry for sexual size dimorphism: Pattern and process in the coevolution of body size in males and females. *Annual Review of Ecology and Systematics, 28*(1), 659–687. https://doi.org/10.1146/annurev.ecolsys.28.1.659

Fairbairn, D. J. (2005). Allometry for sexual size dimorphism: Testing two hypotheses for Rensch's rule in the water strider *Aquarius remigis*. *The American Naturalist, 166*(Suppl 4), S69–S84. https://doi.org/10.1086/444600

Freidline, S. E., Gunz, P., and Hublin, J. J. (2015). Ontogenetic and static allometry in the human face: Contrasting Khoisan and Inuit. *American Journal of Physical Anthropology, 158*(1), 116–131. https://doi.org/10.1002/ajpa.22759

Gardner, J. L., Peters, A., Kearney, M. R., Joseph, L., and Heinsohn, R. (2011). Declining body size: A third universal response to warming? *Trends in Ecology & Evolution, 26*(6), 285–291. https://doi.org/10.1016/j.tree.2011.03.005

Gayon, J. (2000). History of the concept of allometry. *American Zoologist, 40*(5), 748–758. https://doi.org/10.1093/icb/40.5.748

Gomes, V., Carretero, M. A., and Kaliontzopoulou, A. (2016). The relevance of morphology for habitat use and locomotion in two species of wall lizards. *Acta Oecologica, 70*, 87–95. https://doi.org/10.1016/j.actao.2015.12.005

Gomes, V., Herrel, A., Carretero, M. A., and Kaliontzopoulou, A. (2020). New insights into bite performance: Morphological trade-offs underlying the duration and magnitude of bite force. *Physiological and Biochemical Zoology, 93*(3), 175–184.

Gravel, D., Guichard, F., and Hochberg, M. E. (2011). Species coexistence in a variable world. *Ecology Letters, 14*(8), 828–839. https://doi.org/10.1111/j.1461-0248.2011.01643.x

Gunderson, A. R., and Leal, M. (2016). A conceptual framework for understanding thermal constraints on ectotherm activity with implications for predicting responses to global change. *Ecology Letters, 19*(2), 111–120. https://doi.org/10.1111/ele.12552

Hart, S. P., Usinowicz, J., and Levine, J. M. (2017). The spatial scales of species coexistence. *Nature Ecology & Evolution, 1*(8), 1066–1073. https://doi.org/10.1038/s41559-017-0230-7

Herrel, A., Damme, R. V., Vanhooydonck, B., and Vree, F. D. (2001). The implications of bite performance for diet in two species of lacertid lizards. *Canadian Journal of Zoology, 79*(4), 662–670. https://doi.org/10.1139/z01-031

Huey, R. B., Kearney, M. R., Krockenberger, A., Holtum, J. A., Jess, M., and Williams, S. E. (2012). Predicting organismal vulnerability to climate warming: Roles of behaviour, physiology and adaptation. *Philosophical Transactions of the Royal Society B: Biological Sciences, 367*(1596), 1665–1679. https://doi.org/10.1098/rstb.2012.0005

Husak, J. F., Lappin, A. K., Fox, S. F., and Lemos-Espinal, J. A. (2006). Bite-force performance predicts dominance in male venerable collared lizards (*Crotaphytus antiquus*). *Copeia, 2006*(2), 301–306. https://doi.org/10.1643/0045-8511(2006)6

Hutchinson, G.E. (1957). Concluding remarks. *Cold Spring Harbor Symposia on Quantitative Biology. 22*:415–427. https://doi.org/10.1101/SQB.1957.022.01.039

Hutchinson, G. E. (1978). *An introduction to population ecology.* Yale University Press.

Huxley, J. S. (1924). Constant differential growth ratios and their significance. *Nature, 114*, 895–896.

Huxley, J. S., and Teissier, G. (1936). Terminology of relative growth. *Nature, 780*–781.

Huyghe, K., Vanhooydonck, B., Scheers, H., Molina-Borja, M., and Van Damme, R. (2005). Morphology, performance and fighting capacity in male lizards, *Gallotia galloti*. *Functional Ecology*, 800–807. https://www.jstor.org/stable/3599340

IPCC, 2023: Sections. In: Climate Change 2023: Synthesis Report. Contribution of Working Groups I, II and III to the Sixth Assessment Report of the Intergovernmental Panel on Climate Change [Core Writing Team, H. Lee and J. Romero (eds.)]. IPCC, Geneva, Switzerland, pp. 35-115, doi: 10.59327/IPCC/AR6-9789291691647

Irschick, D. J., Meyers, J. J., Husak, J. F., and Le Galliard, J. F. (2008). How does selection operate on whole-organism functional performance capacities? A review and synthesis. *Evolutionary Ecology Research, 10*(2), 177–196. https://doi.org/10.7275/R58G8HX6

Jenkins, D. G., Brescacin, C. R., Duxbury, C. V., Elliott, J. A., Evans, J. A., Grablow, K. R., ... and Williams, S. E. (2007). Does size matter for dispersal distance? *Global Ecology and Biogeography, 16*(4), 415–425. https://doi.org/10.1111/j.1466-8238.2007.00312.x

Kearney, M. (2006). Habitat, environment and niche: What are we modelling? *Oikos, 115*(1), 186–191. https://doi.org/10.1111/j.2006.0030-1299.14908.x

Kearney, M. (2013). Activity restriction and the mechanistic basis for extinctions under climate warming. *Ecology Letters, 16*(12), 1470–1479. https://doi.org/10.1111/ele.12192

Kearney, M. R., and Enriquez-Urzelai, U. (2023). A general framework for jointly modelling thermal and hydric constraints on developing eggs. *Methods in Ecology and Evolution, 14*(2), 583–595. https://doi.org/10.1111/2041-210X.14018

Kearney, M. R., and Porter, W. P. (2017). NicheMapR–an R package for biophysical modelling: The microclimate model. *Ecography, 40*(5), 664–674. https://doi.org/10.1111/ecog.02360

Kearney, M. R., Isaac, A. P., and Porter, W. P. (2014). Microclim: Global estimates of hourly microclimate based on long-term monthly climate averages. *Scientific Data, 1*(1), 1–9. https://doi.org/10.1038/sdata.2014.6

Kearney, M., and Porter, W. (2009). Mechanistic niche modelling: Combining physiological and spatial data to predict species' ranges. *Ecology Letters, 12*(4), 334–350. https://doi.org/10.1111/j.1461-0248.2008.01277.x

Kleiber, M. (1947). Body size and metabolic rate. *Physiological Reviews, 27*(4), 511–541. https://doi.org/10.1152/physrev.1947.27.4.511

Kohlsdorf, T., and Navas, C. (2012). Evolution of form and function: Morphophysiological relationships and locomotor performance in tropidurine lizards. *Journal of Zoology, 288*(1), 41–49. https://doi.org/10.1111/j.1469-7998.2012.00918.x

LaBarbera, M. (1989). Analyzing body size as a factor in ecology and evolution. *Annual review of ecology and systematics*, 97-117. https://www.jstor.org/stable/2097086

Layman, C. A., Newsome, S. D., and Gancos Crawford, T. (2015). Individual-level niche specialization within populations: Emerging areas of study. *Oecologia, 178*, 1–4. https://doi.org/10.1007/s00442-014-3209-y

Loreau, M. (1989). Coexistence of temporally segregated competitors in a cyclic environment. *Theoretical Population Biology, 36*(2), 181–201. https://doi.org/10.1016/0040-5809(89)90029-4

Losos, J. B. (1990). The evolution of form and function: Morphology and locomotor performance in West Indian *Anolis* lizards. *Evolution, 44*(5), 1189–1203.

Lu, X., Gong, G., and Ma, X. (2011). Niche segregation between two alpine rosefinches: To coexist in extreme environments. *Evolutionary Biology, 38*, 79–87. https://doi.org/10.1007/s11692-010-9102-7

Lutterschmidt, W. I., and Reinert, H. K. (2012). Modeling body temperature and thermal inertia of large-bodied reptiles: support for water-filled biophysical models in radiotelemetric studies. *Journal of thermal biology*, *37*(4), 282-285.

Martínez-Freiría, F., Lizana, M., do Amaral, J. P., and Brito, J. C. (2010). Spatial and temporal segregation allows coexistence in a hybrid zone among two Mediterranean vipers (*Vipera aspis* and *V. latastei*). *Amphibia-Reptilia, 31*(2), 195–212.

Masson-Delmotte, V., Zhai, P., Pirani, A., Connors, S. L., Péan, C., Berger, S., ... and Zhou, B. (2023). IPC 2021. Summary for Policymakers. Climate Change 2021: The Physical Science Basis. Contribution of Working Group I to the Sixth Assessment Report of the Intergovernmental Panel on Climate Change.

Maurer, B. A., Brown, J. H., and Rusler, R. D. (1992). The micro and macro in body size evolution. *Evolution, 46*(4), 939–953. https://doi.org/10.1111/j.1558-5646.1992.tb00611.x

Mirth, C. K., Frankino, W. A., and Shingleton, A. W. (2016). Allometry and size control: What can studies of body size regulation teach us about the evolution of morphological scaling relationships? *Current Opinion in Insect Science, 13*, 93–98. https://doi.org/10.1016/j.cois.2016.02.010

Mousseau, T. A. (1997). Ectotherms follow the converse to Bergmann's rule. *Evolution*, 630–632. https://doi.org/10.2307/2411138

Murren, C. J. (2012). The integrated phenotype. *Integrative and Comparative Biology, 52*(1), 64–76. https://doi.org/10.1093/icb/ics043

Navarro, J., Votier, S. C., Aguzzi, J., Chiesa, J. J., Forero, M. G., and Phillips, R. A. (2013). Ecological segregation in space, time and trophic niche of sympatric planktivorous petrels. *PloS One, 8*(4), e62897. https://doi.org/10.1371/journal.pone.0062897

Nunez, S., Arets, E., Alkemade, R., Verwer, C., and Leemans, R. (2019). Assessing the impacts of climate change on biodiversity: Is below 2° C enough? *Climatic Change, 154*, 351–365. https://doi.org/10.1007/s10584-019-02420-x

Ohlberger, J. (2013). Climate warming and ectotherm body size–from individual physiology to community ecology. *Functional Ecology, 27*(4), 991–1001. https://doi.org/10.1111/1365-2435.12098

Parratt, S. R., Walsh, B. S., Metelmann, S., White, N., Manser, A., Bretman, A. J., ... and Price, T. A. (2021). Temperatures that sterilize males better match global species distributions than lethal temperatures. Nature Climate Change, 11(6), 481-484. https://doi.org/10.1038/s41558-021-01047-0

Peters, R. H. (1983). *The ecological implications of body size.* Cambridge University Press.

Pélabon, C., Firmat, C., Bolstad, G. H., Voje, K. L., Houle, D., Cassara, J., Rouzic, A. L., and Hansen, T. F. (2014). Evolution of morphological allometry. *Annals of the New York Academy of Sciences, 1320*(1), 58–75. https://doi.org/10.1111/nyas.12470

Pianka, E. R., and Huey, R. B. (1978). Comparative ecology, resource utilization and niche segregation among gekkonid lizards in the southern Kalahari. *Copeia, 1978*, 691–701. https://doi.org/10.2307/1443698

Pita, R., Mira, A., and Beja, P. (2011). Assessing habitat differentiation between coexisting species: The role of spatial scale. *Acta Oecologica, 37*(2), 124–132. https://doi.org/10.1016/j.actao.2011.01.006

Porter, E. E., and Hawkins, B. A. (2001). Latitudinal gradients in colony size for social insects: Termites and ants show different patterns. *American Naturalist, 157*, 97–106. https://doi.org/10.1086/317006

Ramalho, Q., Vale, M. M., Manes, S., Diniz, P., Malecha, A., and Prevedello, J. A. (2023). Evidence of stronger range shift response to ongoing climate change by ectotherms and high-latitude species. *Biological Conservation, 279*, 109911. https://doi.org/10.1016/j.biocon.2023.109911

Rensch, B. (1950). Die Abhängigkeit der relativen Sexualdifferenz von der Körpergrösse. *Bonner Zoologische Beiträge, 1*, 58–69.

Rensch, B. (1959). *Evolution above the species level.* Columbia University Press.

Rocha, M. P., Bini, L. M., Siqueira, T., Hjort, J., Grönroos, M., Lindholm, M., ... and Heino, J. (2018). Predicting occupancy and abundance by niche position, niche breadth

and body size in stream organisms. *Oecologia*, *186*, 205-216. https://doi.org/10.1007/s00442-017-3988-z

Rohr, J. R., and Palmer, B. D. (2013). Climate change, multiple stressors, and the decline of ectotherms. *Conservation Biology, 27*(4), 741–751. https://doi.org/10.1111/cobi.12086

Sales, L. P., Hayward, M. W., and Loyola, R. (2021). What do you mean by “niche”? Modern ecological theories are not coherent on rhetoric about the niche concept. *Acta Oecologica, 110*, 103701. https://doi.org/10.1016/j.actao.2020.103701

Scheffers, B. R., Edwards, D. P., Diesmos, A., Williams, S. E., and Evans, T. A. (2014). Microhabitats reduce animal's exposure to climate extremes. *Global change biology*, *20*(2), 495-503. https://doi.org/10.1111/gcb.12439

Seebacher, F., White, C. R., and Franklin, C. E. (2015). Physiological plasticity increases resilience of ectothermic animals to climate change. *Nature Climate Change, 5*(1), 61–66.

Singh, S. H. I. P. R. A. (2018). Understanding the role of slope aspect in shaping the vegetation attributes and soil properties in montane ecosystems. *Tropical Ecology, 59*(3), 417–430.

Sillero, N., and Gonçalves-Seco, L. (2014). Spatial Structure Analysis of a Reptile Community with Airborne LiDAR Data. *International Journal of Geographical Information Science 28*(8): 1709–22. https://doi.org/10.1080/13658816.2014.902062

Shingleton, A. W., Mirth, C. K., and Bates, P. W. (2008). Developmental model of static allometry in holometabolous insects. *Proceedings of the Royal Society B: Biological Sciences, 275*(1645), 1875-1885.

Smart, H. J., and Gee, J. H. (1979). Coexistence and resource partitioning in two species of darters (Percidae), *Etheostoma nigrum* and *Percina maculata*. *Canadian Journal of Zoology, 57*(10), 2061–2071. https://doi.org/10.1139/z79-272

Streinzer, M., Huber, W., and Spaethe, J. (2016). Body size limits dim-light foraging activity in stingless bees (Apidae: Meliponini). *Journal of Comparative Physiology A, 202*, 643–655. https://doi.org/10.1007/s00359-016-1118-8

Tokeshi, M. (2009). *Species coexistence: Ecological and evolutionary perspectives.* John Wiley & Sons.

Valladares, F., Bastias, C. C., Godoy, O., Granda, E., and Escudero, A. (2015). Species coexistence in a changing world. *Frontiers in Plant Science, 6*, 866. https://doi.org/10.3389/fpls.2015.00866

Van Heerwaarden, B., and Sgrò, C. M. (2021). Male fertility thermal limits predict vulnerability to climate warming. *Nature Communications, 12*(1), 2214. https://doi.org/10.1038/s41467-021-22546-w

Verwaijen, D., Van Damme, R., and Herrel, A. (2002). Relationships between head size, bite force, prey handling efficiency and diet in two sympatric lacertid lizards. *Functional Ecology, 16*(6), 842–850. https://doi.org/10.1046/j.1365-2435.2002.00696.x

Walsh, B. S., Parratt, S. R., Hoffmann, A. A., Atkinson, D., Snook, R. R., Bretman, A., and Price, T. A. (2019). The impact of climate change on fertility. *Trends in Ecology & Evolution, 34*(3), 249-259. https://doi.org/10.1016/j.tree.2018.12.0022

Webber, Q. M., and McGuire, L. P. (2022). Heterothermy, body size, and locomotion as ecological predictors of migration in mammals. *Mammal Review, 52*(1), 82–95. https://doi.org/10.1111/mam.12263

Weil, S. S., Gallien, L., Nicolaï, M. P., Lavergne, S., Börger, L., and Allen, W. L. (2023). Body size and life history shape the historical biogeography of tetrapods. *Nature Ecology & Evolution, 7*(9), 1467–1479. https://doi.org/10.1038/s41559-023-02150-5

White, E. P., Ernest, S. M., Kerkhoff, A. J., and Enquist, B. J. (2007). Relationships between body size and abundance in ecology. *Trends in Ecology & Evolution, 22*(6), 323–330. https://doi.org/10.1016/j.tree.2007.03.007

Wojczynski, M. K., and Tiwari, H. K. (2008). Definition of phenotype. *Advances in genetics*, *60*, 75-105.

Woodward, G., Ebenman, B., Emmerson, M., Montoya, J. M., Olesen, J. M., Valido, A., and Warren, P. H. (2005). Body size in ecological networks. *Trends in Ecology & Evolution, 20*(7), 402–409. https://doi.org/10.1016/j.tree.2005.04.005

Chapter 2

Objectives and Thesis Structure

2.1. General objectives

The main goal of this thesis is to advance the understanding of size variation on species' phenotypic diversification, coexistence and vulnerability to global change through the following goals: 1) To evaluate the role of allometric effects in shaping morphological diversity through the analysis of macroevolutionary patterns of sexual differentiation; 2) To infer the functional and physiological effects of morphological variation, namely body size, through laboratory experiments in two model species; 3) To unravel coexistence and segregation mechanisms of two model species through a combination of laboratory and field approaches; 4) To assess the climate change vulnerability of model species through fine-tuning mechanistic models.

2.2. Thesis outline

This thesis is divided into seven chapters, as follows:

Chapter 1 provides a general introduction to the most relevant topics for this thesis, initially addressing the role of body size in phenotypic and ecological traits as a central axis in ecology and macroevolution, with an emphasis on Rensch's Rule. It then explores phenotypic diversification, niche segregation, and their connection to species coexistence and niche segregation. Finally, it offers a general overview of the vulnerability of ectotherms to climate change, with a particular focus on the application of mechanistic models.

Chapter 2 presents the main objectives and the thesis outline

Chapter 3 focuses on the relationship between intraspecific and evolutionary allometry, exploring how body size influences other traits within and between species. It investigates Rensch's Rule as a framework for understanding allometry and discusses the ecological and evolutionary implications of allometric relationships. As a study system it uses the green lizard clade of the genera *Timon* and *Lacerta*.

This research was published as:

- Reyes-Puig, C., Adams, D. C., Enriquez-Urzelai, U., and Kaliontzopoulou, A. (2023). Rensch's rule: linking intraspecific to evolutionary allometry. *Evolution*, *77*(12), 2576– 2589. https://doi.org/10.1093/evolut/qpad172

Chapter 4 explores the role of body size and other phenotypic traits in niche segregation and species coexistence using *Timon lepidus* and *Lacerta schreiberi* as model organisms. Through an integrated approach, it examines how morphology, functional performance, and ecophysiology contribute to niche segregation within a multidimensional context.

This research was published as:

- Reyes-Puig, C., Enriquez-Urzelai, U., Carretero, M. A., and Kaliontzopoulou, A. (2024). Is it all about size? Dismantling the integrated phenotype to understand species coexistence and niche segregation. *Functional Ecology*, *38*(11), 2350-2368. https://doi.org/10.1111/1365-2435.14646

Chapter 5 investigates niche differentiation in *T. lepidus* and *L. schreiberi* by combining field data on activity patterns, microhabitat use and environmental preferences. The study highlights the role of spatial and temporal niche segregation, as well as the influence of microclimatic conditions, in allowing species coexistence.

This research has been submitted as:

- Reyes-Puig, C., Enriquez-Urzelai, U., Sillero, N., and Kaliontzopoulou, A. (2025). Niche differentiation in coexisting species: ecological insights into the role of activity patterns, space use and environmental preferences. *Oecologia*, *in revision.*

Chapter 6 uses fine tune mechanistic models to assess how climate change affects the physiological responses and microhabitat use of *T. lepidus* and *L. schreiberi*. This chapter assesses changes in basking and foraging activity, water loss, times at preferred temperatures and shade requirements, as well as local distribution under future climate warming scenarios, highlighting the critical role of microhabitats in mediating heat and water stress.

This research will be submitted as:

- Reyes-Puig, C., Kaliontzopoulou, A., Sillero, N., and Enriquez-Urzelai, U. (2025). Microhabitats mediate the thermal and hydric challenges under climate change: a mechanistic perspective on similar yet distinct lizard species. *In preparation*.

Chapter 7 presents a general discussion of all the previous chapters covering the key findings of each one and the integration between all of them to answer the objectives of the thesis, as well as significant conclusions.

Chapter 3

Rensch’s rule: linking intraspecific to evolutionary allometry

3.1. Introduction

Sexual dimorphism (SD) refers to the difference in phenotypic traits between the sexes of a species (Casselman and Schulte-Hostedde, 2004; Ralls and Mesnick, 2009). One of the most conspicuous patterns of SD in animals relates to differences in body size, although many other traits, such as coloration, shape, sound, behavior, or appendage development, are also frequently dimorphic (Mori et al., 2017; Ralls and Mesnick, 2009). Sexual size dimorphism (SSD) is the pattern of significant differences in size between males and females of a species or population (Cox and Calsbeek, 2010; Fairbairn et al., 2007). SSD may vary in directionality, being expressed with the presence of larger males (male-biased) or larger females (female-biased). This directionality, as well as the magnitude of SSD, exhibits variation across taxa associated with differences in mating system, reproductive mode, or the fitness of a population (e.g., high fitness in larger males as a consequence of competitive behavior) (Blanckenhorn et al., 2007; Nali et al., 2014).

The study of evolutionary allometry can provide useful insights into the evolution of SD in size and other phenotypic traits. Evolutionary allometry describes variation in trait size concerning to body size across species or evolutionarily closely related groups (Figure 3.1; Gayon, 2000; Pélabon et al., 2014; Voje et al., 2014). Likewise, the degree of SD may vary across species or populations (Cox and Calsbeek, 2010; Tubaro and Bertelli, 2003). Such variation in the degree of dimorphism is often examined in light of its covariation with body size, and considerable attention has been devoted to determining whether there are allometric patterns of SSD in a macroevolutionary context (Dale et al., 2007; Fairbairn, 2005). Indeed, numerous studies have found that SSD increases with species body size in male-biased groups (Abouheif and Fairbairn, 1997; Fairbairn, 2005; Frýdlová and Frynta, 2010; Frynta et al., 2012; Rensch, 1959), while others have shown that it increases with species body size in female-biased groups (Jannot and Kerans, 2003; Peñalver- Alcázar et al., 2019), a trend known as Rensch's rule (RR) and its converse, respectively. RR proposes that "*the relative sexual difference is generally more important in larger species than in small species of the same kind of group*" (Rensch, 1950, 1959). Rensch (1950) examined the allometric relationship between male and female traits in several biological groups. His revisions concentrated on size dimorphism, but he also considered dimorphism in other traits (e.g., the head, brain, and eyes), and he proposed the "rule of proportioning" (Rensch, 1950, 1959). Currently, RR is defined as the increase or decrease in SD with body size in independent

male-biased or female-biased evolutionary groups, respectively (Abouheif and Fairbairn, 1997; Adams et al., 2020; Dale et al., 2007; Fairbairn, 2005).

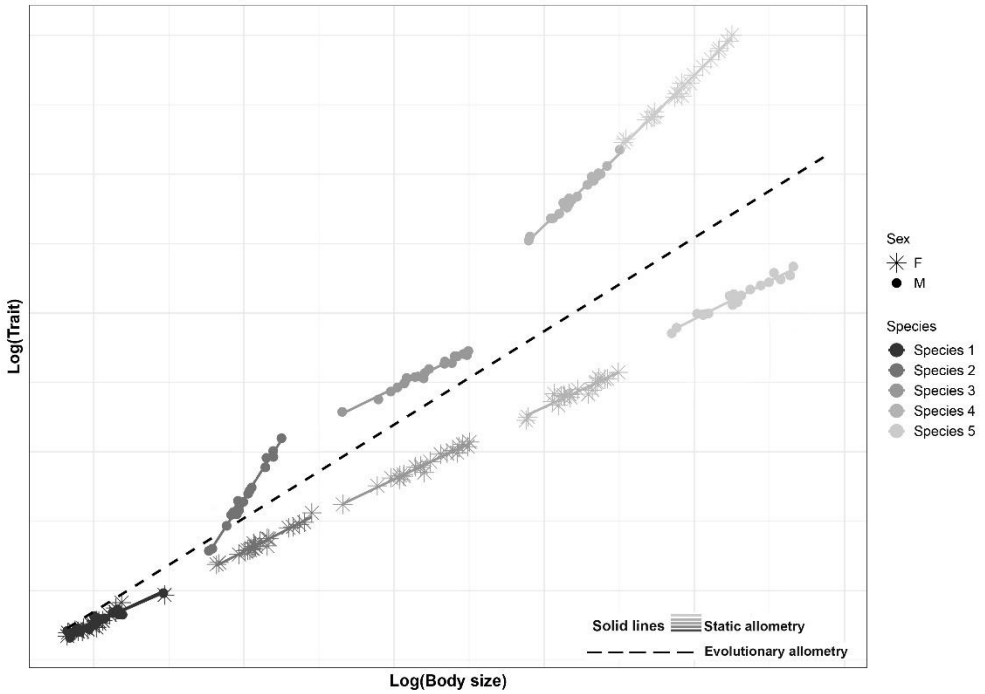

Figure 3.1 Hypothetical scenarios of sexual differentiation in static allometry within species and the emerging evolutionary allometric relationship. Reprinted with permission from Reyes-Puig, C. et al. (2023). Rensch's rule: linking intraspecific to evolutionary allometry. Evolution, 77(12), 2576–2589. © The Society for the Study of Evolution, published by Oxford University Press.

Several hypotheses have been proposed as possible evolutionary drivers of SSD and of the macroevolutionary allometric trends in its occurrence; namely, those that conform with RR and its converse (see Fairbairn, 1997). Of these, many are selection-based, where natural or sexual selection on one sex drives body size changes. For instance: (a) sexual selection favors positive evolutionary allometry in males (RR pattern) mainly when they show male-male competition and do not have displays with agility, so males do not have to exhibit attraction maneuvers for females (Cox et al., 2003; Dale et al., 2007; Fairbairn, 2005; Fairbairn et al., 2007; Szekely et al., 2004); (b) sexual selection may favor the decrease of body size in males if they exhibit displays with agility (i.e., converse RR), so the maneuverability in stunts is enhanced with smaller body size (Dale et al., 2007; Szekely et al., 2004); (c) natural selection may select for increased body sizes in females to produce large number of offspring, so that females present larger trunk lengths compared to males (i.e., converse RR) (Cox et al., 2003; Pincheira-Donoso and Hunt, 2017) or bodies of equal size as males (i.e., isometry for RR), depending on the balance with sexual selection also acting on males; (d) natural selection may act on the body size of one of the sexes and its relationship with the

surrounding habitat, favoring either larger males (RR pattern) or females (converse RR) (Cox, 1981; Pearson et al., 2002). Genetic-based hypotheses have also been explored, where there is evidence of greater phenotypic plasticity of body size in males compared to females (Fairbairn, 1997). Thus, these hypotheses (one of them or a combination thereof) could act on one of the sexes directionally, maintaining an RR pattern. However, sexual selection has been the most widely accepted and supported hypothesis for explaining RR and differences in the degree of SSD across taxa (Ceballos et al., 2013; Cox et al., 2003; Dale et al., 2007; Fairbairn, 2005; Fairbairn and Preziosi, 1994; Szekely et al., 2004). Some evidence suggests that, under sexual selection, female body size evolves in concert with male body size. If natural selection decreases for females, it could reverse this effect, leading to males stabilizing at a size balanced by sexual selection (Andersson, 1994; Fairbairn, 1997).

Complementary to evolutionary allometry, intraspecific allometry describes the rate of change between trait size and overall size in individuals of the same species at the same ontogenetic stage (i.e., static allometry), or throughout growth (i.e., ontogenetic allometry) (Eberhard et al., 2018; Freidline et al., 2015; Gould, 1966a, 2000; Pélabon et al., 2013). Variation in intraspecific allometry has been explored in several taxonomic groups, providing information regarding the potential association between allometric trends within and among species (Klingenberg and Zimmermann, 1992; Voje et al., 2014). For instance, differentiation between the sexes in static allometry has been frequently linked to sexual selection, and the evolvability of sexually selected traits with respect to body size has been the focal point for understanding morphological functionality (Eberhard et al., 2018). Here, positive static allometry has been interpreted as an indication of sexual selection. However, this will only occur if the combined influence of sexual and natural selection on the size of a trait and body size leads to a comparatively greater benefit of larger trait size in larger individuals (Bonduriansky and Day, 2003; Bonduriansky, 2007). Nonetheless, sexual selection is not the only explanation that may result in this pattern. Merely focusing on the selection of either the absolute or relative size of a trait in isolation is insufficient to generate a trait that exhibits positive allometry (Bertin and Fairbairn, 2007; Bonduriansky, 2007).

Given the shared research foci on how sexual and natural selection affect intraspecific and evolutionary trends of SD, investigating possible links between them seems paramount to better comprehend how the interplay between trait and body size coevolution shapes SD patterns. Some studies have analyzed the effects of intraspecific on evolutionary allometry, suggesting that the former acts mainly as a constraint to the

latter, possibly by shaping genetic lines of least resistance (Brombacher et al., 2017; Schluter, 1996; Tejero-Cicuéndez et al., 2022; Voje et al., 2022). However, this association between levels of allometry has been poorly explored from the perspective of SD evolution and the trend expressed as RR. This connection becomes particularly relevant when considering that RR may or may not occur in traits other than body size (Colleoni et al., 2014; Liang and Shi, 2017). Thus, both types of allometries (i.e., intraspecific and evolutionary) can occur in a clade, and investigating them in concert may provide insights into the mechanisms of selection operating within and across species (Firmat et al., 2014; Tejero-Cicuéndez et al., 2022; Voje et al., 2014).

From the perspective of understanding SD, we may characterize sexual differentiation within species in trait size–body size allometry expressed through linear relationships (on a log-log scale) (Figure 3.1). Here, the two sexes may exhibit the exact same allometric trend and no differences in their intercept and slope (e.g., species 1 in Figure 3.1). By contrast, there may be differences in both the intercept and the slope (species 4 and 5), in the intercept but not in the slope (species 3), or vice versa (species 2) (Figure 3.1). Then changes in these parameters could affect the evolutionary allometric slope in light of RR. The static or intraspecific slope, being one of the most studied parameters, has garnered significant attention from numerous researchers who have explored its relationship with species' size (Gould, 1966a; Voje and Hansen, 2013). Gould (1966a, b) suggested that larger species tend to exhibit shallower intraspecific slopes. However, subsequent investigations have yielded inconclusive results to find evidence supporting this relationship (Kawano, 2002; Voje and Hansen, 2013; Voje et al., 2013). Therefore, delving into the connections between intraspecific allometry and species size could also offer valuable insights into the effect of within-species allometric slope on the evolutionary slope in the context of SD.

Here we examined intraspecific and evolutionary allometry through the implementation of a series of computer simulations. We first used these simulations to establish when RR in body size is identified given different degrees of SSD. Then, we explored the interplay between intraspecific and evolutionary allometry of SD (RR) in a trait by simulating differences between the sexes in intraspecific slope and intercept and then assessing their effect on the evolutionary slope of RR. To illustrate how the results of the simulations can be reflected in a real-life example, we examined intraspecific and evolutionary allometry in several morphological traits in Mediterranean green lizards as an empirical case. First, we tested whether RR occurred in body size and in four other

morphological traits, and then we explored whether differences between the sexes in intraspecific allometric slope and intercept contributed to determining RR patterns.

3.2. Simulations

3.2.1. Methods

3.2.1.1. Rensch's rule in body size

To set up a hypothetical interspecific dataset that encompassed RR in body size, we performed a series of computational simulations across different degrees of SSD. For this, we first generated a pure-birth phylogenetic tree of 50 species and simulated mean values for the body size of females (Y_F) under a Brownian motion model of evolution. From these, we then obtained male body sizes (Y_M) through the allometric equation of Huxley (1924) and Huxley and Tessier (1936) as: $Y_M = \beta_0 Y_F^{\beta 1} + \varepsilon$, where β_1 is a uniform factor with value 1 + SSD and ε represents small random error drown from a normal distribution with $\mu = 0$ and $\sigma = 0.01$. We defined SSD to range from −0.05 to 0.05 in intervals of 0.001 to simulate different evolutionary patterns for SSD. These scenarios included an isometric relationship between Y_M and Y_F (i.e., a lack of RR) when SSD = 0 ($Y_M = Y_F$) and all species are monomorphic. On the other hand, our simulations encompassed male-biased SSD when SSD > 1 (e.g., when SSD = 0.05, $Y_M = Y_F^{1.05}$), and female-biased SSD when SSD < 1 (e.g., with SSD = −0.05, $Y_M = Y_F^{0.95}$).

Once female and male species means for body size were generated, we simulated body size for 50 individuals per sex, by drawing 50 random values from a normal distribution with a standard deviation of 0.1, around each of the species-mean elements (Y_F and Y_M). This provided a database containing simulated values of body size for 50 individuals per sex, for each of 50 species on a random phylogeny. These individual values were later used to explore the association between within-species allometric patterns and the emergence of RR in body traits other than body size. We repeated these simulations 1,000 times.

From each of these matrices of 5,000 individual male and female values for 50 species, we explored RR for body size. We first calculated means by sex and by lineage. Then, we performed a phylogenetic generalized least-squares regression (PGLS) between the SD ratio (i.e., $\log(Y_M/Y_F)$) and log-transformed species body size, following the equivalence between the later and the standard regression for testing for RR (Abouheif and Fairbairn, 1997) as shown by Adams et al. (2020) (see details in page 1911) and tested whether the slope of this regression was significantly different from 0 through a t-test.

3.2.1.2. Rensch's rule in other traits and linking intraspecific allometry to evolutionary allometry

We explored how the occurrence of RR in a trait other than body size is linked to its occurrence in body size and investigated whether variation in sexual differentiation of intraspecific allometric intercept and slope influences RR in the trait. To obtain simulated data expressing variation in a second trait, we used the empirically observed values of intercept and slope between a morphological trait (head size) and body size in our dataset of green lizards (see further on), ensuring realistic relationships that may allow us to abstract the results to an organism of interest. We ran a set of 1,000 trait simulations for each of the SSD variation scenarios previously considered: (a) isometry (no dimorphism in body size), (b) male-biased SSD, and (c) female-biased SSD. To evaluate the effect of sexual differentiation in intraspecific allometric intercepts on the emergence of RR in the trait, we kept the static slope of both sexes constant and generated trait values under variable intraspecific intercepts. Based on female and male body sizes simulated before (Y_F and Y_M), we generated trait values as $Z_F = \beta_0 * Y_F^{\beta 1} + \varepsilon$ and $Z_M = \beta_0' * Y_M^{\beta 1'} + \varepsilon$, where $\beta_0' = \beta_0 + ID$. Here, ID (intercept difference) is the simulated intercept difference between the sexes, ranging from −1 to 1 at intervals of 0.02 in our simulations, and ε random error $N(\mu = 0, \sigma = 0.001)$.

Similarly, to evaluate the effect of sexual differences in intraspecific allometric slope on the emergence of RR in the trait, we kept the intraspecific intercept (β_0) constant and generated traits with varying differences between the sexes in intraspecific slopes (β_1 for females and β_1' for males, with $\beta_1' = \beta_1 + SLD$), the slope difference (SLD) taking values between −1 and 1 (in intervals of 0.02). A matrix with 50 individuals per sex and species with two variables (i.e., body size and a second trait) was created for each value of simulated body size, ID, and SLD. To evaluate the effect of sexual differentiation in intraspecific allometric intercept and slope on RR we followed the same procedure mentioned above. To test whether RR was identifiable in the simulated trait, we first standardized individual trait values over body size (i.e., trait/ size). Then we calculated means by sex and lineage for the size-corrected, log-transformed trait values, and performed a PGLS regression in the same way as for body size (i.e., SD ratio ~ log(mean species size)).

Finally, to assess the stability of the simulation results with smaller sample sizes we performed a rarefaction analysis. For this, we chose 40, 30, 20, and 10 random

individuals of each sex from the 50 originally simulated individuals per lineage. Using these data, we ran the RR tests mentioned above with these sample sizes.

We performed all analyses in R (R Core Team, 2020) using the packages ape (Paradis et al., 2019), phytools (phytools. Revell, 2014), geiger (Harmon et al., 2015), RRPP (Collyer and Adams, 2018), and tidyverse (Wickham and Wickham, 2017).

3.2.2. Results

Based on the simulations of RR in body size we identified that RR emerges at SSD values greater than 0.025 in male-biased groups and lower than −0.025 in female-biased groups (Figure 3.2A–C; Appendix A Figure A1.1-A1.13). Importantly, this SSD value follows Huxley's allometric power law and therefore increases when species body size does. So, the minimum value for RR to be detected was |SSD| = 0.025. That is, if the increase in SSD was greater than 0.025, the slope resulted in a pattern of RR according to the regression of SD ratio on log mean species size ($\beta_1 > 0$). Conversely, for SSD values lower than −0.25 the converse RR pattern emerged ($\beta_1 < 0$; Figure 3.2; Appendix A Figure A1.1-A1.13).

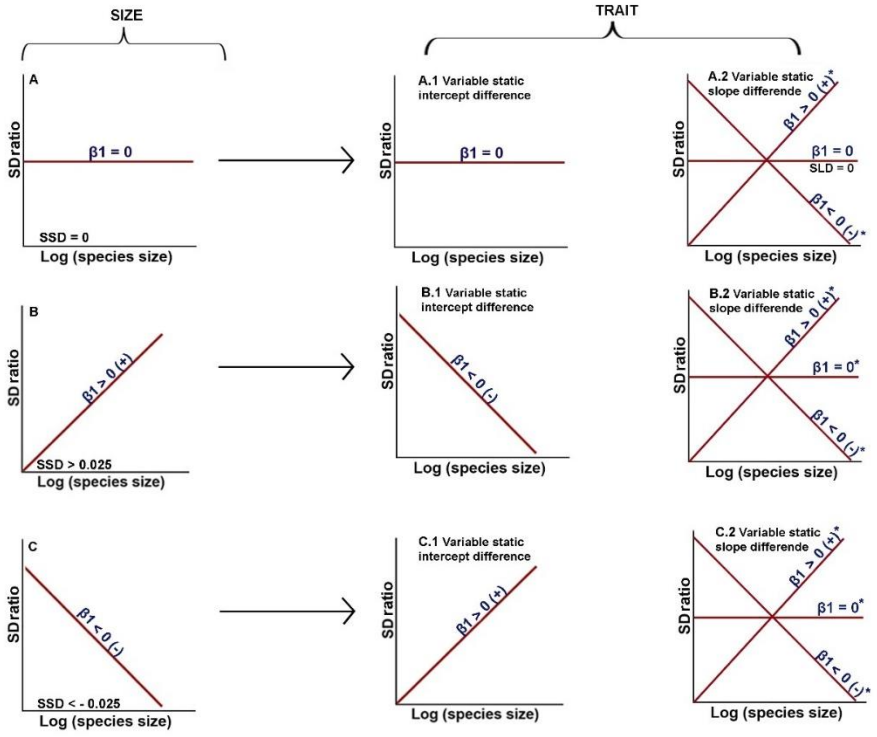

Figure 3.2 Summary of results obtained from RR test simulations, SD ratio = $\log(Y_M/Y_F)$ vs. log(mean species size), β_1: estimated evolutionary slope. RR pattern is equivalent to $\beta_1 > 0$, converse RR pattern is equivalent to $\beta_1 < 0$. (A) Isometric relationship of body size between males and females, so absence of RR in size. (B) Allometric relationship of body size between males and females following a male-biased pattern. (C) Allometric relationship of body size between males and females following a female-biased pattern. (A.1, B.1, C.1) RR simulations in trait with variable static intercept difference between sexes. (A.2, B.2, C.2) RR simulations in trait with variable static slope difference between sexes. *Asterisks

correspond to thresholds within the simulations, in which the static slope can stabilize its value with body size and the trait could lack RR. For details, see Appendix A Figure A1.1-A1.13. SLD = slope difference, so in scenario (A) lack of RR in the trait is due to no differences in the static slope. (+) means that the evolutionary slope of the regression is different from 0 and positive and (−) means that the evolutionary slope of the regression is different from 0 and negative. Reprinted with permission from Reyes-Puig, C. et al. (2023). Rensch's rule: linking intraspecific to evolutionary allometry. Evolution, 77(12), 2576–2589. © The Society for the Study of Evolution, published by Oxford University Press.

3.2.2.1. Rensch's rule in traits when there is no SSD

The simulations conducted to examine how RR in body size and sexual differences in intraspecific allometry influence the occurrence of RR in other traits showed that, in the absence of RR in body size (i.e., $\beta_1 = 0$), intercept differences between the sexes do not affect RR in the trait. Thus, the RR pattern in the trait would resemble that observed for body size regardless of any sexual variation in intraspecific allometric intercept (Figure 3.2A.1). Instead, it is possible to observe RR in a trait other than body size if there are differences between the sexes in intraspecific allometric slope (Figure 3.2A.2; Appendix A Table A1.1). If the slope difference is negative (i.e., the trait slope is steeper in females than in males), RR could be observed (that is, in female-biased groups SD decreases as the species body size increases); if the slope difference is positive then converse RR would be detected. If no differences exist in the intraspecific slope, RR is not observed in the trait (Figure 3.2A.2).

3.2.2.2. Rensch's rule in traits when there is SSD and RR in body size ($\beta_1 > 0$) and converse of RR ($\beta_1 < 0$)

Simulations introducing variation in intraspecific intercept difference show the inverse pattern of RR than that observed in body size. That is, for trait data simulated on a pattern of body size RR under varying values of intercept differentiation between the sexes, the resulting value of the allometric evolutionary slope for RR for the trait is the inverse of that observed for body size (Figure 3.2B.1 and C.1; Appendix A Figure A1.4-1.6). Complicating things further, if a difference in static slope between the sexes is introduced when simulating trait variation, both RR and the converse of RR may appear, and also the lack of RR ($\beta_1 = 0$) in the trait (Figure 3.2B.2 and C.2; Appendix A Figure 1.6 and 1.7). It is important to mention that based on our simulations the static intercept difference alone has little effect on the expression of RR (when the static slope is uniform between the sexes).

Finally, the rarefaction procedures showed that the patterns and trends of RR were the same as those mentioned above, even with sample sizes as low as 10–20 individuals per sex per lineage (Appendix A Figure 1.8-1.13). However, as expected, the variance increased with smaller sample sizes.

3.3. Real-life empirical example

3.3.1. Methods

To explore how the aforementioned links between intraspecific sexual differentiation in allometric trajectories and evolutionary allometry of SD (i.e., Rench's rule) may occur and be interpreted in a real-life situation, we explored their occurrence in several body traits in a group of Mediterranean green lizards. Green lizards of the genera *Timon* and *Lacerta* (Squamata: Lacertidae) represent a monophyletic clade of species distributed in a variety of ecosystems and habitats in the Mediterranean basin (Ahmadzadeh et al., 2016; Verwaijen and Van Damme, 2007). They exhibit a remarkable diversity of body sizes and the relative size of other morphological traits (e.g., head size) between species (Enriquez-Urzelai et al., 2022), as well as between sexes of the same species (Adams et al., 2020; Arnold et al., 2007; Braña, 1996). Together, these features make them an excellent model system for linking micro- and macroevolutionary patterns of static vs. evolutionary allometry in the context of SD and RR.

We examined 1,097 preserved individuals from 24 lineages of green lizards from natural history museum collections (see Acknowledgments of Reyes-Puig et al., 2023), an initial dataset that fully overlapped that of Adams et al. (2020). We based our taxon sampling on a phylogenetic criterion, and we considered each lineage as an independent and divergent group, so we used the same criteria as Adams et al. (2020) and Enriquez-Urzelai et al. (2022). To avoid any effects of growth and because our objectives are not related to ontogenetic allometry, all measured individuals were adults, whereas juveniles and neonates were excluded from data collection. The specimens measured were chosen to adequately cover morphological variation across the distribution range of each lineage. To take into account variation in traits that exhibit SD in adult individuals and to avoid sampling bias due to unequal sample size in each lineage, we selected the 15 largest individuals per sex and lineage. This decision is based (a) on the fact that the samples were obtained from scientific collections of natural history museums, therefore, larger individuals have less preservation effects and measurements can be easily taken, (b) our study is focused on SD and body size, so we assume that larger individuals represent more visible and more expressive maturation features, and (c) to reduce the bias introduced by non-random sampling, this is an approach to standardize the sampling. In addition, similar approaches have been proposed for comparative studies (Martínez-Gil et al., 2022; Stamps and Andrews, 1992). Lineages with a small sample size ($n < 10$) were removed from analyses (i.e., *Lacerta boemica*, *Lacerta bosnica*, *Lacerta ciliciensis*, *Lacerta guentherpetersi*, and *Lacerta pamphylica*). This provided a

final database of 515 individuals from 19 lineages. A set of linear measurements were taken on each individual with a digital caliper, rounded to the nearest 0.01 mm, always recorded by the same observer to reduce measurement error. These measurements were: (a) snout to vent length, SVL, as a proxy for body size; (b) trunk length, TRL; (c) head length, HL; (d) head width, HL; (e) head height, HH; (f) forelimb length, FLL; and (g) hindlimb length, HLL (Figure 3.3). To summarize head size (HS), we calculated the geometric mean of HL, HW, and HH, so finally we analyzed five traits: SVL, TRL, HS, FLL, and HLL.

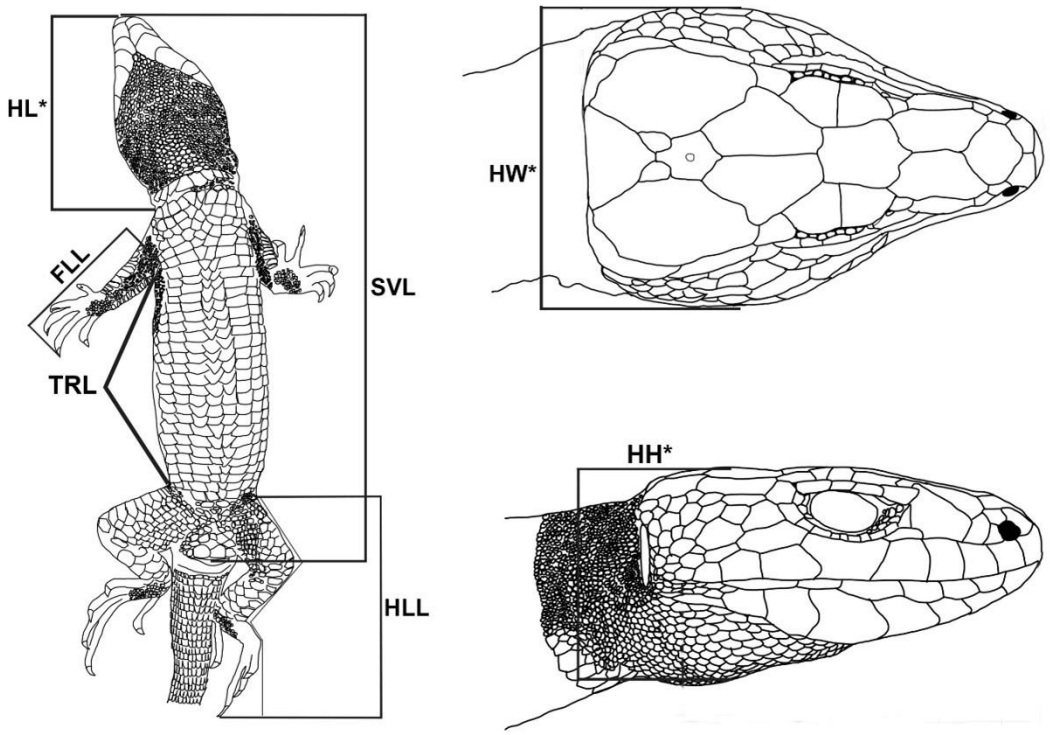

Figure 3.3 Linear measurements used to assess static allometry and RR in shape in green lizards. *Measurements used to calculate head size. Reprinted with permission from Reyes-Puig, C. et al. (2023). Rensch's rule: linking intraspecific to evolutionary allometry. Evolution, 77(12), 2576–2589. © The Society for the Study of Evolution, published by Oxford University Press.

3.3.1.1. Intraspecific and evolutionary (Rensch's rule) allometry

To examine the variation in static allometric relationships between trait size (TRL, HS, FLL, and HLL) and body size (SVL), and test whether allometric slopes and intercepts varied between the sexes and across lineages, we fit general linear models (GLMs) between each linear measurement and body size (all log-transformed). We also included sex, lineage, and all interactions in GLMs. We performed analysis of variance

tests on those models to determine whether males and females differed in their allometric slopes and intercepts and whether the degree of sexual differentiation in allometric parameters varied evolutionarily (i.e., across lineages), as can be inferred through the interaction terms of the aforementioned models. Next, to quantify the amount of allometric differentiation between the sexes in each individual lineage, we fit separate within-lineage GLMs including body size and sex to explain variation in body size. From these models, we extracted the difference in static allometric slopes and intercepts between sexes to subsequently link intraspecific allometries with RR (see further on).

To perform all analyses across lineages accounting for evolutionary relationships, we used the updated green lizard phylogeny presented in Adams et al. (2020), which included all 24 initial lineages mentioned above. We calculated the mean of each morphological trait by lineage and sex. In addition, to consider the effect of body size on the other traits, we standardized these measurements as Y/SVL (following Mosimann, 1970). With these values, we evaluated whether RR occurred in body size and the other four size-standardized traits. For this, we first performed a PGLS between the SD ratio (i.e., $\log(Y_M/Y_F)$) and log-transformed species body size, following the same reasoning of the simulations explained above. This procedure was implemented for both body size dimorphism and dimorphism in size-corrected traits. Then, we used a PGLS to test whether the difference in static (i.e., intraspecific) allometric slopes and intercepts between males and females had an effect on the general pattern of RR. For this, we included the difference between the sexes in static slopes (slope_diff) and intercepts (intercept_diff) for each lineage extracted from the previous within-species allometry analyses (see above) together with average lineage body size in the model used to evaluate RR. Because the contribution of the parameters to trait variance is not additive (Voje et al., 2014), one has to consider all interaction terms to link them in an evolutionary context. Thus, we evaluated the model: $\log(Y_M/Y_F)$ ~ log(species size) * slope_diff * intercept_diff | phylo. This allowed us to investigate how sexual differences in body size, allometric intercept, and allometric slope may conjointly determine evolutionary patterns of RR-in traits other than body size.

We also included a static allometry approach in which we considered two levels: the difference in static allometry between the sexes and the static allometry per species. So, the difference in slope and static intercept (as mentioned in the model above) and the slope and static intercept of the species (including males and females in the same dataset). To relate these parameters to species sizes, we performed a PGLS with the following models: slope_diff ~ log(species size) | phylo, intercept_diff ~ log(species size)

| phylo, species_static_slope ~ log(species size) | phylo, and species_static_intercept ~ log(species size) | phylo.

As the simulations showed that the static allometric slope is a key factor influencing RR we performed a rarefaction analysis on empirical data with a sample size of 10 individuals per sex per lineage to evaluate if the estimates of the static allometric slopes and their effect on the emergence of RR change considerably if smaller sample sizes are used. With this data, we estimated the static allometric intercept and slope and their contribution to the evolutionary allometry of RR.

We evaluated the significance of all models using RRPP (Collyer and Adams, 2018) and 1,000 permutations.

3.3.2. Results

3.3.2.1. Intraspecific allometry

We found significant effects of body size, sex, and lineage on explaining variation in all investigated morphological traits (Appendix A Table A1.1). The interactions of body size and lineage, and body size and sex, were significant for all traits except for forelimb length, so static allometric slopes varied significantly across species and between the sexes (Appendix A Table A1.1). By contrast, the three-way interaction between body size, sex, and lineage was not significant for any trait, suggesting that sexual differences in allometric slopes were similar across lineages. As a general trend, we detected that, in all analyzed traits, species of larger body sizes (*Timon* species) exhibited smaller intercept differences between the sexes, while the opposite was true for smaller species (*Lacerta* species) (Figure 3.4). The examination of static allometries unveiled contrasting patterns of allometric slope variation between different body traits and body size. When examining the relationship between trunk length and body size, larger species generally presented flatter slopes than smaller species (Figure 3.5). By contrast, for head size the static allometric slopes tended to be steeper for larger than for smaller species (Figure 3.5).

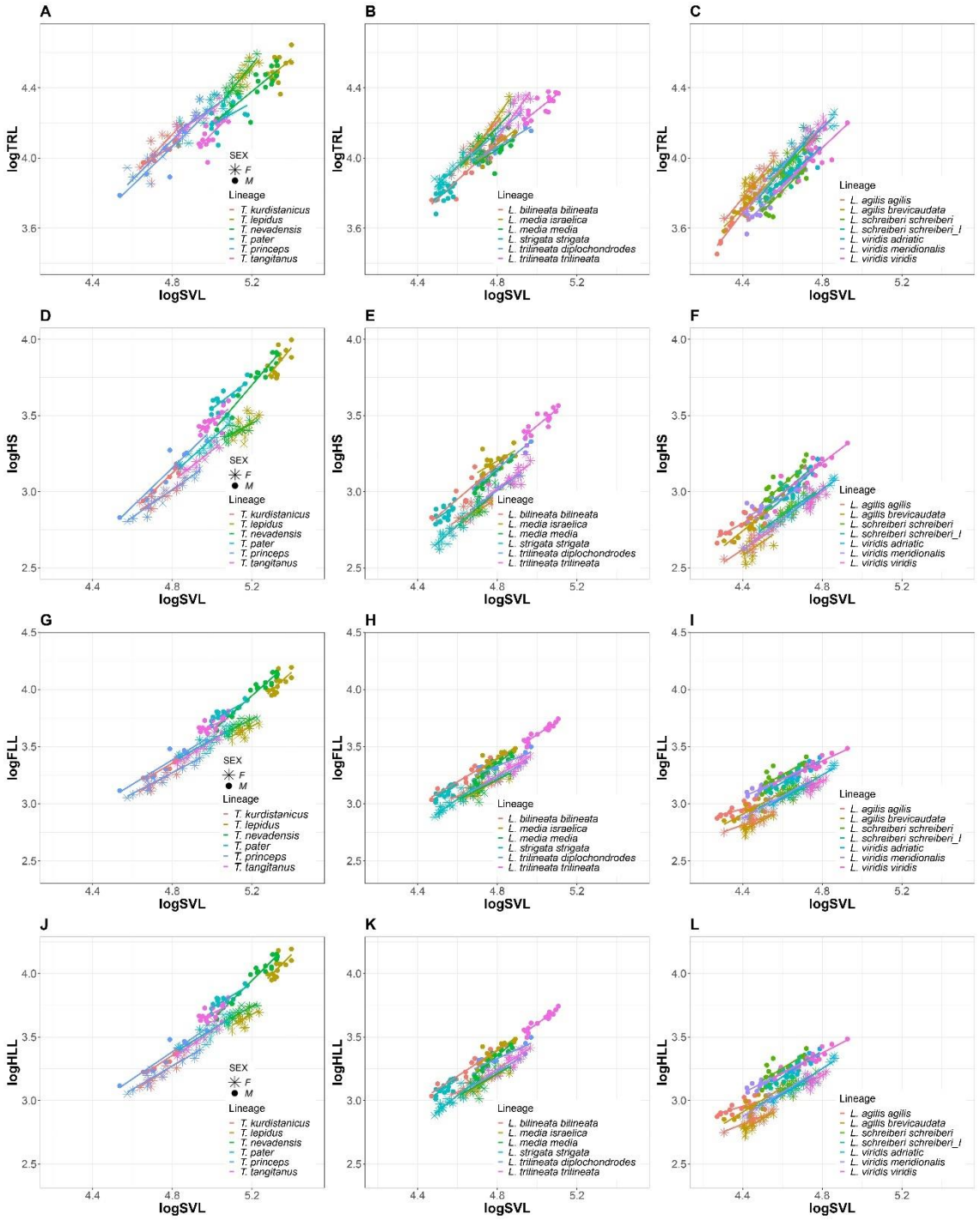

Figure 3.4 Static allometries of studied morphological traits with body size (SVL) within green lizard species. (A)–(C) Trunk length; (D)–(F) head size; (G)–(I) forelimb length; and (J)–(L) hindlimb length. Reprinted with permission from Reyes-Puig, C. et al. (2023). Rensch's rule: linking intraspecific to evolutionary allometry. Evolution, 77(12), 2576–2589. © The Society for the Study of Evolution, published by Oxford University Press.

When evaluating SD in static allometries within each species separately, trunk length only exhibited significant differences in allometric slopes between sexes in *Lacerta media israelica* ($F = 8.608$, $Z = 2.248$, $p = .008$) and *Lacerta trilineata trilineata* ($F = 5.817$, $Z = 1.856$, $p = .032$) (Appendix A Table A1.2-A1.7; Figure 3.4A). For head size only

Timon nevadensis (F = 13.226, Z = 2.637, p = .003) and *Timon princeps* (F = 4.350, Z = 1.592, p = .046) showed sexual differences in allometric slopes (Figure 3.4D; Appendix A Table A1.2-A1.7). On the other hand, all lineages presented significant differences between the sexes in allometric intercepts (details of the individual statistics of each trait per species can be found in Appendix A Table A1.2-A1.7). In addition to differences in trait size caused by sexual differences in intercepts, some species also exhibited sexual differences in body size which further amplified sexual trait differentiation. This is, for example, the case in *Timon lepidus* (Figure 3.4D, G, and J) and *L. trilineata trilineata* (Figure 3.4E, H, and K; Appendix A Table A1.2 and A1.3).

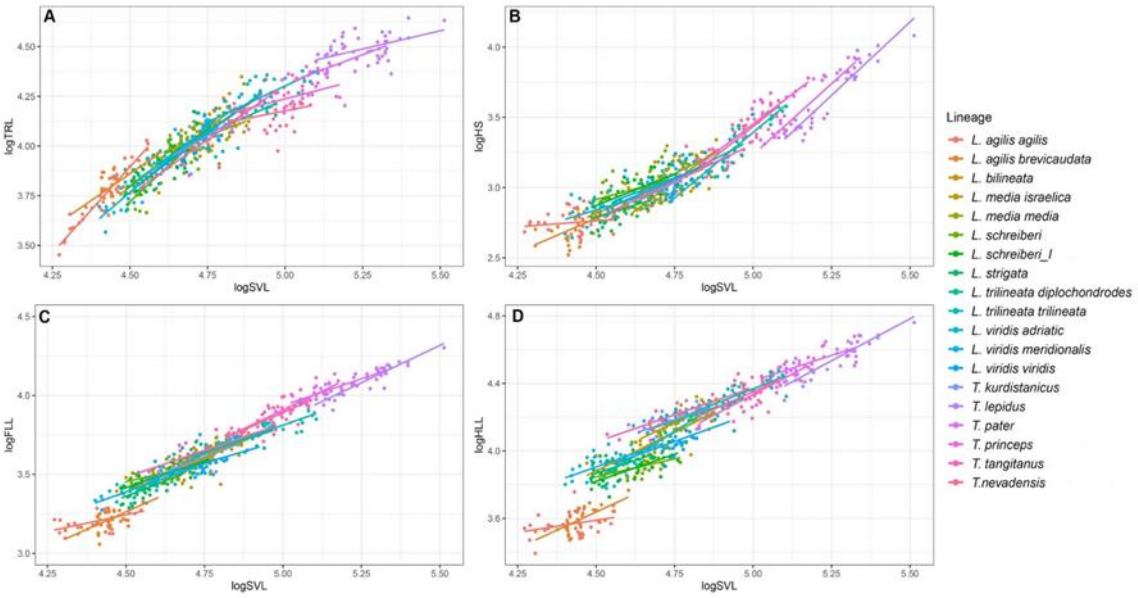

Figure 3.5 Allometric relationships between each of studied morphological traits and body size (SVL) in green lizards, without talking allometric differences between the sexes into account, used to visualize general tendencies of slope variation across species (but see main results for the supported statistical models). A. trunk length; B. head size; C. forelimb length; D. hindlimb length. Reprinted with permission from Reyes-Puig, C. et al. (2023). Rensch's rule: linking intraspecific to evolutionary allometry. Evolution, 77(12), 2576–2589. © The Society for the Study of Evolution, published by Oxford University Press.

3.3.2.2. Evolutionary allometry (Rensch's rule)

Tests for RR revealed that the body size of males and females varied in a congruent way with this macroevolutionary pattern (SD ratio ~ mean species size, F = 20.222, p < .001) (Table 3.1; Figure 3.6). Regarding tests for RR in other body traits, we found a significant relationship between the SD ratio of head size and mean species size, a pattern consistent with RR (Table 3.1; Figure 3.6). We did not find a significant relationship between the SD ratio of trunk length and mean species size. SD ratio of hindlimb length and forelimb length exhibited the converse pattern of RR with negative slope values different from 0 (Table 3.1; Figure 3.6).

Table 3.1 Statistics of tests for Rensch's rule with sexual dimorphism ratio (SD ratio) approach. β_1: estimated allometric slope, SE: standard error of the slope estimate, t and p value: corresponding t and p values of significance testing for slope estimates ($\beta_1 \neq 0$). Significant patterns (using a threshold of $\alpha = 0.05$) are highlighted with asterisks.

Trait	β	SE	*t* value	*p* value
SVL	0.29	0.064	4.478	**<0.001*** **
TRL	0.044	0.067	0.663	0.52
HS	0.194	0.069	2.794	**<0.05***
FLL	−0.065	0.016	−3.946	**<0.05***
HLL	−0.125	0.038	−3.298	**<0.05***

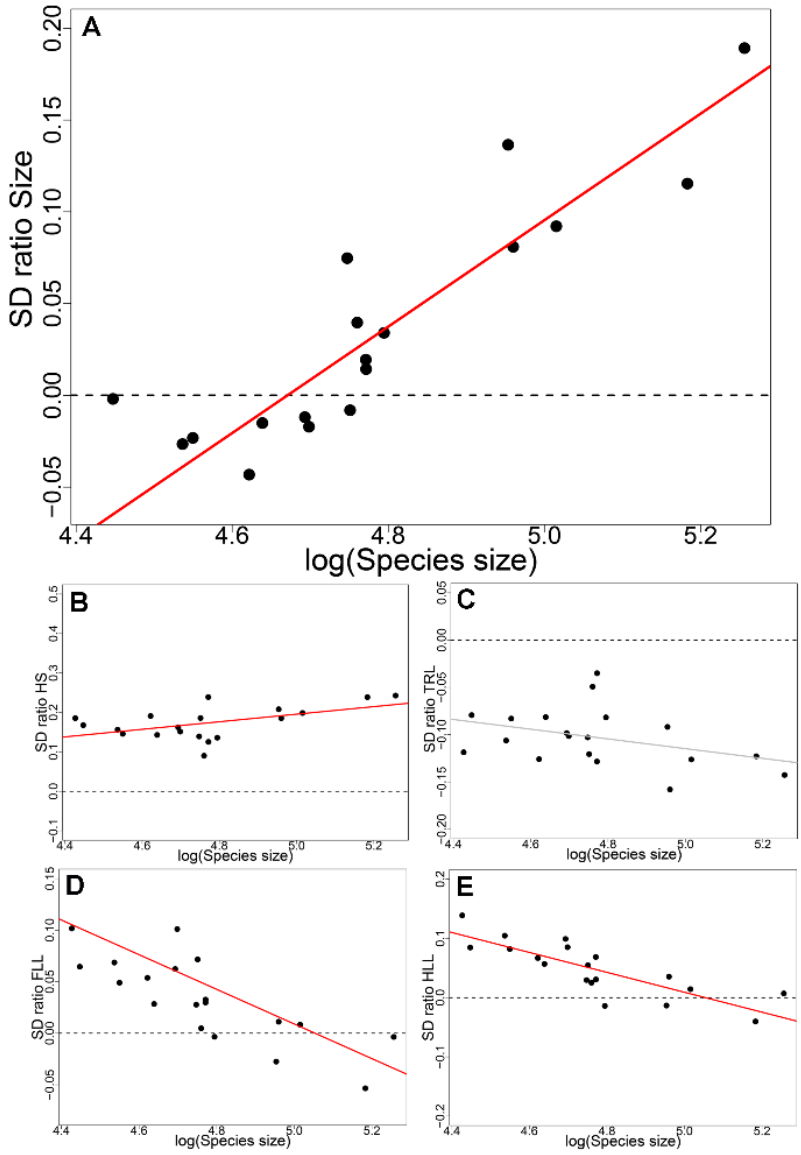

Figure 3.6 Rensch's rule (RR) pattern for five morphological traits in green lizards. (A) Body size (SVL); (B) head size; (C) trunk length; (D) forelimb length; and (E) hindlimb length. The gray line (in C) represents a non-significant relationship, and the dashed line depicts isometry (lack of RR). Reprinted with permission from Reyes-Puig, C. et al. (2023). Rensch's rule: linking intraspecific to evolutionary allometry. Evolution, 77(12), 2576–2589. © The Society for the Study of Evolution, published by Oxford University Press.

3.3.2.3. Contribution of intraspecific allometry to Rensch's rule

The degree of sexual differentiation in static allometric slopes contributed to explaining RR for most traits (Table 3.2). The interaction between static allometric intercept, slope, and body size had a significant effect on the display of the converse pattern of RR in forelimb length (Table 3.2). In general, static intercepts had no effect on evolutionary allometry (RR) in other traits. Rarefaction analysis with the smaller dataset showed the same trends as the main dataset, including the influence of the static allometric slope on the RR pattern (Appendix A Table A1.6 and A1.7). In this dataset the results of trunk length were the only ones that varied, showing a significant negative relationship between trunk length and mean species size (i.e., converse RR) (Appendix A Table A1.7).

Table 3.2 Analysis of variance (ANOVA) table for the linear model used to test for the effect of intersexual differences in static allometric intercept and slope on the trait Rensch's rule pattern with the SD ratio approach. β_1: estimated allometric slope, β_0: estimated allometric intercept. Interaction factors of the model are depicted with an asterisk. *F* value and *p* values of significance. Significant patterns (using a threshold of $\alpha = 0.05$) are highlighted with bold asterisks.

SD ratio	**TRL**		**HS**		**FLL**		**HLL**	
Source of variation	***F* value**	***p* value**	***F* value**	***p* value**	***F* value**	***p* value**	***F* value**	***p* value**
(Intercept)	51.395	**<0.001*** **	397.2168	**<0.001*****	17.45	**0.001***	9.91	**<0.05***
Species size (SVL)	0.638	0.441	58.354	**<0.001*****	100.669	**<0.001*****	42.164	**<0.001*****
β_1	2.313	0.156	14.478	**<0.05***	22.131	**<0.001*****	0.015	0.903
β_0	10.159	**<0.05***	5.628	0.037	0.704	0.419	0.175	0.686
sp.sz* β_1	24.388	**<0.001*** **	212.966	**<0.001*****	138.146	**<0.001*****	44.083	**<0.001*****
sp.sz* β_0	0.635	0.442	0.998	0.339	0.014	0.906	0.629	0.444
β_0* β_1	5.065	**<0.05***	5.041	**<0.05***	8.825	0.127	2.546	0.138
sp.sz* β_0* β_1	0.264	0.617	0.448	0.516	34.15	**<0.001*****	0.0001	0.992

The species static allometric slope and intercept showed a highly significant relationship with mean species size in all traits. Specifically, the static allometric slope increased and the static allometric intercept decreased for head size as the mean species size increased (Figure 3.7; Appendix A Figure A1.1 and A1.2). By contrast, for trunk length, as mean species size increased its static allometric slope decreased and static allometric intercept increased (Figure 3.7; Appendix A Figure A1.3 and A1.4). Static allometric slopes and intercepts alone had no relationship with mean species size for hindlimb length and forelimb length (Appendix A Figure A1.5-A1.8). However, when

we considered the interaction of the static intercept with the static allometric slope we did detect a highly significant positive relationship between the static allometric slope and mean species size (Figure 3.7; Appendix A Figure A1.9 and A1.10). We found the same pattern when analyzing the static slope and intercept difference against body size, although p values for regression significance ranged from 0.06 to 0.07. Thus, we found a significant relationship between the species static allometry and mean species size rather than with the difference of static intercepts and slopes between the sexes (i.e., intercept_diff and slope_diff) (Appendix A Figure A1.1-A1.13).

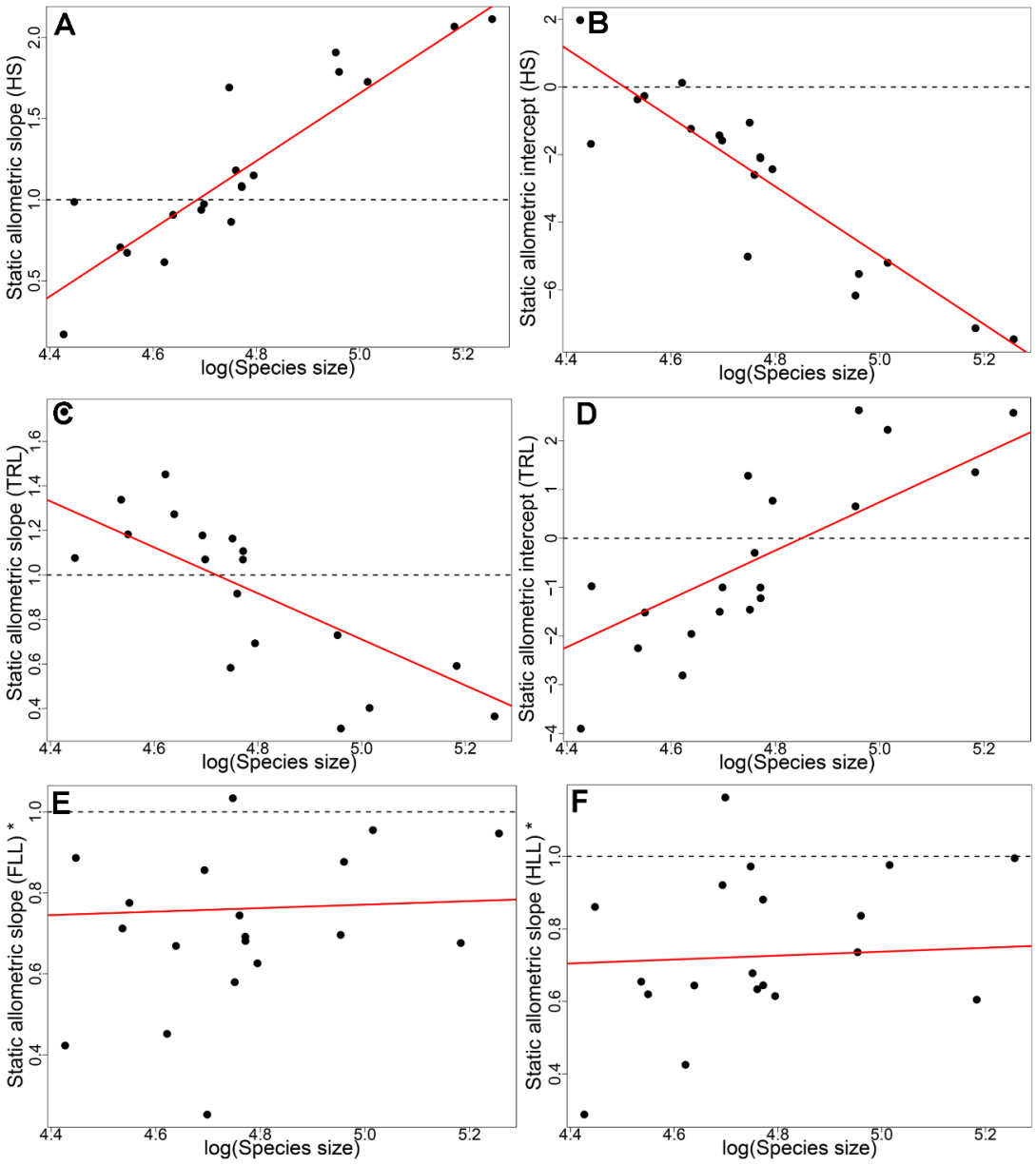

Figure 3.7 Relationship between static allometric parameters and mean species size in green lizards. (A) Slope vs. size in head size (HS). (B) Intercept vs. size in HS. (C) Slope vs. size in trunk length (TRL). (D) Intercept vs. size in TRL. (E) Slope vs. size in forelimb length (FLL). (F) Slope vs. size in hindlimb length (HLL). The asterisk represents the interaction with the static allometric intercept in the model for FLL and HLL. Reprinted with permission from Reyes-Puig, C. et al.

(2023). Rensch's rule: linking intraspecific to evolutionary allometry. Evolution, 77(12), 2576–2589. © The Society for the Study of Evolution, published by Oxford University Press.

3.4. Discussion

Two of the most common phenotypic patterns are changes in trait values that scale with body size (allometry), and systematic differences between the sexes (SD) (Mori et al., 2017; Ralls and Mesnick, 2009). At macroevolutionary scales, SD may also display allometric variation, that is, systematic differences across species of different sizes, a pattern known as Rensch's rule. Interestingly, how intraspecific allometry relates to macroevolutionary trends of SD allometry had not been previously investigated. We filled this gap through a thorough exploration of the links between sexual differentiation in intraspecific trait allometry and evolutionary allometry of SD (RR) using computer simulations and examined a real-life example considering several morphological traits in empirical data. Through computer simulations, we found that RR and converse RR can emerge in a trait depending on whether there are differences in intraspecific allometric slope but not intercept, between the sexes. In the empirical data, we found that intraspecific allometry varies considerably in Mediterranean green lizards, mainly depending on the body size of the species. Furthermore, we detected RR patterns that varied across traits, following the classic pattern of positive evolutionary allometry in body and head size, but the converse RR pattern in limb length. Our results provide several important insights for the study of allometric effects on SD across levels of biological organization.

The thorough simulations conducted here highlighted the importance of the intraspecific allometric slope in shaping evolutionary trends of SD allometry (i.e., RR). Indeed, we identified that sexual differences in static allometric slopes affect RR in a second trait, under different scenarios for RR in body size. Indeed, our simulations revealed that RR may occur in the trait if intraspecific slopes differ between the sexes, even if RR does not occur in body size. In the absence of body size RR, the emerging pattern of RR in a second trait (i.e., following the classic definition of the rule or its converse) will mainly depend on the differences in intraspecific slope between the sexes: if the difference in slope between the sexes is simulated as positive (i.e., the largest sex exhibits also higher intraspecific allometric slope), then the classical RR pattern will occur in the trait. Instead, if the difference in allometric slope between the sexes is negative (i.e., the largest sex exhibits a shallower slope) a reverse RR pattern will be observed. When there is RR or its converse in body size, the pattern may or may not be maintained for a second trait. For instance, slope differences between the sexes may cancel out the

effects of body size causing the RR pattern to disappear in the trait (Appendix A Table 1.1): This is exactly what we can see in the case of trunk length in the empirical example (see Tables 3.1 and 3.2).

In this context, we found that body size and head size followed RR, and the limbs followed its converse in green lizards of the genera *Timon* and *Lacerta*. Linking the simulations with the empirical example, we detected that a trait can also exhibit RR or its converse and that this pattern can be affected by the static allometric slope (Figure 3.2). The traits in which we detected RR (i.e., head size) and its converse (i.e., forelimb length and hindlimb length) suggest that the static slope difference between the sexes acted as an interaction fac- tor for the emergence of RR in that trait (Table 3.2), an example consistent with our simulations (Figure 3.2). We identified a significant relationship between static slope and mean species size. So, from an RR perspective, our results suggest that the effect of larger species exhibiting steeper static slopes shapes this macroevolutionary pattern and its converse trend. That is, species with larger body sizes tend to exhibit either amplification or reduction of the phenotypic characteristic through the static slope (Figure 3.7), resulting in positive or negative evolutionary allometry between the SD ratio and mean species size in that particular trait (Figure 3.6). The outcome of this combination is the classical RR pattern in some traits, such as head size, or its converse in others, such as limb length, or pattern elimination, as is the case for trunk length. All these scenarios are possible and consistent with our simulations (Figure 3.2).

It is important to note that these, as any, simulations are framed in a hypothetical scenario where the intraspecific slope varies between the sexes while the intercept remains constant and vice versa, which may differ somewhat from biological reality (Voje and Hansen, 2013). However, they provide insights into the relative importance of these two parameters, showing that sexual differences in intraspecific allometric slope are the main source of variation in the occurrence of RR and its converse. Further simulations encompassing additional parameters, such as the covariation of intraspecific allometric slope and intercept, or variation in body size SD, may help to better understand how all these intraspecific parameters inter- act to shape evolutionary allometry of SD in traits other than body size. Other authors have highlighted the importance of the intraspecific allometric slope and its effect on evolutionary allometry in contexts other than SD evolution (Cheverud, 1982; Pélabon et al., 2014; Voje et al., 2022), although some results are inconclusive. For example, Voje et al. (2022) found a strong relationship between static and evolutionary allometry for certain traits and not for others, suggesting

that this relationship depends on strong selection over ancient times. Although we found through simulations that sexual differences in intraspecific slope are related to RR, it is important to consider that, evolutionarily, the intraspecific allometric slope is considered a constraint for evolutionary allometry (Pélabon et al., 2014). As such, strong selection may limit the evolutionary potential of intraspecific slopes (Pélabon et al., 2014; Voje et al., 2022), but there is still a lack of available data in this regard.

Following our empirical case and to exemplify the results obtained in the simulations, most species of green lizards exhibited similar static allometric slopes between the sexes except for certain species in some traits (e.g., *L. trilineata trilineata* in trunk length and *T. nevadensis* in head size). This contrasts with the results of Voje and Hansen (2013), who found that static allometric slopes of eye span differed between the sexes in 60% of the species of stalk-eyed flies. Such discordance could be due to the fact that closely related species tend to retain the ancestral static allometric slopes, which have been reported to be evolvable over at least 2-million-year time scales (Pélabon et al., 2014; Voje and Hansen, 2013; Voje et al., 2014). On the other hand, our findings coincide with those of Voje and Hansen (2013) in that static allometric intercepts differed between the sexes in more than 90% of the species studied. This reinforces the observation that evolutionary changes in the static allometric intercept are probably faster than changes in the static slope (Hansen and Houle, 2008; Pélabon et al., 2014). Along the same lines, results regarding the evolution of allometric trajectories across different scales seem to lend support to the constraint hypothesis, which holds that the evolution of morphological characters is more constrained within than across species and that evolutionary allometries are limited by static allometries so that both should be similar (Hansen and Houle, 2008; Pélabon et al., 2014; Voje et al., 2014).

Strikingly, variation in static allometric slopes follows a pattern related to species' body size. This relationship has already been referred to as Gould's hypothesis (Gould, 1966a, b; Voje and Hansen, 2013), where shallower allometric slopes in larger species would prevent anatomically non-functional trait sizes. Indeed, our analyses showed that variation in trait static allometric slopes is tightly linked to species' body size (Figure 3.7; Appendix A Figure A1.9 and A1.10). For trunk length, we found shallower static allometric slopes with increasing body size. Instead, for head size, forelimb length, and hindlimb length the relationship was inverse, that is, the larger the species body size, the steeper the static slope (Figure 3.7; Appendix A Figure A1.9 and A1.10). However, our findings for fore- and hind-limb lengths showed that the association between static slope and body size was only significant if the interaction of the static intercept was also

considered as a factor within the model. This reinforces the importance of considering both allometric parameters in concert, as the intercept is mathematically dependent on the slope (Anzai et al., 2017). As such, important patterns might be missed when examining a single parameter in isolation, whereas identifying significant effects of explanatory variables becomes more efficient by considering both parameters together. In a sexual selection context, several authors have detected that allometric slopes are evolvable at macroevolutionary scales and that mainly species that have sexual selection toward specific traits can evolve steeper slopes (Voje and Hansen, 2013; Voje et al., 2014; Pélabon et al., 2014; Voje et al., 2022).

Our simulation and empirical results allowed us to confirm that the main source of contribution for RR is the static allometric slope and, in some cases, its interaction with the static intercept. Trying to understand the two levels of allometry—within and between species—and their relationship is complex and the theoretical framework does not yield a straightforward answer as to whether allometry is adaptive or not (Ganyon, 2000). However, the available information suggests that allometric static slopes play an important role in the evolution of traits (Pélabon et al., 2014; Voje and Hansen, 2013; Voje et al., 2014; Voje et al., 2022), although their evolvability might be slower than that of static intercepts (Pélabon et al., 2014; Voje et al., 2014). Furthermore, if static allometric slopes evolve, it is mainly due to selective pressure on sexually selected traits (Voje and Hansen, 2013).

Our study stands out as one of the few investigations that not only focus on examining RR in body size but also extends its exploration to other traits. Since the work of Abouheif and Fairbairn (1997) assessments of RR have mainly focused on body size (Blanckenhorn et al., 2007; Ceballos et al., 2013; Frýdlová and Frynta, 2010; Liang et al., 2021; Remeš and SzéKely, 2010) and not on other traits as initially examined by Rensch himself (1950, 1959), with a few remarkable exceptions (Adams et al., 2020; Bidau and Martinez, 2016; Colleoni et al., 2014; Liang and Shi, 2017; Machado et al., 2021; Szekely et al., 2004). Our results from both simulations and an empirical case have allowed us to explore RR in body size and in other traits considering important parameters such as static intercept and slope. We delved into static allometry, finding a link between static allometry and body size, mainly in the relationship between the static allometric slope and the species size, confirming some previous research (Gould, 1966a; Pélabon et al., 2014; Voje et al., 2022). Importantly, we have found concordance between our numerical simulations and the empirical real-life example, in that static allometry can determine the occurrence of RR or its converse in a trait through the

allometric slope. The complex linkage between SD in body and trait size, static allometry, and evolutionary allometry of SD (i.e., RR) is a challenge for current studies. The combination of sexual selection, natural selection, and genetic-based hypothesis may be a possible explanation to understand these intricate patterns. By considering the interplay of these mechanisms, we may gain insights into the underlying explanations for RR. Sexual selection, driven by mate choice and competition for reproductive success, could play a role in shaping certain traits or exaggerating their expression. Natural selection, on the other hand, influences traits that enhance fitness in specific environments, favoring specific features over others. In addition, genetic-based hypotheses highlight the role of genetic factors and mechanisms in configuring trait variation and inheritance patterns. By integrating these factors, we can potentially unravel the complex dynamics behind the observed RR patterns.

The intricate links that connect intraspecific allometry, SD, and RR in body size and other traits established through simulations are exemplified with more realism through the empirical case of green lizards. The analyses focusing on *Lacerta* and *Timon* lineages revealed a strong relationship between intraspecific allometric parameters (slope and intercept) and body size. Traits such as trunk length exhibited steeper static slopes and lower static intercepts in smaller species, and traits such as head size exhibited steeper static slopes and lower static intercepts as species increased in size. Our results support Gould's hypothesis only for trunk length, while not for the other three traits. Interestingly trunk length is the only trait that does not show RR or its converse. This could be linked to physical and anatomical constraints between trait and body size. In conclusion, our results confirm that patterns consistent with Rench's rule can appear in body size and traits and that they can do so consistently with the rule or conversely to it. We provide strong evidence that intraspecific allometry is linked to evolutionary allometry for RR through variations in slope and sometimes through the interaction between slope and intercept. As such, we conclude that the intraspecific allometric slope is a major parameter influencing the evolutionary allometry of sexual differences.

References

Abouheif, E., and Fairbairn, D. J. (1997). A comparative analysis of allometry for sexual size dimorphism: Assessing Rensch's rule. *The American Naturalist*, 149(3), 540–562. https://doi.org/10.1086/286004

Adams, D. C., Glynne, E., and Kaliontzopoulou, A. (2020). Interspecific allometry for sexual shape dimorphism: Macroevolution of multivariate sexual phenotypes with application to Rensch's rule. *Evolution*, 74(9), 1908–1922. https://doi.org/10.1111/evo.14049

Ahmadzadeh, F., Flecks, M., Carretero, M. A., Böhme, W., Ihlow, F., Kapli, P., Miraldo, A., and Rödder, D. (2016). Separate histories in both sides of the Mediterranean: Phylogeny and niche evolution of ocellated lizards. *Journal of Biogeography*, 43(6), 1242–1253. https://doi.org/10.1111/jbi.12703

Andersson, M. (1994). Sexual selection. Princeton University Press. Anzai, H., Oishi, K., Kumagai, H., Hosoi, E., Nakanishi, Y., and Hirooka, H. (2017). Interspecific comparison of allometry between body weight and chest girth in domestic bovids. *Scientific Reports*, 7(1), 1–7. https://doi.org/10.1038/s41598-017-04976-z

Arnold, E. N., Arribas, O., and Carranza, S. (2007). Systematics of the Palaearctic and Oriental lizard tribe Lacertini (Squamata: Lacertidae: Lacertinae), with descriptions of eight new genera. *Zootaxa*, 1430(1), 1–86. https://doi.org/10.11646/zootaxa.1430.1.1

Bertin, A., and Fairbairn, D. J. (2007). The form of sexual selection on male genitalia cannot be inferred from within-population variance and allometry—A case study in *Aquarius remigis*. *Evolution*, 61(4), 825–837. https://doi.org/10.1111/j.1558-5646.2007.00074.x

Bidau, C. J., and Martinez, P. A. (2016). Sexual size dimorphism and Rensch's rule in Canidae. *Biological Journal of the Linnean Society*, 119(4), 816–830. https://doi.org/10.1111/bij.12848

Blanckenhorn, W. U., Dixon, A. F., Fairbairn, D. J., Foellmer, M. W., Gibert, P., Linde, K., Meier, R., Nylin, S., Pitnick, S., Schoff, C., Signorelli, M., Teder, T., and Wiklund, C. (2007). Proximate causes of Rensch's rule: Does sexual size dimorphism in Arthropods result from sex differences in development time? *The American Naturalist*, 169(2), 245–257. https://doi.org/10.1086/510597

Bonduriansky, R. (2007). Sexual selection and allometry: A critical reappraisal of the evidence and ideas. *Evolution*, 61(4), 838–849. https://doi.org/10.1111/j.1558-5646.2007.00081.x

Braña, F., and Brana, F. (1996). Sexual dimorphism in lacertid lizards: Male head increase vs female abdomen increase? *Oikos*, 75(3), 511–523. https://doi.org/10.2307/3545893

Bonduriansky, R., and Day, T. (2003). The evolution of static allometry in sexually selected traits. *Evolution*, 57(11), 2450–2458. https://doi.org/10.1111/j.0014-3820.2003.tb01490.x

Brombacher, A., Wilson, P. A., Bailey, I., and Ezard, T. H. (2017). The breakdown of static and evolutionary allometries during climatic upheaval. *The American Naturalist*, 190(3), 350–362. http://orcid.org/0000-0001-8305-6605

Casselman, S. J., and Schulte-Hostedde, A. I. (2004). Reproductive roles predict sexual dimorphism in internal and external morphology of lake whitefish, *Coregonus clupeaformis. Ecology of Freshwater Fish*, 13(3), 217–222. https://doi.org/10.1111/j.1600- 0633.2004.00053.x

Ceballos, C. P., Adams, D. C., Iverson, J. B., and Valenzuela, N. (2013). Phylogenetic patterns of sexual size dimorphism in turtles and their implications for Rensch's rule. *Evolutionary Biology*, 40(2), 194–208. https://doi.org/10.1007/s11692-012-9199-y

Cheverud, J. M. (1982). Relationships among ontogenetic, static, and evolutionary allometry. *American Journal of Physical Anthropology*, 59(2), 139–149. https://doi.org/10.1002/ajpa.1330590204

Colleoni, E., Denoël, M., Padoa-Schioppa, E., Scali, S., and Ficetola, G.F. (2014). Rensch's rule and sexual dimorphism in salamanders: Patterns and potential processes. *Journal of Zoology*, 293(3), 143–151. https://doi.org/10.1111/jzo.12137

Collyer, M. L., and Adams, D. C (2018). RRPP: An r package for fitting linear models to high-dimensional data using residual randomization. Methods in Ecology and *Evolution*, 9(7), 1772–1779. https://doi.org/10.1111/2041-210x.13029

Cox, P. A. (1981). Niche partitioning between sexes of dioecious plants. *The American Naturalist*, 117(3), 295–307. https://doi.org/10.1086/283707

Cox, R. M., and Calsbeek, R. (2010). Sex-specific selection and intraspecific variation in sexual size dimorphism. *Evolution*, 64(3), 798–809. https://doi.org/10.1111/j.1558-5646.2009.00851.x

Cox, R. M., Skelly, S. L., and John-Alder, H. B. (2003). A comparative test of adaptive hypotheses for sexual size dimorphism in lizards. *Evolution*, 57(7), 1653–1669. https://doi.org/10.1111/j.0014-3820.2003. tb00371.x

Dale, J., Dunn, P. O., Figuerola, J., Lislevand, T., Székely, T., and Whittingham, L. A. (2007). Sexual selection explains Rensch's rule of allometry for sexual size dimorphism. *Proceedings of the Royal Society B: Biological Sciences*, 274(1628), 2971–2979. https://doi.org/10.1098/rspb.2007.1043

Eberhard, W. G., Rodríguez, R. L., Huber, B. A., Speck, B., Miller, H., Buzatto, B. A., and Machado, G. (2018). Sexual selection and static allometry: The importance of function. *The Quarterly Review of Biology*, 93(3), 207–250. https://doi.org/10.1086/699410

Enriquez-Urzelai, U., Martínez-Freiría, F., Freitas, I., Perera, A., Martínez-Solano, I., Salvi, D., Velo-Antón, G., and Kaliontzopoulou, A. (2022). Allopatric speciation, niche conservatism and gradual phenotypic change in the evolution of European green lizards. *Journal of Biogeography*, 49(12), 1–13. https://doi.org/10.1111/jbi.14497

Fairbairn, D. J. (1997). Allometry for sexual size dimorphism: Pattern and process in the coevolution of body size in males and females. *Annual Review of Ecology and Systematics*, 28(1), 659–687. https://doi.org/10.1146/annurev.ecolsys.28.1.659

Fairbairn, D. J. (2005). Allometry for sexual size dimorphism: Testing two hypotheses for Rensch's rule in the water strider *Aquarius remigis*. *The American Naturalist*, 166(Suppl 4), S69–S84. https://doi.org/10.1086/444600

Fairbairn, D. J., and Preziosi, R. F. (1994). Sexual selection and the evolution of allometry for sexual size dimorphism in the water strider, *Aquarius remigis*. *The American Naturalist*, 144(1), 101–118. https://doi.org/10.1086/285663

Fairbairn, D. J.|, Blanckenhorn, W. U., and Székely, T. (Eds.). (2007). Sex, size and gender roles: evolutionary studies of sexual size dimorphism. Oxford University Press, USA. https://doi.org/10.1093/ac-prof:oso/9780199208784.001.0001

Firmat, C., Lozano-Fernández, I., Agusti, J., Bolstad, G. H., Cuenca-Bescós, G., Hansen, T. F., and Pélabon, C. (2014). Walk the line: 600000 years of molar evolution constrained by allometry in the fossil rodent *Mimomys savini*. *Philosophical Transactions of the Royal Society B: Biological Sciences*, 369(1649), 20140057. https://doi.org/10.1098/rstb.2014.0057

Frýdlová, P., and Frynta, D. (2010). A test of Rensch's rule in varanid lizards. *Biological Journal of the Linnean Society*, 100(2), 293–306. https://doi.org/10.1111/j.1095-8312.2010.01430.x

Freidline, S. E., Gunz, P., and Hublin, J. J. (2015). Ontogenetic and static allometry in the human face: Contrasting Khoisan and Inuit. *American Journal of Physical Anthropology*, 158(1), 116–131. https://doi.org/10.1002/ajpa.22759

Frynta, D., Baudyšová, J., Hradcová, P., Faltusová, K., and Kratochvíl, L. (2012). Allometry of sexual size dimorphism in domestic dog. *PLoS One*, 7(9), e46125. https://doi.org/10.1371/journal.pone.0046125

Gayon, S. J. (2000). History of the concept of allometry. *American Zoologist*, 40(5), 748–758. https://doi.org/10.1093/icb/40.5.748

Gould, S. J. (1966a). Allometry and size in ontogeny and phylogeny. *Biological Reviews*, 41(4), 587–638. https://doi.org/10.1111/j.1469-185x.1966.tb01624.x

Gould, S. J. (1966b). Allometry in Pleistocene land snails from Bermuda: The influence of size upon shape. *Journal of Paleontology*, 40(5), 1131–1141.

Gould, S. J. (2000). Of coiled oysters and big brains: How to rescue the terminology of heterochrony, now gone astray. *Evolution & Development*, 2(5), 241–248. https://doi.org/10.1046/j.1525- 142x.2000.00067.x

Hansen, T. F., and Houle, D. (2008). Measuring and comparing evolvability and constraint in multivariate characters. *Journal of Evolutionary Biology*, 21(5), 1201–1219. https://doi.org/10.1111/j.1420-9101.2008.01573.x

Harmon, L., Weir, J., Brock, C., Glor, R., Challenger, W., Hunt, G., and Rcpp, L. (2015). Package "geiger." R Package Version, 2(3), 1–74.

Huxley, J. S. (1924). Constant differential growth-ratios and their significance. *Nature*, 114(2877), 895–896. https://doi.org/10.1038/114895a0

Huxley, J. S., and Teissier, G. (1936). Terminology of relative growth. *Nature*, 137(3471), 780–781. https://doi.org/10.1038/137780b0

Kawano, K. (2002). Character displacement in giant rhinoceros beetles. *The American Naturalist,* 159(3), 255–271. https://doi.org/10.1086/338512

Jannot, J. E., and Kerans, B. L. (2003). Body size, sexual size dimorphism, and Rensch's rule in adult hydropsychid caddisflies (Trichoptera: Hydropsychidae). *Canadian Journal of Zoology*, 81(12), 1956– 1964. https://doi.org/10.1139/z03-194

Klingenberg, C. P., and Zimmermann, M. (1992). Static, ontogenetic, and evolutionary allometry: A multivariate comparison in nine species of water striders. *The American Naturalist*, 140(4), 601–620. https://doi.org/10.1086/285430

Liang, T., and Shi, L. (2017). Sexual dimorphism and morphological variation of three populations of *Phrynocephalus helioscopus*: Test of Bergmann's rule, Allen's rules and Rensch's rule. *Sichuan Journal of Zoology*, 36(3), 249–257.v

Liang, T., Shi, L., Bempah, G., and Lu, C. (2021). Sexual size dimorphism and its allometry in Chinese lizards. *Evolutionary Ecology*, 35(2), 323–335. https://doi.org/10.1007/s10682-021-10104-1

Machado, G., Buzatto, B. A., and Samia, D. S. (2021). It is not always about body size: Evidence of Rensch's rule in a male weapon. *Biology Letters*, 17(6), 0234. https://doi.org/10.1098/rsbl.2021.0234

Martínez-Gil, H., Martínez-Freiría, F., Perera, A., Enriquez-Urzelai, U., Martínez-Solano, I., Velo-Antón, G., and Kaliontzopoulou, A. (2022). Morphological diversification of Mediterranean anurans: The roles of evolutionary history and climate. *Biological Journal of the Linnean Society*, 135(3), 462–477. https://doi.org/10.1093/biolinnean/blab156

Mori, E., Mazza, G., and Lovari, S. (2017). Sexual dimorphism. In J. Vonk, and T. Shakelford (Eds.), Encyclopedia of animal cognition and behavior (pp. 1–7). Springer International Publishing.

Mosimann, J. E. (1970). Size allometry: Size and shape variables with characterizations of the lognormal and generalized gamma distributions. *Journal of the American Statistical Association*, 65(330), 930–945. https://doi.org/10.1080/01621459.1970.10481136

Nali, R. C., Zamudio, K. R., Haddad, C. F., and Prado, C. P. (2014). Size-dependent selective mechanisms on males and females and the evolution of sexual size dimorphism in frogs. *The American Naturalist*, 184(6), 727–740. https://doi.org/10.1086/678455

Paradis, E., Blomberg, S., Bolker, B., Brown, J., Claude, J., Cuong, H. S., and Didier, G. (2019). Package “ape.” Analyses of phylogenetics and evolution. Version, 2(4), 47.

Pearson, D., Shine, R., and How, R. (2002). Sex-specific niche partitioning and sexual size dimorphism in Australian pythons (*Morelia spilota imbricata*). *Biological Journal of the Linnean Society*, 77(1), 113–125. https://doi.org/10.1046/j.1095-8312.1999.00075.x

Pélabon, C., Bolstad, G. H., Egset, C. K., Cheverud, J. M., Pavlicev, M., and Rosenqvist, G. (2013). On the relationship between ontogenetic and static allometry. *The American Naturalist*, 181(2), 195–212. https://doi.org/10.1086/668820

Pélabon, C., Firmat, C., Bolstad, G. H., Voje, K. L., Houle, D., Cassara, J., Rouzic, A. L., and Hansen, T. F. (2014). Evolution of morphological allometry. *Annals of the New York Academy of Sciences*, 1320(1), 58–75. https://doi.org/10.1111/nyas.12470

Peñalver-Alcázar, M., Galán, P., and Aragón, P. (2019). Assessing Rensch’s rule in a newt: Roles of primary productivity and conspecific density in interpopulation variation of sexual size dimorphism. *Journal of Biogeography*, 46(11), 2558–2569. https://doi.org/10.1111/jbi.13680

Pincheira-Donoso, D., and Hunt, J. (2017). Fecundity selection theory: Concepts and evidence. *Biological Reviews*, 92(1), 341–356. https://doi.org/10.1111/brv.12232

R Core Team (2020). R: A language and environment for statistical computing. R Foundation for Statistical Computing. https://www.r-project.org/

Ralls, K., and Mesnick, S. (2009). Sexual dimorphism. In J. G. M. Bernd Würsig, and K. K. Thewissen (Eds.), Encyclopedia of marine mammals (pp. 1005–1011). Academic Press.

Remeš, V., and SzéKely, T. (2010). Domestic chickens defy Rensch’s rule: Sexual size dimorphism in chicken breeds. *Journal of Evolutionary Biology*, 23(12), 2754–2759. https://doi.org/10.1111/j.1420-9101.2010.02126.x

Rensch, B. (1950). Die Abhängigkeit der relativen Sexualdifferenz von der Körpergrösse. *Bonner Zoologische Beiträge*, 1, 58–69.

Rensch, B. (1959). Evolution above the species level. Columbia University Press.

Revell, L. J., and Revell, M. L. J. (2014). Package "phytools." https://cran.r-project.org/web/packages/phytools

Reyes-Puig, C., Adams, D. C., Enriquez-Urzelai, U., and Kaliontzopoulou, A. (2023). Rensch's rule: linking intraspecific to evolutionary allometry. Evolution, 77(12), 2576-2589. https://doi.org/10.1093/evolut/qpad172

Stamps, J. A., and Andrews, R. M. (1992). Estimating asymptotic size using the largest individuals per sample. *Oecologia*, 92(4), 503–512. https://doi.org/10.1007/BF00317842

Schluter, D. (1996). Adaptive radiation along genetic lines of least resistance. *Evolution*, 50(5), 1766–1774. https://doi.org/10.1111/j.1558-5646.1996.tb03563.x

Szekely, T., Freckleton, R. P., and Reynolds, J. D. (2004). Sexual selection explains Rensch's rule of size dimorphism in shorebirds. *Proceedings of the National Academy of Sciences of the United States of America*, 101(33), 12224–12227. https://doi.org/10.1073/pnas.0404503101

Tejero-Cicuéndez, H., Menéndez, I., Talavera, A., Riaño, G., Burriel-Carranza, B., Simó-Riudalbas, M., and Adams, D. C. (2022). Evolution along allometric lines of least resistance: Morphological differentiation in *Pristurus* geckos. *bioRxiv*. 1–34. https://doi.org/10.1101/2022.11.28.518148

Tubaro, P. L., and Bertelli, S. (2003). Female-biased sexual size dimorphism in tinamous: A comparative test fails to support Rensch's rule. *Biological Journal of the Linnean Society*, 80(3), 519–527. https://doi.org/10.1046/j.1095-8312.2003.00252.x

Verwaijen, D., and Van Damme, R. (2007). Does foraging mode mould morphology in lacertid lizards? *Journal of Evolutionary Biology*, 20(5), 1950–1961. https://doi.org/10.1111/j.1420-9101.2007.01367.x

Voje, K. L., Bell, M. A., and Stuart, Y. E. (2022). Evolution of static allometry and constraint on evolutionary allometry in a fossil stickle- back. *Journal of Evolutionary Biology*, 35(3), 423–438. https://doi.org/10.1111/jeb.13984

Voje, K. L., and Hansen, T. F. (2013). Evolution of static allometries: Adaptive change in allometric slopes of eye span in stalk-eyed flies. *Evolution*, 67(2), 453–467. https://doi.org/10.1111/j.1558- 5646.2012.01777.x

Voje, K. L., Hansen, T. F., Egset, C. K., Bolstad, G. H., and Pélabon, C. (2014). Allometric constraints and the evolution of allometry. *Evolution*, 68(3), 866–885. https://doi.org/10.1111/evo.12312

Wickham, H., and Wickham, M. H. (2017). Package tidyverse. Easily install and load the 'Tidyverse'. https://tidyverse.tidyverse.org

Chapter 4

Is it all about size? Dismantling the integrated phenotype to understand species coexistence and niche segregation

4.1. Introduction

The factors promoting species coexistence have puzzled scientists for decades (Amarasekare, 2002; Armstrong and McGehee, 1976; Gravel et al., 2011; Pigot et al., 2016; Zobel, 1992). This occurs when different species share the same habitat or ecosystem without one species being displaced by the presence of the other (Gravel et al., 2011; Valladares et al., 2015). In classical niche theory, coexistence is allowed when each species utilizes a unique combination of biotic and abiotic resources, which are limited regarding the populations of such species, which translate into having different niches (Colwell and Rangel, 2009; Grinnell, 1917; Hutchinson, 1978). Under the same theory, if resources are limited and niches overlap, the less efficient competitor will be displaced (Hutchinson, 1978; Schoener, 1974). As such, species coexistence is typically achieved through niche segregation (Gravel et al., 2011; Tokeshi, 2009), which involves the differentiation of resource use between species that cooccur in a given area (Schoener, 1974; Valladares et al., 2015). Niche segregation facilitates species coexistence by minimizing competitive interactions for resources, thus reducing the risk of one species excluding the other (Larson, 1984; Pianka and Huey, 1978; Valladares et al., 2015). Niche segregation could reduce competition among species by fulfilling its resource requirements either at different times (temporal segregation) or by causing each species to specialize in a particular area of the multivariate niche space (including time as part of it) (Castro-Arellano and Lacher, 2009; Prins et al., 2006; Smart and Gee, 1979).

The ecological niche can be summarized as the multidimensional space shaped by the conditions and resources that allow species to exist (Colwell and Rangel, 2009; Hutchinson, 1978), that is an integrated set of conditions that determine species' survival and reproductive success (Kearney, 2006). Importantly, a comprehensive view of the niche considers it a property of species—and not merely a description of the habitat they occupy—which emerges through the interplay between environmental conditions and species phenotype (i.e. behaviour, morphology, physiology and life history) (Colwell and Rangel, 2009; Elton, 1927; Hutchinson, 1957; Kearney, 2006). Implicitly, phenotypes are also multidimensional and interact with the environment in order to determine species' niches. Among phenotypic traits, morphology influences—among other things—how organisms exploit their structural habitat (e.g. foraging, sheltering, escaping) (Kaliontzopoulou et al., 2012; Peterson and Husak, 2006; Williams, 1983). Morphology also affects locomotor performance (e.g. sprint speed, manoeuvrability) mediated by the surrounding environment and anatomical adaptations (e.g. elasticity, joint flexibility)

(Farley, 1997; Farley and Ko, 1997; Gomes et al., 2016; Goodman et al., 2008; Vasilopoulou-Kampitsi, 2020). Also, it is linked to the trophic and social axes of the niche through head proportions and bite force (Gomes et al., 2018; Gomes et al., 2020; Huyghe et al., 2005; Lappin and Husak, 2005; McBrayer and White, 2002). Furthermore, organisms' physiology (e.g. heat and water exchange) is related to the surrounding environment (Kearney, 2006; Mi et al., 2022), and in terrestrial organisms, it is associated with morphological and functional adaptations to minimize dehydration and to enhance heat interchange (Angilletta Jr., 2009; de la Vega and Schilman, 2017; Eynan and Dmi'el, 1993; Kearney and Porter, 2009; Mautz, 1980; Morales and Giannini, 2010). However, it is crucial to understand that while morphology influences different aspects of an organism's behaviour and performance with its surrounding habitat, it does not mean that it exclusively defines the ecological niche. Rather, morphology is tightly connected to niche utilization, regarded as a proxy indicator of niche segregation. Thus, describing multidimensional phenotypes—and how and to what extent they overlap—can shed light on the mechanisms that facilitate niche segregation in coexisting species (Garland Jr and Losos, 1994; Vasil'ev, 2021).

The overall dimensions of an organism and the distinct anatomical features of which it is composed represent its size. In this regard, body size is a key phenotypic trait that can affect each of the niche axes through allometric and biophysical effects. That is, body size is tightly linked to each of the aforementioned morphological, functional performance and physiological traits (Angilletta Jr. et al., 2004; Sears and Angilletta Jr., 2004). Body size has a significant impact on functional performance, since muscle strength is positively related to body size and mass (Aasa et al., 2003; Irschick et al., 2008). For example, relative head and limb sizes are well known to contribute to variation in bite and locomotor performance (Herrel et al., 2001; Huyghe et al., 2005). Similarly, there is a well-established relationship between body size and thermal physiology (Angilletta Jr., 2009; Baudier and O'Donnell, 2018; Streinzer et al., 2016). For instance, larger organisms tend to have higher tolerance to higher temperatures and smaller ones tend to have lower minimum critical temperature values, also, variation in body size may be related to regional heterothermic capacity (Baudier and O'Donnell, 2018; Olalla-Tárraga et al., 2006; Webber and McGuire, 2022). In addition, smaller animals usually have higher per gram relative metabolic rates due to lower thermal inertia (Angilletta Jr., 2009; Kearney and Porter, 2009). Finally, larger ectotherms exhibit a lower surface area-to-volume ratio, thus reducing water loss (Chown and Klok, 2003). Thus, in this context, body size is particularly relevant since it covaries with most phenotypic traits (Ayers and

Shine, 1997; Carlson et al., 2008; Tobalske and Dial, 2000), and it may therefore serve as a primary mechanism for species differentiation, facilitating niche segregation and promoting species coexistence. Still, residual trait differentiation between coexisting species may further contribute to niche segregation, after size is accounted for.

With this integrated multivariate approach, we intend to identify the main directions of species' differentiation pinpointing those that could allow their coexistence. Here, we used as our study model syntopic populations (i.e. populations of species that occur at the same time in a particular locality) of *Timon lepidus* and *Lacerta schreiberi* in Northern Portugal (Brito, Paulo, and Crespo, 1998; Enriquez-Urzelai et al., 2022 Loureiro et al., 2008). Both species are considerably different in body size, being *T. lepidus* larger than *L. schreiberi* (Brito, Luis, et al., 1998; Brito, Paulo, and Crespo, 1998; Marco and Pollo, 1993; Mateo and Castanet, 1994), and they frequently share habitats. However, *T. lepidus* tends to show varied spatial patterns in Mediterranean habitats such as shrublands and other more semi-arid areas (Renet et al., 2022). It usually moves on rocky substrates and open areas, using rock holes as shelter (Ferreira et al., 2016). Other studies have also detected the presence of *T. lepidus* in structures of anthropogenic origin, reflecting the adaptability of the species to different microhabitat conditions (Delgado and Gómez, 2016). On the other hand, *L. schreiberi* prefers microhabitats with an increased presence of shrubs and bushes (Salvador, 1988), where soil and vegetation characteristics are important for the occurrence of this species (Brito, Luis, et al., 1998; Brito, Paulo, and Crespo, 1998). Given its elevated dependence on vegetation, the relative humidity of the surrounding environment is a potential factor to be examined. Regarding their trophic niche, there is some evidence that both species consume similar items such as beetles, grasshoppers, ants and spiders among others (Pérez Mellado, 1982; Salvador, 1988; Salvidio et al., 2006). Thus, these species are appropriate for investigating phenotypic differentiation in coexisting species, and for understanding the contribution of body size to niche segregation. Specifically, we aim to provide a comprehensive framework for examining phenotypic space partitioning between coexisting species to infer the potential drivers of niche segregation, combining morphological, performance and physiological traits. Through this approach, we want to clarify the interplay between morphology and function, with special emphasis on the relationship between body size and different phenotypic traits. We hypothesize the existence of differences in morphology, functional performance, thermal and water balance between both species. Since body size is closely linked to allometric trait relationships, we predict that the effect of body size will be significant in all traits, with

the greatest influence on morphology. Since *T. lepidus* and *L. schreiberi* are known to occupy relatively different microhabitats in particular areas (Marco and Pollo, 1993; Mateo and Cheylan, 1997), we expect niche segregation to be maintained once the effect of body size is removed from performance and ecophysiological traits. Likewise, we expect greater phenotypic overlap between species when the body size effect is removed and greater segregation when it is included. By investigating the integration of phenotypic axes, we expect to gain insights on the mechanisms and traits underlying the differences between coexisting species. Thus, in this way, we anticipate identifying phenotypic traits that are species-specific and not a consequence of body size scaling and to gain a better understanding of the available phenotypic components that may contribute to niche segregation.

4.2. Materials and Methods

4.2.1. Study species, sampling and animal husbandry

The ocellated green lizard *Timon lepidus* (Daudin, 1802) is a European reptile typical of western Mediterranean regions, mainly distributed in northeastern Italy, southern France, and the Iberian Peninsula, from sea level to 2000 meters of elevation (Mateo and Cheylan, 1997; Mateo, 2017). The Schreiber's green lizard *Lacerta schreiberi* Bedriaga, 1879 is an Atlantic species, endemic to Western Iberian Peninsula, distributed from sea level to 2100 meters of elevation (Brito, Paulo, and Crespo, 1998; Marco and Pollo, 1993). Despite their overall morphological resemblance, the two species are distinguished mainly by their difference in body size, *T. lepidus* being one of the largest species of the green lizard clade in Europe reaching more than 240 mm of snout to vent length (SVL), while *L. schreiberi* is about 130 mm of SVL (Brito, Luis, et al., 1998; Mateo, 2017). Both species are relatively flexible ecologically; however, *T. lepidus* is generally considered to have a broad plasticity for habitat preferences (Galán, 2003; Llorente et al., 1995), while *L. schreiberi* is very linked to humid environments (e.g. moist deciduous forests, heathlands and locations close to running streams; Brito, Paulo, and Crespo, 1998).

In May and June 2022, we sampled individuals of *T. lepidus* and *L. schreiberi* from a sympatric locality in northern Portugal (Castro de São Paio; 41.312257° N, 8.737074° W; 12 m a.s.l.). Since both species are sexually dimorphic, we restricted our sampling to adult males to avoid sex-, pregnancy- and ontogeny-related biases (Carretero et al., 2005). We collected a total of 26 males of *T. lepidus* and 16 *L. schreiberi* by noosing as described by Sillero and García-Muñoz (2010). Once the specimens were

collected, they were transported to the laboratory of CIBIO. Individuals were assigned a unique code with non-toxic marker paint to identify them during the experiments and were individually housed in terraria with water *ad libitum* with no food. Between experiments, the terraria were cleaned and provided with clean water, and the air temperature maintained at 25°C. All animals rested one day before starting the experiments.

All the processes of collection, management and experimentation with green lizards were carried out with the collection and research permits LICENÇA No. 344-348/2022/CAPT obtained from the Instituto da Conservação da Natureza e Florestas. In addition, the Órgão Responsável pelo Bem-Estar dos Animais (ORBEA) was informed about the practices and details of the project.

4.2.2. Experimental procedures and data analysis

4.2.2.1. Replication statement

Our study involves co-occurring populations of two species of green lizards. Specifically, we examined 26 individuals of *T. lepidus* and 16 individuals of *L. schreiberi*, allowing us to analyse the scale of inference at the population level within each species.

4.2.2.2. Morphology

We recorded the following linear measurements in all collected individuals, using electronic callipers with a precision of 0.01 mm: snout-to-vent length (SVL), trunk length (TRL), head length (HL), head width (HW), head height (HH), fore limb length (FLL) and hind limb length (HLL). The individuals were also weighed using a precision balance (± 0.0001 g; Sartorius M-Pact AX224, Sartorius AG, Goettingen, Germany). We used SVL as a proxy of body size. To obtain a single metric for head size (HS), we calculated the geometric mean of HL, HW and HH. To investigate morphological differences between species, we used ANOVA comparisons for SVL, and ANCOVAs for the other morphological traits with SVL as covariate and species as factor. For downstream analyses (see further on), we obtained size-corrected variables for each species by regressing each morphological trait on body size and we used the residuals from this regression for further analyses. The decision on using SVL for size correction was based on the AIC values observed after including body size or body weight as a covariate (Appendix B Table B2.1). The size-corrected morphological variables are abbreviated in figures and tables as res.TRL, res.HS, res.FLL and res.HLL. Measurement data collection lasted 2 h for each set of 8 specimens and were taken on the first day.

All ANOVA and ANCOVA comparisons for morphology as well as the performance and ecophysiology analyses detailed below were evaluated for significance using residual randomization procedures with 1000 permutation cycles as implemented in the package 'RRPP' (Collyer and Adams, 2019). We used this approach since it does not rely on parametric assumptions and is suitable for relatively small sample sizes (Collyer and Adams, 2019). For generalized linear models we used the 'lme4' R package (Bates et al., 2014), and 'tidyverse' (Wickham et al., 2019) for data cleaning, wrangling and visualization.

4.2.2.3. Locomotor performance

We started the locomotor performance experiment on the morning of the first day, therefore, the lizards were in conditions most similar to the field. Racetrack experiments lasted between in total 4 and 5 h for each set of 8 specimens, this means that each lizard rested at least 20 min in thermal chambers after each trial. Thus, no lizard performed sequential runs on the racetracks (see details in Appendix B). We followed standard procedures for locomotor performance experiments (Gomes et al., 2018; Herrel et al., 2000). We examined locomotor performance in two different ecologically relevant settings (Figure 4.1a,b). A straight racetrack to assess maximum sprint speed (MaxSPR) (Figure 4.1a) and a double L-racetrack to assess manoeuvrability (MNV) (Figure 4.1b). Details on racetrack specifications and exact experimental conditions are available in Appendix B. Each individual performed the runs in each racetrack three times to guarantee that maximal locomotor performance was recorded. To motivate lizards to run, we chased them during the trials in both racetracks. We filmed all trials with a digital camera (specifications in Appendix B). We excluded from analyses all the trials in which the lizards completely stopped or turned to face the researchers.

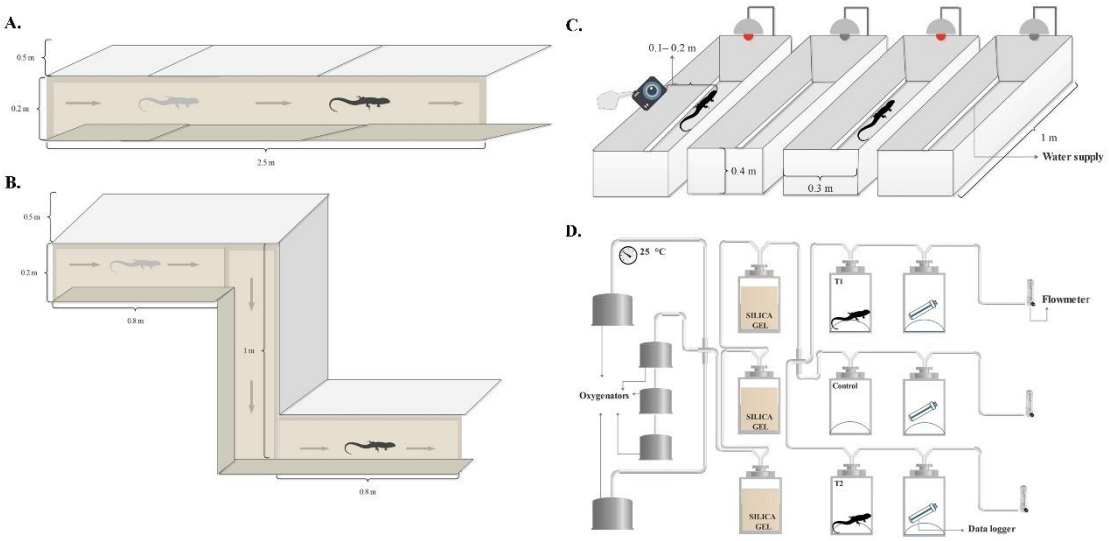

Figure 4.1 Schematic representation of the experiments carried out to record phenotypic traits. (A) Straight racetrack, (B) double-L racetrack (i.e. a straight surface of 0.8 m, an angle of 90°, a straight surface of 1 m, a second angle of 90° and a final straight surface of 0.8 m), (C) thermogradient chambers and (D) evaporative water loss quantification system. Reprinted with permission from Reyes-Puig, C. (2024). Is it all about size? Dismantling the integrated phenotype to understand species coexistence and niche segregation. Functional Ecology, 38(11), 3081–3099. © John Wiley & Sons Ltd.

For MaxSPR, we calculated the maximum instantaneous speed (evaluated between consecutive frames, Gomes et al., 2018) across all trial repetitions. We considered the following variables to describe MNV: (i) success of the turn, considering as unsuccessful any turns in which the lizard collided or climbed the walls, (ii) maximal speed during the path and turn; (iii) maximum bending angle of the trunk and head during a turn; and (iv) manoeuvring strategy (MS), modified from the categories proposed by Vasilopoulou-Kampitsi (2020): MS_0 trials in which lizards crashed against the walls and therefore, unsuccessful turns; MS_1 trials in which lizards completed the turns stopping before the turns; MS_2 trials in which the lizards completed the turn without stopping. All data on locomotor performance were log-transformed prior to analyses.

To explore differences in maximum sprint speed (MaxSPR), we performed an ANCOVA including body size as a covariate and species as a factor. To explore how other morphological traits biomechanically associated with locomotor capacity contribute to variation between species in sprint speed, we performed ANCOVA comparisons on sprint speed using size-corrected limb traits and species as predictors. To evaluate turning success as a measure of manoeuvrability, we used a chi-squared proportions test, implemented in the function prop.test of the ‘stats’ R-package (R Core Team, 2024) to assess whether the proportions of turning success are significantly different between the two species. To investigate the combined effect of body size and running speed while

in the double-L racetrack, we performed binomial generalized mixed models with turning success as the response variable, body size and manoeuvring strategy (i.e. whether the lizard stopped before the turn or not) as interacting explanatory factors and maximum speed in the double-L corridor as an additive factor. For downstream analyses (as detailed later on), we obtained size-corrected variables by regressing each locomotor trait on body size and extracting the residuals from this regression for further analyses. We used body size to correct manoeuvrability traits based on the AIC values observed after including body size or body weight as a covariate (Appendix B Table B2.1). The size-corrected locomotor variables are abbreviated in figures and tables as res.MaxSPR, res.HA, res.Max_L (for each abbreviation of locomotion traits see Appendix B).

4.2.2.4. Bite force

We measured bite force (BF) with an isometric Kistler force transducer, using standard procedures (Herrel et al., 2001; Appendix B). Bite force measurements took 2 h for eight specimens during the end of first day of experiments, after the lizards had rested for at least 2 h from the previous performance experiments. We put two marks on the edge of the plates to delimit where the lizards should bite to ensure an equal distance and thus standardize the point of effort of the bite force (Gomes et al., 2020). We tested each individual five times to ensure that we quantified the maximal bite force of each lizard. We retained the maximum bite force (in N) per lizard and log- transformed the data before statistical analyses. At the end of the first day of experiments, the lizards rested for 48 h with water *ad libitum* (see details in Appendix B).

We used an ANOVA to investigate the differences in bite force between species and ANCOVA including body weight and head size as covariate and species as factor, considering all interaction terms.

For subsequent analyses (see further on), we acquired residuals of size-corrected bite force values by conducting a regression between bite force on body weight (res.BF). We based this decision on the AIC values observed once body size or body weight were accounted for (Appendix B Table B2.1). Finally, we performed and ANCOVA between size-corrected bite force with size-corrected head size as covariate and species as factor to explore if head size had an effect on size- corrected bite force.

4.2.2.5. Preferred body temperatures

To quantify the thermal preference of individuals, we conducted selected temperature experiments between 9 h and 17:30 h on the fourth day, as the second and

third days were intended for the lizards to rest and acclimatize to the thermogradients. We measured body temperatures every half an hour, resulting in 19 temperature measurements per individual. To measure body temperatures, we used a FLIR T335 thermal camera (Flir Systems Inc., Wilsonville, Oregon, USA). Details on the preparation of the lizards prior to the experiments, as well as specifications and dimensions of the experimental arena and the instrumentation used are available in Appendix B and Figure 4.1c.

To summarize the thermal preference of each species, we calculated the mean (i.e. preferred, T_{pref}), median, minimum, maximum, variance ($T_{pref}V$) and set point range of body temperature per individual (25%–75% quartile) (Angilletta Jr., 2009). To evaluate differences in preferred temperatures (T_{pref} and $T_{pref}V$) between species we performed an ANOVA with species as the explanatory variable. In a second ANCOVA model, body weight was added as a covariate to incorporate the effect of size, as used in other similar studies (Barroso et al., 2020) and based in the AIC values displayed on models with body size or body weight (Appendix B Table B2.1). For downstream analyses of species differentiation across a size-free multivariate phenotypic space, we obtained the residual values from a regression of T_{pref} and $T_{pref}V$ on body weight (res.*Tpref* and res.*TprefV*, respectively).

4.2.2.6. Water loss

Water loss experiments were conducted on the fifth day, after the lizards had rested for at least 15 h from the previous experiment (thermogradients). We used a three-channel, open-air circulation system to measure water loss (Figure 4.1d). Experimental design specifications, dimensions, and materials are available in Appendix B. Experiments lasted for 2.5 h. Once the data were extracted from data loggers, we obtained the minimum of relative humidity (RH) values from the five most stable periods of data recordings for further analysis, thus excluding the initial values of the experiment which tend to be the highest due to stress (Žagar et al., 2022). At the end of the fifth day, after water loss experiments, the lizards were fed with yellow mealworms and rested for another day. Lizards were then transported to a mesocosm where they were monitored during a week in natural conditions for habitat use and occupancy in a different study. Finally, the individually marked lizards were released at the exact collection points in Castro São Paio to avoid the recapture of individuals.

We evaluated water loss rates by estimating evaporative water loss (EWL) and effective proportion of surface area that is wet (p_wet) (Kearney and Porter, 2017;

Kearney et al., 2018). A full description of the process to calculate EWL and p_wet is detailed in Appendix B. Subsequently, we performed ANOVA and ANCOVA models to test for differences in evaporative water loss and effective proportion of surface area that is wet between species, where we included body weight as a covariate, since body mass (rather than SVL) is an appropriate proxy for size in water loss analysis (Le Galliard et al., 2021). We also supported this decision based on the AIC values obtained, once we included body size or body weight as covariate (Appendix B Table B2.1). We also calculated the residual values of EWL and p_wet on weight (res. EWL and res.p_wet) for downstream multivariate analyses.

4.2.2.7. Species position, overlap and association in multivariate phenotypic space

We performed a set of multivariate analyses to understand niche segregation between the two coexisting species in the multivariate phenotypic space composed by morphological, performance and physiological traits. To gain insights into the importance of body size for the segregation of niches of coexisting species and the contribution of different variables to phenotypic space once the effect of body size was removed, we performed these analyses twice: first with the raw variables, that is including body size effects, and then with size-corrected variables. Before running multivariate analyses, and because our dataset included traits quantified in different scales and units, we standardized all variables by mean-centring them and scaling them to unit variance. To better explore phenotypic space and investigate which aspects of the phenotype are more relevant for niche segregation between species, we distinguished three variable subsets: one for morphology (MORPH), including trunk length, head size, hindlimb length and forelimb length; one for functional performance (PERFORM), including bite force, trunk max bending angle, head max bending angle, maximum sprint speed and maximum instantaneous speed in the double-L racetrack; and one for ecophysiology (ECOPHY), including mean preferred temperature, preferred temperature variance, evaporative water loss and proportion of surface area that is wet. The same subsets were considered using size-corrected variables (res.MORPH, res.PERFORM and res. ECOPHY). All analyses described below were therefore conducted considering a global dataset for the same individuals, with all traits together and each of the three subsets separately, both before and after size-correction.

To identify the most correlated phenotypic variables and the ones with the greatest weight in explaining their ordination in the multivariate space, we performed a principal component analysis (PCA) on the datasets. We used the ‘factoextra’ R package

(Kassambara, 2016) to perform the PCA analysis and the prcomp function which uses a covariance matrix. Note, however, that since all variables were mean-centred and scaled before analyses, this is fully corresponding to an analysis using the correlation matrix. With this, we identified the amount of variation retained in each component and the associated variables. For the final representation of most of the datasets, we retained the axes that accounted for more than 50% of the variance. To test whether the multivariate phenotypic spaces composed of the subset datasets MORPH, PERFORM and ECOPHY differed significantly between species, and examine how each contributed to niche segregation, we performed a multivariate analysis of covariance (MANCOVA) considering size as a covariate and species as a factor, with the R package 'RRPP' (Collyer and Adams, 2019) and using residual randomization procedures with 1000 permutations.

To identify the phenotypic variables that maximize the separation between the two species we used discriminant analyses in all datasets. Due to the non-normality of some variables, we applied a flexible discriminant analysis (FDA), as implemented in the fda function of the 'mda' package (Hastie and Tibshirani, 2023). We extracted the linear discriminant scores and calculated their correlations with the predictor variables to identify the most important ones for species segregation. In addition, to investigate the multivariate association between the phenotypic spaces, we conducted a two-block partial least squares (PLS) regression with the plsr function of the R package pls (Mevik et al., 2011). We first used a PLS with raw variables in each set (MORPH, PERFORM, ECOPHY) and then we performed a PLS with size-corrected sets (res.MORPH, res. PERFORM, res.ECOPHY).

To obtain a comprehensive representation of the different phenotypic trait spaces defined by the subset datasets described above, and to evaluate niche overlap between species, we used a hypervolume analysis approach (Blonder et al., 2014; Blonder, 2018). Specifically, we calculated four hypervolumes, including those phenotypic trait combinations previously identified as most relevant for differentiating the two species. This resulted in a morphological hypervolume (including size-corrected hindlimb length, forelimb length and snout-to-vent length), a bite force hypervolume (size- corrected head size and bite force), a locomotor performance hypervolume (including size-corrected maximum instantaneous speed in the double-L racetrack, trunk max bending angle and head max bending angle) and an ecophysiological hypervolume (including size-corrected mean preferred temperature, preferred temperature variance and effective proportion of surface area that is wet). To estimate the shape and volume of

multidimensional datasets and identify intersection (i.e. shared space that intersects between two or more hypervolumes.), overlap and unique components within the hypervolumes, we used the 'hypervolume' package, and the functions hypervolume, hypervolume_set, hypervolume_distance and hypervolume_overlap_statistics (Blonder et al., 2018). For the construction of hypervolumes, we used the Silverman bandwidth estimator and the kernel density Gaussian method. To estimate the overlap of hypervolumes between species, we used the Sørensen and Jaccard indices, which are based on the similarity of the groups, and range from 0 (no overlap) to 1 (complete overlap) (Blonder et al., 2014; Blonder, 2018).

4.3. Results

4.3.1. Morphology

Timon lepidus and *Lacerta schreiberi* differed significantly in body size (F = 271.114, p = 0.001) and in all raw morphological traits due to body size (Attachment 4.3.1), with *T. lepidus* being the largest species (= 144.3 mm in *T. lepidus* vs. = 91.4 mm in *L. schreiberi*, Table 4.1). However, we found no differences between species in trunk length and head size once the effect of body size was taken into account (p > 0.05, Appendix B Table B2.2). On the other hand, forelimb length and hindlimb length showed significant differences between species even after accounting for size effects (p < 0.05, Appendix B Table B2.2), with *T. lepidus* being the lizard with relatively longer limbs.

Table 4.1 Mean values of variables obtained from morphological, performance and ecophysiological spaces. The values are followed by the standard deviation of each variable. The abbreviations of the variables are as follows: Weight (W), snout to vent length (SVL), head size (HS), trunk length (TRL), fore limb length (FLL), hind limb length (HLL), bite force (BF), maximum sprint speed (MaxSPR), maximum trunk angle bending (TA), maximum head angle bending (HA), and minimum time to complete double-L racetrack (min_T), preferred temperature (T_{pref}), preferred temperature variance ($T_{pref}V$), evaporative water loss (EWL) and effective proportion of surface area that is wet (p_wet). Asterisks (*) denote statistically significant differences at an alpha level of 0.05 and dots (·) represent marginal differences (p ≈ 0.059).

Variable	*L. schreiberi*	*T. lepidus*	Significant differences	Significance adjusted for size
W	21.9 ± 4.3	84.5 ± 21.6	*	—
SVL	91.4 ± 7.4	144.3 ± 13.2	*	—
HS	19.7 ± 1.7	30.9 ± 3.5	*	—
TRL	46.1 ± 4.9	69.1 ± 7.3	*	—
HLL	45.7 ± 4.6	69.7 ± 5.2	*	*
FLL	32.4 ± 1.4	44.7 ± 3.1	*	*
BF	2.4 ± 0.1	2.8 ± 0.2	*	*
MaxSPR	5.6 ± 0.3	5.7 ± 0.4	—	—
Max_L	6.6 ± 2.9	5.2 ± 2.9	—	*
TA	147.1 ± 6.7	136.9 ± 12.2	*	—
HA	152.1 ± 10	151.4 ± 9.2	—	—
min_T	6.7 ± 2.9	5.15 ± 2.9	*	.
T_{pref}	30.4 ± 0.9	30.3 ± 0.6	—	—
$T_{pref}V$	4.5	2.4	*	—
EWL	0.9 ± 0.3	1.1 ± 0.4	*	—
P_wet	0.02 ± 0.008	0.01 ± 0.003	*	.

4.3.2. Locomotor and bite performance

We did not identify significant differences in maximum sprint speed between the two species ($F = 0.938$, $p = 0.346$, Table 4.1). Likewise, we did not detect any relationship between sprint speed and body size or any of the other size-corrected morphological traits (e.g. size- corrected forelimb length and hindlimb length) nor their interaction with species ($p > 0.05$ in all cases, Appendix B Table B2.3).

Concerning manoeuvrability, we found significant differences between species in trunk maximum bending angle ($F = 9.394$, $p = 0.004$), where *T. lepidus* exhibited lower angles than *L. schreiberi* (Table 4.1), but not in head maximum bending angle ($F = 0.033$, $p = 0.843$, Table 4.1). We found a significant negative relationship between trunk max bending angle and body size (Table 4.1), but once size effects were accounted for, differences between species were rendered non-significant (Appendix B Table B2.3). Variation in head max bending angle was not related to body size nor species (Appendix B Table B2.3). The maximum instantaneous speed in the double-L racetrack was not related to body size, and once size effects were considered, *L. schreiberi* was relatively faster (Appendix B Table B2.3). However, *L. schreiberi* took significantly longer to complete the racetrack ($F = 3.898$, $p = 0.048$, Table 4.1), and the time to complete the racetrack was inversely related to body size. Differences between species became marginally non-significant when accounting for size variation (Appendix B Table B2.3). Overall, *L. schreiberi* had a higher proportion of successful turns in the manoeuvrability experiments, and it showed a higher proportion of successful turns in the first turn ($X^2 = 6.232$, $p = 0.012$, Figure 4.2), but not in the second turn ($X^2 = 3 \times 10^{-30}$, $p = 0.999$, Figure 4.2). *T. lepidus* had more crashes on the wall during the first turn ($X^2 = 5.552$, $p = 0.018$, Figure 4.2), but not during the second turn ($X^2 = 3 \times 10^{-32}$, $p = 0.999$, Figure 4.2). *Lacerta schreiberi* was significantly more successful in stopping before both the first ($X^2 = 11.162$, $p = 0.001$, Figure 4.2) and the second turn ($X^2 = 9.267$, $p = 0.002$, Figure 4.2), whereas *T. lepidus* had a higher proportion of successful turns without stopping in the second ($X^2 = 15.121$, $p = 0.0001$, Figure 4.2), but not in the first turn ($X^2 = 2.275$, $p = 0.131$, Figure 4.2). Binomial mixed models showed that body size did not significantly relate to turning success, stops before the turn or maximum speed in the racetrack ($p > 0.05$ in all cases, Appendix B Table B2.4). However, in the second turn, when maximum speed and stops before the turn were added to body size in the model, there was a significant effect on turn success and species ($p < 0.05$, Appendix B Table B2.4).

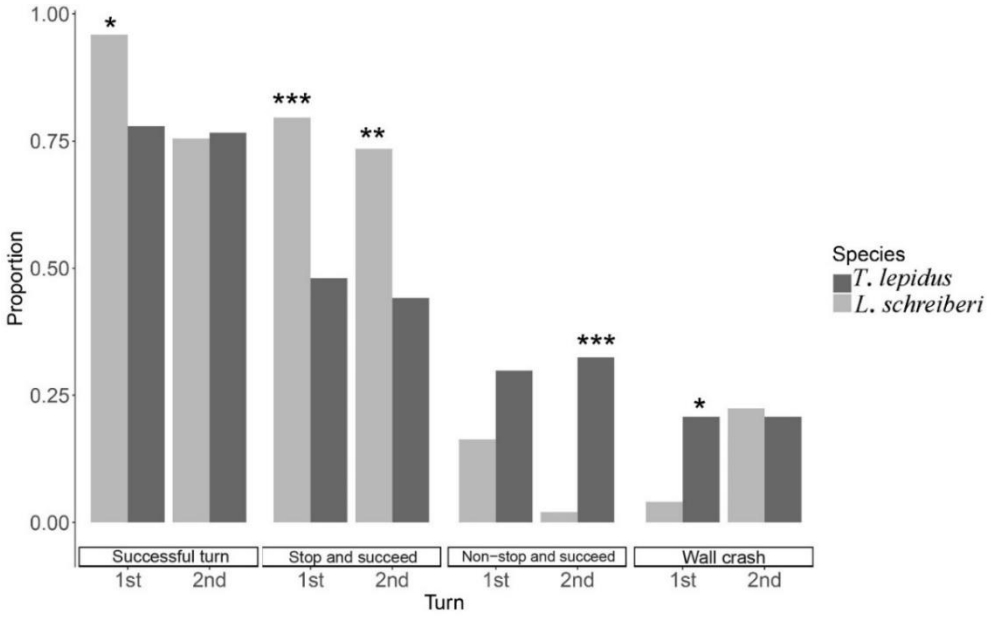

Figure 4.2 Proportion of exhibiting each turning behavior during the first and second turn of the double-L racetrack in the two species studied. Statistically significant differences between species are marked with * (α <0.05), ** (α <0.01) and *** (α <0.001). Reprinted with permission from Reyes-Puig, C. (2024). Is it all about size? Dismantling the integrated phenotype to understand species coexistence and niche segregation. Functional Ecology, 38(11), 3081–3099. © John Wiley & Sons Ltd.

There was also a significant positive relationship between bite force and body size, with *T. lepidus* exhibiting the highest raw bite force values (Table 4.1). Additionally, we detected a significant difference between species (Table 4.2), with *L. schreiberi* showing relatively higher adjusted bite force values. However, we found no significant differences in bite force when using head size as a covariate, independent of body size (Table 4.2).

Table 4.2 Results of ANCOVAs performed on bite force (BF) to test for differences between the two species (Sp) of green lizards (*Timon lepidus* and *Lacerta shreiberi*), considering weight (log W) and size corrected head size (res.HS) as covariate.

Model	Source	Df	SS	Rsq	Z	Pr(>F)
BF ~ Sp	**Sp**	1	1.373	0.604	4.641	**0.001****
	Residuals	41	0.898	0.395		
	Total	42	2.272			
BF ~ log(W)*Sp	**log(W)**	1	1.808	0.796	6.113	**0.001****
	Sp	1	0.052	0.023	1.755	**0.032***
	log(W)*Sp	1	0.001	0.001	-0.624	0.730
	Residulas	39	0.409	0.180		
	Total	42	2.272			
res.bf ~ res.HS*Sp	**res.HS**	1	0.014	0.031	0.711	0.245
	Sp	1	0.005	0.012	0.084	0.471
	res.HS*Sp	1	0.011	0.024	0.526	0.310
	Residulas	39	0.431	0.931		
	Total	42	0.463			

4.3.3. Preferred body temperatures and water loss rates

Mean and median preferred temperatures did not differ significantly between the two species (F = 0.066, p = 0.840 and F = 0.995, p = 0.343, respectively, Table 4.1). However, temperature variance did (F = 21.347, p = 0.001): *L. schreiberi* showed greater amplitude in body temperature values and a skewed distribution towards lower temperatures than *T. lepidus* (Table 4.2 and 4.3). Body size had no effect on preferred temperature but significantly negatively affected temperature variance, making species differences non-significant (Table 4.3). Raw evaporative water loss differed significantly between species (F = 6.731, p = 0.001), with *T. lepidus* showing higher values than *L. schreiberi* (Table 4.1). However, this relationship became non-significant when accounting for body weight (Table 4.3). The effective proportion of surface area that was wet was higher in *L. schreiberi* compared to *T. lepidus* (F = 126.12, p = 0.001, Table 4.1), but this difference became marginally non- significant when accounting for body weight (Table 4.3).

Table 4.3 Results of ANCOVAs performed on ecophysiological traits to test for differences between the two species (Sp) of green lizards (*Timon lepidus* and *Lacerta shreiberi*), considering body weight (log W) as a covariate. The abbreviations of the variables are as follows: preferred temperature (T_{pref}), preferred temperature variance (T_{pref} V), evaporative water loss (EWL), and effective proportion of surface area that is wet (p_wet).

Model	Source	Df	SS	Rsq	Z	Pr(>F)
T_{pref} ~ log(W)*Sp	**log(W)**	1	0.008	3.5×10^{-4}	-1.382	0.910
	Sp	1	0.629	0.025	0.526	0.321
	log(W)*Sp	1	0.050	0.002	-0.718	0.750
	Residuals	39	23.666			
	Total	42	24.354			
T_{pref} V~ log(W)*Sp	**log(W)**	1	46.995	0.207	2.761	**0.002***
	Sp	1	0.722	0.160	-0.486	0.692
	log(W)*Sp	1	3.860	0.017	0.386	0.367
	Residuals	39	175.036			
	Total	42	226.613			
EWL ~ log(W)*Sp	**log(W)**	1	1.071	0.233	2.401	**0.005****
	Sp	1	0.076	0.016	0.367	0.383
	log(W)*Sp	1	0.006	0.001	-0.888	0.784
	Residuals	39	3.439			
	Total	42	4.593			
p_wet ~ log(W)* Sp	**log(W)**	1	0.003	0.413	6.128	**0.001***
	Sp	1	9×10^{-5}	0.010	1.497	0.059.
	log(W)*Sp	1	1×10^{-5}	0.001	-0.116	0.562
	Residuals	39	0.005		-1.382	0.910
	Total	42	0.009			

4.3.4. Species position, overlap and association in multivariate phenotypic space

PCA on the dataset of all raw variables showed two clearly distinguishable groups, corresponding to the two species (Figure 4.3a). The first two PCs retained about 56% of variation in the data (Appendix B Table B2.5). The most important variables for interpreting the PCs were the linear morphological variables, which were highly correlated, plus bite force for PC1; the ecophysiological variables (mean preferred temperature, preferred temperature variance, effective proportion of surface area that is wet and evaporative water loss); and the trunk maximum bending angle (TA) for PC2 (Appendix B Table B2.6). On the other hand, the PCA analysis with the size-corrected variables resulted in a high overlap between species (Figure 4.3b). The first two PCs retained 49% variation (Appendix B Table B2.7). The size-corrected variables with the highest loadings on the PCs were size-corrected effective proportion of surface area that is wet, evaporative water loss, bite force and preferred temperature variance for PC1, and head size and trunk maximum bending angle for PC2 (Appendix B Table B2.8). Concerning the PCA analyses for raw morphological, performance and ecophysiological traits separately, the first two PCs captured 97%, 56%, and 64% of total variance, respectively (Appendix B Table B2.9). PC results for PERFORM and ECOPHY suggest that there was no major axis variation and rather indicate a spherical distribution of points in multivariate space (Appendix B Table B2.9). All variables were equally important for interpreting the PC1 in the MORPH dataset, and trunk length and hindlimb length for PC2; bite force and trunk maximum bending angle for PC1 and maximum sprint speed for PC2 in the PERFORM dataset; preferred temperature variance and evaporative water loss for PC1 and effective proportion of surface area that is wet for PC2 in the ECOPHY dataset (Appendix B Table B2.10). The relative overlap of PCs in MORPH variables showed two clearly distinguishable groups (Figure 4.3c), while in the PERFORM and ECOPHY datasets the PCs showed partial and total overlap respectively (Figure 4.3e–g). We identified that for the size-corrected res.MORPH, res.PERFORM and res.ECOPHY datasets the first two PCs cumulatively captured 62%, 56% and 75% of variance, respectively (Appendix B Table B2.11). The most important size-corrected variables for interpreting the PCs were size-corrected head size and trunk length for PC1 and forelimb length for PC2 in the res.MORPH dataset, bite force and head maximum bending angle for PC1 and trunk maximum bending angle for PC2 in the res.PERFORM, and effective proportion of surface area that is wet and evaporative water loss for PC1 and mean preferred temperature and preferred temperature variance for PC2 in the res.ECOPHY (Appendix B Table B2.12). Within the size-corrected datasets, we

identified that trunk length (res.TRL) was inversely related to head size, forelimb length and hindlimb length (res.HS, res.FLL and res.HLL). Likewise, bite force was inversely related to the components of manoeuvrability and sprint speed (res. HA, res.TA and res.MaxSRP). On the other hand, evaporative water loss (res.EWL) and surface area that is wet (res.p_wet) were positively correlated, while preferred temperature variance (res.$T_{pref}V$) and preferred temperature (T_{pref}) were inversely related among them (Appendix B Table B2.12; Figure 4.3h). The relative overlap of PCs was high in res. MORPH, res.PERFORM and res.ECOPHY (Figure 4.3).

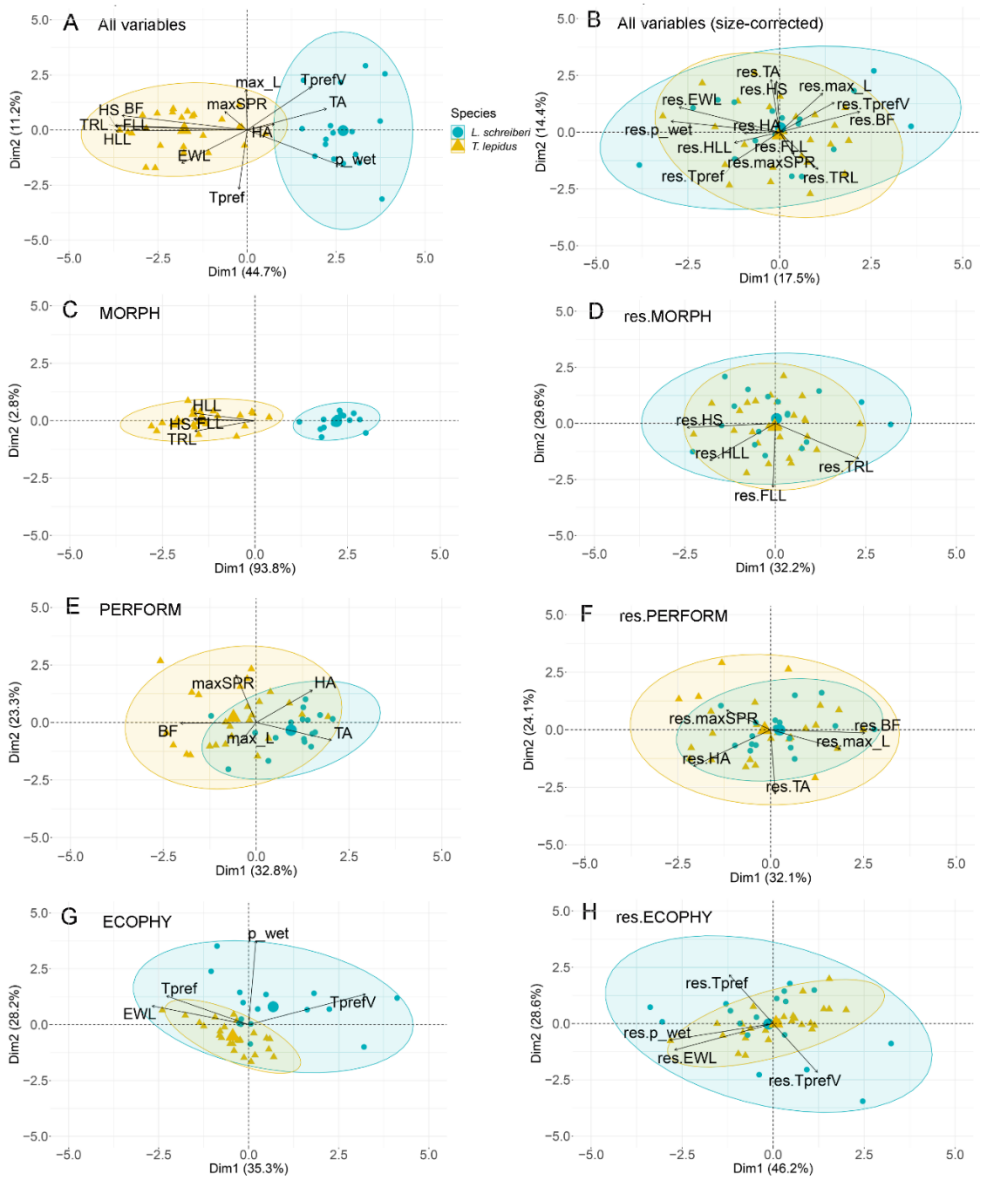

Figure 4.3 PCA plots representing the ordering of individuals of *Timon lepidus* (yellow triangles) and *Lacerta schreiberi* (blue dots) into the first two principal components of recorded phenotypic traits, before (left column) and after (right column) size correction, for different variable blocks. (A and B) All variables and (C and D) morphology (MORPH and res.MORPH datasets). (E and F) Functional performance (PERFORM and res.PERFORM datasets). (G and H) Ecophysiology (ECOPHY and res.ECOPHY datasets). The largest point and triangle in each group represents the centroid of each dataset. Reprinted with permission from Reyes-Puig, C. (2024). Is it all about size? Dismantling the integrated

phenotype to understand species coexistence and niche segregation. Functional Ecology, 38(11), 3081–3099. © John Wiley & Sons Ltd.

We found that, without correcting for body size effects, the variables with the greatest weight for discriminating species included all morphological traits, as well as bite force and to a lesser extent evaporative water loss, effective proportion of surface area that is wet, trunk maximum bending angle and preferred temperature variance (Figure 4.4; Appendix B Table B2.13). Once size effects were removed from the data, the variables that showed the greatest importance for species discrimination included forelimb length and maximum sprint speed in the positive and mean preferred temperature and bite force in the negative direction (Figure 4.4c; Appendix B Table B2.13).

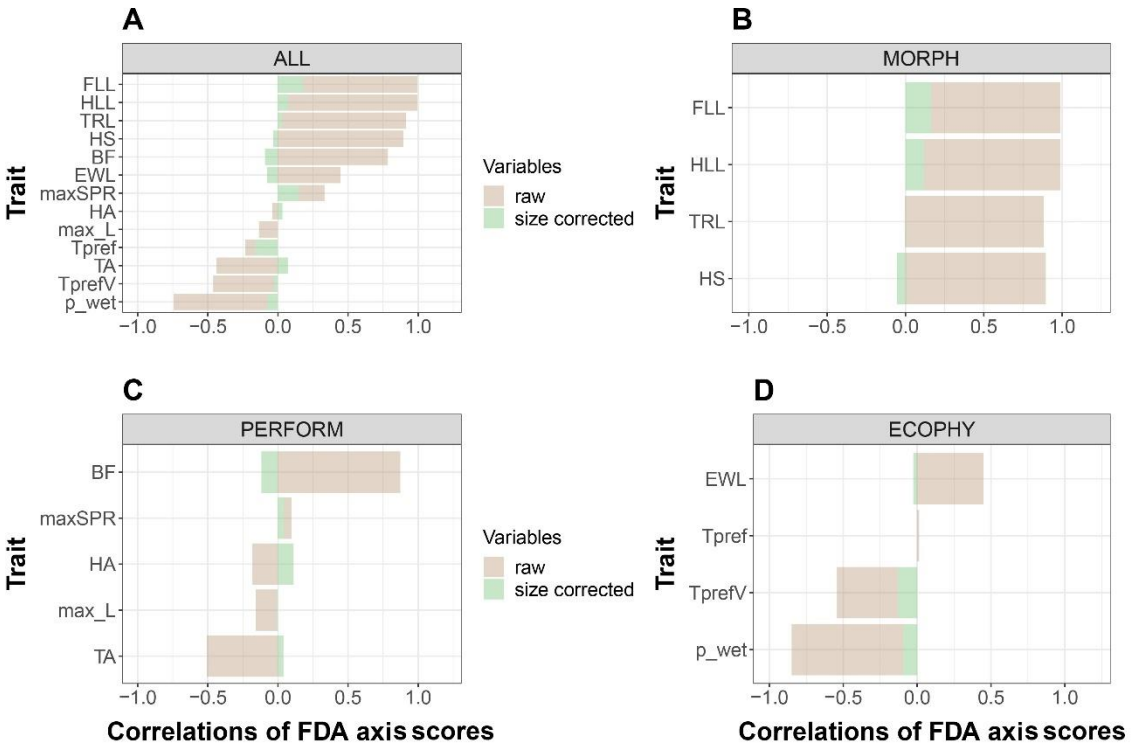

Figure 4.4 Correlations of FDA axis scores with phenotypic variables in two species of green lizards (*Timon lepidus* and *Lacerta schreiberi*). (A) FDA axes scores considering all raw and size-corrected variables in the dataset together. (B) FDA axes scores considering MORPH raw and size-corrected variables. (C) FDA axes scores considering PERFORM raw and size-corrected variables. (D) FDA axes scores considering ECOPHY raw and size-corrected variables (MORPH, PERFORM, ECOPHY). The abbreviations of the variables are as follows: Trunk length (TRL), head size (HS), fore limb length (FLL), hind limb length (HLL), maximum sprint speed (MaxSPR), maximum speed in the double-L racetrack (Max_L), maximum trunk angle bending (TA), maximum head angle bending (HA), bite force (BF), preferred temperature (T_{pref}), preferred temperature variance ($T_{pref}V$), evaporative water loss (EWL) and effective proportion of surface area that is wet (p_wet). Reprinted with permission from Reyes-Puig, C. (2024). Is it all about size? Dismantling the integrated phenotype to understand species coexistence and niche segregation. Functional Ecology, 38(11), 3081–3099. © John Wiley & Sons Ltd.

When we separated the raw variables MORPH, PERFORM and ECOPHY datasets, we detected that morphological variables are equally important with slightly

greater weight on limb length for the separation between groups (Figure 4.4b; Appendix B Table B2.13) in the MORPH dataset, bite force in the positive and trunk maximum bending angle in the negative direction (Figure 4.4c; Appendix B Table B2.13) in the PERFORM dataset, and evaporative water loss with positive direction, effective proportion of surface area that is wet in a negative direction (Figure 4.4d; Appendix B Table B2.13) in the ECOPHY dataset. When we separated variables obtained from their residuals (size-corrected), forelimb length, hindlimb length and head maximum bending angle, and bite force were the variables with the highest weight in res.MORPH and res.PERFORM dataset, respectively (Figure 4.4; Appendix B Table B2.13). By contrast, in the res.ECOPHY dataset the variables with the highest weight were the size-corrected preferred temperature variance and effective proportion of surface area that is wet (Figure 4.4; Appendix B Table B2.13). The two-block partial least-squares regression per- formed on raw variables showed significant association between MORPH and PERFORM (r = 0.85, p < 0.01), ECOPHY and MORPH (r = 0.85, p < 0.01) and also between PERFORM and ECOPHY (r = 0.77, p < 0.01). On the other hand, in the size-corrected data the PLS still showed significant association between res.MORPH and res.PERFORM (r = 0.49, p < 0.01), res.PERFORM and res.ECOPHY (r = 0.33, $p \leq 0.05$). PLS showed no association between res.MORPH and res.ECOPHY (r = 0.02, p = 0.87).

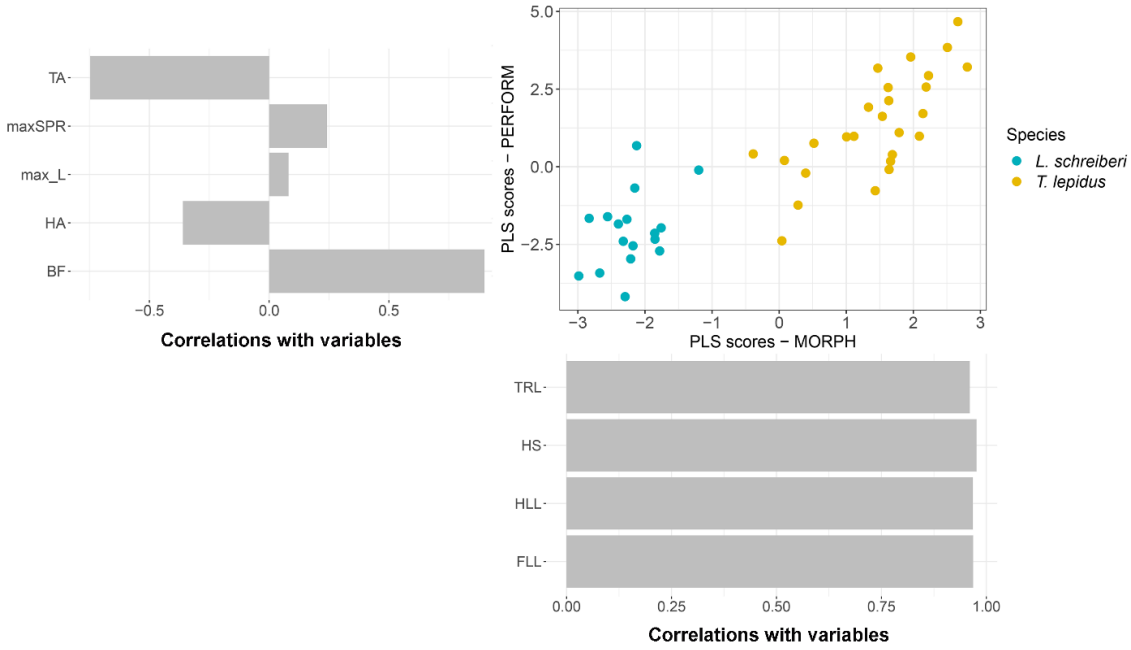

Figure 4.5 Scatter-plot of two species of green lizards scores obtained from partial least-squares (PLS) analysis between MORPH and PERFORM data sets, variables are not corrected by size. The bar-plots next to MORPH axis correspond to the correlations observed between that axis and PERFORM. The abbreviations of the variables are as follows: maximum sprint speed (maxSPR), maximum speed in the double-L racetrack (max_L) maximum trunk angle bending (TA), maximum head angle bending (HA), bite force (BF), trunk length (TRL), head size (HS), fore limb length (FLL), and hind limb length (HLL). Reprinted with permission from Reyes-Puig, C. (2024). Is it all about size? Dismantling the integrated

phenotype to understand species coexistence and niche segregation. Functional Ecology, 38(11), 3081–3099. © John Wiley & Sons Ltd.

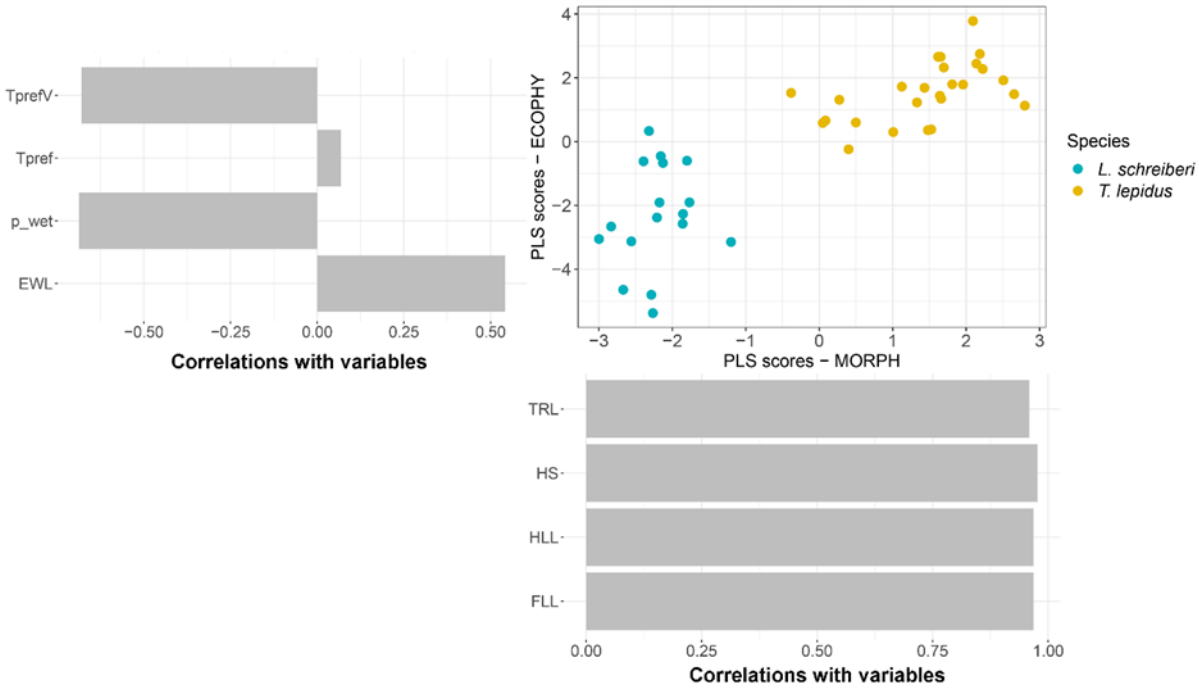

Figure 4.6 Scatter-plot of two species of green lizards scores obtained from partial least-squares (PLS) analysis between MORPH and ECOPHY data sets, variables are not corrected by size. The bar-plots next to MORPH axis correspond to the correlations observed between that axis and ECOPHY. The abbreviations of the variables are as follows: preferred temperature (T_{pref}), preferred temperature variance ($T_{pref}V$), evaporative water loss (EWL), effective proportion of surface area that is wet (p_wet), trunk length (TRL), head size (HS), fore limb length (FLL), and hind limb length (HLL). Reprinted with permission from Reyes-Puig, C. (2024). Is it all about size? Dismantling the integrated phenotype to understand species coexistence and niche segregation. Functional Ecology, 38(11), 3081–3099. © John Wiley & Sons Ltd.

The two-block partial least-squares regression performed on raw variables showed significant association between MORPH and PERFOM ($r = 0.85$, $p < 0.01$), ECOPHY and MORPH ($r = 0.85$, $p < 0.01$) and also between PERFOM and ECOPHY ($r = 0.77$, $p < 0.01$). On the other hand, in the size-corrected data the PLS still showed significant association between res.MORPH and res.PERFORM ($r = 0.49$, $p < 0.01$), and res.PERFORM and res.ECOPHY ($r = 0.33$, $p = < 0.05$). PLS showed no association between res.MORPH and res.ECOPHY ($r = 0.02$, $p = 0.87$). As expected, all PLSs incorporating body size have the effect of this trait on the associations in the data set (Figure 4.5, 4.6, 4.7). The PLS performed between MORPH and PERFORM showed that the variables most associated with morphology are bite force (BF) and trunk maximum bending angle (TA). With larger individuals having higher values of BF and lower values of TA (Figure 4.5). PLS between MORPH and ECOPHY showed that morphology is significantly associated with evaporative water loss (EWL), effective proportion of surface area that is wet (p_wet) and variance of preferred temperature ($T_{pref}V$); with

larger individuals having higher values of EWL and lower values of p_wet and $T_{pref}V$ (Figure 4.6). PLS between PERFORM and ECOPHY showed that larger individuals showed higher values of BF, lower values of TA, higher of EWL and lower values of p_wet and $T_{pref}V$ (Figure 4.7). On the other hand, PLSs performed on size-corrected data sets showed that morphology (res.MORPH) still associates with performance (res.PERFORM), being bite force (res.BF), trunk maximum bending angle (res.TA), maximum instantaneous speed in the double-L racetrack (res.max_L) and head size (res.HS) associated in the same direction (Figure 4.8), and maximum sprint speed (res.maxSPR) and trunk length (res.TRL) associated in the opposite direction to previous traits (Figure 4.8). As we did not find significant associations between res.MORPH and res.ECOPHY we did not interpret scatter-plot from PLS analysis (Figure 4.9). Finally, PLS between res.PERFORM and res.ECOPHY showed an association in same direction of res.TA, res.HA, res.p_wet and res.EWL, and res.BF, res.max_L and TprefV in the opposite direction to the previous traits (Figure 4.10).

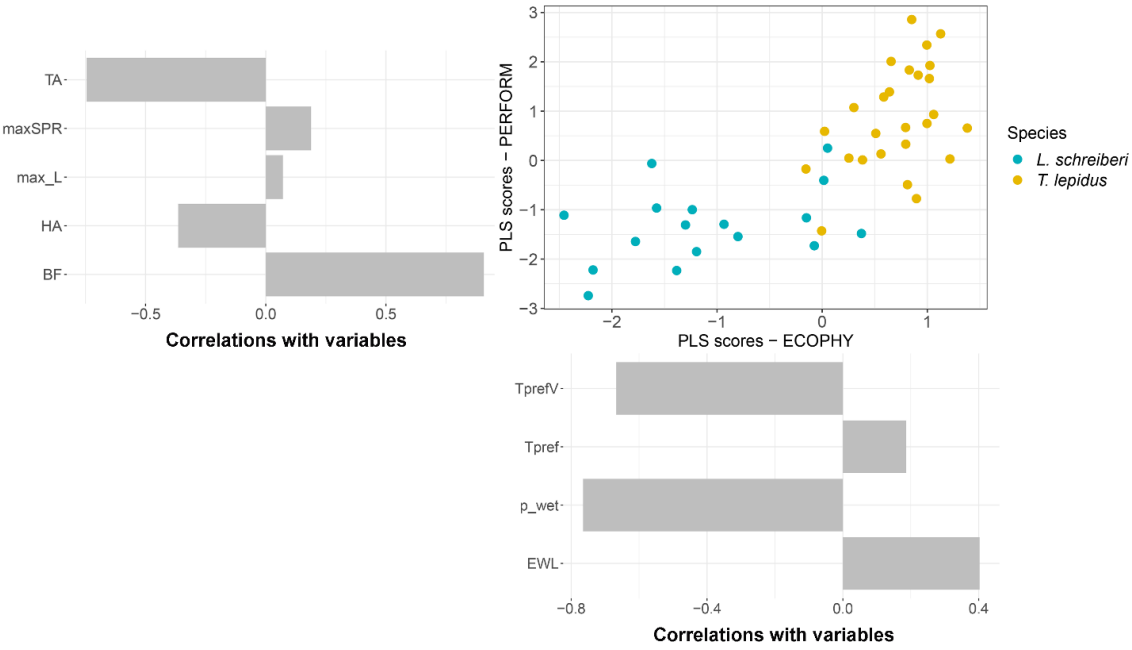

Figure 4.7 Scatter-plot of two species of green lizards scores obtained from partial least-squares (PLS) analysis between ECOPHY and PERFORM data sets, variables are not corrected by size. The bar-plots next to ECOPHY axis correspond to the correlations observed between that axis and PERFORM. The abbreviations of the variables are as follows: maximum sprint speed (maxSPR), maximum speed in the double-L racetrack (max_L) maximum trunk angle bending (TA), maximum head angle bending (HA), bite force (BF), preferred temperature (T_{pref}), preferred temperature variance (T_{pref} V), evaporative water loss (EWL), and effective proportion of surface area that is wet (p_wet). Reprinted with permission from Reyes-Puig, C. (2024). Is it all about size? Dismantling the integrated phenotype to understand species coexistence and niche segregation. Functional Ecology, 38(11), 3081–3099. © John Wiley & Sons Ltd.

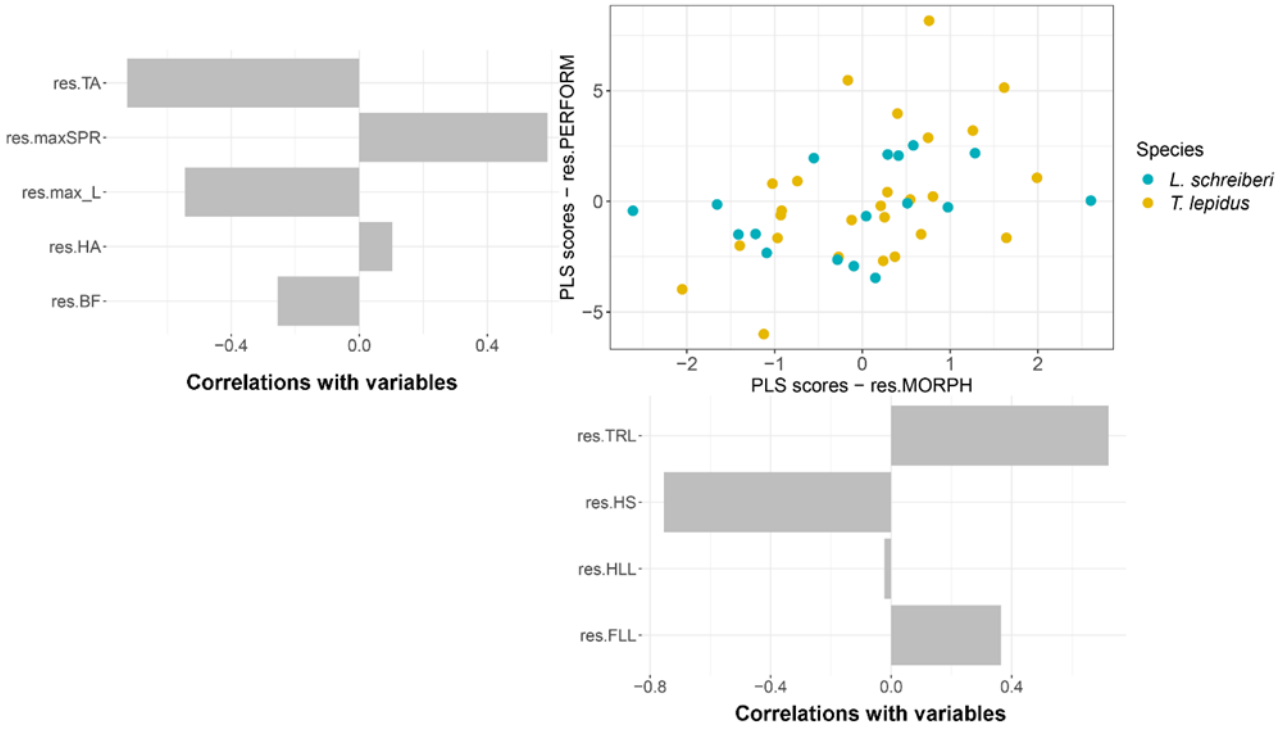

Figure 4.8 Scatter-plot of two species of green lizards scores obtained from partial least-squares (PLS) analysis between res.MORPH and res.PERFORM data sets, variables are corrected by size. The bar-plots next to res.MORPH axis correspond to the correlations observed between that axis and res.PERFORM. Trait abbreviations can be found in methodology. The abbreviations of the size corrected variables are as follows: maximum sprint speed (res.maxSPR), maximum speed in the double-L racetrack (res.max_L) maximum trunk angle bending (res.TA), maximum head angle bending (res.HA), bite force (res.BF), trunk length (res.TRL), head size (res.HS), fore limb length (res.FLL), and hind limb length (res.HLL). Reprinted with permission from Reyes-Puig, C. (2024). Is it all about size? Dismantling the integrated phenotype to understand species coexistence and niche segregation. Functional Ecology, 38(11), 3081–3099. © John Wiley & Sons Ltd.

The MANCOVA analysis showed a significant effect of body size when considering all raw variables (Table 4.4). However, we found no differences between species. The MANCOVA analysis for each data- set showed significant differences between species for the MORPH and ECOPHY datasets even when the effect of body size was taken into account (Table 4.4). In contrast, the PERFORM dataset exhibited no differences between species (Table 4.4).

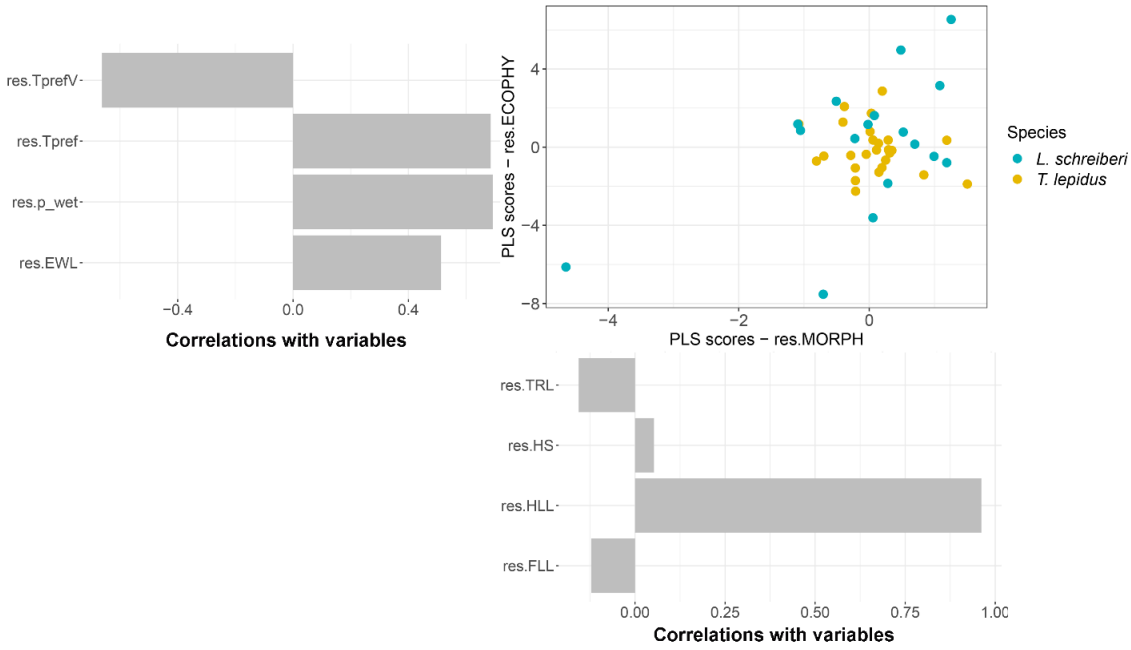

Figure 4.9 Scatter-plot of two species of green lizards scores obtained from partial least-squares (PLS) analysis between res.MORPH and res.ECOPHY data sets —variables are corrected by size. The bar-plots next to res.MORPH axis correspond to the correlations observed between that axis and res.ECOPHY. The abbreviations of the size corrected variables are as follows: preferred temperature (res.Tpref), preferred temperature variance (res.Tpref V), evaporative water loss (res.EWL), effective proportion of surface area that is wet (res.p_wet), trunk length (res.TRL), head size (res.HS), fore limb length (res.FLL), and hind limb length (res.HLL). Reprinted with permission from Reyes-Puig, C. (2024). Is it all about size? Dismantling the integrated phenotype to understand species coexistence and niche segregation. Functional Ecology, 38(11), 3081–3099. © John Wiley & Sons Ltd.

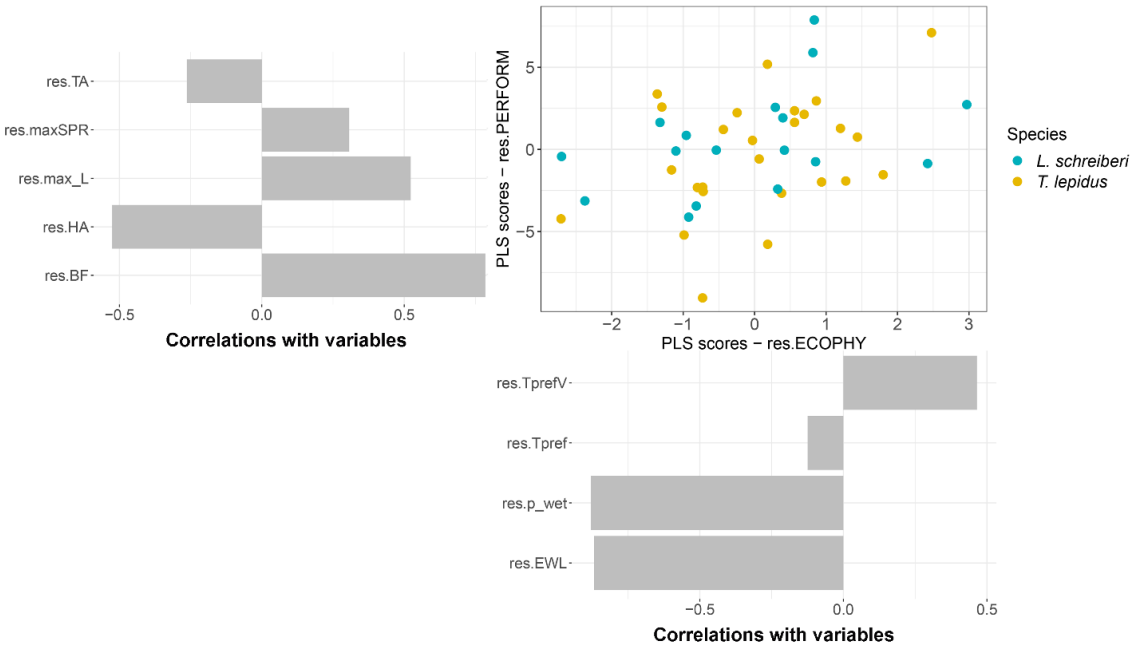

Figure 4.10 Scatter-plot of two species of green lizards scores obtained from partial least-squares (PLS) analysis between res.ECOPHY and res.PERFORM data sets —variables are not corrected by size. The bar-plots next to res.ECOPHY axis correspond to the correlations observed between that axis and res.PERFORM. The abbreviations of the size corrected variables are as follows: maximum sprint speed (res.maxSPR), maximum speed in the double-L racetrack (res.max_L) maximum trunk angle bending (res.TA), maximum head angle bending (res.HA), bite force (res.BF), preferred temperature (res.T_{pref}), preferred temperature variance (res.T_{pref}V), evaporative water loss (res.EWL), and effective proportion of

surface area that is wet (res.p_wet). Reprinted with permission from Reyes-Puig, C. (2024). Is it all about size? Dismantling the integrated phenotype to understand species coexistence and niche segregation. Functional Ecology, 38(11), 3081–3099. © John Wiley & Sons Ltd.

Table 4.4 MANCOVA table reporting multivariate comparisons between species in different datasets, considering body size as a covariate. Variables' abbreviations are shown in the methodology section. *p* value in bold when alpha α < 0.05. Abbreviations: df, degrees of freedom; Roy, Roy's maximum root.

MANCOVA	df	Roy	Z	Pr(>Roy)	MANCOVA	df	Roy	Z	Pr(>Roy)
All variables					PERFORM				
Size	1	19.195	12.189	**0.001**	Size	1	1.14	4.52	**0.001**
Species	1	0.056	0.401	0.356	Species	1	0.09	0.944	0.188
Size × Species	1	0.055	0.393	0.359	Size × Species	1	0.028	−0.257	0.604
Full model	3	19.249	11.429	**0.001**	Full model	3	1.153	4.069	**0.001**
Residuals	39				Residuals	39			
MORPH					ECOPHY				
Size	1	39.766	13.136	**0.001**	Size	1	1.652	5.651	**0.001**
Species	1	0.228	1.961	**0.023**	Species	1	0.176	1.687	**0.044**
Size × Species	1	0.032	−0.122	0.552	Size × Species	1	0.09	0.823	0.218
Full model	3	39.959	14.602	**0.001**	Full model	3	1.889	4.992	**0.001**
Residuals	39				Residuals	39			

Complementarily, we quantitatively identify multivariate spaces using a hypervolume approach. Hypervolume overlap analyses showed that hypervolumes associated with bite force and performance had the greatest overlap, whereas morphological and eco- physiological hypervolumes had the least overlap (Table 4.5); however, the morphological hypervolume was the only one that included body size, and its difference in overlap was mainly due to the inclusion of this variable (Figure 4.11). The degree of hypervolume intersection varied between the morphological (∩ 1.7%; due to body size; see Figure 4.11), ecophysiological (∩ 16%), performance (∩ 64%) and bite force hypervolumes (∩ 74%) (Table 4.5). Hypervolume overlap assessed through Sørensen and Jaccard similarity indices showed that the morphological hypervolume including body size has the lowest degree of overlap between species, while the performance hyper- volumes (locomotor traits and bite force) have the highest degree of overlap. On the other hand, the ecophysiological hypervolumes showed that even when body size was removed, there was separation of spaces between species (Table 4.5).

Table 4.5 Metrics of phenotypic space occupancy and overlap estimated through hypervolume analyses between the two species of green lizards from northern Portugal.

Space	Species	Volume	Intersection	% intersection	Unique	% unique	Jaccard	Sørensen
Morphological	*T. lepidus*	0.024	0.008	1.7	0.022	97.02	0.015	0.0284
	L. schreiberi	0.035			0.017	96.17		
Bite force	*T. lepidus*	20.853	18.325	74.03	2.529	12.13	0.741	0.851
	L. schreiberi	22.225			3.9	17.55		
Locomotor performance	*T. lepidus*	95.965	76.147	63.73	19.818	20.65	0.637	0.779
	L. schreiberi	99.656			23.51	23.59		
Ecophysiology	*T. lepidus*	15.889	3.193	15.75	12.695	79.9	0.154	0.267
	L. schreiberi	7.571			4.378	57.83		

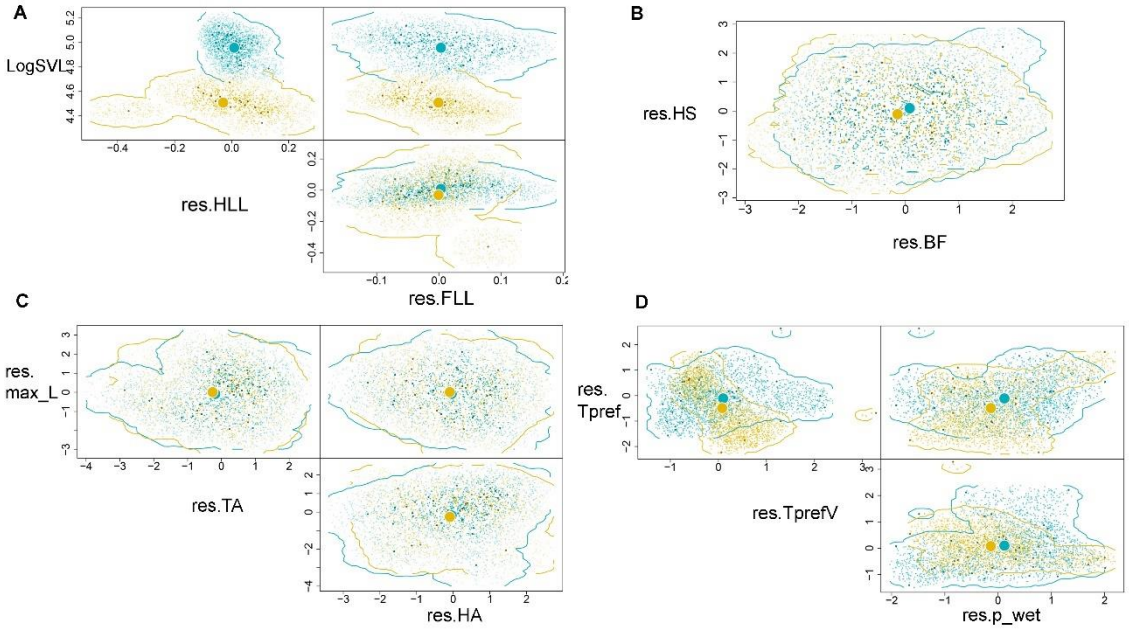

Figure 4.11 Phenotypic hypervolumes of *Timon lepidus* (yellow) and *Lacerta schreiberi* (blue). (A) Morphological hypervolume, (B) bite force hypervolume, (C) locomotor performance hypervolume and (D) ecophysiological hypervolume. Small dots represent resampled points derived from original data values while big dots represent the hypervolume centroids. The abbreviations of the variables are as follows: Snout to vent length (SVL), size-corrected head size (res.HS), size-corrected fore limb length (res.FLL), size-corrected hind limb length (res. HLL), size-corrected maximum speed in the double-L racetrack (res.max_L), maximum trunk angle bending corrected by size (res.TA), head angle bending corrected by size (res.HA), size-corrected bite force (res.BF), preferred temperature corrected by size (res. T_{pref}), preferred temperature variance corrected by size (res. $T_{pref}V$) and effective proportion of surface area that is wet corrected by size (res.p_wet). Reprinted with permission from Reyes-Puig, C. (2024). Is it all about size? Dismantling the integrated phenotype to understand species coexistence and niche segregation. Functional Ecology, 38(11), 3081–3099. © John Wiley & Sons Ltd.

4.4. Discussion

The phenotypic space is multidimensional, including all traits associated with morphology, physiology and behaviour (Murren, 2012; Wojczynski and Tiwari, 2008). With different ecological functions tightly linked to each of the axes of this

multidimensional phenotypic space, niche segregation along some or all of those axes can facilitate species coexistence (Valladares et al., 2015). However, research combining several phenotypic dimensions to systematically understand species coexistence and the role of size variation on different aspects of the phenotype are scarce. To address this research gap, we performed a comprehensive comparison of different phenotypic dimensions and their degree of overlap/segregation in two coexisting lizard species, while also putting body size variation into perspective.

By integrating the multivariate phenotypic space including morphological, functional performance and ecophysiological traits we were able to identify body size as the main driver that dominates variation, and therefore a major factor contributing to niche segregation. This reinforces the importance of size, which mediates most of the functions of organisms from metabolism (Angilletta Jr., 2009) to reproductive and behavioural strategies (Eldøy et al., 2021; Quinn and Foote, 1994; Wells, 1988). The effect of body size on phenotypic traits is pervasive, causing most other traits to respond directly to body size scaling (Chown and Gaston, 2010; Chown and Klok, 2003; Laube et al., 2013). Size effects can directly impact the trophic niche, for example, where larger animals with larger heads consume larger prey items that are not available to smaller organisms (Kaliontzopoulou et al., 2012). Instead, by looking at size-free phenotypic spaces it is possible to unveil the extent to which specific traits further contribute to niche segregation in co-occurring species, independently of body size. Across the three distinct phenotypic spaces, we detected that only the morphological and ecophysiological spaces maintain niche segregation after body size effects were accounted for. Specific traits in each space appear to have a greater contribution to such segregation, including relative limb length and traits associated with both thermal and hydric physiology. Other investigations have been concordant in finding size-free axes of major importance for niche segregation (Attum et al., 2007; Lu et al., 2011; Redtfeldt and Davis, 1996). For instance, in studies with Darwin's finches it has been observed that beak size, independent of body size, correlates with the ability to exploit different types of seeds, influencing diet preferences and ecological niches in coexisting species (Herrel et al., 2005; Van der Meij and Bout, 2006). Another example comes from dune lizards, where changes in morphological traits such as limb lengths and their relationship to habitat adaptations, highlighting the importance of size-independent traits in understanding habitat preferences and strategies for coping with coexistence (Attum et al., 2007). Although several authors have recently emphasized the relevance of understanding multivariate niche spaces (e.g. Anderson et al., 2023; Carvalho and Cardoso, 2020;

Castro-Arellano and Lacher, 2009), studies that implement an integrated framework to disentangle the different axes of phenotypic space and better understand the mechanisms that contribute to species coexistence are limited.

For instance, the interplay between performance and morphology is a well-known established paradigm for understanding phenotypic trait coevolution (Arnold, 1983). Here, it aids us in gaining a clearer understanding on how segregation occurs to support species coexistence. It appears that, at least in the system of green lizards studied here, body size contributes to species differentiation in traits related to trophic ecology and spatial behaviour, such as bite force and angles of locomotor manoeuvrability (Gomes et al., 2018; Huyghe et al., 2005; Vasilopoulou-Kampitsi, 2020; Verwaijen et al., 2002), but not in other traits such as maximum speed (Gomes et al., 2016; Irschick and Losos, 1998). Interestingly, other studies have already reported sprint speed equivalence in co-existing species (Gomes et al., 2018; Žagar et al., 2017), and apparently the lack of direct competition between *T. lepidus* and *L. schreiberi* could be related to our results. Furthermore, *T. lepidus* uses more open spaces, in which it might encounter fewer obstacles when escaping, while *L. schreiberi* is more associated with vertical vegetation (Salvador, 1988), so it probably manoeuvres better in this stratum. Further differences between species existed in the strategy used for successfully manoeuvring and turning in complex environments, where *L. schreiberi* turned successfully when stopping before curving at the double L-racetrack angles, while, on the contrary, *T. lepidus* tended not to stop before curving. Put together, these results suggest that predator escape or territory defence, as might be reflected in sprinting performance, are not as important for niche segregation, but instead the conformation of the structural habitat used by both species seems more relevant. Indeed, *L. schreiberi* typically moves within and on top of vegetation and strata such as shrubs, ferns, etc., both for thermoregulation and when escaping predators, and it even has the ability to swim (Brito, Luis, et al., 1998; Brito, Paulo, and Crespo, 1998; Mateo, 2017). This kind of spatial behaviour gives it a potential advantage of first observing the environment and then, in case of an eventual threat, deciding to flee. Instead, *T. lepidus* tends to move in more open and exposed environments, and it typically has a fast escape behaviour mainly on the ground or on rock walls (Fargallo et al., 2020; Mateo, 2017; Sannolo et al., 2019). Thus, the behaviour of organisms affects their performance and other phenotypic traits of the niche. Some individuals depending on their size may be bolder to run or may have different strategies to cope with species' interactions (e.g. more exploratory behaviour) (Damas-Moreira et al., 2019; Žagar et al., 2022). Thus, in the context of species coexistence, mechanisms

to segregate niches may also relate to complex behavioural strategies and trophic level (e.g. size-dependent bite force) (Herrel et al., 2001; Ho et al., 2021). Preliminary results with the individuals analysed in this work using stable isotopes have shown that *T. lepidus* and *L. schreiberi* differ in their overall diet based on the proportions of carbon and nitrogen signatures (unpublished data).

In the context of our study and with the aim of understanding niche segregation free from the effect of body size in coexisting species, we followed a multivariate strategy. From this perspective, the size-corrected morphological space examined in isolation shows differentiation between species (Table 4.4). The results of the PCA, FDA, and univariate data (Appendix B Table B2.2) establish relative limb lengths as the main traits contributing to species differentiation in the morphological space, after accounting for variations in body size. However, we did not find a direct relationship with any of the variables studied in our experiments. Limb variation may be a consequence of differential habitat use that is not related to escape speed in our study models. As mentioned by other authors (Brito, Paulo, and Crespo, 1998; Marco and Pollo, 1993) and by our direct observations in Castro de São Paio, *T. lepidus* uses more open areas, and *L. schreiberi* tends to occupy more closed and shrubby areas. So, these variations in the composition of the vertical stratum may shape the morphology of the limbs, where lizards that use open areas tend to change their limb posture and vary the use of the habitat stratum (Fuller et al., 2011; Vanhooydonck and Van Damme, 2003).

On the other hand, species distribution in (size corrected) ecophysiological space highlights that, apart from the metabolic functions that respond directly to body size (Angilletta Jr., 2009; Angilletta Jr. et al., 2004; Nagy, 2005), there are size-free processes that differentiate species and may therefore contribute to a more efficient segregation of the ecophysiological niche. A closer examination of individual ecophysiological traits revealed that mean and median preferred temperature was not different between species, but the temperature variance was, and it was also negatively related to body size. That is, smaller individuals showed a greater temperature variance during the experimental period, with greater variance in the afternoon hours in contrast to the morning hours (Table 4.3). This variation may be due to constraints associated with morphological traits, thermoregulation behaviour, metabolic rate variation or genetic variability (Angilletta Jr., 2009; Kohlsdorf and Navas, 2006; Phillips et al., 2016; Sannolo et al., 2018; S'khifa et al., 2020). Thus, one of the likely explanations for this variation in preferred temperatures is that the thermoregulation of *L. schreiberi* may be more limited by its hydro-regulatory processes. As such, *L. schreiberi* may struggle to maintain its T_{pref}

over longer periods of time, unlike *T. lepidus*. Consequently, individuals have more variable body temperatures leading to an overall skewed distribution of temperatures (as shown in Appendix B Table B2.5). In this context larger animals tend to retain heat more effectively and for a longer period of time (thermal inertia), while smaller animals lose heat more easily (Angilletta Jr., 2009), which could change their thermoregulatory behaviour and increase the variance in temperature. Concerning water loss, it can be explained primarily by differences in skin exposure relative to body size. However, adaptations associated with skin texture and morphology may influence the rates associated with evaporative water loss (Eynan and Dmi'el, 1993) even when the effect of body size is removed. Although size-corrected evaporative water loss was not different between the two species (Appendix B Table B2.6) and the effective surface area that is wet was marginally non-significant (Appendix B Table B2.12), the multivariate results from the ECOPHY dataset (Tables 4.4 and 4.5; Figure 4.11) reinforce that this space is highly relevant for species segregation, when variables are considered in concert. These results make sense in light of field observations at a geographic scale, where *L. schreiberi* has a more hydrophilic behaviour, while *T. lepidus* is more related to the Mediterranean climate (Llorente et al., 1995).

The partitioning of multivariate spaces allows us to understand that niche segregation occurs simultaneously on several combined axes of the phenotype, rather than on univariate traits. For example, univariate ecophysiological traits (i.e. mean preferred temperature, preferred temperature variance, effective surface area that is wet) did not show clear differences between species. However, when we used a multivariate approach and assessed the entire ecophysiological phenotypic space, we verified that species' segregation is evident (Tables 4.4 and 4.5). Our field observations on thermal and hydric ecology, conducted separately, align closely with those from our laboratory results (*pers. obs*.). Additionally, our observations suggest microhabitat differences in relative humidity between the two species, alongside temporal activity variations, which may contribute to niche segregation, as has already been observed in other organisms (Martínez-Freiría et al., 2010; Navarro et al., 2013).

Contrary to our expectations, we detected greater intersection and therefore suggested an overlap of the corresponding niches in the size-corrected hypervolumes of variables associated to functional performance (bite force and locomotor performance). Indeed, the shape of these hypervolumes was homogeneous and without gaps between species (Figure 4.11b,c). On the other hand, the hypervolume representing the ecophysiological niche showed gaps and shape constrictions in the niche spaces (Figure

4.11d). By contrast, species segregation across the morphological hypervolume was totally dominated by body size, as we had predicted (Figure 4.11a). However, the phenotypic space associated with relative limb lengths still encompassed distinct hypervolumes for each species (Figure 4.11a). Interestingly, these results suggest that while body size facilitates niche segregation mostly through phenotypic shifts (changes in average position across phenotypic space), the ecophysiological space displays differentiation mainly through niche expansions and contractions (differences in niche amplitude) (Carvalho and Cardoso, 2020). Niche expansions refer to the broadening of a species' ecological niche, allowing it to tolerate a wider range of ecological components. On the other hand, niche contractions imply a reduction of the niche, indicating a more specialized and limited tolerance to particular ecological factors (Carvalho and Cardoso, 2020). In general terms, these species overlap their geographic distribution in certain regions, mainly in the north of the Iberian Peninsula. However, the complex spatial arrangement could provide niche spaces (e.g. ecophysiology, behaviour) for both species, which seem mainly when considering spaces related to water ecology, as thermal ecology seems to be more phylogenetically restricted within the family (Enriquez- Urzelai et al., 2022; Garcia-Porta et al., 2019; S'khifa et al., 2022). In this sense, multivariate phenotypic spaces are complex, and their interpretation becomes easier when decomposing them into variables that represent different niche aspects (Carvalho and Cardoso, 2020; Holt, 2009; Hothorn et al., 2011). By analysing our variables in separate hypervolumes, we were able to better understand each space, with a restricted number of variables responding to a particular dimension and to evaluate their relative contribution towards coexisting species' segregation.

Our findings confirm the usefulness of establishing integrated multivariate spaces not only to better understand ecological niche characterization but also niche segregation in coexisting species. This methodological view incorporating different lines of evidence is key to elucidate the mechanisms that facilitate coexistence among species. Taking into account our experimental trait view, we show that the ecological niche can be effectively segregated even when body size is removed from the phenotypic space. Trait-based approaches have been effective in integrating functional ecology with species coexistence theories, considering that trait dissimilarity is linked to reduced niche overlap between coexisting species (Kraft et al., 2008; Stubbs and Bastow Wilson, 2004). The view of species coexistence is not merely the competition for resources but also involves complex ecological interactions shaped by factors that define the niche (McPeek, 2014). This is confirmed by our results, in which physiological traits act differently in each

species, forming a segregated ecological niche. When species are similar in size, direct interspecific competition with interference may be expected (Martin and Martin, 2001; Zeng and Lu, 2009). However, when body sizes are relatively different, and trophic resources are available there are other areas of the niche that can be exploited (i.e. use of microhabitat strata, dietary composition), for example, size allows species to lengthen or shorten the dietary profile (Damas-Moreira et al., 2020; Gomez et al., unpublished data; Lu et al., 2011) without competing directly, although exploitative competition via ecological resources remains possible. Ecophysiological space has been shown in other research to be useful for understanding the mechanisms by which niche segregation may be enhanced (Horn and Riegle, 1981; Le Lagadec et al., 1998). With our contribution, we highlight that through niche segregation of ecophysiological traits, aided by a less marked segregation in other aspects of performance, organisms are able to exploit the available resources. This culminates in a differential use of the structural niche (free of size effect), including its microclimatic and physical characteristics, thus allowing species to potentially reduce direct competition.

References

Aasa, U., Jaric, S., Barnekow-Bergkvist, M., and Johansson, H. (2003). Muscle strength assessment from functional performance tests: Role of body size. *The Journal of Strength & Conditioning Research*, 17(4), 664–670. https://doi.org/10.1519/1533-4287(2003)017<0664:msaffp>2.0.co;2

Amarasekare, P. (2002). Interference competition and species coexistence. *Proceedings of the Royal Society of London. Series B: Biological Sciences*, 269(1509), 2541–2550. https://doi.org/10.1098/rspb.2002.2181

Anderson, R. O., Tingley, R., Hoskin, C. J., White, C. R., and Chapple, D. G. (2023). Linking physiology and climate to infer species distributions in Australian skinks. *Journal of Animal Ecology*, 92(10), 2094–2108. https://doi.org/10.1111/1365-2656.14000

Angilletta, M. J., Jr., Steury, T. D., and Sears, M. W. (2004). Temperature, growth rate, and body size in ectotherms: Fitting pieces of a life-history puzzle. *Integrative and Comparative Biology*, 44(6), 498–509. https://doi.org/10.1093/icb/44.6.498

Angilletta, M. J., Jr. (2009). Thermal adaptation: A theoretical and empirical synthesis. Oxford University Press.

Armstrong, R. A., and McGehee, R. (1976). Coexistence of species competing for shared resources. *Theoretical Population Biology*, 9(3), 317–328. https://doi.org/10.1016/0040-5809(76)90051-4

Arnold, S. J. (1983). Morpholgy, performance and fitness. *American Zoologist*, 23, 347–361.

Attum, O., Eason, P., and Cobbs, G. (2007). Morphology, niche segregation, and escape tactics in a sand dune lizard community. *Journal of Arid Environments*, 68(4), 564–573. https://doi.org/10.1016/j.jaridenv.2006.07.010

Ayers, D. Y., and Shine, R. (1997). Thermal influences on foraging ability: Body size, posture and cooling rate of an ambush predator, the python *Morelia spilota*. *Functional Ecology*, 11(3), 342–347. https://doi.org/10.1046/j.1365-2435.1997.00093.x

Barroso, F. M., Riaño, G., Sannolo, M., Carretero, M. A., and Rato, C. (2020). Evidence from *Tarentola mauritanica* (Gekkota: Phyllodactylidae) helps validate

thermography as a tool to infer internal body temperatures of lizards. *Journal of Thermal Biology*, 93, 102700. https://doi.org/10.1016/j.jtherbio.2020.102700

Bates, D., Mächler, M., Bolker, B., and Walker, S. (2014). Fitting linear mixed-effects models using lme4. *arXiv preprint*, arXiv:1406.5823. https://doi.org/10.18637/jss.v067.i01

Baudier, K., and O'Donnell, S. (2018). Complex body size differences in thermal tolerance among army ant workers (*Eciton burchellii parvispinum*). *Journal of Thermal Biology*, 78, 277–280. https://doi.org/10.1016/j.jtherbio.2018.10.011

Bedriaga, J. (1879). Herpetologische Studien. Archiv für Naturgeschichte, XLIV, 259–320.

Blonder, B. (2018). Hypervolume concepts in niche-and trait-based ecology. *Ecography*, 41(9), 1441–1455. https://doi.org/10.1111/ecog.03187

Blonder, B., Lamanna, C., Violle, C., and Enquist, B. J. (2014). The n-dimensional hypervolume. *Global Ecology and Biogeography*, 23(5), 595–609. https://doi.org/10.1111/geb.12146

Blonder, B., Morrow, C. B., Maitner, B., Harris, D. J., Lamanna, C., Violle, C., Enquist, B., and Kerkhoff, A. J. (2018). New approaches for delineating n-dimensional hypervolumes. *Methods in Ecology and Evolution*, 9(2), 305–319. https://doi.org/10.1111/2041-210X.12865

Brito, J. C., Luis, C., Godinho, M. R., Paulo, O. S., and Crespo, E. G. (1998). Bases para a Conservação do Lagarto-de-água (*Lacerta schreiberi*). Estudos de Biologia e Conservação da Natureza no 23 Instituto da Conservação da Natureza Ministerio do Ambiente, Lisboa.

Brito, J. C., Paulo, O. S., and Crespo, E. G. (1998). Distribution and habitats of Schreiber's green lizard (*Lacerta schreiberi*) in Portugal. *Herpetological Journal*, 8(4), 187–194.

Carlson, S. M., Olsen, E. M., and Vøllestad, L. A. (2008). Seasonal mortality and the effect of body size: A review and an empirical test using individual data on brown trout. *Functional Ecology*, 22, 663–673. https://doi.org/10.1111/j.1365-2435.2008.01416.x

Carretero, M. A., Roig, J. M., and Llorente, G. A. (2005). Variation in preferred body temperature in an oviparous population of *Lacerta* (*Zootoca*) *vivipara*. *The Herpetological Journal*, 15(1), 51–55.

Carvalho, J. C., and Cardoso, P. (2020). Decomposing the causes for niche differentiation between species using hypervolumes. *Frontiers in Ecology and Evolution*, 8, 243. https://doi.org/10.3389/fevo.2020.00243

Castro-Arellano, I., and Lacher, T. E. (2009). Temporal niche segregation in two rodent assemblages of subtropical Mexico. *Journal of Tropical Ecology*, 25(6), 593–603. https://doi.org/10.1017/S0266467409990186

Chown, S. L., and Gaston, K. J. (2010). Body size variation in insects: A macroecological perspective. *Biological Reviews*, 85(1), 139–169. https://doi.org/10.1111/j.1469-185X.2009.00097.x

Chown, S. L., and Klok, C. J. (2003). Water-balance characteristics respond to changes in body size in subantarctic weevils. *Physiological and Biochemical Zoology*, 76(5), 634–643. https://doi.org/10.1086/376919

Collyer, M. L., and Adams, D. C. (2019). RRPP: Linear model evaluation with randomized residuals in a permutation. *Procedure*. https://CRAN.R-project.org/package=RRPP

Colwell, R. K., and Rangel, T. F. (2009). Hutchinson's duality: The once and future niche. Proceedings of the National Academy of Sciences of the United States of America, 106(supplement_2), 19651–19658. https://doi.org/10.1073/pnas.0901650106

Damas-Moreira, I., Riley, J. L., Carretero, M. A., Harris, D. J., and Whiting, M. J. (2020). Getting ahead: Exploitative competition by an invasive lizard. *Behavioral Ecology and Sociobiology*, 74, 117. https://doi.org/10.1007/s00265-020-02893-2

Damas-Moreira, I., Riley, J. L., Harris, D. J., and Whiting, M. J. (2019). Can behaviour explain invasion success? A comparison between sympatric invasive and native lizards. *Animal Behaviour*, 151, 195–202. https://doi.org/10.1016/j.anbehav.2019.03.008

Daudin, F. M. (1802). Histoire Naturelle, génerale et particulièredes reptiles, ouvrage faisant suite, a l'histoiure naturelle, générale et particulière composée par Leclerc de Buffon, et redigée par C. S. *Sonnini. Dufart*, 3, 452.

de la Vega, G. J., and Schilman, P. E. (2017). Using eco-physiological traits to understand the realized niche: The role of desiccation tolerance in Chagas disease vectors. *Oecologia*, 185(4), 607–618. https://doi.org/10.1007/s00442-017-3986-1

Delgado, J. D., and Gómez, M. D. L. Á. (2016). Evidence of use of road drainage culverts by *Timon lepidus* (Daudin, 1802) in Western Andalusia*. Anales de Biologia*, 38, 63–67. https://doi.org/10.6018/analesbio.38.05

Eldøy, S. H., Bordeleau, X., Lawrence, M. J., Thorstad, E. B., Finstad, A. G., Whoriskey, F. G., Crossin, G. T., Cooke, S. J., Aarestrup, K., Rønning, L., Sjursen, A. D., and Davidsen, J. G. (2021). The effects of nutritional state, sex and body size on the marine migration behaviour of sea trout. *Marine Ecology Progress Series*, 665, 185–200. https://doi.org/10.3354/meps13670

Elton, C. (1927). The animal community. In C. S. Elton (Ed.), *Animal ecology* (pp. 239–256). The Macmillan Company.

Enriquez-Urzelai, U., Martínez-Freiría, F., Freitas, I., Perera, A., Martínez-Solano, Í., Salvi, D., Velo-Antón, G., and Kaliontzopoulou, A. (2022). Allopatric speciation, niche conservatism and gradual phenotypic change in the evolution of European green lizards. *Journal of Biogeography*, 49(12), 2193–2205. https://doi.org/10.1111/jbi.14497

Eynan, M., and Dmi'el, R. (1993). Skin resistance to water loss in agamid lizards. *Oecologia*, 95, 290–294. https://doi.org/10.1007/BF00323502

Fargallo, J. A., Navarro-López, J., Palma-Granados, P., and Nieto, R. M. (2020). Foraging strategy of a carnivorous-insectivorous raptor species based on prey size, capturability and nutritional components. *Scientific Reports*, 10(1), 7583. https://doi.org/10.1038/s41598-020-64504-4

Farley, C. T. (1997). Maximum speed and mechanical power output in lizards. *Journal of Experimental Biology*, 200(16), 2189–2195. https://doi.org/10.1242/jeb.200.16.2189

Farley, C. T., and Ko, T. C. (1997). Mechanics of locomotion in lizards. *Journal of Experimental Biology*, 200(16), 2177–2188. https://doi.org/10.1242/jeb.200.16.2177

Ferreira, C. C., Santos, X., and Carretero, M. A. (2016). Does ecophysiology mediate reptile responses to fire regimes? Evidence from Iberian lizards. *PeerJ*, 4, e2107. https://doi.org/10.7717/peerj.2107

Fuller, P. O., Higham, T. E., and Clark, A. J. (2011). Posture, speed, and habitat structure: Three-dimensional hindlimb kinematics of two species of padless geckos. *Zoology*, 114(2), 104–112. https://doi.org/10.1016/j.zool.2010.11.003

Galán, P. (2003). Anfibios y Reptiles del Parque Nacional de las Islas Atlánticas de Galicia. Naturaleza y Parques Nacionales. Serie Técnica, Ministerio de Medio Ambiente, Madrid.

Garcia-Porta, J., Irisarri, I., Kirchner, M., Kirchhof, S., Brown, J. L., MacLeod, A., Turner, A. P., Ahmadzadeh, F., Albadalejo, G., Crnobrnja-Isailović, J., de la Riva, I., Fawzi, A., Galán, P., Göçmen, B., Harris, D. J., Jiménez-Robles, O., Joger, U., Jovanović-Glavaš, O., Karış, M., … Wollemberg-Valero, K. C. (2019). Environmental temperatures shape thermal physiology as well as diversification and genome-wide substitution rates in lizards. *Nature Communications*, 10, 4077. https://doi.org/10.1038/s41467-019-11943-x

Garland, T., Jr., and Losos, J. B. (1994). Ecological morphology of locomotor performance in squamate reptiles. In T. Garland, Jr. and J. B. Losos (Eds.), Ecological morphology: Integrative organismal biology (pp. 240–302). University of Chicago Press.

Gomes, V., Carretero, M. A., and Kaliontzopoulou, A. (2016). The relevance of morphology for habitat use and locomotion in two species of wall lizards. *Acta Oecologica*, 70, 87–95. https://doi.org/10.1016/j.actao.2015.12.005

Gomes, V., Carretero, M. A., and Kaliontzopoulou, A. (2018). Run for your life, but bite for your rights? How interactions between natural and sexual selection shape functional morphology across habitats. *The Science of Nature*, 105, 1–12. https://doi.org/10.1007/s0011 4-017-1537-6

Gomes, V., Herrel, A., Carretero, M. A., and Kaliontzopoulou, A. (2020). New insights into bite performance: Morphological trade-offs underlying the duration and magnitude of bite force. *Physiological and Biochemical Zoology*, 93(3), 175–184. https://doi.org/10.1086/708248

Goodman, B. A., Miles, D. B., and Schwarzkopf, L. (2008). Life on the rocks: Habitat use drives morphological and performance evolution in lizards. *Ecology*, 89(12), 3462–3471. https://doi.org/10.1890/07-2093.1

Gravel, D., Guichard, F., and Hochberg, M. E. (2011). Species coexistence in a variable world. *Ecology Letters*, 14(8), 828–839. https://doi.org/10.1111/j.1461-0248.2011.01643.x

Grinnell, J. (1917). The niche-relationships of the California thrasher. *Auk*, 34(4), 427–433. https://doi.org/10.2307/4072271

Hastie, T., and Tibshirani. (2023). mda: Mixture and flexible discriminant analysis. R package version 0.5-4. https://search.r-project.org/CRAN0/refmans/mda/html/fda.html

Herrel, A., Damme, R. V., Vanhooydonck, B., and Vree, F. D. (2001). The implications of bite performance for diet in two species of lacertid lizards. *Canadian Journal of Zoology*, 79(4), 662–670. https://doi.org/10.1139/z01-031

Herrel, A., Podos, J., Huber, S. K., and Hendry, A. P. (2005). Bite performance and morphology in a population of Darwin's finches: Implications for the evolution of beak shape. *Functional Ecology*, 19(1), 43–48. https://doi.org/10.1111/j.0269-8463.2005.00923.x

Herrel, A., Van Damme, R., Vanhooydonck, B., Zaaf, A., and Aerts, P. (2000). Lizard locomotion: How morphology meets ecology. *Netherlands Journal of Zoology*, 50(2), 261–277. https://doi.org/10.1163/156854200505865

Ho, H. C., Tylianakis, J. M., and Pawar, S. (2021). Behaviour moderates the impacts of food-web structure on species coexistence. *Ecology Letters*, 24(2), 298–309. https://doi.org/10.1111/ele.13643

Holt, R. D. (2009). Bringing the Hutchinsonian niche into the 21st century: Ecological and evolutionary perspectives. *Proceedings of the National Academy of Sciences of the United States of America*, 106(supplement_2), 19659–19665. https://doi.org/10.1073/pnas.0905137106

Horn, M. H., and Riegle, K. C. (1981). Evaporative water loss and inter- tidal vertical distribution in relation to body size and morphology of stichaeoid fishes from California. *Journal of Experimental Marine Biology and Ecology*, 50(2–3), 273–288. https://doi.org/10.1016/0022-0981(81)90054-X

Hothorn, T., Müller, J., Schröder, B., Kneib, T., and Brandl, R. (2011). Decomposing environmental, spatial, and spatiotemporal components of species distributions. *Ecological Monographs*, 81(2), 329–347. https://doi.org/10.1890/10-0602.1

Hutchinson, G. E. (1957). Concluding remarks. *Cold Spring Harbor Symposia on Quantitative Biology*, 22, 415–427.

Hutchinson, G. E. (1978). An introduction to population ecology. Yale University Press.

Huyghe, K., Vanhooydonck, B., Scheers, H., Molina-Borja, M., and Van Damme, R. (2005). Morphology, performance and fighting capacity in male lizards, *Gallotia galloti*. *Functional Ecology*, 19, 800–807. https://doi.org/10.1111/j.1365-2435.2005.01038.x

Irschick, D. J., and Losos, J. B. (1998). A comparative analysis of the ecological significance of maximal locomotor performance in Caribbean Anolis lizards. *Evolution*, 52(1), 219–226. https://doi.org/10.1111/j.1558-5646.1998.tb05155.x

Irschick, D. J., Meyers, J. J., Husak, J. F., and Le Galliard, J. F. (2008). How does selection operate on whole-organism functional performance capacities? A review and synthesis. *Evolutionary Ecology Research*, 10(2), 177–196. https://doi.org/10.7275/R58G8HX6

Kaliontzopoulou, A., Adams, D. C., van der Meijden, A., Perera, A., and Carretero, M. A. (2012). Relationships between head morphology, bite performance and ecology in two species of *Podarcis* wall lizards. *Evolutionary Ecology*, 26, 825–845. https://doi.org/10.1007/s10682-011-9538-y

Kassambara, A. (2016). Factoextra: Extract and visualize the results of multivariate data analyses. R package version, 1.

Kearney, M. (2006). Habitat, environment and niche: What are we modelling? *Oikos*, 115(1), 186–191. https://doi.org/10.1111/j.2006.0030-1299.14908.x

Kearney, M., and Porter, W. (2009). Mechanistic niche modelling: Combining physiological and spatial data to predict species' ranges. *Ecology Letters*, 12(4), 334–350. https://doi.org/10.1111/j.1461-0248.2008.01277.x

Kearney, M. R., Munns, S. L., Moore, D., Malishev, M., and Bull, C. M. (2018). Field tests of a general ectotherm niche model show how water can limit lizard activity and distribution. *Ecological Monographs*, 88(4), 672–693. https://doi.org/10.1002/ecm.1326

Kearney, M. R., and Porter, W. P. (2017). NicheMapR—An R package for biophysical modelling: The microclimate model. *Ecography*, 40(5), 664–674. https://doi.org/10.1111/ecog.04680

Kohlsdorf, T., and Navas, C. A. (2006). Ecological constraints on the evolutionary association between field and preferred temperatures in Tropidurinae lizards. *Evolutionary Ecology*, 20, 549–564. https://doi.org/10.1007/s10682-006-9116-x

Kraft, N. J., Valencia, R., and Ackerly, D. D. (2008). Functional traits and niche-based tree community assembly in an Amazonian forest. *Science*, 322(5901), 580–582. https://doi.org/10.1126/science.1160662

Lappin, A. K., and Husak, J. F. (2005). Weapon performance, not size, determines mating success and potential reproductive output in the collared lizard (*Crotaphytus collaris*). *The American Naturalist*, 166(3), 426–436. https://doi.org/10.1086/432564

Larson, D. W. (1984). Habitat overlap/niche segregation in two *Umbilicaria* lichens: A possible mechanism. *Oecologia*, 62, 118–125. https://doi.org/10.1007/BF00377384

Laube, I., Korntheuer, H., Schwager, M., Trautmann, S., Rahbek, C., and Böhning-Gaese, K. (2013). Towards a more mechanistic understanding of traits and range sizes. *Global Ecology and Biogeography*, 22(2), 233–241.

Le Galliard, J. F., Chabaud, C., de Andrade, D. O. V., Brischoux, F., Carretero, M. A., Dupoué, A., Gavira, R. S. B., Lourdais, O., Sannolo, M., and Van Dooren, T. J. (2021). A worldwide and annotated data- base of evaporative water loss rates in squamate reptiles. *Global Ecology and Biogeography*, 30(10), 1938–1950. https://doi.org/10.1111/j.1466-8238.2012.00798.x

Le Lagadec, M. D., Chown, S. L., and Scholtz, C. H. (1998). Desiccation resistance and water balance in southern African keratin beetles (Coleoptera, Trogidae): The influence of body size and habitat. *Journal of Comparative Physiology B*, 168, 112–122. https://doi.org/10.1007/s003600050127

Llorente, G. A., Montori, A., Santos, X., and Carretero, M. A. (1995). Atlas de distribució dels Anfibis y Rèptils de Catalunya y Andorra. *El Grau, Figueres*: 192 pp.

Loureiro, A., Ferrand, N., Carretero, M. A., and Paulo, O. (Eds.). (2008). Atlas dos Anfíbios e Répteis de Portugal. Instituto da Conservação da Natureza e da Biodiversidade.

Lu, X., Gong, G., and Ma, X. (2011). Niche segregation between two alpine rosefinches: To coexist in extreme environments. *Evolutionary Biology*, 38, 79–87. https://doi.org/10.1007/s11692-010-9102-7

Marco, A., and Pollo, C. (1993). Análisis biogeográfico de la distribución del lagarto verdinegro (*Lacerta schreiberi* Bedriaga 1878). *Ecología*, 7, 457–466.

Martin, P. R., and Martin, T. E. (2001). Behavioral interactions between two coexisting wood warblers (Parulidae: *Vermivora*): *Experimental and empirical tests. Ecology,* 82, 207–218. https://doi.org/10.2307/2680097

Martínez-Freiría, F., Lizana, M., do Amaral, J. P., and Brito, J. C. (2010). Spatial and temporal segregation allows coexistence in a hybrid zone among two Mediterranean vipers (*Vipera aspis* and *V*. *latastei*). *Amphibia-Reptilia*, 31(2), 195–212. https://doi.org/10.1163/156853810791069001

Mateo, J. A. (2017). Lagarto ocelado—*Timon lepidus*. In A. Salvador and A. Marco (Eds.), Enciclopedia Virtual de los Vertebrados Españoles (pp. 1–52). Museo Nacional de Ciencias Naturales.

Mateo, J. A., and Castanet, J. (1994). Reproductive strategies in three Spanish populations of the ocellated lizard, *Lacerta lepida* (Sauria, Lacertidae). *Acta Oecologica*, 1, 215–229.

Mateo, J. A., and Cheylan, M. (1997). *Lacerta lepida* Daudin 1802. SEH & Muséum National d'Histoire Naturelle.

Mautz, W. J. (1980). Factors influencing evaporative water loss in lizards. *Comparative Biochemistry and Physiology Part A: Physiology*, 67(3), 429–437. https://doi.org/10.1016/S0300-9629(80)80019-3

McBrayer, L. D., and White, T. D. (2002). Bite force, behavior, and electromyography in the teiid lizard, *Tupinambis teguixin*. *Copeia*, 2002(1), 111–119. https://doi.org/10.1643/0045-8511(2002)002

McPeek, M. A. (2014). Limiting factors, competitive exclusion, and a more expansive view of species coexistence. *The American Naturalist*, 183(3), iii–iv. https://doi.org/10.1086/675305

Mevik, B. H., Wehrens, R., and Liland, K. H. (2011). pls: Partial least squares and principal component regression. R package version, 2(3).

Mi, C., Ma, L., Wang, Y., Wu, D., Du, W., and Sun, B. (2022). Temperate and tropical lizards are vulnerable to climate warming due to in- creased water loss and heat stress. *Proceedings of the Royal Society B: Biological Sciences*, 289(1980), 20221074. https://doi.org/10.1098/rspb.2022.1074

Morales, M. M., and Giannini, N. P. (2010). Morphofunctional patterns in Neotropical felids: Species co-existence and historical assembly. *Biological Journal of the Linnean Society*, 100(3), 711–724. https://doi.org/10.1111/j.1095-8312.2010.01461.x

Murren, C. J. (2012). The integrated phenotype*. Integrative and Comparative Biology*, 52(1), 64–76. https://doi.org/10.1093/icb/ics043

Nagy, K. A. (2005). Field metabolic rate and body size. *Journal of Experimental Biology*, 208(9), 1621–1625. https://doi.org/10.1242/jeb.01553

Navarro, J., Votier, S. C., Aguzzi, J., Chiesa, J. J., Forero, M. G., and Phillips, R. A. (2013). Ecological segregation in space, time and trophic niche of sympatric planktivorous petrels. *PLoS One*, 8(4), e62897. https://doi.org/10.1371/journal.pone.0062897

Olalla-Tárraga, M. Á., Rodríguez, M. Á., and Hawkins, B. A. (2006). Broad- scale patterns of body size in squamate reptiles of Europe and North America. *Journal of Biogeography*, 33(5), 781–793.

Pérez Mellado, V. (1982). Estructura en una taxocenosis de Lacertidae (Sauria, Reptilia) del sistema central. In Mediterránea. Serie de Estudios Biológicos, N. 6 (diciembre 1982) (pp. 39–64). Universidad de Alicante.

Peterson, C. C., and Husak, J. F. (2006). Locomotor performance and sexual selection: Individual variation in sprint speed of collared lizards (*Crotaphytus collaris*). *Copeia*, 2006(2), 216–224. https://doi.org/10.1643/0045-8511(2006)6

Phillips, B. L., Munoz, M. M., Hatcher, A., Macdonald, S. L., Llewelyn, J., Lucy, V., and Moritz, C. (2016). Heat hardening in a tropical lizard: Geographic variation explained by the predictability and variance in environmental temperatures. *Functional Ecology*, 30(7), 1161– 1168. https://doi.org/10.1111/1365-2435.12609

Pianka, E. R., and Huey, R. B. (1978). Comparative ecology, resource utilization and niche segregation among gekkonid lizards in the south- ern Kalahari. *Copeia*, 1978, 691–701. https://doi.org/10.2307/1443698

Pigot, A. L., Trisos, C. H., and Tobias, J. A. (2016). Functional traits reveal the expansion and packing of ecological niche space underlying an elevational diversity gradient in passerine birds. *Proceedings of the Royal Society B: Biological Sciences*, 283(1822), 20152013. https://doi.org/10.1098/rspb.2015.2013

Prins, H. H., De Boer, W. F., Van Oeveren, H., Correia, A., Mafuca, J., and Olff, H. (2006). Co-existence and niche segregation of three small bovid species in southern Mozambique. *African Journal of Ecology*, 44(2), 186–198. https://doi.org/10.1643/0045-8511(2006)6

Quinn, T. P., and Foote, C. J. (1994). The effects of body size and sexual dimorphism on the reproductive behaviour of sockeye salmon, *Oncorhynchus nerka*. *Animal Behaviour*, 48(4), 751–761. https://doi.org/10.1371/journal.pone.0216448

R Core Team. (2024). R: A language and environment for statistical computing. R Foundation for Statistical Computing. https://www.R-project.org/

Redtfeldt, R. A., and Davis, S. D. (1996). Physiological and morphological evidence of niche segregation between two co-occurring species of Adenostoma in California chaparral. *Ecoscience*, 3(3), 290–296. https://doi.org/10.1080/11956860.1996.11682345

Renet, J., Dokhelar, T., Thirion, F., Tatin, L., Pernollet, C. A., and Bourgault, L. (2022). Spatial pattern and shelter distribution of the ocellated lizard (*Timon lepidus*) in two distinct Mediterranean habitats. *Amphibia-Reptilia*, 43(3), 263–276.

Salvador, A. (1988). Selección de microhabitat del lagarto verdinegro (*Lacerta schreiberi*) (Sauria: Lacertidae). *Amphibia-Reptilia*, 9(3), 265–275. https://doi.org/10.1163/156853888X00350

Salvidio, S., Calvi, G., Lamagni, L., and Gardini, G. (2006). Primi dati sulla dieta della lucertola ocellata *Timon lepidus* (Daudin, 1802) in Italia. *Acta Herpetologica*, 1(1), 73–76. https://doi.org/10.13128/Acta_Herpetol-1253

Sannolo, M., Barroso, F. M., and Carretero, M. A. (2018). Physiological differences in preferred temperatures and evaporative water loss rates in two sympatric lacertid species. *Zoology*, 126, 58–64.

Sannolo, M., Ponti, R., and Carretero, M. A. (2019). Waitin'on a sunny day: Factors affecting lizard body temperature while hiding from predators. *Journal of Thermal Biology*, 84, 146–153. https://doi.org/10.1016/j.jtherbio.2019.07.001

Schoener, T. W. (1974). Resource partitioning in ecological communities: Research on how similar species divide resources helps reveal the natural regulation of species diversity. *Science*, 185(4145), 27–39. https://doi.org/10.1126/science.185.4145.27

Sears, M. W., and Angilletta, M. J., Jr. (2004). Body size clines in Sceloporus lizards: Proximate mechanisms and demographic constraints. *Integrative and Comparative Biology*, 44(6), 433–442. https://doi.org/10.1093/icb/44.6.433

Sillero, N., and García-Muñoz, E. (2010). Two new types of noose for capturing herps. *Acta Herpetologica*, 5, 259–263. https://doi.org/10.13128/Acta_Herpetol-9033

S'khifa, A., Carretero, M. A., Harris, D. J., and Slimani, T. (2022). Ecophysiological conservativeness and size-mediated plasticity in the High Mountain lizard *AtlantoLacerta andreanskyi* confirm its vulnerability to climate change. *Salamandra*, 58(2), 139–150.

S'khifa, A., Koziel, G., Vences, M., Carretero, M. A., and Slimani, T. (2020). Ecophysiology of a lacertid community in the high Moroccan mountains suggests conservation guidelines. *Journal of Thermal Biology*, 94, 102743. https://doi.org/10.1016/j.jtherbio.2020.102743

Smart, H. J., and Gee, J. H. (1979). Coexistence and resource partitioning in two species of darters (Percidae), *Etheostoma nigrum* and *Percina maculata*. *Canadian Journal of Zoology*, 57(10), 2061–2071. https://doi.org/10.1139/z79-272

Stevenson, R. D., Peterson, C. R., and Tsuji, J. S. (1985). The thermal dependence of locomotion, tongue flicking, digestion, and oxygen consumption in the wandering garter snake. *Physiological Zoology*, 58(1), 46–57. https://doi.org/10.1086/physzool.58.1.30161219

Streinzer, M., Huber, W., and Spaethe, J. (2016). Body size limits dim-light foraging activity in stingless bees (Apidae: Meliponini). *Journal of Comparative Physiology A*, 202, 643–655. https://doi.org/10.1007/s00359-016-1118-8

Stubbs, W. J., and Bastow Wilson, J. (2004). Evidence for limiting similarity in a sand dune community. *Journal of Ecology*, 92(4), 557–567. https://doi.org/10.1111/j.0022-0477.2004.00898.x

Tobalske, B. W., and Dial, K. P. (2000). Effects of body size on take-off flight performance in the Phasianidae (Aves). *Journal of Experimental Biology*, 203(21), 3319–3332. https://doi.org/10.1242/jeb.203.21.3319

Tokeshi, M. (2009). Species coexistence: Ecological and evolutionary perspectives. John Wiley & Sons.

Valladares, F., Bastias, C. C., Godoy, O., Granda, E., and Escudero, A. (2015). Species coexistence in a changing world. *Frontiers in Plant Science*, 6, 866. https://doi.org/10.3389/fpls.2015.00866

Van der Meij, M. A. A., and Bout, R. G. (2006). Seed husking time and maximal bite force in finches. *Journal of Experimental Biology*, 209(17), 3329–3335. https://doi.org/10.1242/jeb.02379

Vanhooydonck, B., and Van Damme, R. (2003). Relationships between locomotor performance, microhabitat use and antipredator behaviour in lacertid lizards. *Functional Ecology*, 17, 160–169.

Vasil'ev, A. G. (2021). The concept of morphoniche in evolutionary ecology. *Russian Journal of Ecology*, 52(3), 173–187. https://doi.org/10.1134/S1067413621030097

Vasilopoulou-Kampitsi, M. (2020). Manoeuvrability and the anotomy of the inner ear in lacertid lizards. An ecological approach. PhD thesis, University of Antwerp.

Verwaijen, D., Van Damme, R., and Herrel, A. (2002). Relationships between head size, bite force, prey handling efficiency and diet in two sympatric lacertid lizards. *Functional Ecology*, 16(6), 842–850. https://doi.org/10.1046/j.1365-2435.2002.00696.x

Webber, Q. M., and McGuire, L. P. (2022). Heterothermy, body size, and locomotion as ecological predictors of migration in mammals. *Mammal Review*, 52(1), 82–95. https://doi.org/10.1111/mam.12263

Wells, M. S. (1988). Effects of body size and resource value on fighting behaviour in a jumping spider. *Animal Behaviour*, 36(2), 321–326. https://doi.org/10.1016/S0003-3472(88)80001-0

Wickham, H., Averick, M., Bryan, J., Chang, W., McGowan, L. D., François, R., Grolemund, G., Hayes, A., Henry, L., Hester, J., Kuhn, M., Pedersen, T. L., Miller, E., Bache, S. M., Müller, K., Ooms, J., Robinson, D., Seidel, D. P., Spinu, V., … Yutani, H. (2019). Welcome to the tidyverse. *Journal of Open-Source Software*, 4(43), 1686. https://doi.org/10.21105/joss.01686

Williams, E. E. (1983). Ecomorphs, faunas, Island size, and diverse end points in Island radiations of Anolis. In R. B. Huey, E. R. Pianka, and T. W. Schoener (Eds.), Lizard ecology: Studies of a model organism (pp. 326–370). Harvard University Press.

Wojczynski, M. K., and Tiwari, H. K. (2008). Definition of phenotype. *Advances in Genetics*, 60, 75–105. https://doi.org/10.1016/S0065-2660(07)00404-X

Žagar, A., Carretero, M. A., and de Groot, M. (2022). Time changes everything: A multispecies analysis of temporal patterns in evaporative water loss. *Oecologia*, 198(4), 905–915.

Žagar, A., Carretero, M. A., Vrezec, A., Drašler, K., and Kaliontzopoulou, A. (2017). Towards a functional understanding of species coexistence: Ecomorphological variation in relation to whole-organism performance in two sympatric lizards. *Functional Ecology*, 31(9), 1780–1791. https://doi.org/10.1111/1365-2435.12878

Zeng, X., and Lu, X. (2009). Interspecific dominance and asymmetric competition with respect to nesting habitats between two snow finch species in a high-altitude extreme environment. *Ecological Research*, 24, 607–616. https://doi.org/10.1007/s11284-008-0530-0

Zobel, M. (1992). Plant species coexistence: The role of historical, evolutionary and ecological factors. *Oikos*, 65, 314–320. https://doi.org/10.2307/3545024

Chapter 5

Niche differentiation in coexisting species: ecological insights into the role of activity patterns, space use and environmental preferences

5.1. Introduction

For decades, the definition of the ecological niche has been a subject of debate among scientists (Elton, 1927; Grinnell, 1917; Hutchinson ,1957, 1978; Sales et al., 2021; Soberon and Peterson, 2005). From Hutchinson's seminal contribution in 1978 to the most current, biogeographically driven views of Soberon and Peterson in 2005, there is consensus that the ecological niche is a property of species, defined by a multidimensional space. This multidimensional space encompasses the species' interactions with their environment and with other species, including the use of available resources, while factors such as dispersal patterns, and life history traits influence how species occupy their niche. Together, this combination of factors shapes and defines the structure of the ecological niche (Sales et al., 2021). The ecological niche of a species comprises the fundamental niche, which includes abiotic, or scenopoetic, variables, and the realised niche, which is further moulded by biotic interactions with other species. Biotic interactions impose additional constraints, refining the niche beyond abiotic environmental conditions (Pearson, 2007).

Ecologically similar coexisting species—those that live in the same area with similar requirements—may interact in three ways: through direct interference (individuals interact directly via aggression), exploitation-competition (indirect competition for shared resources, which can lead to reduced availability of those resources), or by partitioning their niche (niche differentiation) (Begon et al., 1986; Dufour et al., 2015; Messerman et al., 2022; Pianka, 1974; Pianka, 2000;). Niche differentiation or segregation refers to the process through which coexisting species reduce competition and share the same geographical area without displacing each other (Chapman and Reiss, 1999; Pianka and Huey, 1978; Valladares et al., 2015). To reduce competition, coexisting species often specialize in different resources. These resources can include microhabitats with specific structural and physical configurations, microclimatic conditions (e.g., thermal and hydric regulation), thermoregulation spots, and trophic resources. Indeed, co-occurring species with generally similar environmental preferences may exhibit subtle differences in their particular ecophysiological requirements (e.g., selected temperatures, environmental humidity) (Díaz and Cabezas-Díaz, 2004; Reyes-Puig et al., 2024). These differences not only influence their rates of development, growth, survival, and behaviour but also enable them to exploit slightly different resources (Kearney and Porter, 2009; Messerman et al., 2022; Wolf, 1996).

On the other hand, the spatial distribution of coexisting species at local scales is a key factor in understanding niche differentiation (Dufour et al., 2015), as species may

utilize different types of available microhabitats, such as varying amounts of vegetation, structural features, or water sources (Dufour et al., 2015; Ganem et al., 2012; Meynard et al., 2012). Similarly, temporal segregation can be observed in the differential timing of foraging, breeding, and resting behaviours. This includes variations in daily and seasonal activity patterns, which are particularly relevant for investigating how species segregate their niche (Dufour et al., 2015; Ganem et al., 2012; Meynard et al., 2012). While studies addressing niche differentiation at the trophic level in coexisting species are abundant (Andriollo et al., 2021; Bezerra et al., 2024; Kingsbury et al., 2020; Kouete and Balckburn, 2020; MacArthur, 1958; Ramellini et al., 2024), other ways of reducing competition, including spatial (e.g., partitioning of space), environmental (e.g., differentiation in abiotic factors), temporal (e.g., activity levels or patterns) and, particularly, their combination are less explored overall.

A key factor in understanding how different species modulate resource use, segregate their niches, reduce competition, and achieve coexistence is body size (Anaya-Rojas et al., 2021; Basset, 1995; Reyes-Puig et al., 2024). Body size influences dispersal capacity and resource utilisation, enabling species of distinct sizes to exploit distinct resources, thereby reducing competition (Weil et al., 2023). Additionally, different phenotypic traits, such as head size and bite force, allow selective access to prey (Huyghe et al., 2005; Verwaijen et al., 2002), while limb length enables the use of different habitat structures (Irschick and Losos 1998). Since food resources are often limited by size (Prins and Olff, 1998; Ritchie and Olff, 1999), species with substantial differences in body size experience relaxed competition pressure when coexisting.

Due to notable differences in body size and ecophysiological parameters relevant for microhabitat use (Brito et al., 1998a, b; Marco, 2017; Reyes-Puig et al., 2024), *Timon lepidus* (ocellated lizard) and *Lacerta schreiberi* (Iberian emerald lizard) offer an outstanding model to explore niche segregation and obtain insights into how microhabitat use, space partitioning, environmental preferences, activity patterns and other components of the ecological niche are involved in species coexistence. Both species coexist in northern Portugal, allowing simultaneous observations, although they potentially exhibit differential use of microhabitats (Ferreira et al., 2016). *Timon lepidus* typically favours more open and semi-arid areas (Ferreira et al., 2016; Renet et al., 2022), whereas *L. schreiberi* shows a stronger preference for humid environments with abundant surrounding vegetation (Brito et al., 1998a, b; Salvador, 1988). Another relevant difference between the two species is in body size, where *T. lepidus* is quite larger (reaching 240 mm) than *L. schreiberi* (reaching 130 mm) (Brito et al., 1998b;

Mateo, 2017). Previous research suggested that body size differences between the two species may influence how they utilize environmental resources, leading to niche segregation (Reyes-Puig et al., 2024). Indeed, based on laboratory experiments, we found that the primary driver of niche segregation between both species is body size, but we also showed that morphological and ecophysiological traits, independent of size, also significantly contributed to such segregation (Reyes-Puig et al., 2024). Some of our previous observations revealed that niche differentiation primarily occurs in hydric ecophysiology, while thermal preferences were more uniform between both species (Reyes-Puig et al., 2024). Based on these laboratory observations, we suggested that microhabitat segregation may be a strong mechanism allowing the coexistence of these species in nature. Although there is some evidence that *T. lepidus* and *L. schreiberi* use microhabitats differently (e.g., Brito et al., 1998a; Ferreira et al., 2016), further investigation is needed to understand how their body size and ecophysiological differences determine spatial and temporal niche segregation in the field.

To fill this gap, here we integrate former knowledge on the physiology of these species from a field ecology perspective, to investigate real-world consequences of previous experimental findings and better understand how they drive species coexistence and niche differentiation in nature. For this purpose, we explore activity patterns, humidity and temperature in selected microhabitats, and inquire into their relationship with behaviour (type of activity in the field), microhabitat use, and fine-scale distribution. If the physiological differentiation between ocellated and the Iberian emerald lizards, as derived from lab experiments, drives their capacity for segregation and niche differentiation, we expect to find no significant differences in body temperatures between species but significant differences in the relative humidity of their microhabitats. We also anticipate observing differentiation in space use and microhabitat composition, considering that fine-scale spatial segregation allows for resource partitioning and thus may reduce interspecific competition in coexisting species. We expect some degree of overlap in activity patterns, as species living in similar environments may have comparable thermoregulatory strategies, resulting in overlapping active periods to optimize conditions for basking or foraging (Žagar et al., 2015). However, we speculate there may be variations between species, since seasonal activity patterns can vary in lizards (Adolph and Porter, 1993). Also, we presume specific relationships between activity time, abiotic variables, and body size, where lizards with larger body sizes may require extended basking periods, starting earlier in the morning to achieve optimal body temperatures (Angilletta Jr., 2009); while smaller lizards may be active at differential time

windows since their bodies reach optimal temperatures faster (Adolph and Porter, 1993; Angilletta Jr., 2009). In terms of behavioural observations (i.e., activities such as basking, foraging and sheltering) and their relationship to environmental variables, we hypothesize that temperature and humidity differentiation will be influenced by the type of activity. Given the influence of landscape conformation on microhabitat availability, we expect to find a spatial distribution of species occurrences related to this landscape structure.

5.2. Materials and Methods

5.2.1. Study area, model organisms and sampling design

In this study, we focused on two species of green lizards distributed in the north of Portugal, *Timon lepidus* (Daudin, 1802) *and Lacerta schreiberi* Bedriaga, 1879. The ocellated lizard *T. lepidus* is typically found in western Mediterranean regions (Sillero et al., 2009) and it is distributed in the Iberian Peninsula, southern France and Italy, ranging from sea level to 2000 meters in elevation (Mateo and Cheylan, 1997; Mateo, 2017). In contrast, the Iberian emerald lizard *L. schreiberi*, is an Atlantic species, endemic to the western Iberian Peninsula (Sillero et al., 2009), found from sea level to 2100 meters in elevation (Brito et al., 1998a; Marco and Pollo, 1993). The most remarkable morphological characteristic that distinguishes both species is their body size, with the ocellated lizard being the largest (reaching an SVL of 240 mm) and the Iberian emerald lizard the smallest (up to 130 mm) (Brito et al., 1998a; Marco, 2017). While *T. lepidus* is recognized for its high ecological flexibility (Galán, 2003; Llorente et al., 1995), *L. schreiberi* is closely associated with humid habitats such as moist deciduous forests and areas close to streams (Brito et al., 1998a).

In the period from January 2022 to mid-July2022 we sampled different areas and microhabitats in Castro de São Paio in northern Portugal (41.31°N, 8.74°W; 12 m asl, Figure 5.1), where syntopic (co-occurring) populations of *T. lepidus* and *L. schreiberi* are found. The landscape in Castro de São Paio comprises a diverse array of coastal features, including rocky shores, sandy beaches, and coastal vegetation (Araújo and Abrunhosa, 2012). To document landscape heterogeneity, capture variation in microhabitat abundance, and investigate their relationship with environmental variables, and with lizard activity, space use, and behaviour, we conducted random samplings throughout the study area, prioritising the most abundant microhabitats (Figure 5.1): i) herbaceous vegetation, areas with abundance of grasses, ferns, *Ulex* sp., *Carpobrotus* sp., and maize; ii) rocky substrates, including exposed natural rocks without direct

vegetation cover, stone walls following boundaries and delimiting agricultural zones in the study area, isolated rocks or groups of rocks emerging from the ground; iii) cement/rubble, encompassing area with materials such as cement debris, bricks, generally derived from building structures, forming artificial substrates; iv) walkway, that is, a wooden structure elevated above the ground, allowing safe passage of people across paths in the study area; v) soil devoid of herbaceous vegetation, composed of mineral particles and organic matter. Sampling was conducted during the normal activity hours of the lizards, from 8:30 to 18:00, with one or two visits per week. We visited each zone of the study area randomly, covering all zones both in the morning and afternoon, without sampling the same points within less than 4 hours to ensure independent observations.

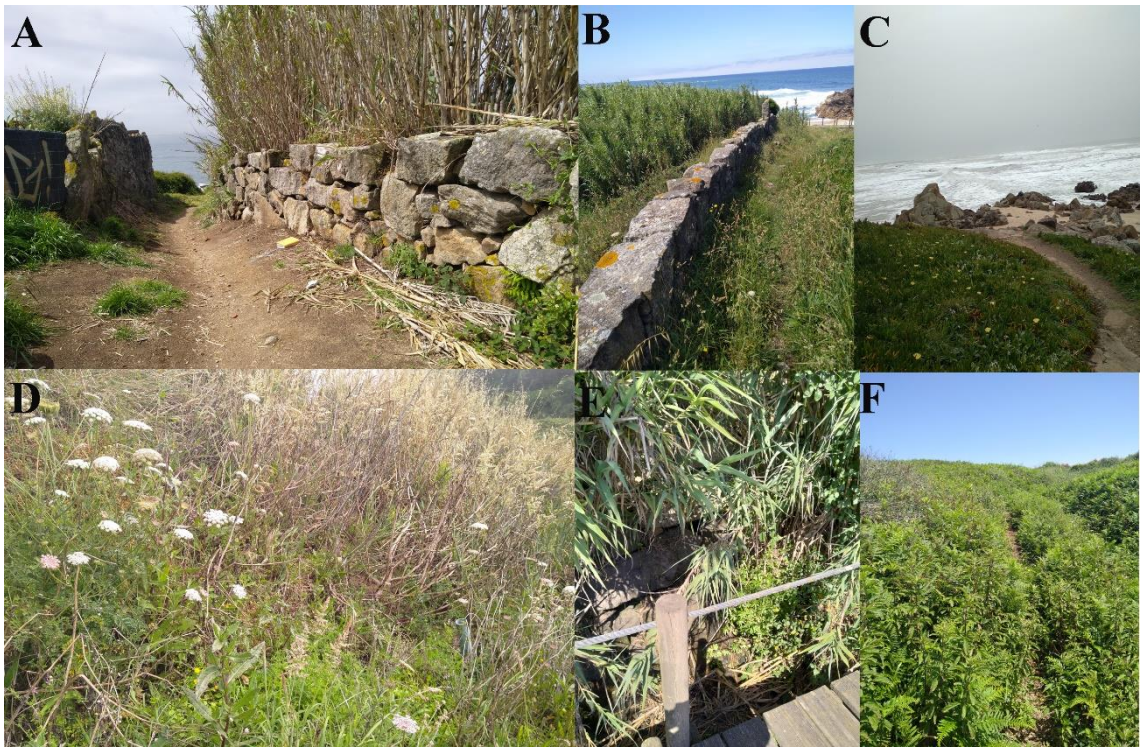

Figure 5.1 Microhabitats most commonly used by the two species of Mediterranean green lizards in Castro de São Paio. A-C. *Timon lepidus*, D-F. *Lacerta schreiberi*

Once a green lizard was detected it was assigned a unique code and its position was recorded by registering the exact geographic coordinates of observation using a sub-meter precision GPS (Trimble GeoXT). We also recorded the time, microhabitat type, air temperature and relative humidity (measured with a Lanaform LA 120701 Thermo-Hygrometer), substrate temperature (measured with an GM320 infrared thermometer), and the lizard's behaviour. We defined behaviour as the type of activity that each lizard engaged in at the moment it was observed, and identified four types of

behaviour: basking (immobile basking in the sun), foraging (actively searching for food and/or consuming it), sheltering (taking refuge in holes or hiding under the shade of vegetation or rocks), mating (interactions related to copulation), and fleeing (escaping from the proximity of humans). Similar classifications to define behaviour activities have been used (Díaz, 1991; Pavey and Geiser, 2008). To avoid pseudoreplications we visually observed the animals and took individual photographs with a camera, ensuring that each photo contained detail of the head and characteristic markings of each individual to later confirm their unique ID. We photographed each individual and the surroundings of its point of observation, including a scale mark. Whenever possible, we then collected lizards with a noose to measure their snout-to-vent length (SVL), and for those that could not be collected, we estimated body size from the scaled photographs. From May 2022 onwards we extracted field body temperatures using a thermal camera (Cat® S6Cat with an integrated FLIR TM Lepton camera), and we recorded the amount of light at the observation points with a light meter (ATP Electronics MT-912).

5.2.2. Data Analyses

5.2.2.1. Environmental variables and microhabitat preferences

To identify differences between species in the utilization of different microhabitats, we applied a Chi-Square test of proportions on the number of observations using the chisq.test R function (R Core Team, 2024) and assuming that each microhabitat is equally utilized by both species as the null hypothesis. To identify differences between species in air temperature, substrate microhabitat temperature and relative humidity of the points of observation, as well as illuminance and body temperature, we used analyses of variance (ANOVA), including these environmental parameters as dependent variables and species, sex and their interaction as predictors. We considered only adults, as we had very few juvenile observations. As the effect of sex was not significant for any of the above analyses, we did not consider it a factor of interest for subsequent analyses.

To investigate whether differences between species in air temperature, substrate microhabitat temperature, relative humidity, illuminance, and body temperature depending on the type of microhabitat where lizards were observed, we performed an ANOVA with species, microhabitat and their interaction as factors. Note that, as we did not record observations of *L. schreiberi* in the walkway, this microhabitat category was removed from the ANOVA. To investigate whether variation in the recorded variables depended on the combined effects of species and type of behaviour, we performed an ANOVA with these factors and their interaction as predictors.

Finally, we explored seasonal variation across species in the recorded traits.

As we did not record any observations of *L. schreberi* during the winter, and the observations during March and April were very few (Figure 5.2), we only considered the data from spring and summer (from May to July) for this analysis, and we used an ANOVA to test for variation in air temperature, substrate microhabitat temperature, relative humidity, illuminance and body temperature in response to species, month and their interaction.

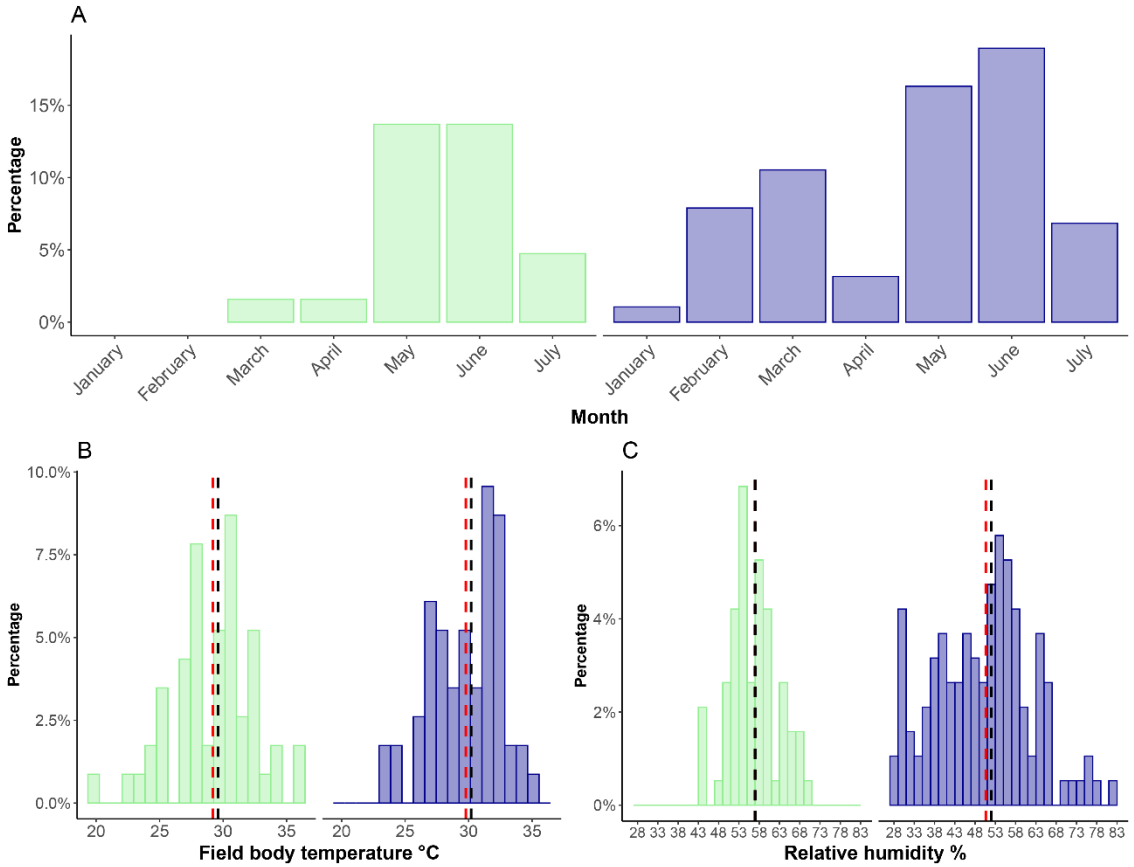

Figure 5.2 Percentage of observations during the sampling period (A), field body temperatures (C) and relative humidity (D) for *T. lepidus* (blue) and *L. schreiberi* (green) during the entire sampling period. Bars represent the percentage of individuals across body temperature and relative humidity values throughout the entire sampling period. Red dashed lines indicate the mean and black dashed lines the median. 100% of the observations in C and D correspond to the sum of all bins.

We assessed the significance of all ANOVAs via residual randomization procedures with 1000 permutations using the package “RRPP” (Collyer and Adams, 2019) in R (R Core Team, 2024). We performed post hoc pairwise comparisons whenever a significant effect or interaction was identified in ANOVAs involving factors with more than two categories with the function “pairwise” of the same package.

5.2.2.2. Activity patterns

We used independent lizard observations to assess species' seasonal distribution (i.e., activity patterns) and proportion of the daily cycle that a species is active (i.e., activity levels). We first evaluated differences in levels of activity between species for the complete data set, i.e., including all observations from January through July. We then evaluated differences between and within species in activity patterns. For this purpose, observations were grouped into seasons based on solstice limits for the Northern Hemisphere, i.e. divided into winter (January, February, and up to 21 March), spring (22 March - 21 June), and summer (22 June - 31 July). We considered only spring and summer months for interspecific comparisons, as winter observations were very scarce for *L. schreiberi*. We conducted activity analyses using the 'activity' package (Rowcliffe, 2023) in R version 4.3.3 (R Core Team, 2024). First, we converted dates and times to radians and calculated the circular mean for each species (i.e., the mean direction of activity hours expressed as angles across a 24-hour cycle, in radians). We then used the "fitact" function with 9999 replicates to fit kernel density functions that describe lizard activity. We compared daily activity between the two species, using the Wald test with the function "compareAct", and compared and identified differences in seasonal activity patterns using the function "compareCkern" with 9999 replicates, which tests for the probability that two circular observations come from the same distribution. In order to assess the degree of temporal niche overlap, we estimated the overlap coefficient (Δ) between *T. lepidus* and *L. schreiberi* patterns, where, $\Delta = 0$ reflects no overlap and $\Delta = 1$ indicates total overlap (Ridout and Linkie, 2009). We used Δ_1 as recommended by Ridout and Linkie (2009) and Meredith et al. (2024) for small sample sizes ($n < 70$), which provide lower root mean square error (RMSE) when the sample size is small. We used the “overlap” package (Meredith et al., 2024) for overlap estimations and for producing kernel density plots of lizard activity with the 'overlapPlot' function.

To evaluate whether activity times are influenced by environmental variables, body temperatures and body size, we performed Bayesian circular GLMs, since time follows a circular distribution (Ridout and Linkie 2009; Lee, 2010). We used the package "circglmbayes" (Mulder and Klugkist, 2017) which allows regressing a circular variable on linear and categorical predictors. We used the "circGLM" function, which implements a Markov chain-based Monte Carlo (MCMC) approach. We estimated the coefficients, standard deviations (SD) and 95% credible intervals of the estimated coefficients. The

credible intervals (lower bound, LB, and upper bound, UB) were obtained from the posterior distribution of the coefficients, and we considered a relationship to be significant if the credible intervals did not include the value 0, as this would indicate no effect (Hespanhol et al., 2019). We ran the models with 9999 iterations. To assess model predictions, we compared the values of the Deviance Information Criterion (DIC) and the Watanabe-Akaike Information Criterion (WAIC). To evaluate the convergence of the model we used the "coda" package (Plummer et al., 2006) and the "gelman.diag" function, which calculates the Gelman and Rubin convergence diagnostic. Convergence diagnostics ascertain whether the MCMCs have adequately explored the parameters and converged to a stable distribution. The Gelman and Rubin diagnostic compares the within-chain variance with the between-chain variance. Convergence is indicated by $\hat{R}$ values, where values closer to 1 denote good convergence.

5.2.2.3. Micro-scale distribution

To compare how species are distributed locally (i.e., in the same population) at a microscale, we first obtained a detailed orthophoto to spatially record the occurrences of the two species in the study area**.** Occurrence data were imported into ArcGIS Pro (Esri, 2024) and projected to the WGS 1984 UTM Zone 29N coordinate system. We then plotted the occurrence points on the map to visualize the spatial distribution of the species. To identify hotspots of occurrence for each species and relate them to potential spatial segregation, we used Kernel density estimation (KDE) implemented in ArcGIS Pro 10.x (Esri, 2024). This technique smooths discrete location data to generate a continuous estimate of the density of occurrence points (Esri, 2024). We chose KDE because it effectively captures the intensity of occurrence points across space, providing a clear visualization of data presence. Moreover, it does not assume an underlying distribution of the data (Baíllo and Chacón, 2021). We identified the hotspots based on densities that fall within the 75th percentile of the Kernel Density Estimation (KDE) output, representing areas where 75% of the highest density aggregations are located.

5.3. Results

We recorded a total of 206 lizard observations with concomitant standardised records of different field variables (body temperature, microhabitat substrate temperature, air temperature, relative humidity, illuminance, behaviour, microhabitat type, month and hour). Of these observations, 134 were of *Timon lepidus* (♂ = 83, ♀ = 44, juveniles = 7), and 68 of *Lacerta schreiberi* (♂ = 48, ♀= 22, juveniles = 2). Observations of *T. lepidus* occurred from January to the end of the sampling period in

July; the months with the most observations were February, March, May and June (Table 5.1, Figure 5.2A). On the other hand, we did not record individuals of *L. shreiberi* during January and February, but only from March until July, the months with the highest number of observations being May and June (Table 5.1, Figure 5.2A). *Timon lepidus* generally exhibited greater variation in relative humidity, with peaks in winter and spring, while *L. schreiberi* had higher average values and a narrower range (Figure 5.2A–C, ANOVA on relative humidity, $Z = 3.415$, $p < 0.001$).

Table 5.1 Summary of environmental variables and body temperature measurements across species, sexes, months, behaviors, and microhabitat categories. The table presents mean values (± standard deviation) for air temperature (°C), relative humidity (%), substrate microhabitat temperature (°C), illuminance (lx), and body temperature (°C) for *T. lepidus* and *L. schreiberi*. Sample sizes (n) are indicated for each category.

Factor	Species	Category (sample size)	Air T °C	Relative humidity %	Substrate microhabitat T °C	Illuminance (lx)	Body T °C
Sex	*T. lepidus*	Males (n = 83)	22.53 ± 3.6	50.9 ± 12.2	29.4 ± 5.1	61.9 ± 10.9	29.9 ± 2.6
		Females (n = 44)	22.29 ± 2.5	50.1 ± 11.8	30.6 ± 6.3	65.3 ± 11	29.6 ± 2.9
	L. schreiberi	Males (n = 48)	23.23 ± 2.6	58.1 ± 6.2	30.2 ± 4.3	63.4 ± 7.5	29.2 ± 2.3
		Females (n = 22)	23.23 ± 2.5	54.1 ± 4.7	30.6 ± 4.7	61.4 ± 9.2	29.2 ± 4.5
Month	*T. lepidus*	January (n = 2)	18.1 ± 2.8	52.2 ± 4.9	18.2 ± 3.1	-	-
		February (n = 17)	21.2 ± 2.2	40.0 ± 11.3	30.1 ± 5.7	-	-
		March (n = 24)	19.2 ± 1.9	40.3 ± 7.1	25.7 ± 4.5	-	-
		April (n = 8)	21.2 ± 2.6	75.7 ± 5.4	23.5 ± 1.4	-	-
		May (n = 34)	24.3 ± 4.3	49.8 ± 7.6	29.8 ± 5.7	60.5 ± 9.8	29.0 ± 3.4
		June (n = 37)	22.6 ± 1.6	59.8 ± 8.8	30.7 ± 4.1	68.0 ± 8.0	29.8 ± 3.0
		July (n = 13)	23.3 ± 2.4	53.5 ± 6.1	32.5 ± 5.3	54.6 ± 9.7	29.9 ± 2.6
	L. schreiberi	March (n =5)	20.3 ± 3.4	52.2 ± 4.8	26.0 ± 6.8	-	-
		April (n = 3)	19.2 ± 0.01	68.3 ± 1.5	29.3 ± 0.7	-	-
		May (n =25)	24.4 ± 2.6	57.5 ± 4.6	30.3 ± 5.1	61.3 ± 7.9	28.9 ± 2.2
		June (n = 26)	22.5 ± 1.7	56.5 ± 6.9	31.1 ± 3.8	67.7 ± 6.4	28.5 ± 3.5
		July (n = 10)	23.8 ± 2.8	54.9 ± 2.9	30.9 ± 4.4	56.4 ± 6	32.4 ± 3.3
Behaviour	*T. lepidus*	Basking (n = 83)	22.3 ± 3.0	50.2 ± 12.5	30.0 ± 5.4	64.1 ± 10.4	29.2 ± 2.8
		Fleeing (n = 9)	23.7 ± 4.9	44.8 ± 6.8	26.1 ± 5.1	62.4 ± 6.2	31.5 ± 1.2
		Foraging (n = 9)	21.7 ± 1.9	57.9 ± 12.2	30.5 ± 5.4	59.3 ± 9.5	29.6 ± 3.6
		Mating (n = 8)	24.9 ± 0.1	58.5 ± 1.2	34.3 ± 0.0001	75.3 ± 0.9	31.6 ± 0.4
		Sheltering (n =	21.7	47.9 ±	27.8 ± 6.8	46.9 ± 6.5	30.4

		14)	± 4.6	12.1			± 2.2
		Basking (n = 36)	23.4 ± 2.7	57.0 ± 6.2	30.9 ± 4.1	63.9 ± 6.8	28.8 ± 2.7
		Fleeing (n = 9)	22.5 ± 2.1	58.0 ± 4.7	23.9 ± 1.3	60.2 ±5.9	26.3 ± 2.1
	L. schreiberi	Foraging (n =8)	23.1 ± 1.3	58.5 ± 1.7	27.8 ± 2.5	63.0 ± 13.1	32.2 ± 1.3
		Mating (n = 8)	20.5 ± 0.2	51 ± 7.0	34.6 ± 3.0	66.2 ± 1.7	31.8 ± 0.2
		Sheltering (n =10)	24.2 ± 2.7	59.8 ± 5.6	28.2 ± 4.7	47.4 ± 7.2	28.6 ± 2.7
Microhabitat	*T. lepidus*	Rocky substrate (n = 88)	22.4 ± 3.3	50.9 ± 12.8	29.5 ± 5.1	64.3 ± 11.7	30.0 ± 2.4
		Herbaceous vegetation (n = 13)	23.0 ± 2.2	51.5 ± 9.6	28.7 ± 4.2	59.6 ± 8.3	29.7 ± 2.2
		Ground (n = 5)	22.6 ± 3.8	46.6 ± 6.2	32.8 ± 9.9	48.4 ± 10.7	29.4 ± 3.0
		Cement/rubble (n = 12)	20.8 ± 2.9	49.9 ± 11.3	31.0 ± 6.9	66.3 ± 5.5	28.9 ± 3.9
		Walkway (n = 5)	25.1 ± 5.3	50.2 ± 13	34.1 ± 9.0	65.2 ± 7.3	28.2 ± 5.2
	L. schreiberi	Rocky substrate (n = 5)	24.5 ± 2.8	59.4 ± 0.6	34 ± 6.8	60.8 ± 5.6	30.4 ± 0.3
		Herbaceous vegetation (n = 54)	23.1 ± 2.4	56.3 ± 6.0	29.9 ± 4.3	63.5 ± 8.5	29.2 ± 3.5
		Ground (n = 5)	26.8 ± 1.3	53.3 ± 1.0	32.2 ± 0.6	64.5 ± 0.6	28.8 ± 0.9
		Cement/rubble (n = 5)	19.8 ± 1.2	66.3 ± 4.3	29.4 ± 0.7	54.1 ± 1.3	25.4 ± 2.3

5.3.1. Microhabitat use and microclimatic preferences

Mean values for all variables, factors, and the numbers of observations are available in Table 5.1. We did not detect significant differences in air temperature, illuminance, field body temperature, or microhabitat substrate temperature at the observation points of *T. lepidus* and *L. schreiberi*, nor between sexes (Appendix C Table C3.1). However, we found significant differences in relative humidity between species but not between sexes (Appendix C Table C3.1).

We found significant variation in the frequency of using different microhabitats for both *T. lepidus* ($X^2 = 206.55$, $p < 2.2e\text{-}16$) and *L. schreiberi* ($X^2 = 101.65$, $p < 0.001$), and between species ($X^2 = 14.83$, $p = 0.020$). *T. lepidus* predominantly used rocky substrate (70.1%), followed by cement/brick (12.7%), herbaceous vegetation (9.7%), bare soil (3.7%), and walkway (3.7%). In contrast, *L. schreiberi* mainly used herbaceous vegetation (86.4%), with lower proportions of cement/brick (5.1%), rocky substrate (3.4%), bare soil (3.4%), and walkway (1.7%).

We detected a significant effect of microhabitat on air temperature and a significant species-microhabitat interaction on illuminance (Appendix C Table C3.2). Pairwise analyses confirmed differences in illuminance (Appendix C Table C3.3). For *T. lepidus*, substrate temperature in rocky microhabitats varied significantly across months ($Z = 3.999$, $p = 0.001$, Figure 5.3A), while relative humidity showed marginal differences ($Z = 1.636$, $p = 0.057$, Figure 5.3B), and illuminance differed significantly ($Z = 3.448$, $p = 0.001$, Figure 5.3D). Field body temperature did not vary across months in rocky microhabitats ($Z = 0.525$, $p = 0.299$, Figure 5.3C). For *L. schreiberi*, no monthly differences were detected in substrate temperature ($Z = 0.767$, $p = 0.241$, Figure 5.3A) or relative humidity ($Z = 0.051$, $p = 0.488$, Figure 5.3B) in herbaceous vegetation. However, body temperature ($Z = 2.145$, $p = 0.017$, Figure 5.3C) and illuminance ($Z = 2.949$, $p = 0.001$, Figure 5.3D) showed significant monthly variation. Microhabitat substrate temperatures were similar between species (Figure 5.3A, Appendix C Table C3.2). By contrast, body temperatures peaked in July for *L. schreiberi* and in June for *T. lepidus* (Appendix C Table C3.4).

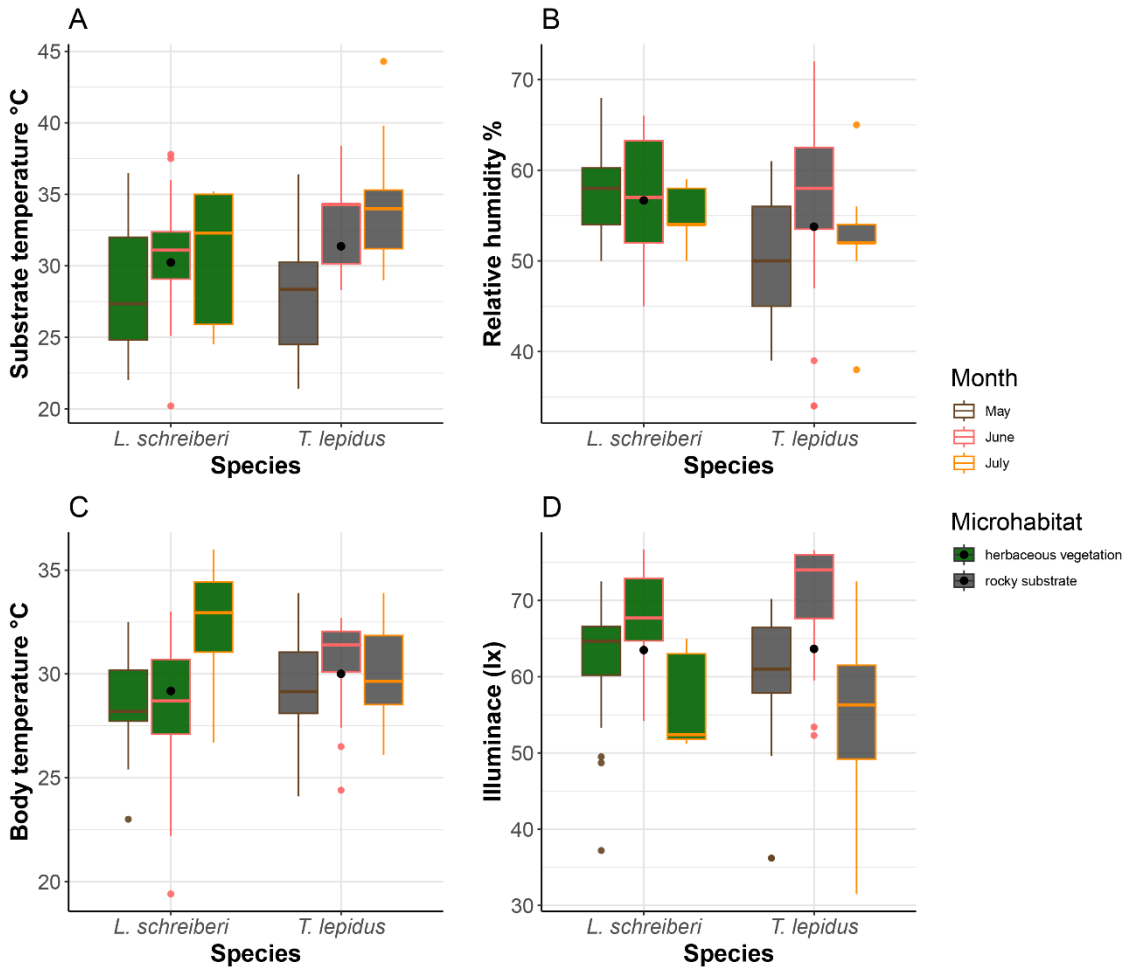

Figure 5.3 Substrate microhabitat temperature (A), relative humidity (B), body temperature (C), and illuminance (D) for *T. lepidus* and *L. schreiberi* in herbaceous vegetation and rocky substrate across different months (May-July).

We detected significant differences depending on behaviour for illuminance, field body temperature, and microhabitat substrate temperature (Appendix C Table C3.5). Additionally, we found a significant interaction between species and behaviour for air temperature (Appendix C Table C3.5). Most green lizards in Castro de São Paio were observed basking, with *T. lepidus* showing the highest activity in February, March, May, and June, and *L. schreiberi* in May, June, and July (Figure 5.4A). We observed mating in June for both species (Figure 5.4A) and detected significant differences in air temperature during mating between species (Figure 5.4B, Appendix C Table C3.6). We did not detect a significant effect of behaviour on relative humidity (Appendix C Table C3.5, Figure 5.4C). Illuminance was highest during mating and lowest during sheltering (Figure 5.4D), although pairwise analyses found no significant differences (Appendix C Table C3.7). Finally, observations of body temperature and microhabitat substrate

temperature were heterogeneous, with no significant pairwise differences (Figure 5.4E, Appendix C Table C3.8-A3.9).

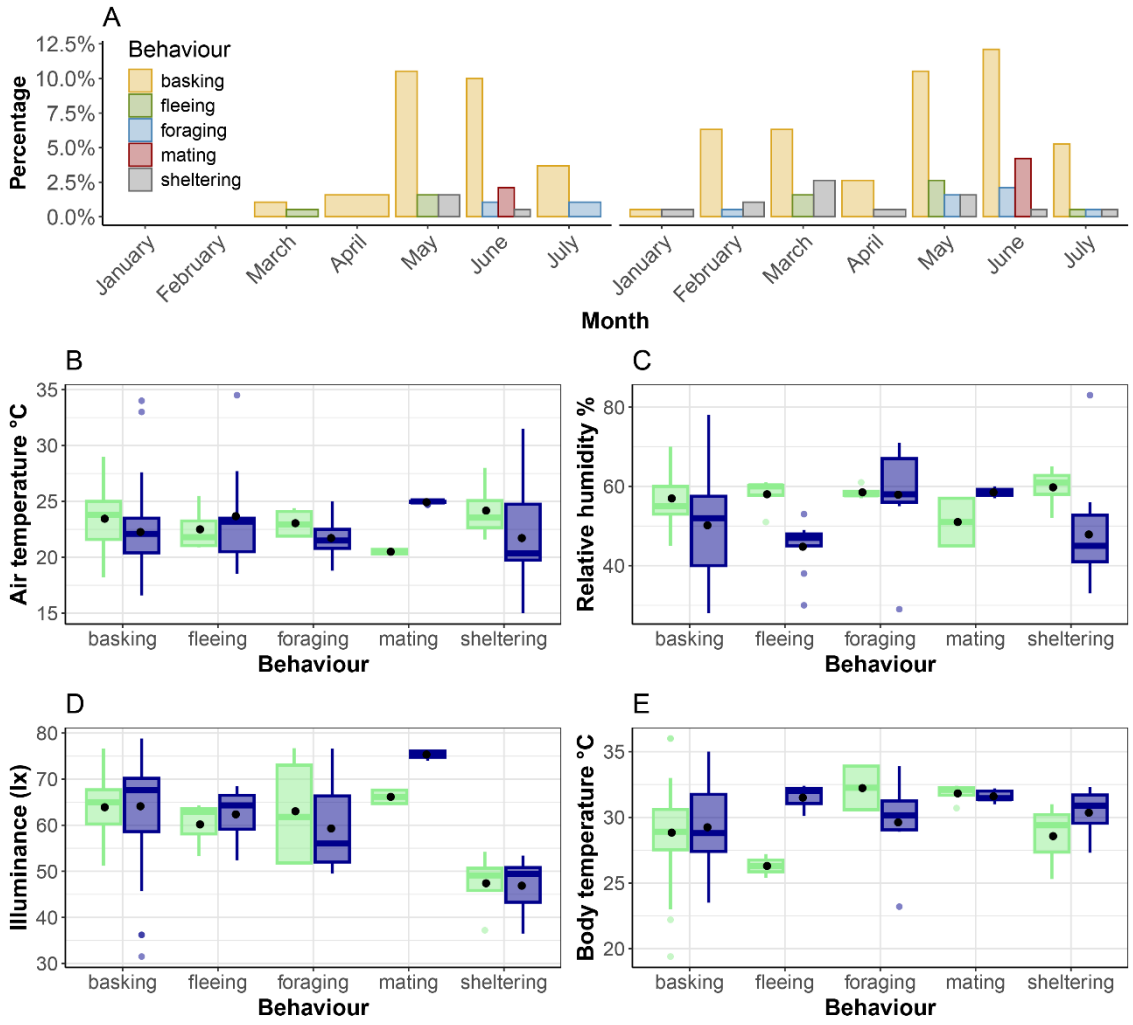

Figure 5.4 Behaviour and environmental conditions of *T. lepidus* and *L. schreiberi* over time. Percentage distribution of behaviours observed for. *T. lepidus* (right) and *L. schreiberi* (left) from January to July (A). Behaviours include basking, fleeing, foraging, mating, and sheltering. Air temperature (B), relative humidity (C), illuminance (D), and body temperature associated with each behaviour (E). The blue and green boxplots represent *T. lepidus* and *L. schreiberi*, respectively.

Seasonal variation in air temperature showed lower values in winter and spring and humidity peaking between February and May (Figure 5.5). We detected significant monthly differences in air temperature (Appendix C Table C3.10, Figure 5.6A), although the subsequent pairwise comparisons were not significant (Appendix C Table C3.11). When analysing relative humidity during months with higher observations (May, June, July), we found a significant effect of species, months, and their interaction (Appendix C Table C3.10). Significant differences occurred in May, with *T. lepidus* showing lower values than *L. schreiberi* (Figure 5.6B, Appendix C Table C3.12). A similar pattern was observed in March, although not statistically tested. We also found significant monthly

variation in illuminance (Appendix C Table C3.10, Figure 5.6C), although pairwise analyses showed no differences (Appendix C Table C3.13). Field body temperature varied significantly across months, with differences mainly occurring in June and July (Figure 5.6D, Appendix C Table C3.4 and A3.10).

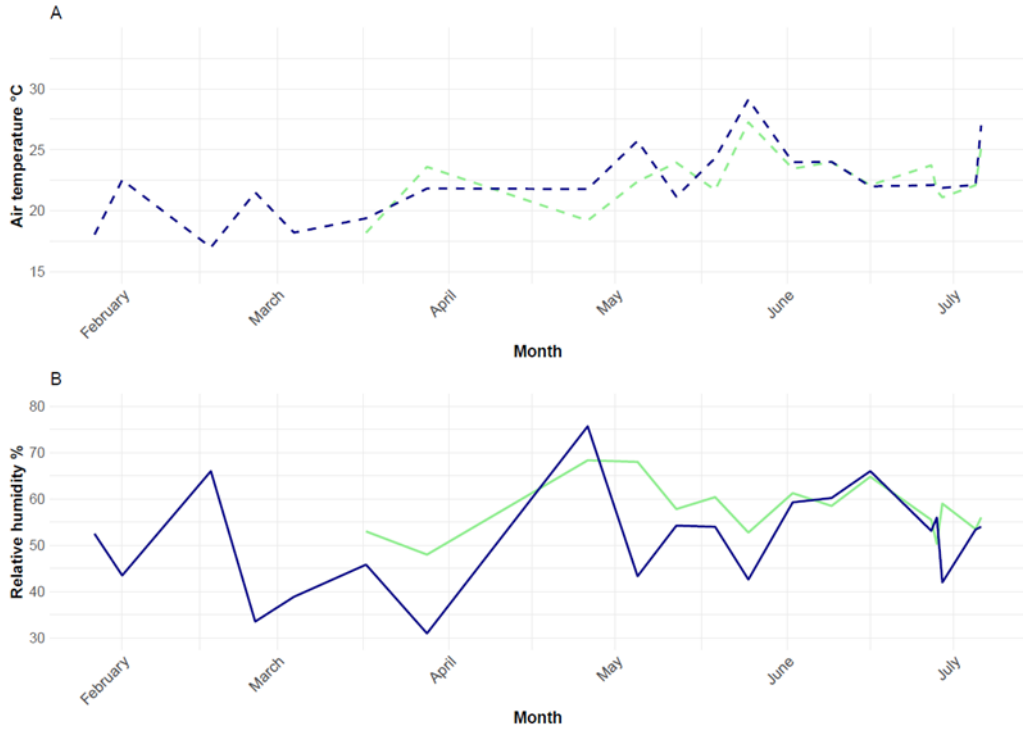

Figure 5.5 Mean air temperature (dashed lines) (A) and mean relative humidity (solid lines) (B) during the sampling period.

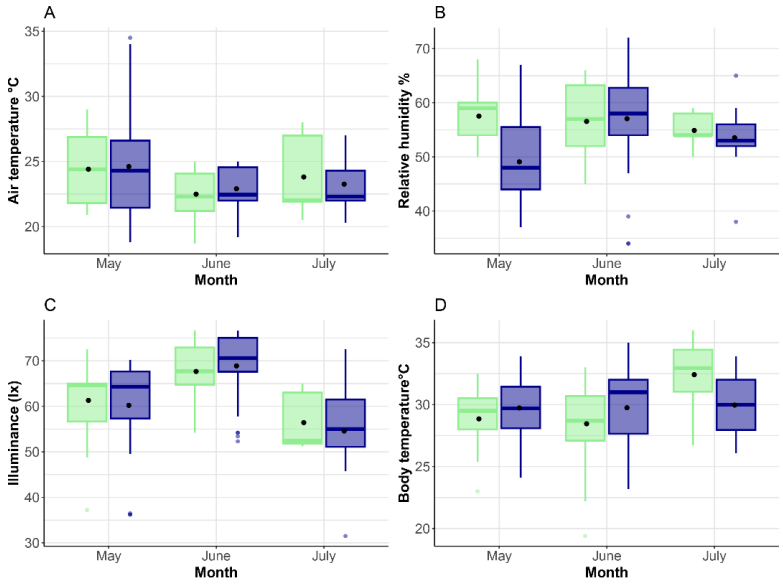

Figure 5.6 Boxplots of variables during the sampling period related to the observations of *T. lepidus* (blue) and *L. schreiberi* (green). and air temperature (A), relative humidity (B), illuminance (C), and body temperature (D).

5.3.2. Activity Patterns

Our observations indicate that *T. lepidus* exhibits a unimodal activity pattern with a pronounced peak around midday (Figure 5.7A), a trend that was maintained through all three seasons (winter, spring and summer) (Figure 5.7A). On the other hand, *L. schreiberi* showed a bimodal pattern with activity concentrations mainly at two hours past noon between 1:00 and 2:00 p.m., and another peak in the afternoon mainly between 5 and 6 p.m. (Figure 5.7B). This pattern was similar in the spring and summer data (Figure 5.7A).

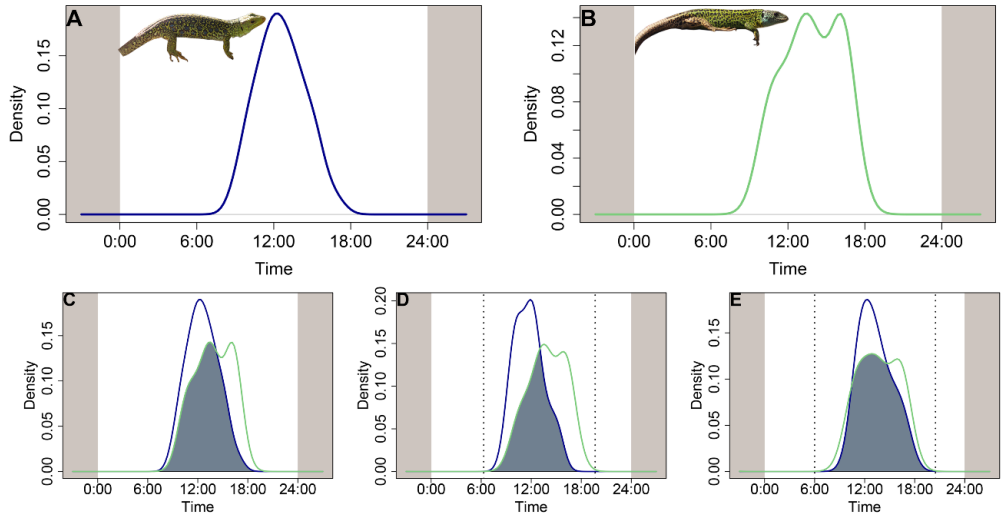

Figure 5.7 Activity patterns of *Timon lepidus* (blue) (A) and *Lacerta schreiberi* (green) (B), and overlap (blue-grey shaded area) between species for general activity patterns (C), spring activity patterns (D), and summer activity patterns (E).

Regarding activity levels (i.e., the proportion of the daily cycle that the species is active), we detected significant differences between the two species with *T. lepidus* being more active ($W = 4.74$, $p = 0.030$). On the other hand, the distribution of the activity patterns of both species differed significantly ($p < 0.001$), despite a relatively high overlap coefficient ($\Delta = 0.76$, 95% CI = 0.65 – 0.97, Figure 5.7). When we analyzed the spring dataset, we observed that the overlap between species in activity patterns was the most reduced, with significant differences between the patterns of *T. lepidus* and *L. schreiberi* ($\Delta = 0.59$, 95% CI = 0.44 – 0.70, $p < 0.001$, Figure 5.7D). By contrast, the summer dataset exhibited the highest overlap coefficient and activity pattern distributions did not differ significantly ($\Delta = 0.84$, 95% CI = 0.69 – 0.99, $p = 0.275$, Figure 5.7E).

Our Bayesian circular GLMs showed that the models that best explain differences in activity times were those that included environmental temperature (Appendix C Table C3.14). We detected significant differences in activity times between species: we found

a significant interaction between air temperature and species *T. lepidus* Appendix C Table C3.14) suggesting that *L. schreiberi* tends to be active earlier in the day as air temperature increases. We did not detect significant interactions between body size and other variables (air temperature, relative humidity, body temperature and illuminance) in the best models explaining activity time (Appendix C Table C3.14).

5.3.3. Spatial distribution of species

Our observations of nearly seven months of sampling allowed us to pinpoint spatial hot spots where sightings of each species were concentrated. *T. lepidus* was predominantly detected in open areas and along human-accessible pathways (edges of walkways, abandoned structures with debris, etc.). Observation points indicate that *T. lepidus* could be found around rocky edges and natural rock strata, including areas with vegetation or along coastal sandy substrates (Figure 5.1, Figure 5.8). In contrast, *L. schreiberi* was observed in areas covered by herbaceous vegetation (Figure 5.1, Figure 5.8). While some overlap exists in the spatial distribution of observations, distinct areas of occurrence were evident between the species. For *T. lepidus*, we identified at least three high-density hotspots in the study area, all closely associated with rocky microhabitats (Figure 5.8). Meanwhile, *L. schreiberi* exhibits at least two high-density hotspots: one associated with a small stream flowing towards the coast and another in areas densely vegetated with shrubs and herbaceous plants (Figure 5.1, Figure 5.8).

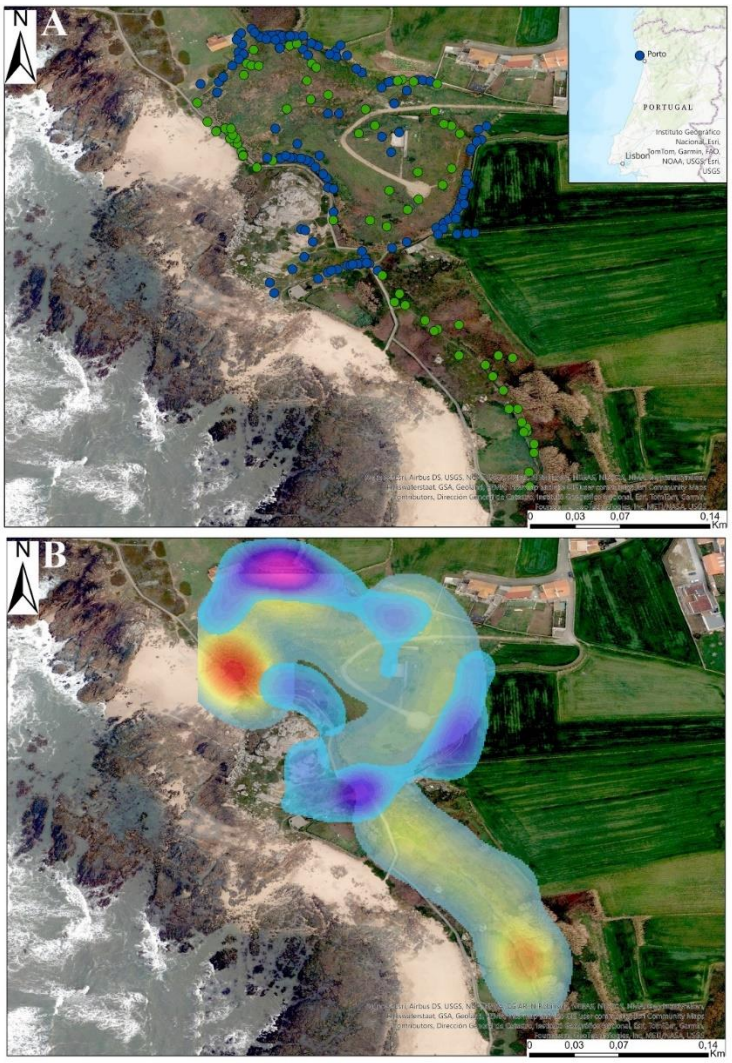

Figure 5.8 Spatial distribution and density of observations of *T. lepidus* and *L. schreiberi* in the study area. (A). Distribution of observation points for *T. lepidus* (blue points) and *L. schreiberi* (green points) along the coastal and inland areas in Castro de São Paio. The inset map shows the location of the study area near Porto, Portugal. (B). Kernel density estimation (KDE) map showing the density of occurrences for both species. Areas with higher densities are indicated by warmer colors, red and yellow for *L. schreiberi* and blue and purple for *T. lepidus*.

5.4. Discussion

Niche segregation among co-occurring species remains a critical point of debate in current ecology (Amarasekare, 2002; Gravel et al., 2011; Valladares et al., 2015). Experimental evidence and empirical field observations are essential to thoroughly understand the mechanisms by which ecologically similar species can thrive in the same localities. Our field study of green lizards in northern Portugal revealed significant differences in microhabitat use and preferred conditions of relative humidity between *T. lepidus* and *L. schreiberi*, which appear to contribute to their niche segregation. Specifically, *L. schreiberi* preferred relatively humid microhabitats and it followed a bimodal activity pattern, whereas *T.lepidus* used drier, more exposed habitats and it

exhibited a pick of daily activity fitting a unimodal pattern. These findings suggest that physiological, ecological, temporal, and spatial factors—including microhabitat humidity, spatial arrangement, and activity patterns—promote niche segregation between the two species.

During the sampling period, which encompassed the months of highest activity and the reproductive period of both species, we obtained a higher number of observations for *T. lepidus* than for *L. schreiberi*. This may be the result of a combination of various factors, including detectability (MacKenzie et al., 2017). Field observations indicated that *L. schreiberi* prefers microhabitats with dense herbaceous vegetation over rocky or open areas, consistent with findings from other researchers (Brito et al., 1998a; Brito et al. 1999). This suggests that although *L. schreiberi* may occasionally use other types of microhabitats such as stone walls (Brito et al., 1998a), it shows a preference for herbaceous and bushy vegetation (Brito et al., 1998a, b; 1999), which may reduce our potential for observing it. Although our sampling covered all microhabitats present in Castro de São Paio, factors such as vegetation height, the noise produced by the researchers during sampling, the lizards' size and cryptic colouration, and the ease of access to certain areas may have directly reduced detectability (Driscoll et al., 2020; MacKenzie et al., 2017). Nonetheless, considering that we sampled the entire study area across different months, we identified that *L. schreiberi* is less observable during the winter months, potentially due to its reduced activity during this period (Marco and Pérez-Mellado, 1998; Pérez-Mellado 1998). On the other hand, *T. lepidus* was detectable in the sampled period in the winter, although in a smaller proportion than in the spring and summer, which implies that this species could be more adaptable to seasonal variations in temperature and rainfall (Figure 5.5). Previous studies have shown that a reduction of lacertid activity during the autumn and winter is related to the preparation for the breeding period and the accumulation of lipid reserves (Carretero, 2006; Rachid et al., 2006; Sannolo et al., 2019). Given its larger body size and associated greater thermal inertia, *T. lepidus* is expected to be more active during winter, as it can maintain more stable body temperatures even amid extreme thermal fluctuations (Stevenson, 1985). This is consistent with our observations, where *L. schreiberi*, significantly smaller than *T. lepidus*, was scarcely detected during the winter and early spring months.

Our findings suggest that air temperature, illuminance, and field body temperature do not contribute to niche segregation between the two species. Although these variables exhibit seasonal variation (Brito et al., 1999; Salvador, 1988), they do so similarly in both *T. lepidus* and *L. schreiberi* (Appendix C Table C3.10). These field data

corroborate laboratory experiments on thermal ecology with the same populations, where no differences were detected in the preferred temperature of the two species (Reyes-Puig et al., 2024). Additionally, our results show no differences in these variables between the sexes, which suggests that both sexes of the two species have a similar ability to regulate their temperature within the thermal ranges available in their environment. However, it is well established that females may exhibit differential thermoregulatory behaviour during periods of intensified physiological demand, such as oogenesis and embryogenesis (Lailvaux, 2007; Shine, 2004). While our study did not specifically focus on these reproductive periods, variations in body temperatures between sexes may likely occur before and after the breeding period. Although our results showed that *T. lepidus* and *L. schreiberi* use different microhabitats (Figure 5.3), it seems that these can provide similar thermal conditions allowing both species to reach comparable body temperatures. This observation is supported by the fact that both species thermoregulate on average at similar temperatures, both experimentally (Reyes-Puig et al., 2024) and in nature (see Appendix C Table C3.1-A3.13). Since thermal conditions alone do not appear to significantly contribute to niche segregation between the two species, it is likely that the spatial configuration of microhabitats, combined with microclimatic conditions, plays a more influential role in driving spatial niche differentiation (Prieto-Ramírez et al., 2018). Such a hypothesis still needs to be corroborated, though, potentially through fine-scale microclimatic modelling of the habitats used by the two species.

Another key factor which could influence niche segregation, but that unfortunately has been largely overlooked in squamate ecophysiology, is water balance (Kearney et al., 2018). Our results, in line with other research (Brito et al., 1999; Ferreira et al., 2016; Reyes-Puig et al., 2024), underscore the importance of water balance traits for *L. schreiberi* and for the coexistence of the two species. The relative humidity of the microhabitats where we observed individuals of this species was significantly higher than that of the microhabitats used by *T. lepidus*, which tend to be open, stony, and more exposed, similar to findings reported by other authors (Mateo, 2017; Mateo, Escoriza and Amat, 2021). Herbaceous and shrub vegetation store more moisture and receive less radiation, reducing direct evaporation and increasing microenvironmental and body temperatures (Adams, 2009). Consequently, organisms occurring in highly humid habitats may face increased water loss during periods of elevated temperatures, as these conditions can intensify evaporative stress (How and Lee, 2014; Weaver et al., 2023). Consistent with our field findings, *L. schreiberi* not only uses wetter sites in the

landscape but specifically prefers areas near streams with flowing or semi-flowing water, as noted by several other researchers (Brito et al., 1999; Pérez-Mellado, 1998; Salvador, 1988). Recently published evidence (Reyes-Puig et al., 2024) confirms that the Iberian Emerald lizard has higher water loss rates than *T. lepidus* and also holds a higher proportion of wet skin surface. Skin permeability appears to be a crucial trait for coping with physiological changes associated with water loss (Sannolo et al., 2018; Weaver et. al., 2023), which may explain why *L. schreiberi* needs to be near bodies of water and humid places, to avoid higher desiccation rates, as observed in other organisms (Cain et al., 2010; Weaver et al., 2023). Likewise, laboratory experiments have identified that skin water loss in lizards is greater in hot and humid environments. This phenomenon may be related to vapour pressure and the amount of water in the environment (Weaver et al., 2023). However, reptiles from humid habitats tend to exhibit lower resistance to skin water loss, reflecting a lower selective pressure for water retention compared to species from arid environments (Dmi'el, 2001).

In the context of niche segregation among coexisting species, behaviour plays a crucial role, especially when thermoregulatory strategies are closely tied to it (Días and Cabezas-Díaz, 2004). The type of behaviour or activity is directly related to the internal metabolism of the species (Angilletta, 2009). For instance, when ectotherms mate, body temperature increases mainly because organisms seek out exposed sites with higher radiation to copulate (Angilletta, 2009; Licht, 1972). Our observations corroborate this, as body temperatures were higher for both species when mating compared to basking, which was also associated with higher illuminance in the exposed sites (Figure 5.4). Likewise, when we analysed our data by type of behaviour, we found that *L. schreiberi* had higher body temperatures while foraging compared to other activities. Although both species are considered active foragers, this could suggest that *L. schreiberi* requires a higher energetic output or adopts distinct thermoregulatory strategies during foraging. In this sense, trophic niche segregation is likely influenced not only by dietary differences (Kaliontzopoulou et al., unpublished data) but also by the energy demands and thermoregulatory behaviours associated with foraging mode (Angilletta, 2009; Bowker, 1984).

Within the landscape arrangement of the study area (Figure 5.8), the spatial organization of microhabitats is shaped by structural features and human accessibility. Castro de São Paio is a highly frequented touristic site (Araújo and Abrunhosa, 2012) where anthropogenic structures like rocky edges bordering agricultural zones, as well as open, vegetation-free areas such as coastal rocks, provide ideal conditions for observing

T. lepidus (Figure 5.1, Figure 5.4). Conversely, *L. schreiberi* is more restricted to areas covered by herbaceous vegetation, often with limited human accessibility, dominated by ferns and grasslands within the study site (Figure 5.8). Spatial aggregations of both species in distinct areas reflect that spatial segregation is an important driver of niche differentiation as pointed out by several authors (Darmon et al., 2012; Dufour et al., 2015; Hart et al., 2017).

On the other hand, temporal niche segregation allows coexisting species to access exclusive resources, such as food and space. Therefore, understanding the timing of activities and periods of peak activity provides valuable information on how species successfully segregate their niches. Our results support the idea that *T. lepidus* and *L. schreiberi* segregate their niches not only through phenotypic differentiation—primarily due to divergence in body size, which in turn leads to differences bite force, manoeuvrability, and physiological traits (Reyes-Puig et al., 2024)—but also spatially and temporally. While both species are diurnal, they exhibited noticeable differences in their activity peaks. *T. lepidus* exhibits a clear unimodal peak around midday, whereas *L. schreiberi* is more active after noon, particularly between 5 and 6 p.m. There is limited detailed information on the activity patterns of both species. Previous studies have reported temporal activity ranges primarily during autumn (Sannolo et al., 2019) and spring (e.g., Marco and Pérez-Mellado, 1998; Martín and López, 2010), in areas where lizard activity is more restricted compared to Castro de São Paio. In contrast, our observations indicate that green lizards, particularly *T. lepidus*, in Castro de São Paio are active almost year-round. Specifically, we found that *T. lepidus* is more active during the day and tends to initiate its activity earlier as temperature rises, potentially linked to foraging strategies and thermoregulatory behaviour (Bergallo and Rocha, 1993).

Our data reveal distinct activity patterns between *T. lepidus* and *L. schreiberi*, particularly during spring, likely driven by the breeding period (Carretero, 2006; Mateo, 2017). During this season, temporal segregation is more pronounced, with *T. lepidus* being more active before noon and at midday, while *L. schreiberi's* peaks activity in the afternoon (Figure 5.7). Although both species reproduce during similar periods (Marco, 2017; Mateo, 2017), their activity may vary due to differences in microhabitat use and responses to environmental factors such as temperature and humidity. For instance, *T. lepidus*, with its larger body size and greater thermal inertia, likely selects warmer, drier microhabitats like rocky substrates in the morning, enabling faster heat absorption (Goldenberg et al., 2021). In contrast, *L. schreiberi*, being smaller and more sensitive to thermal and humidity fluctuations, may prefer cooler, more humid microhabitats later in

the day to avoid overheating and dehydration (Stevenson, 1985). While the average body, microhabitat, and environmental temperatures do not differ significantly between species, temporal analyses show that *L. schreiberi* experiences higher body temperatures around midday and lower temperatures in the afternoon (Figure 5.9). This may reflect physiological adjustments to meet reproductive demands while maintaining water balance. These findings highlight that temporal niche segregation, influenced by seasonal variation in behaviour and microhabitat use, plays a critical role in reducing competition and promoting coexistence between these two species.

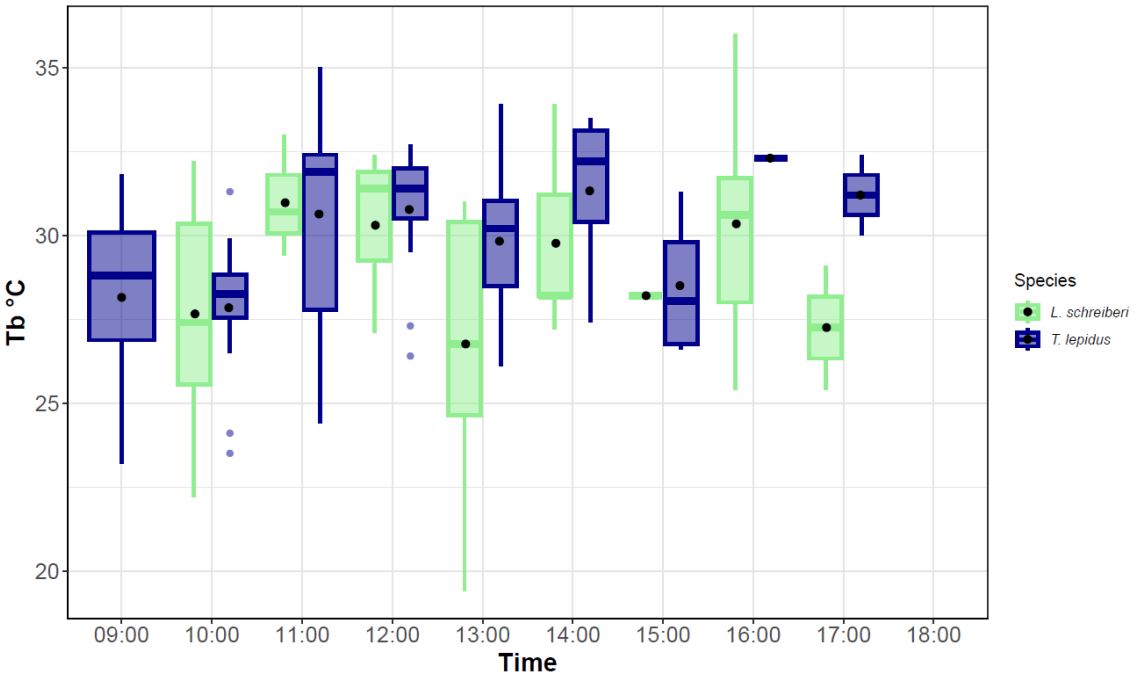

Figure 5.9 Field body Temperature (Tb) of *L. schreiberi* (green) and *T. lepidus* (blue). Each box represents the interquartile range with the median value indicated by a thick horizontal line inside the box. Outliers are shown as individual points. The black dots represent the mean body temperatures for each time period.

Finally, our study provides valuable insights into the mechanisms driving niche segregation and species coexistence, with emphasis on our study system *Timon lepidus* and *Lacerta schreiberi*. Thus, by integrating laboratory experimental findings with real-world field observations, we found a general congruence between the two, especially in relation to thermal preferences and water balance. However, our field observations also reveal that spatial and temporal factors such as microhabitat use, and activity patterns play a crucial and complementary role in shaping niche differentiation. Body size appears as a fundamental trait influencing most traits and is much more evident in laboratory-derived variables (Reyes-Puig et al., 2024). These findings underline the importance of combining experimental and field approaches to comprehensively understand niche

segregation, not only in green lizards but also in other organisms. By highlighting the interplay between physiological and ecological factors, our study contributes to a broader understanding of how coexistence is maintained in ecologically similar species.

References

Adams, J. (2009). Vegetation-climate interaction: how plants make the global environment. Springer Science and Business Media.

Adolph, S. C., and Porter, W. P. (1993). Temperature, activity, and lizard life histories. *The American Naturalist*, *142*(2), 273–295. https://doi.org/10.1086/285538

Amarasekare, P. (2002). Interference competition and species coexistence*. Proceedings of the Royal Society of London. Series B: Biological Sciences, 269*(1509), 2541–2550. https://doi.org/10.1098/rspb.2002.2181

Anaya-Rojas, J. M., Bassar, R. D., Potter, T., Blanchette, A., Callahan, S., Framstead, N., Reznick, D. and Travis, J. (2021). The evolution of size-dependent competitive interactions promotes species coexistence. *Journal of Animal Ecology, 90*(11), 2704-2717. https://doi.org/10.1111/1365-2656.13577

Andriollo, T., Michaux, J. R., and Ruedi, M. (2021). Food for everyone: Differential feeding habits of cryptic bat species inferred from DNA metabarcoding. *Molecular Ecology, 30*(18), 4584–4600. https://doi.org/10.1111/mec.16073

Angilletta, M. J., Jr. (2009). Thermal Adaptation: A Theoretical and Empirical Synthesis. Oxford University Press.

Araújo, A., and Abrunhosa, M. (2012). Geologia e Geomorfologia. S. Paio: Centro de Interpretação.

Baíllo, A., and Chacón, J. E. (2021). Statistical outline of animal home ranges: an application of set estimation. In Handbook of statistics (Vol. 44, pp. 3-37). Elsevier.

Basset, A., and Angelis, D. L. (2007). Body size mediated coexistence of consumers competing for resources in space. *Oikos*, 116(8), 1363-1377. https://doi.org/10.2307/1940913

Bedriaga, J. (1879). Herpetologische Studien. Archiv für Naturgeschichte XLIV: 259–320

Begon M, Harper J. L., and Townsend C. R. (1986). Ecology: individuals, populations and communities. Blackwell, Boston, MA.

Bergallo, H. G., and Rocha, C. F. D. (1993). Activity patterns and body temperatures of two sympatric lizards (*Tropidurus torquatus* and *Cnemidophorus ocellifer*) with

different foraging tactics in southeastern Brazil. *Amphibia-Reptilia, 14*(3), 312-315.

Bezerra, M. F., Barrios-Rodriguez, C. A., Rezende, C. E., López-Castro, M. C., and Lacerda, L. D. (2024). Trophic ecology of sympatric sea turtles in the tropical Atlantic coast of Brazil. *Marine Environmental Research, 196*, 106406. https://doi.org/10.1016/j.marenvres.2024.106406

Bowker, R. G. (1984). Precision of thermoregulation of some African lizards. *Physiological Zoology, 57*(4), 401–412.

Bowker, R. G., Damschroder, S., Sweet, A. M., and Anderson, D. K. (1986). Thermoregulatory behavior of the North American lizards *Cnemidophorus velox* and *Sceloporus undulatus*. *Amphibia-Reptilia, 7*(4), 335–346.

Brito, J. C., Godinho, R., Luís, C., Paulo, O. S., and Crespo, E. G. (1999). Management strategies for conservation of the lizard *Lacerta schreiberi* in Portugal. *Biological Conservation, 89*(3), 311–319. https://doi.org/10.1016/S0006-3207(99)00002-6

Brito, J. C., Paulo, O. S., and Crespo, E. G. (1998a). Distribution and habitats of Schreiber's green lizard (*Lacerta schreiberi*) in Portugal. *Herpetological Journal, 8*(4), 187–194.

Brito, J.C., Luis, C., Godinho, M.R., Paulo, O.S. and Crespo EG. (1998b). Bases para a Conservação do Lagarto-de-água (*Lacerta schreiberi*). Estudos de Biologia e Conservação da Natureza nº 23 Instituto da Conservação da Natureza Ministerio do Ambiente, Lisboa.

Cain III, J. W. C., Krausman, P. R., Rosenstock, S. S., and Turner, J. C. (2006). Mechanisms of thermoregulation and water balance in desert ungulates. *Wildlife Society Bulletin, 34*(3), 570–581. https://doi.org/10.2193/0091-7648(2006)34

Chapman, J. L., and Reiss, M. J. (1999). Ecology: principles and applications. Cambridge University Press.

Darmon, G., Calenge, C., Loison, A., Jullien, J. M., Maillard, D., and Lopez, J. F. (2012). Spatial distribution and habitat selection in coexisting species of mountain ungulates. *Ecography, 35*(1), 44–53. https://doi.org/10.1111/j.1600-0587.2011.06664.x

Daudin, F. M. (1802). Histoire Naturelle, génerale et particulièredes reptiles, ouvrage faisant suite, a l'histoiure naturelle, générale et particulière composée par LECLERC DE BUFFON, et redigée par C. S. SONNINI. *Dufart 3*: 452 pp

Diaz, J. A. (1991). Temporal patterns of basking behaviour in a Mediterranean lacertid lizard. *Behaviour, 118*(1-2), 1-14. https://www.jstor.org/stable/4534950

Díaz, J. A., and Cabezas-Díaz, S. (2004). Seasonal variation in the contribution of different behavioural mechanisms to lizard thermoregulation. *Functional Ecology*, *18*(6), 867–875.

Dmi'el, R. (2001). Skin resistance to evaporative water loss in reptiles: a physiological adaptive mechanism to environmental stress or a phyletically dictated trait?. *Israel Journal of Zoology, 47*(1), 56-67. https://doi.org/10.1560/ENQ9-KD7R-WFGW-KUQW

Driscoll, D. A., Smith, A. L., Blight, S., and Sellar, I. (2020). Interactions among body size, trophic level, and dispersal traits predict beetle detectability and occurrence responses to fire. *Ecological Entomology, 45*(2), 300–310. https://doi.org/10.1111/een.12798

Dufour, C. M., Meynard, C., Watson, J., Rioux, C., Benhamou, S., Perez, J., ... and Ganem, G. (2015). Space use variation in co-occurring sister species: response to environmental variation or competition?. *PLoS One*, *10*(2), e0117750. https://doi.org/10.1371/journal.pone.0117750

Elton, C. (1946). Competition and the structure of ecological communities. *The Journal of Animal Ecology*, 54–68. https://doi.org/10.2307/1625

Elton, C., 1927. Animal Ecology. Sedgwick and Jackson, London.

Escoriza, D., and Amat, F. (2021). Habitat partitioning and overlap by large lacertid lizards in southern Europe. *Diversity, 13*(4), 155. https://doi.org/10.3390/d13040155

Esri (2024). ArcGIS Pro: Professional GIS application. Version 2024. Redlands, CA: Environmental Systems Research Institute. https://www.esri.com/en-us/arcgis/products/arcgis-pro/overview

Ferreira, C. C., Santos, X., and Carretero, M. A. (2016). Does ecophysiology mediate reptile responses to fire regimes? Evidence from Iberian lizards*. PeerJ*, *4*, e2107. https://doi.org/10.7717/peerj.2107

Galán, P. (2003). Anfibios y Reptiles del Parque Nacional de las Islas Atlánticas de Galicia. Naturaleza y Parques Nacionales. Serie Técnica, Ministerio de Medio Ambiente, Madrid.

Ganem, G., Meynard, C. N., Perigault, M., Lancaster, J., Edwards, S., Caminade, P., ... and Pillay, N. (2012). Environmental correlates and co-occurrence of three mitochondrial lineages of striped mice (*Rhabdomys*) in the Free State Province (South Africa). *Acta Oecologica, 42*, 30-40. https://doi.org/10.1016/j.actao.2012.01.003

Goldenberg, J., D'Alba, L., Bisschop, K., Vanthournout, B., and Shawkey, M. D. (2021). Substrate thermal properties influence ventral brightness evolution in ectotherms. *Communications biology, 4*(1), 26. https://doi.org/10.1038/s42003-020-01524-w

Grinnell, J. (1917). The Niche-Relationships of the California Thrasher. *Auk*, *34*(4):427–433 https://doi.org/10.2307/4072271

Hart, S. P., Usinowicz, J., and Levine, J. M. (2017). The spatial scales of species coexistence. *Nature Ecology and Evolution, 1*(8), 1066–1073.

Hespanhol, L., Vallio, C. S., Costa, L. M., and Saragiotto, B. T. (2019). Understanding and interpreting confidence and credible intervals around effect estimates. *Brazilian journal of physical therapy*, *23*(4), 290–301. https://doi.org/10.1016/j.bjpt.2018.12.006

How, Y. F., and Lee, C. Y. (2014). Effects of temperature and humidity on the survival and water loss of *Cimex hemipterus* (Hemiptera: Cimicidae). *Journal of Medical Entomology, 47*(6), 987–995. https://doi.org/10.1603/ME10018

Hutchinson, G.E. (1957). Concluding remarks. Cold Spring Harbor Symp. *Quant. Biol*. 22, 415–427.

Hutchinson, G.E. (1978). An Introduction to Population Ecology. Yale University Press, New Haven.

Huyghe, K., Vanhooydonck, B., Scheers, H., Molina-Borja, M., and Van Damme, R. (2005). Morphology, performance and fighting capacity in male lizards, *Gallotia galloti*. *Functional Ecology*, 800-807. https://www.jstor.org/stable/3599340

Irschick, D. J., and Losos, J. B. (1998). A comparative analysis of the ecological significance of maximal locomotor performance in Caribbean Anolis lizards. *Evolution, 52*(1), 219-226. https://doi.org/10.1111/j.1558-5646.1998.tb05155.x

Kearney, M. R., Munns, S. L., Moore, D., Malishev, M., and Bull, C. M. (2018). Field tests of a general ectotherm niche model show how water can limit lizard activity and distribution. *Ecological monographs, 88*(4), 672–693. https://doi.org/10.1002/ecm.1326

Kearney, M., and Porter, W., 2009. Kearney, M., and Porter, W. (2009). Mechanistic niche modelling: combining physiological and spatial data to predict species' ranges. *Ecology letters, 12*(4), 334–350. https://doi.org/10.1111/j.1461-0248.2008.01277.x

Kingsbury, K. M., Gillanders, B. M., Booth, D. J., and Nagelkerken, I. (2020). Trophic niche segregation allows range-extending coral reef fishes to co-exist with temperate species under climate change. *Global Change Biology, 26*(2), 721–733. https://doi.org/10.1111/gcb.14898

Kingsolver, J.G., Woods, H.A., Buckley, L.B., Potter, K.A., MacLean, H.J., and Higgins, J.K., 2011. Complex life cycles and the responses of insects to climate change. *Integrative and Comparative Biology, 51*, 719–732. https://doi.org/10.1093/icb/icr015

Kiszka, J., Simon-Bouhet, B., Martinez, L., Pusineri, C., Richard, P., and Ridoux, V. (2011). Ecological niche segregation within a community of sympatric dolphins around a tropical island. *Marine Ecology Progress Series, 433*, 273–288. https://doi.org/10.3354/meps09165

Kouete, M. T., and Blackburn, D. C. (2020). Dietary partitioning in two co-occurring caecilian species (*Geotrypetes seraphini* and *Herpele squalostoma*) in Central Africa. *Integrative Organismal Biology, 2*(1), obz035. https://doi.org/10.1093/iob/obz035

Lailvaux, S. P. (2007). Interactive effects of sex and temperature on locomotion in reptiles. *Integrative and Comparative Biology, 47*(2), 189-199. https://doi.org/10.1093/icb/icm011

Lee, A. (2010). Circular data. Wiley Interdisciplinary Reviews: *Computational Statistics*, *2*(4), 477–486. https://doi.org/10.1002/wics.98

Licht, P. (1972). Environmental physiology of reptilian breeding cycles: role of temperature. *General and comparative endocrinology, 3*, 477–488.

Llorente, G.A., Montori, A., Santos, X., Carretero, M.A. (1995). Atlas de distribució dels Anfibis y Rèptils de Catalunya y Andorra. El Grau, Figueres: 192 pp.

MacArthur, R. H. (1958). Population ecology of some warblers of northeastern coniferous forests. *Ecology*, *39*(4), 599–619. https://doi.org/10.2307/1931600

MacKenzie, D. I., Nichols, J. D., Royle, J. A., Pollock, K. H., Bailey, L., and Hines, J. E. (2017). Occupancy estimation and modeling: inferring patterns and dynamics of species occurrence. Elsevier.

Marco, A. (2017). Lagarto verdinegro - *Lacerta schreiberi*. En: Enciclopedia Virtual de los Vertebrados Españoles. Salvador, A., Marco, A. (Eds.). Museo Nacional de Ciencias Naturales, Madrid. http://www.vertebradosibericos.org/

Marco, A., and Pérez-Mellado, V. (1998). Influence of clutch date on egg and hatchling sizes in the annual clutch of *Lacerta schreiberi* (Sauria, Lacertidae). *Copeia*, 145–150. https://www.jstor.org/stable/1447710

Marco, A., and Pollo, C. (1993). Análisis biogeográfico de la distribución del lagarto verdinegro (*Lacerta schreiberi* Bedriaga 1878). *Ecología, 7*, 457–466.

Martín, J., and López, P. (2010). Thermal constraints of refuge use by Schreiber's green lizards, *Lacerta schreiberi*. *Behaviour*, 275–284. https://www.jstor.org/stable/40599663

Mateo, J.A. (2017). Lagarto ocelado - *Timon lepidus*. In Enciclopedia Virtual de los Vertebrados Españoles. Salvador, A., and A. Marco (Eds.). Museo Nacional de Ciencias Naturales, Madrid, Spain. Pp. 1–52.

Mateo, J.A. and Cheylan, M. (1997). *Lacerta lepida* Daudin 1802. SEH and Muséum National d'Histoire Naturelle, París.

Mathur, V. (1991). The ecological interaction between habitat composition, habitat quality and abundance of some wild ungulates in India (Doctoral dissertation, University of Oxford).

Meredith, M., Ridout, M., and Campbell, L.A. (2024). overlap: Estimates of Coefficient of Overlapping for Animal Activity Patterns. R package version 0.3.9, https://CRAN.R-project.org/package=overlap

Messerman, A. F., Turrell, M., and Leal, M. (2022). Divergent physiological acclimation responses to warming between two co-occurring salamander species and

implications for terrestrial survival. *Journal of Thermal Biology, 106*, 103228. https://doi.org/10.1016/j.jtherbio.2022.103228

Meynard, C. N., Pillay, N., Perrigault, M., Caminade, P., and Ganem, G. (2012). Evidence of environmental niche differentiation in the striped mouse (*Rhabdomys* sp.): inference from its current distribution in southern Africa. *Ecology and evolution, 2*(5), 1008–1023. https://doi.org/10.1002/ece3.219

Mulder and Klugkist (2017). Bayesian estimation and hypothesis tests for a circular Generalized Linear Model. *Journal of Mathematical Psychology, 80*, 4–4.

Pavey, C. R., and Geiser, F. (2008). Basking and diurnal foraging in the dasyurid marsupial *Pseudantechinus macdonnellensis*. *Australian Journal of Zoology*, *56*(2), 129-135. https://doi.org/10.1071/ZO08032

Pearson, R. G. (2007). Species' distribution modeling for conservation educators and practitioners. Synthesis. *American Museum of Natural History, 50*, 54–89.

Pérez-Mellado, V. 1998. *Lacerta schreiberi* (Bedriaga, 1878). In: Salvador A (ed) Reptiles, Fauna Ibérica, vol 10. *Museo Nacional de Ciencias Naturales*, CSIC, Madrid, pp 218–227.

Pianka, E. R. (1974). Niche overlap and diffuse competition. *Proceedings of the National Academy of Sciences, 71*(5), 2141–2145. https://doi.org/10.1073/pnas.71.5.2141

Pianka, E. R. (2000) Evolutionary ecology. Addison Wesley, San Francisco, USA.

Pianka, E. R., and Huey, R. B. (1978). Comparative ecology, resource utilization and niche segregation among gekkonid lizards in the southern Kalahari. *Copeia*, 691–701. https://doi.org/10.2307/1443698

Plummer, M., Best, N., Cowles, K., and Vines, K. (2006). CODA: convergence diagnosis and output analysis for MCMC. *R news*, *6*(1), 7-11.

Prieto-Ramirez, A. M., Pe'er, G., Rödder, D., and Henle, K. (2018). Realized niche and microhabitat selection of the eastern green lizard (*Lacerta viridis*) at the core and periphery of its distribution range. *Ecology and evolution, 8*(22), 11322–11336. https://doi.org/10.1002/ece3.4612

Prins, H.H.T. and Olff, H. (1998) Species richness of African grazer assemblages: towards a functional explanation. In: Dynamics of Tropical Communities;

Symposia of the British Ecological Society 37 (Eds D. M. Newbery, H. H. T. Prins and N. D. Brown). Blackwell Science, Oxford.

R Core Team (2024). R: A language and environment for statistical computing. R Foundation for Statistical Computing, Vienna, Austria. URL https://www.R-project.org/.

Ramellini, S., Crepet, E., Lapadula, S., and Romano, A. (2024). Trophic niche segregation in a guild of top predators within the Mediterranean Basin. *Current Zoology*, zoae001. https://doi.org/10.1093/cz/zoae001

Renet, J., Dokhelar, T., Thirion, F., Tatin, L., Pernollet, C. A., and Bourgault, L. (2022). Spatial pattern and shelter distribution of the ocellated lizard (*Timon lepidus*) in two distinct Mediterranean habitats*. Amphibia-Reptilia, 43*(3), 263–276.

Reyes-Puig, C., Enriquez-Urzelai, U., Carretero, M. A., and Kaliontzopoulou, A. (2024). Is it all about size? Dismantling the integrated phenotype to understand species coexistence and niche segregation. *Functional Ecology*, *38*(11), 2350-2368.

Ridout, M. S., and Linkie, M. (2009). Estimating overlap of daily activity patterns from camera trap data. *Journal of Agricultural, Biological, and Environmental Statistics, 14*, 322–337.

Ritchie, M.E. and Olff, H. (1999) Spatial scaling laws yield a synthetic theory of biodiversity. *Nature 400*, 557–560. https://doi.org/10.1038/23010

Rowcliffe M (2023). activity: Animal Activity Statistics. R package version 1.3.4, https://CRAN.R-project.org/package=activity

Sales, L. P., Hayward, M. W., and Loyola, R. (2021). What do you mean by “niche”? Modern ecological theories are not coherent on rhetoric about the niche concept. *Acta Oecologica, 110*, 103701. https://doi.org/10.1016/j.actao.2020.103701

Salvador, A. (1988). Selección de microhabitat del lagarto verdinegro (*Lacerta schreiberi*) (Sauria: Lacertidae). *Amphibia-Reptilia, 9*(3), 265–275. https://doi.org/10.1163/156853888X00350

Sannolo, M., Barroso, F. M., and Carretero, M. A. (2018). Physiological differences in preferred temperatures and evaporative water loss rates in two sympatric lacertid species. *Zoology, 126*, 58–64. https://doi.org/10.1016/j.zool.2017.12.003

Sannolo, M., Ponti, R., and Carretero, M. A. (2019). Waitin'on a sunny day: Factors affecting lizard body temperature while hiding from predators. *Journal of thermal biology, 84*, 146–153. https://doi.org/10.1016/j.jtherbio.2019.07.001

Sfenthourakis, S., Tzanatos, E., and Giokas, S. (2006). Species co-occurrence: the case of congeneric species and a causal approach to patterns of species association. *Global Ecology and Biogeography, 15*(1), 39–49. https://doi.org/10.1111/j.1466-822X.2005.00192.x

Shine, R. (2004). Does viviparity evolve in cold climate reptiles because pregnant females maintain stable (not high) body temperatures?. *Evolution, 58*(8), 1809-1818. https://doi.org/10.1111/j.0014-3820.2004.tb00463.x

Soberon, J., and Peterson, A. T. (2005). Interpretation of models of fundamental ecological niches and species' distributional areas. https://doi.org/10.17161/bi.v2i0.4

Stevenson, R. D. (1985). Body size and limits to the daily range of body temperature in terrestrial ectotherms. *The American Naturalist, 125*(1), 102–117.

Valladares, F., Bastias, C. C., Godoy, O., Granda, E., and Escudero, A. (2015). Species coexistence in a changing world. *Frontiers in plant science*, *6*, 866. https://doi.org/10.3389/fpls.2015.00866

Verwaijen, D., Van Damme, R., and Herrel, A. (2002). Relationships between head size, bite force, prey handling efficiency and diet in two sympatric lacertid lizards. *Functional Ecology*, *16(*6), 842-850. https://doi.org/10.1046/j.1365-2435.2002.00696.x

Weaver, S. J., McIntyre, T., van Rossum, T., Telemeco, R. S., and Taylor, E. N. (2023). Hydration and evaporative water loss of lizards change in response to temperature and humidity acclimation. *Journal of Experimental Biology, 226*(20), jeb246459. https://doi.org/10.1242/jeb.246459

Weil, S. S., Gallien, L., Nicolaï, M. P., Lavergne, S., Börger, L., and Allen, W. L. (2023). Body size and life history shape the historical biogeography of tetrapods. *Nature Ecology and Evolution, 7*(9), 1467-1479.10.1038/s41559-023-02150-5

Williams, C.B. (1964) Patterns in the balance of nature. Academic Press, N.Y

Wolff, J.O. (1996). Coexistence of white-footed mice and deer mice may be mediated by fluctuating environmental conditions. *Oecologia 108*, 529–533. https://doi.org/10.1007/BF00333730

Žagar, A., Carretero, M. A., Osojnik, N., Sillero, N., and Vrezec, A. (2015). A place in the sun: interspecific interference affects thermoregulation in coexisting lizards. *Behavioral Ecology and Sociobiology, 69*, 1127-1137. https://www.jstor.org/stable/43599866

6. Chapter 6

Physiology-microhabitat matching may help organisms cope with the thermal and hydric challenges under climate change: a tale of two lizards

6.1. Introduction

The effects of climate change on biodiversity are pervasive (Habibullah et al., 2022), manifesting through several impacts such as shifts in species distribution (Ramalho et al., 2023), changes in phenology and trophic interactions (Ramalho et al., 2023), and alterations in growth and reproduction rates (Paaijmans et al., 2013). Ectotherms are particularly vulnerable to climate change because their physiological state (e.g. body temperature) entirely depends on their surroundings. Furthermore, in the case of thermoregulating ectotherms, their ability to maintain their body within a preferred body temperature range—actively selected in controlled conditions to optimise physiological processes—is limited and highly dependent on the features of their surrounding microhabitats (Angilletta Jr., 2009; Huey et al., 2012; Ramalho et al., 2023; Woods et al., 2015). In natural settings, some authors consider body temperature as a proxy for preferred temperature (Angilletta Jr., 2009; Barber and Crawfor Jr., 1977). Microhabitats play a crucial role for ectotherms to avoid heat stress by balancing internal and external temperatures (Burraco et al., 2020; Enriquez-Urzelai et al., 2020). However, one of the most pressing threats posed by global warming is the potential for significant changes in the microclimatic conditions of microhabitats, which may render them unsuitable as thermal refugia, thus increasing extinction risk for ectotherms (Burraco et al., 2020; Kearney, 2013). Consequently, understanding the physiological processes that link organisms to their external environment is crucial for anticipating the fine-scale impacts of climate change on biodiversity.

Increases in temperature extremes could lead to substantial physiological changes in ectothermic organisms due to heat stress (Huey et al., 2012; Kingsolver et al., 2013; Ramalho et al., 2023). Furthermore, altered daily temperature fluctuations can result in reduced levels of performance (Huey et al., 2012; Paaijmans et al., 2013) and activity, and they could create energy imbalances and impair essential functions such as feeding and reproduction (Gunderson and Leal, 2016; Huey et al., 2012). In addition, extreme temperatures can exacerbate water loss, altering water balance and increasing the water intake necessary for physiological homeostasis, further impacting activity and survival rates (Kearney et al., 2018; Pirtle et al., 2019). Unfortunately, most climate change studies have focused on the impacts of thermal environment changes, whereas aspects related to the hydric ecology of species have been largely overlooked (Pirtle et al., 2019; but see Enriquez-Urzelai and Gvozdik 2024; Rozen-Rechels et al., 2019; Wu et al., 2024). Key traits such as activity times (e.g. foraging and basking times), period during which individuals can attain preferred body temperatures, water loss rates and

shade requirements (proportion of shade to mitigate heat stress). Understanding how these traits respond to climate change is critical to predicting shifts in species' microhabitat use and local distribution patterns (Habibullah et al., 2022; Ramalho et al., 2023).

In the face of the strong effects of climate change, microclimates can play a role in mitigating its consequences. However, this mitigation is limited and depends on the ability of ectotherms to exploit favourable conditions in microhabitats (Woods et al., 2015). The presence of microhabitats and associated microclimates is essential to ensure effective thermo- and hydroregulation in ectotherms (Kearney et al., 2014). The spatial configuration of the landscape, such as topography and vegetation, determines the spatiotemporal availability of microhabitats that serve as climatic refugia. When species lack access to microhabitats with favourable microclimates, the risks of population decline increase (Kearney et al., 2009; Kearney et al., 2014). Even the shelter-seeking behaviour of animals in extreme heat conditions is associated with a reduction in the need for short-term physiological adaptations, which helps mitigate heat stress (Kearney et al., 2009). The main climatic factors of microhabitats are temperature and humidity. Undeniably, temperature has been the most studied factor (e.g., Keppel et al., 2017; Rubalcaba et al., 2023; Scheffers et al., 2013); humidity, in conjunction with temperature, has received less attention, leaving its direct effects on physiological water balance less well understood (Enriquez-Urzelai and Gvoždík, 2024; Kearney and Enriquez-Urzelai, 2023). Kearney et al. (2018) showed that access to water may be even more limiting than temperature for ectotherms in some climates. Therefore, the availability of water sources in microhabitats influences the growth, activity, and distribution of populations, as hydration is key to regulating water stress.

Body size is closely related to ectothermic physiology (Angilletta Jr., 2009; Reyes-Puig et al., 2024); for example, smaller ectothermic animals heat faster, while larger ectotherms, due to thermal inertia, retain heat for longer periods of time, which potentially affects internal physiological processes (Huey et al., 2012). The impacts of global warming on body size have already been evidenced and associated with a reduction in body size linked to the consequences of temperature on development and growth (Ohlberger, 2013; Kearney et al., 2009). The effects of increased temperatures on body size are mainly driven by changes in rates of biochemical reactions, heat stress, and disruptions in energy balance (Gardner et al., 2011; Olhberger, 2013; Sentis et al., 2024). All this evidence suggests that species of different sizes could be unequally susceptible to the impacts of climate change (Foden et al., 2018). In addition to temperature related

differences between organisms of different sizes, body size is also of uppermost importance for water balance. For example, water loss in larger ectotherms is relatively lower due to their reduced surface-to-volume ratio, enabling them to conserve water more effectively (Chown and Klok, 2003). In contrast, smaller ectotherms, with a higher surface-to-volume ratio, are more susceptible to water stress. Consequently, body size plays a pivotal role in determining the vulnerability of species to the impacts of climate change (Claunch et al., 2020; Foden et al., 2018).

Some of the indirect effects of climate change, on which less information is available, are related to species' interactions. For instance, shifts in species abundance can lead to changes in their distributions, influenced by interspecific relationships such as competition or predation (Angert et al., 2013; Ramalho et al., 2023). Similarly, behavioural traits can be affected by metabolism and internal physiology due to increased temperature, thus causing disruptions in interaction networks between species, particularly those that coexist and maintain close relationships (Boukal et al., 2019; Brambilla et al., 2019). These indirect effects, although complex, can be more significant than direct climatic impacts (Gilman et al., 2010). Understanding how climate change reshapes biotic interactions, such as predator-prey dynamics or competition for resources, is key to predicting ecosystem responses. Altered species interactions can cascade through ecosystems, modifying species composition, habitat use, and microhabitat selection (Åkesson et al., 2021; Boukal et al., 2019; Brambilla et al., 2019).

Here we focused on how microhabitat variability and physiological traits mediate the impacts of climate change on two coexisting green lizard species, *Timon lepidus* and *Lacerta schreiberi*, in northern Portugal. Specifically, we aimed to assess how their physiological attributes influence thermoregulation, activity, water balance, and microhabitat preferences under current and projected future climatic conditions. *T. lepidus* has a more Mediterranean distribution, preferring open areas (Ferreira et al., 2016), while *L. schreiberi* has a more Atlantic distribution, restricted to wetter environments with abundant vegetation (Salvador, 1988; Sillero et al., 2009). As such, these two species seem to differ substantially in their landscape-level ecological requirements. Additionally, previous findings revealed significant physiological differences between the two species, with *L. schreiberi* displaying distinct physiological traits related to water balance and variance in preferred temperature within a multidimensional ecophenotypic space (Reyes-Puig et al., 2024). Furthermore, both species differ significantly in their body size, with *T. lepidus* being the largest (reaching a snout-vent length, SVL, of 240 mm) and *L. schreiberi* the smallest (reaching a SVL of

130 mm) (Brito et al., 1998; Mateo, 2017). Body size plays a crucial role in defining the ecological niche of these species and facilitating their coexistence (Reyes-Puig et al., 2024). This difference enables us to examine how physiological requirements, largely related to differences in body sizes, will mediate the impacts of climate change on populations of coexisting species that differ in size. By analysing these two species with different ecological requirements we will be able to provide a better understanding of the role of microhabitat variability and physiological adaptation in mitigating the effects of climate change.

Specifically, we hypothesize that time spent in activity will decrease in future and warmer conditions, primarily due to the need to avoid overheating, which could restrict both daily and seasonal activity periods (Huey et al., 2012; Kearney and Porter, 2009). However, if favourable microclimatic conditions in microhabitats are maintained, and maximum thermal limits are not exceeded, activity times could potentially increase as individuals exploit microhabitats to mitigate rising temperatures (Angilletta Jr., 2009; Nagy et al., 1984;). Additionally, we aim to quantify evaporative water loss in both species under current and future conditions. We expect evaporative water loss to increase for both species under climate change, as a result of rising environmental temperatures and lower humidity levels. As temperatures rise, the need for efficient thermoregulation and water balance intensifies (Burraco et al., 2020; Kearney et al., 2018). However, given previous data on the hydrophilic nature of *L. schreiberi* and the importance of this trait for the species (Brito et al., 1998; Reyes-Puig et al., 2024; Salvador, 1988), we expect that it will present higher water loss than *T. lepidus*, even after considering the effect of body size. We anticipate that increasing environmental temperatures will drive both species to seek more shade during periods of high activity and elevated temperatures, such as in spring and summer, such as to reduce thermal stress (Kingsolver et al., 2013; Paaijmans et al., 2013). We also expect a reduction in time spent within their preferred temperature range, mainly because increasing environmental temperatures may cause organisms to exceed their thermal limits. As a result, individuals may need to retreat to shaded or cooler microhabitats to avoid overheating or shift their activity windows to cooler periods of the day (Kingsolver et al., 2013). Furthermore, we suspect that *L. schreiberi* will require more shade than *T. lepidus* to maintain physiological balance and water retention, as suggested by its preference for moist environments (Brito et al., 1998; Salvador, 1988). Finally, we aim to explore potential changes in the fine-scale distribution of both species as they search for more favourable habitats for thermo- and hydroregulation under a climate change scenario.

We anticipate that both species will shift their local distribution in search of cooler and more shaded microhabitats, as has been estimated in previous research on shifts in species distributions under climate change (Angert et al., 2013; Burraco et al., 2020; Ramalho et al., 2023).

6.2. Methods

6.2.1. Study area and microhabitat identification

The study area, located at Castro São Paio, northern Portugal (41.312257° N, 8.737074° W; 12 m a.s.l.), exhibits diverse microhabitats, classified into four main types: **i)** herbaceous vegetation, characterised by low-growing, non-woody, and fast-growing plants, including maize, grass, and Ulex; **ii)** rocky and exposed substrates, comprising natural formations or human-made structures like rocky walls and construction remnants, characterised by bare soil, solid mineral surfaces, cracks, and holes; **iii)** areas dominated by succulent and creeping plants of the genus *Carpobrotus*; and **iv)** walkways, transit areas made of wood, primarily designed for tourists. This region is particularly interesting due to the coexistence of *L. schreiberi* and *T. lepidus*, whose distinct ecological adaptations allow them to exploit different microhabitats (Reyes-Puig et al., unpubl. data. Chapter 5)

To classify the microhabitats throughout the extent of the study area, we classified with ArcGIS Pro (ESRI, 2024) the microhabitats in Castro de São Paio using a high-resolution orthophoto (1 metre resolution). We selected representative areas of each previously defined microhabitat (herbaceous vegetation, rocky and exposed substrates, *Carpobrotus* vegetation, and walkway), using the Training Samples Manager panel. The areas were manually selected (n = 100) based on detailed knowledge of the study area and covered the spectral variability of each class. We applied the supervised classification algorithm Support Vector Machines (SVM), configured with the radial kernel values and using the default values for penalty coefficient and gamma. After training the model, we classified the whole orthophoto to generate a detailed map of the microhabitats present in the study area. We validated the classification with a confusion matrix, using independent samples that were not used for training (80% training, 20% testing), and calculated the Overall Accuracy and Cohen's Kappa coefficient. Finally, we visually reviewed the generated map.

6.2.2. Modeling microclimates in microhabitats and model calibration

To investigate how microhabitat conditions influence thermal and hydric challenges faced by lizards under climate change we developed mechanistic models using NicheMapR (Kearney and Porter, 2017). These models include a microclimate and an organismal model, for our purposes, an ectotherm model. The microclimate model reconstructs environmental conditions experienced by an organism by combining weather data (as measured by weather stations) and terrain characteristics. The terrain is characterised with features such as slope, aspect, elevation, soil properties, and available shade (Kearney and Porter, 2017). Forcing weather variables of the microclimate model include air temperature, precipitation, cloud cover, relative humidity, and wind speed, among others (Kearney and Porter, 2017). We extracted aspect and slope from a digital elevation model obtained in R using the “elevatr” package, which retrieves elevation data from the USGS National Map and Mapzen Terrain Tiles, ensuring access to high-resolution elevation information (Hollister et al., 2023). We resampled terrain layers to match the resolution of a high-definition orthophoto of the study area (1 metre resolution) using bilinear interpolation with the “resample” function from the “raster” R package (Hijmans, 2024). This method estimates the value of each new pixel by taking a weighted average of the four nearest cell values, ensuring smooth transitions.

In order to determine the parameters associated with microhabitat environmental conditions and adjust the predictions generated by the NicheMapR microclimate model (Kearney et al., 2014; Kearney and Porter, 2017) (see below), we installed Thermochron and Hygrochron iButton dataloggers in the four microhabitats at Castro São Paio. We placed four iButtons at strategic locations within each microhabitat: one exposed, one in intermediate shade, one in full shade, and one buried approximately 15 cm below the soil surface. The dataloggers exposed and shaded recorded temperature and humidity, while those in the intermediate shade and buried recorded only temperature. The dataloggers were programmed to record temperature and humidity hourly from May 2021 to June 2022.

Once the data were collected over a full year, we processed and cleaned the dataset, converting dates into appropriate formats for analysis. The data were organised into time series using the R packages “chron” (James and Hornik, 2020) and “lubridate” (Grolemund and Wickham, 2011). We combined the iButton data with meteorological station records obtained from

https://www.wunderground.com/dashboard/pws/IMODIV1, synchronising the time series and unifying temperature and humidity data. This process was automated, and the script used for downloading daily data, organising, and cleaning the dataset can be found here https://github.com/Pristimantis2016/microclimates/blob/main/code/prepare_weather.R. We then used customised NicheMapR microclimate models (Kearney and Porter, 2017) to simulate environmental conditions in each microhabitat. A custom function, "micro_custom", was developed based on the original "micro_global" function to use the hourly weather data from the meteorological station as input variables and modify parameters (with the "habitat" argument) according to the specific microhabitats in the study area. The parameters modified according to microhabitat type were roughness height (*RUF*), substrate longwave IR emissivity (*SLE*), soil mineral density (*Density*, Mg/m^3), soil type (*soiltype*), soil mineral thermal conductivity (*Thcond*, W/m°C), and maximum available shade (*maxshade*). The ranges of parameter values used for model calibration were extracted from revision of literature, including key sources such as Campbell and Norman (1999), Snyder et al. (1998), Hillel (2003), ISRIC (1998), Farouki (1981), and Monteith and Unsworth (1994). The parameter values adjusted per microhabitat were as follows: herbaceous vegetation, *RUF*: 0.02, *SLE*: 0.984, *Density*: 1.42, *soiltype*: 8, *Thcond*: 3, *maxshade*: 85; *Carpobrotus*-dominated areas, *RUF*: 0.01, *SLE*: 0.97, *Density*: 2.5, *soiltype*: 3, *Thcond*: 3, *maxshade*: 90; walkways, *RUF*: 0.005, *SLE*: 0.96, *Density*: 1.75, *soiltype:* 6, *Thcond*: 3, *maxshade*: 70; and rocky and exposed microhabitats, *RUF*: 0.09, *SLE*: 0.96, *Density*: 2.0, *soiltype*: 3, *Thcond*: 3, *maxshade*: 99. The predictive accuracy of the microclimatic models was evaluated using root mean square error (RMSE), calculated for each variable and microhabitat.

6.2.3. Lizard biophysical models

We used the outputs of microclimate models as inputs for the ectotherm model. The ectotherm model incorporates morphological, physiological, and behavioural parameters to simulate how the studied organisms maintain thermal and hydric balance with their environment. The model solves coupled heat and (partial) mass balance equations to calculate body temperatures and water loss at each time step and based on those body temperatures it estimates potential hours of activity (Kearney and Porter, 2020). We executed steady-state ectotherm models, which assume that variables such as body temperatures reach equilibrium within each time step and therefore do not account for thermal inertia over time (Kearney and Porter, 2020). The set of parameters used for our study species were: for *Timon lepidus*, we established a wet body weight

(*Ww_g*) of 84.5 g, a 'lizard' body shape (*shape* = 3), and a skin percentage that is wet (*pct_wet*) of 0.01. The minimum body temperature for foraging (*T_F_min*) was set at 23.2 °C, while the maximum temperature for foraging (*T_F_max*) was 34 °C. The preferred temperature (*T_pref*) was established at 30.3 °C. The minimum body temperature to leave the refuge (*T_RB_min*) was set at 15 °C, and the minimum body temperature for basking (*T_B_min*) was also 15 °C. For *Lacerta schreiberi* we set body weight Ww_g = 21.96 g, shape = 3, and *pct_wet* = 0.02. *T_F_min* was set at 25.4 °C, while *T_F_max* = 34 °C, and *T_pref* = 30.4 °C. Both *T_RB_min* and *T_B_min* were set to 17 °C. We considered both *T. lepidus* and *L. schreiberi* as only diurnal species (*diurn = 1; nocturn = 0; crepus = 0*), with shade seeking behaviour for thermoregulation (shade_seek = 1), and with burrowing behaviour (*burrow = 1*). The parameters were obtained from laboratory experiments and extensive fieldwork (Reyes-Puig et al., 2024; Reyes-Puig et al., unpubl. data. Chapter 5). Using the described parameters, we ran ectotherm models in each cell of the study area. Within each cell we extracted the total sum of foraging hours, basking hours, evaporative water loss during activity, the number of hours within the preferred body temperature range, and the average shade in their respective microhabitats, during the peak activity period of the lizards, which corresponds to spring and summer (20 March to 20 September).

6.2.4. Climate change simulations

To simulate climate change scenarios, we increased current temperature data by 2 °C, which represents a plausible scenario that aligns with the projections of the Sixth Assessment Report of the Intergovernmental Panel on Climate Change (IPCC). The IPCC has already pointed out that global average temperatures have risen by approximately 1.1 °C compared to pre-industrial levels, and since our planet is on track to surpass 2 °C of warming by mid-century under high-emission scenarios (IPCC, 2023). Furthermore, the Copernicus Climate Change Service (C3S) has confirmed that in 2024, global average temperatures temporarily exceeded 1.5 °C above pre-industrial levels for consecutive months, highlighting the ongoing trends of global warming (C3S, 2024). Likewise, and based on current trends, we considered a more extreme scenario and increased the temperature by 4 °C. This scenario corresponds to high-emission pathways described in the Sixth Assessment Report of the IPCC, which indicates that under scenarios with limited mitigation, global temperatures could increase by up to 4.4 °C by the end of the 21st century (IPCC, 2023). To run the climate change scenarios, we added the offsets (+2 ºC or +4ºC) to the baseline weather data and we re-run

microclimate models. With the outputs of those models, we re-run ectotherm models for the whole study area and extracted the abovementioned parameter predictions.

6.2.5. Data analysis

To evaluate spatial patterns of biological rates derived from mechanistic models we generated raster maps using the “rast” function from the terra package (Hijmans, 2024) for each species and climatic scenario (current and two future scenarios). These variables included foraging and basking times, hours within the preferred temperature range, total and size-corrected water loss, and average selected shade. Subsequently, we calculated the differences between scenarios, creating raster maps that reflect the changes in these variables between the present and future scenarios. Additionally, to explore the effect of terrain and microclimates in our forecasts, and compare between species, we analysed variation in the variables as a function of slope, aspect, microhabitats, and species. Slopes were classified into two categories: low (<7 degrees) and high (≥7 degrees), while aspects were divided into four main categories: slopes were classified into two categories: low (<7 degrees) and high (≥7 degrees), while aspects were divided into four main categories: north (0° to 45° and 315° to 360°), east (45° to 135°), south (135° to 225°), and west (225° to 315°). We categorised aspect into four main categories (north, east, south, and west) instead of using continuous values to simplify the analysis and focus on ecologically meaningful trends, as has been done in several research following a similar approach (e.g., Gottlieb and Caldwell, 1967; Guisan and Hofer, 2003). For microhabitats, the categories corresponded to the previously classified microhabitats. These groupings allowed us to explore potential variations associated with topographical and environmental characteristics and their relationship with species physiology.

We extracted spatial coordinates using the “crds” function from the terra package and generated spatial and geographical representations integrating the results of ectothermal models across the different scenarios and categories. We visualised the data using violin plots to clearly identify the distributions of the variables by species, climatic scenario, slope, aspect, and microhabitat. All spatial representations and graphs were created using the ggplot2 package (Wickham, 2016).

6.3. Results

Our orthophoto classification (Figure 6.1) with the Support Vector Machine (SVM) algorithm yielded an Overall Accuracy of 88.71%. Thus, we found a relatively high level of agreement between the classified and actual categories. Furthermore, Cohen's Kappa coefficient was 0.839, representing substantial agreement beyond chance (Cohen, 1960; 1968).

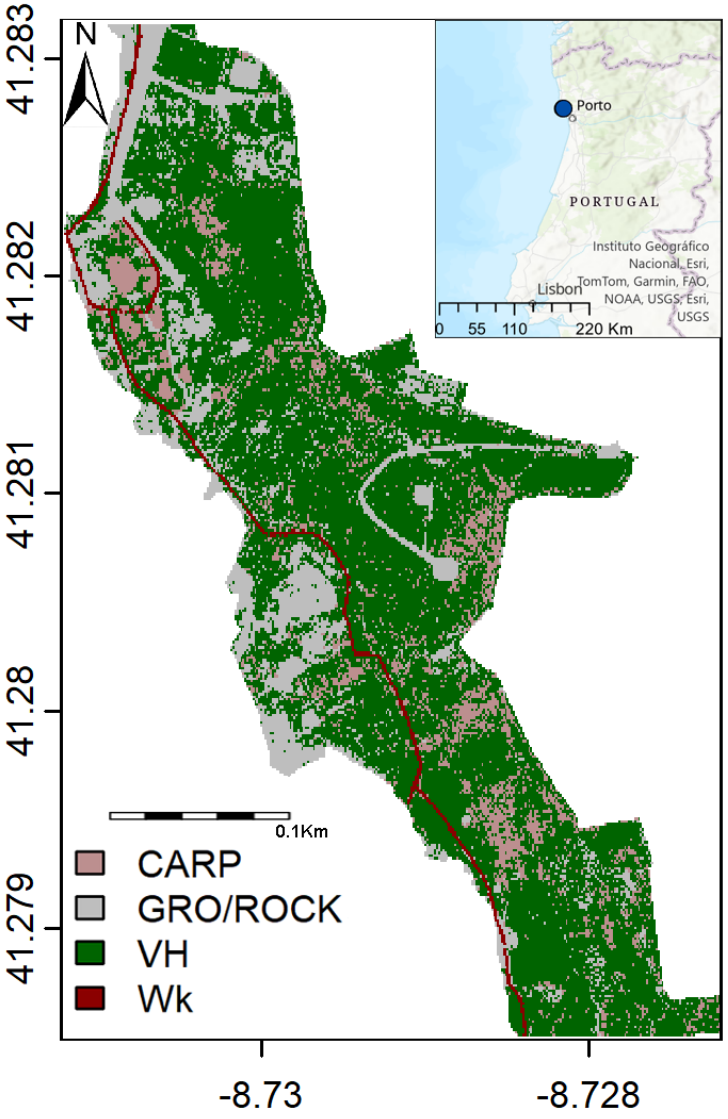

Figure 6.1 Map of the study area in Castro de São Paio, Portugal, showing the classification of microhabitats based on the high-resolution georeferenced orthophoto. Categories include VH (herbaceous vegetation), GRO/ROCK (rocky substrate and bare soil), CARP (*Carpobrotus* vegetation), and Wk (walkway). The inset displays the location of the study site in Portugal.

6.3.1. Microclimates in microhabitats

After adjusting parameters in the microclimate model, we achieved a high predictive accuracy. The predictions obtained with NicheMapR's microclimate model closely matched our observations of empirical temperature and relative humidity data collected over one year, confirming that the microclimate model is able to accurately represent microclimatic conditions in different microhabitats (Figure 6.2). Overall, we obtained RMSE values for temperature ranging from 1.29°C to 5.03°C across the different microhabitats. In the in herbaceous vegetation habitat, RMSE values varied from 1.29°C to 4.35°C. Similarly, rocky habitat, RMSE values ranged between 1.86°C to 5.03°C, and in *Carpobrotus*-dominated areas, the RMSE ranged from 1.54°C to 3.69°C. Finally, in the walkway habitat, RMSE values ranged from 2.25°C to 4.47°C. Additionally, the different microhabitats exhibit distinct patterns in terms of temperature and relative humidity, reflected both in the field data and the model predictions (Figure 6.2, Appendix D Table D4.1). Herbaceous and *Carpobrotus* vegetation showed more moderate temperatures and more stable humidity levels compared to other microhabitats (Figure 6.2). In contrast, the greatest thermal fluctuations were observed in rocky microhabitats and walkways, the latter reaching the highest temperatures, even in shaded areas (Figure 6.2). Finally, model predictions for relative humidity appear to align less closely with empirical data during April to July, particularly in shadowed and buried microhabitats (Figure 6.2).

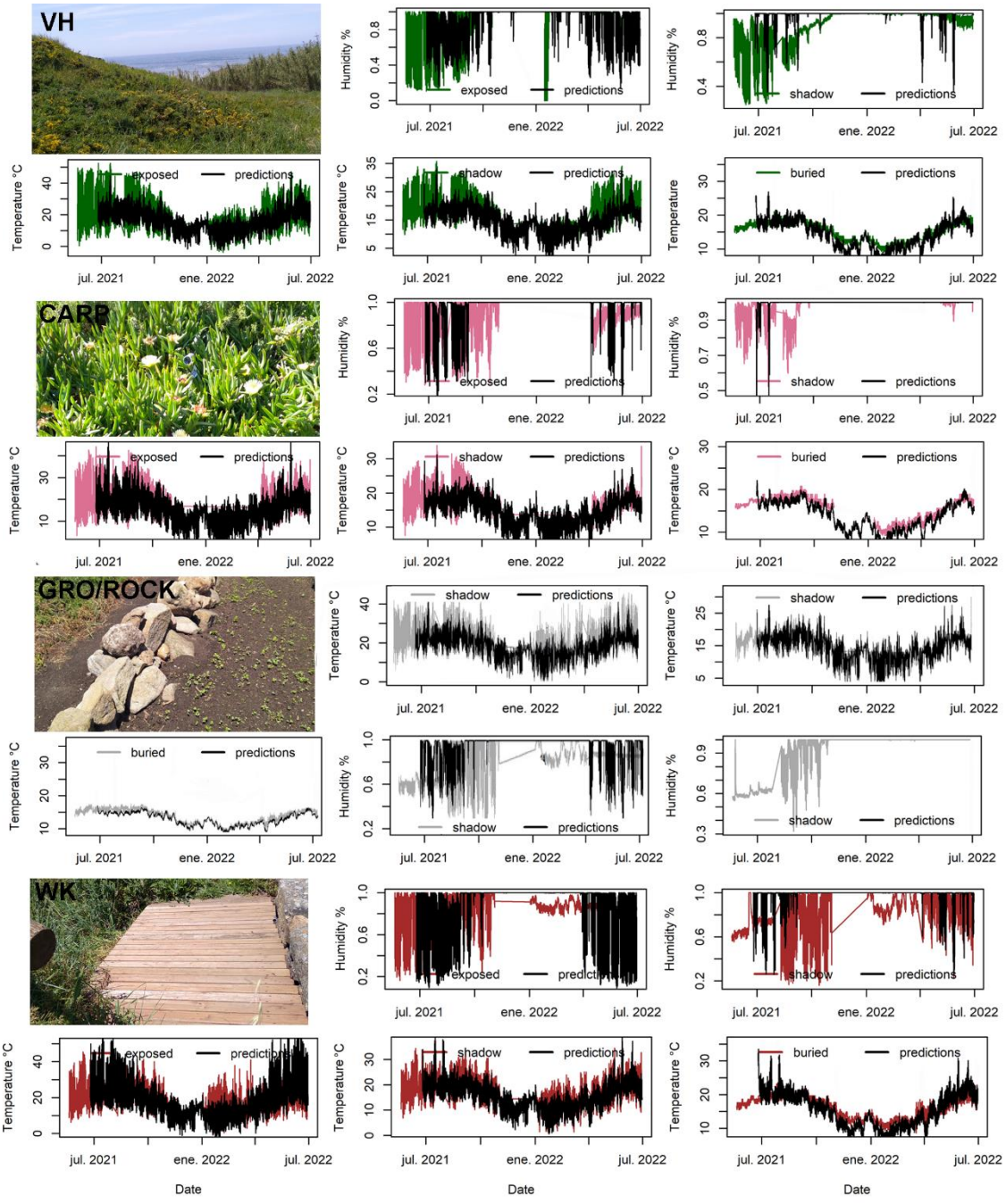

Figure 6.2 Predictions from the microclimate model projected by NicheMapR (black lines) and field data collected using dataloggers (colored lines) over one year of monitoring (May 2021-July 2022). The variables shown are temperature (°C) and relative humidity (%). The datalogger colors represent different microhabitats: dark green for herbaceous vegetation, pink for *Carpobrotus*, grey for rocky microhabitats, and dark brown for walkways. VH (herbaceous vegetation), GRO/ROCK (rocky substrate and bare soil), CARP (*Carpobrotus* vegetation), and Wk (walkway).

6.3.2. Biophysical predictions for lizards in different microhabitats

Regarding variables derived from ectotherm models, we observed a clear spatial variation in foraging time, time spent at the preferred temperature, and shade selection (Figure 6.3). Under current climatic conditions, *T. lepidus* forages for longer periods than

L. schreiberi. Both species tend to have more potential hours for foraging in rocky bare soil microhabitats, although this is more pronounced in *T. lepidus* (Figure 6.3A, D; Figure 6.4A). A similar pattern is observed for basking time, however, *T. lepidus* exhibits a more heterogeneous spatial distribution of basking activity, with greater intensity in rocky and walkway areas but high values across the entire study area (Appendix D Table D4.1). In contrast, *L. schreiberi* restricts basking activity primarily to rocky areas that are surrounded by denser vegetation (Figure 6.1; Appendix Figure D4.1, Table D4.1).

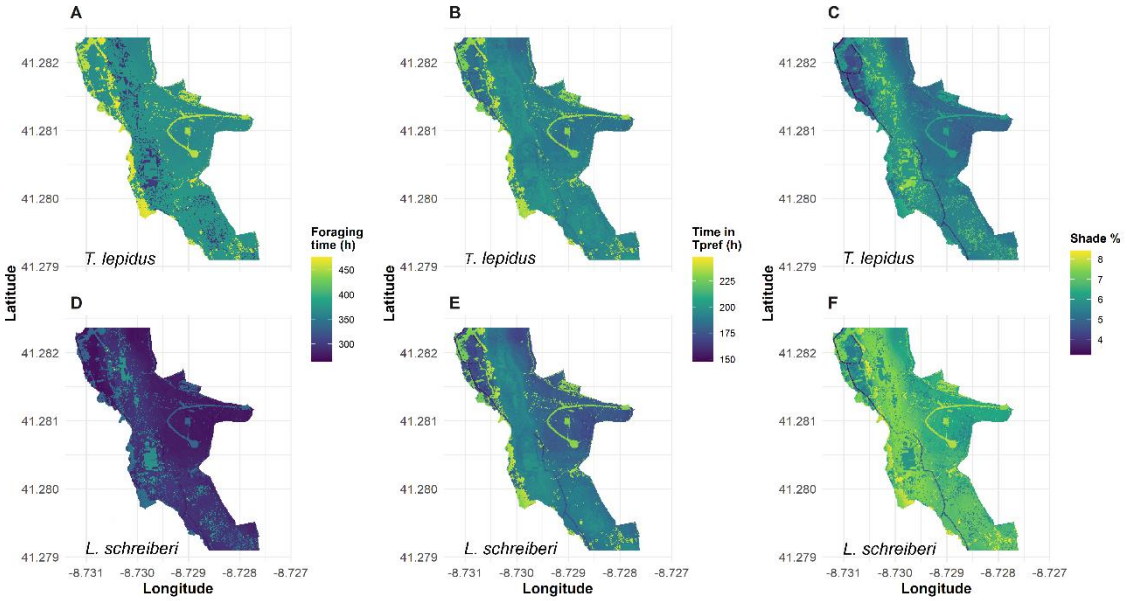

Figure 6.3 Maps of the variables obtained from mechanistic niche models for *T. lepidus* (top: A-C) and *L. schreiberi* (bottom: D-F) under current climatic conditions in Castro São Paio, northern Portugal. Panels A and D show the total foraging time accumulated (in hours) over the spring and summer period; panels B and E represent the time spent at the preferred temperature accumulated (in hours) over the spring and summer period; and panels C and F indicate the percentage of shade selected (in percentage).

Regarding the time both species spend at their preferred temperature, *T. lepidus* shows slightly longer periods of time (Figure 6.3B, E) and dominates in rocky habitats, followed by microhabitats associated with vegetation (i.e., herbaceous vegetation and *Carpobrotus*) (Figure 6.3B). On the other hand, we observed a clear spatial differentiation in shade selection by *L. schreiberi*, with selected higher levels of shade, particularly in geographic areas close to bare soil, rocky and herbaceous microhabitats (Figure 6.3C, F; Figure 6.4C). Concerning total water loss (i.e., without adjusting for body size), *T. lepidus* loses more water (Figure 6.5A, D). However, when size corrected, *L. schreiberi* emerges as the species with higher relative water loss (Figure 6.5B, E). This phenomenon is particularly evident in walkway microhabitats, where the highest water loss for this species is predicted (Figure 6.4D). In contrast, *T. lepidus* maintains relatively low and fairly homogeneous water loss across microhabitats (Figure 6.4D; Figure 6.5B).

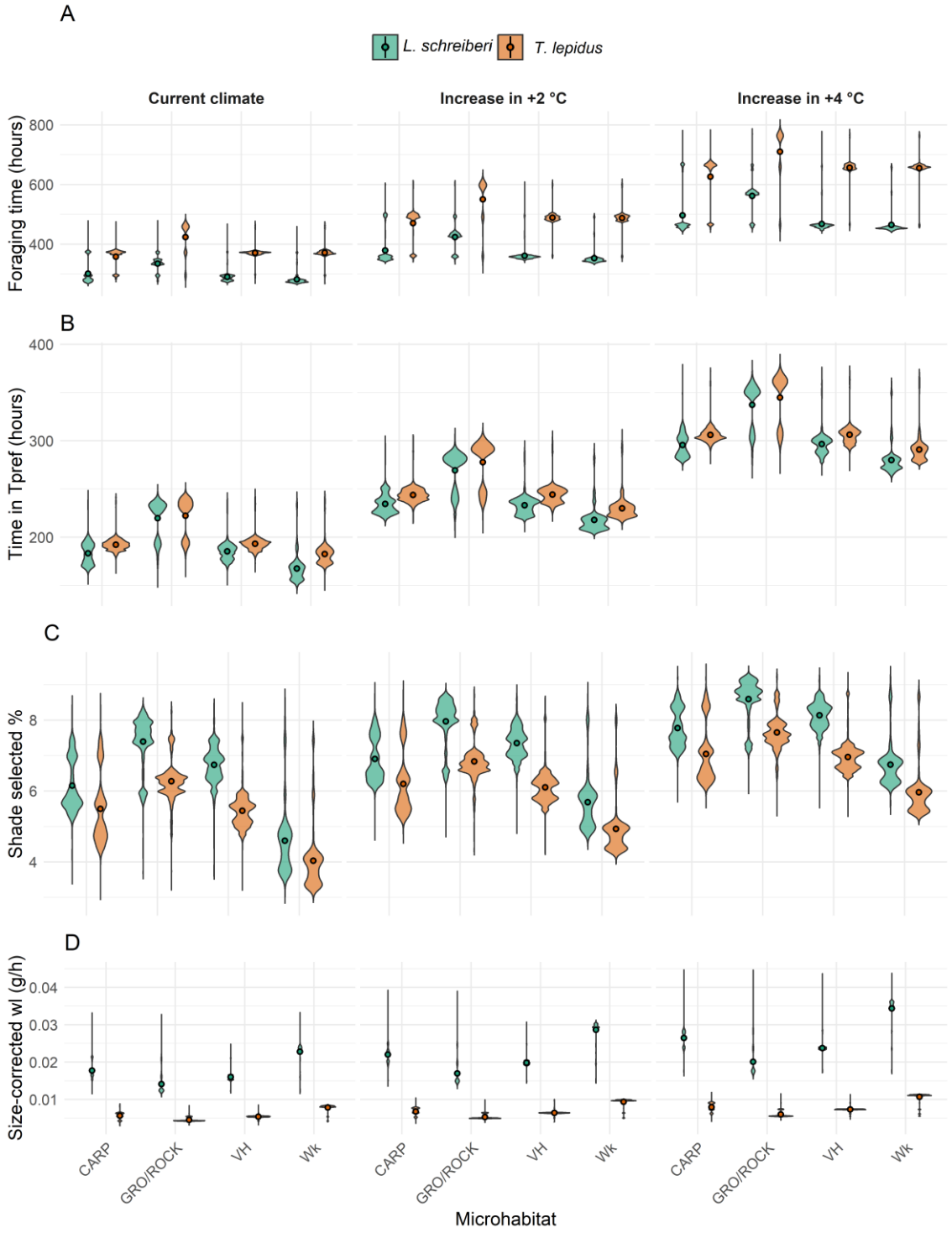

Figure 6.4 (A) Total foraging time (h), (B) time within preferred temperature (h), (C) selected (%), and (D) size-corrected water loss (g/h). The facets indicate climatic scenarios: Current climate, increase in +2 °C, and Increase in +4 °C. The x-axis represents microhabitats: CARP (*Carpobrotus* microhabitat), GRO/ROCK (rocky and bare soil microhabitat), VH (herbaceous vegetation), and Wk (walkway). The colours correspond to the two species studied: orange for *T. lepidus* and green for *L. schreiberi*. Dots inside the violins represent means.

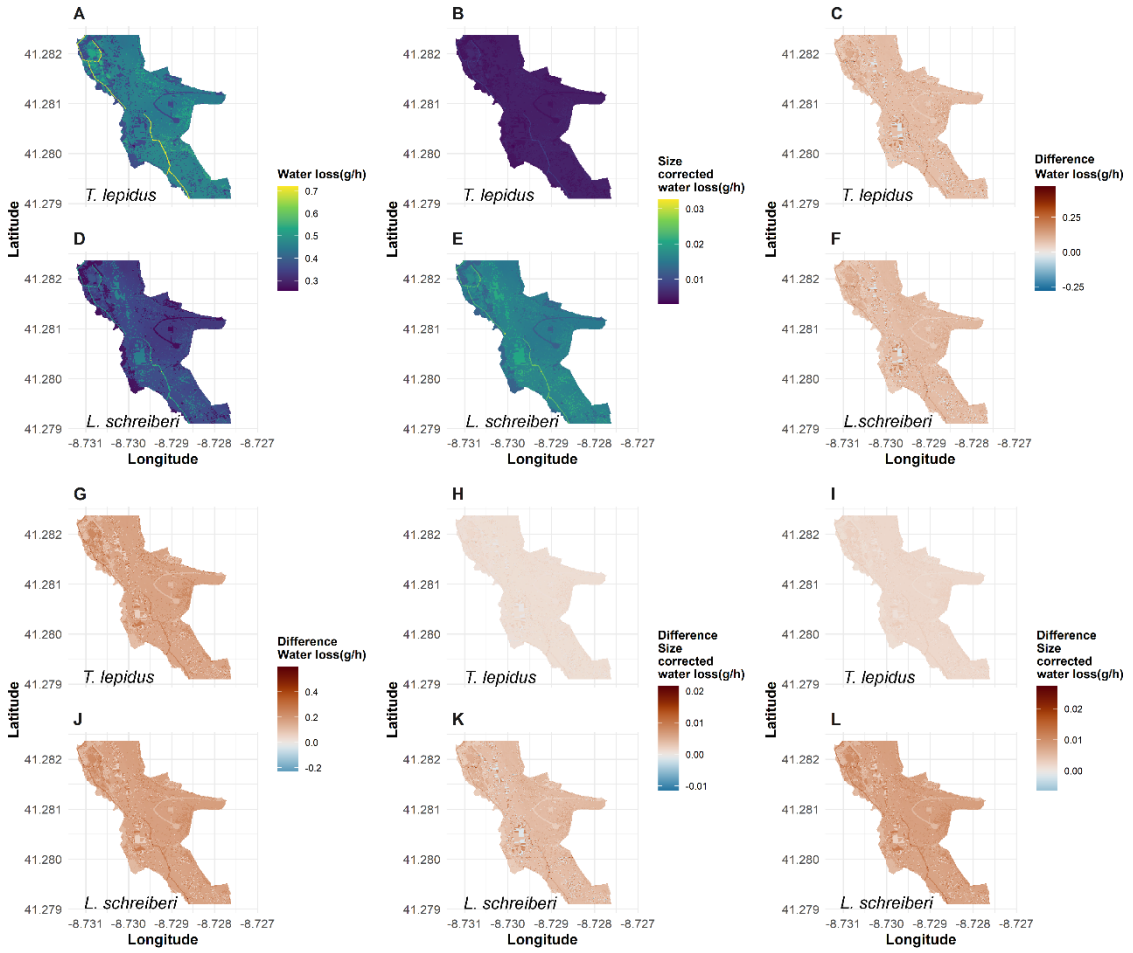

Figure 6.5 Maps of variables related to water loss for *T. lepidus* (panels A–C and G–I) and *L. schreiberi* (panels D–F and J–L) under different climatic scenarios in Castro São Paio, northern Portugal. Total water loss (g/h) (A, D), size-corrected water loss (g/h) (B, E), differences in water loss between scenario +2 °C and current climate (C, F), differences in water loss between scenario +4 °C and current climate (G, J), differences in size-corrected water loss between scenario +2 °C and current climate (H, K), and differences in size-corrected water loss between scenario +4 °C and current climate (G, J).

Regarding slope, higher foraging time values were observed on lower slopes for both species (Figure 6.6A), while time spent at the preferred temperature was relatively similar between low and high slopes (Figure 6.6B). On the other hand, higher slopes exhibited greater shade selection values (Figure 6.6C), whereas total water loss showed similar values across slopes for *T. lepidus* but increased values for *L. schreiberi* (Appendix D Figure D4.5), and size-corrected water loss displayed higher values on steeper slopes (Figure 6.6D). Regarding the aspect, we detected that foraging and basking times varied across orientations (North, East, South, and West), generally being higher in the South and West under current climatic conditions (Figure 6.7A; Appendix D Figure D4.6). We observed that hours within the preferred temperature range (*Tpref*) were relatively uniform across orientations under current climate conditions. Shade selection

varied moderately across orientations, with slightly higher values in the North and West, and the highest values always observed for *L. schreiberi*. Finally, total water loss exhibited the highest maximum values in the East and South orientations, although the means remained relatively uniform across all aspects (Appendix D Figure D4.7).

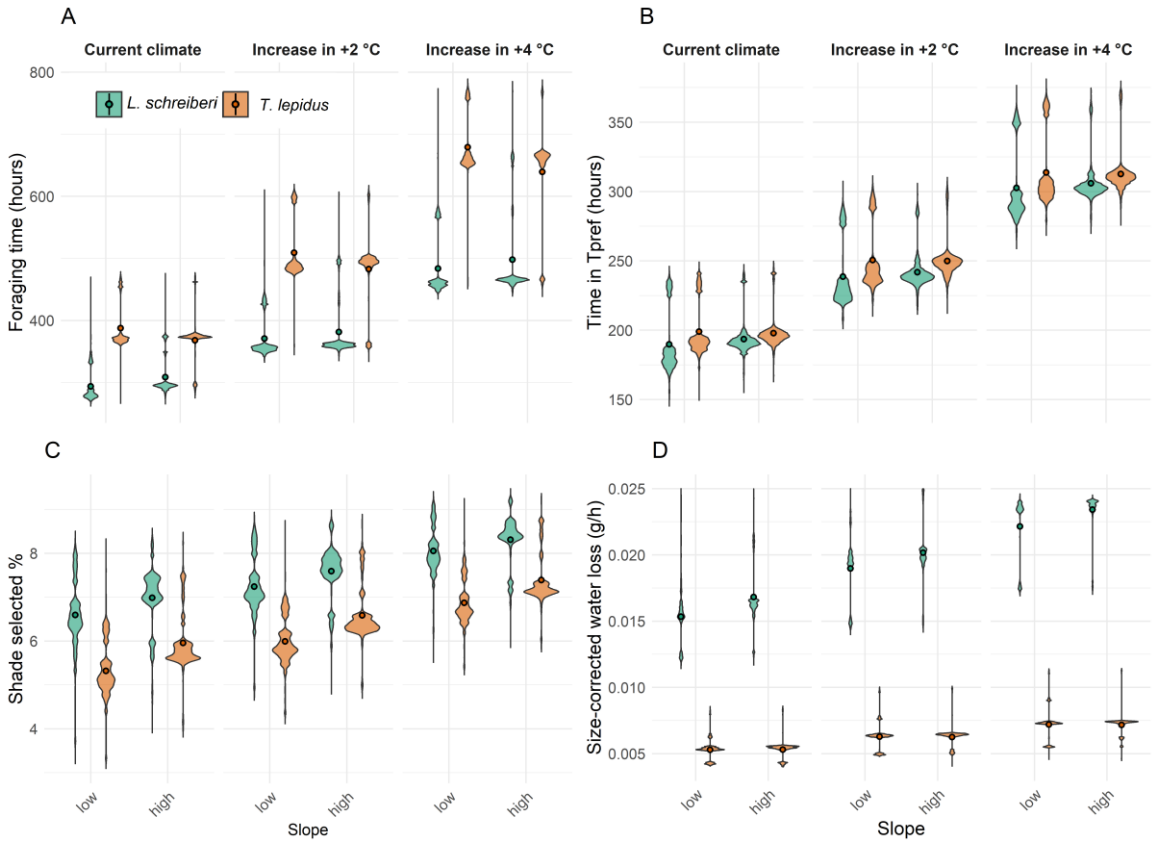

Figure 6.6 Physiological traits derived from mechanistic models in different climatic scenarios. Total foraging time in hours (A), Time within preferred temperature in hours (B), Shade selected % (C), and Size-corrected water loss (g/h) (D). The facets indicate slope categories (Low and High), and the colours correspond to the two species studied: orange for *T. lepidus* and green for *L. schreiberi*. Dots inside the violins represent means.

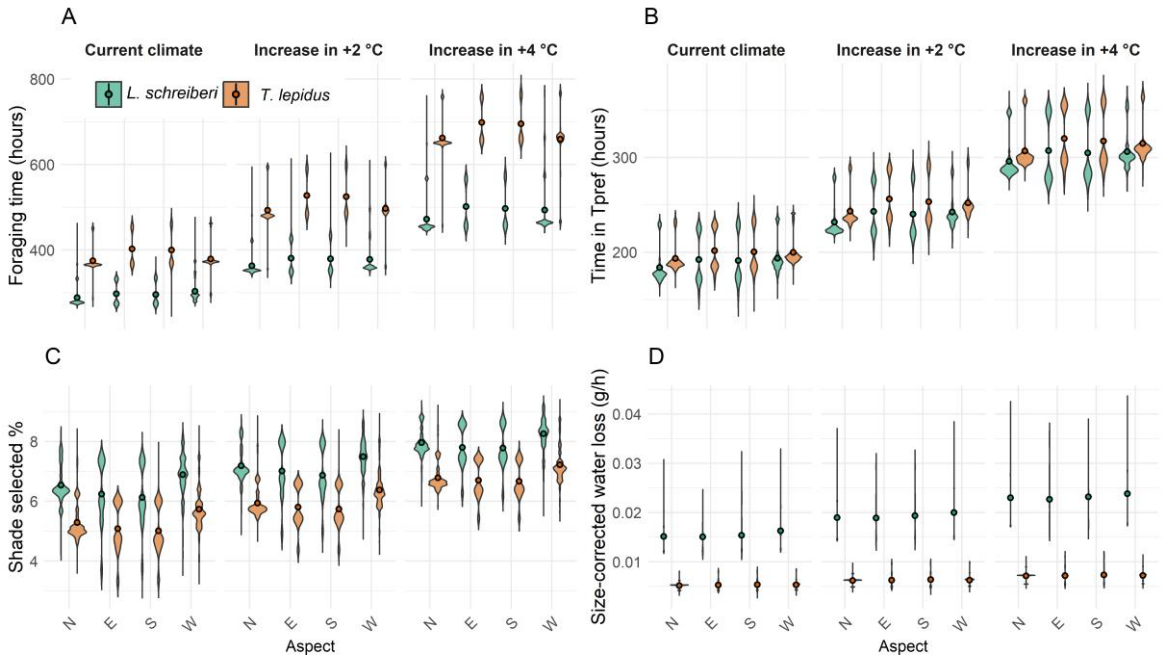

Figure 6.7 Physiological traits derived from mechanistic models in different climatic scenarios. Total foraging time in hours (A), Time within preferred temperature in hours (B), Shade selected % (C), and Size-corrected water loss (g/h) (D). The facets indicate aspect categories (North, East, South, and West), and the colours correspond to the two species studied: orange for *T. lepidus* and green for *L. schreiberi*. Dots inside the violins represent means.

6.3.3. Climate change predictions

When forecasting species' responses to future scenarios with a temperature increase of 2 and 4 ºC, we observed an increase in potential foraging and basking hours for both species and both scenarios (Figure 6.4A, 6.4B; Appendix D Figure D4.2), with a more pronounced increase under the 4°C scenario (Figure 6.4A, 6.4B). We also found greater spatial differences in foraging time for *T. lepidus* in both scenarios (Figure 6.8A, 6.8B, 6.8D, 6.8F, Table 6.1). A more pronounced increase was observed in the time that the species remained within their preferred temperature under the +4°C scenario (Figure 6.8G, 6.8J, Table 6.1). Selected shade remained at higher values across all scenarios and microhabitats for *L. schreiberi* (Figure 6.4C), although differences between the current scenario and the +2°C scenario were relatively similar (Figure 6.8H, 6.8K). Under the +4°C scenario, *T. lepidus* increased its shade selection requirement to a greater extent (Figure 6.8I, 6.8L) but without ever exceeding the shade selected by *L. schreiberi* (Figure 6.4C). Finally, we detected that total water loss also increased under future scenarios for both species (Appendix D Figure D4.3). However, when considering size-corrected water loss, the increase was more pronounced for *L. schreiberi* (Figure 6.5D), with the largest differences occurring primarily under the +4°C scenario (Figure 6.5H-I, 6.5K-L, Table 6.1).

Table 6.1 Summary of the mean, minimum, and maximum difference values for physiological variables between current climate and two climate scenarios: +2°C and +4°C derived from mechanistic models for two species of green lizards, *Timon lepidus* and *Lacerta schreiberi*. Variables include foraging time, basking time, time spent in the preferred temperature range (Tpref), shade selection, water loss, and size-corrected water loss. Foraging and basking times are in hours, time in $_{Tpref}$ in °C, shade selected in % and water loss metrics are in g/h.

Variable	*T. lepidus*	*L. schreiberi*	*T. lepidus*	*L. schreiberi*
	Scenario +2 °C	**Scenario +2 °C**	**Scenario +4 °C**	**Scenario +4 °C**
Foraging time	118.74 (-106-314)	75.29 (-106-316)	283.36 (-5-486)	189.50 (-1-491)
Basking time	156.68 (-31-369)	165.69 (-34-368)	300.77 (136-527)	342.82 (133-512)
Shade selected	0.65 (-2.19-3.39)	0.63 (-2.54-4.28)	1.50 (-1.38-4.25)	1.40 (-1.42-4.88)
Time in Tpref	51.86 (-16-124)	48.67 (-20-124)	114.80 (45-188)	112.71 (37-195)
Water loss	0.08 (-0.28-0.47)	0.08 (-0.25-0.47)	0.16 (-0.23-0.59)	0.17 (-0.14-0.60)
Size-corrected water loss	0.001 (-0.003-0.006)	0.004 (-0.012-0.022)	0.002 (-0.003-0.007)	0.008 (-0.006-0.027)

Under future scenarios with temperature increases of +2 °C and +4 °C, foraging and basking times also increased, while maintaining the pattern of higher activity in the East and South (Figure 6.7A; Appendix D Figure D4.6). Additionally, under the +4 °C scenario, the increase in *T. lepidus* activity was much greater compared to the relative increase in *L. schreiberi* (Figure 6.7A). We observed that the number of hours spent at the preferred temperature range (*Tpref*) were relatively uniform across orientations under current climate conditions and increased under the +2 °C and +4 °C scenarios (Figure 6.7B). However, the highest proportion of activity was still associated with the East and South (Figure 6.7B). Shade selection varied moderately across orientations, with slightly higher values in the North and West, and the highest values always observed for *L. schreiberi*. Foraging time increased on low slopes for *T. lepidus* under both scenarios, while in *L. schreiberi* increased in high slopes (Figure 6.6A). Time at preferred temperatures increased on low slopes for both species (Figure 6.6B). Shade selection increased on high slopes for *L. schreiberi*, while *T. lepidus* showed higher shade selection on low slopes (Figure 6.6C). Size-corrected water loss increased for *L.*

schreiberi on high slopes, while remaining relatively low and constant for *T. lepidus* across slopes (Fig. Figure 6.6D). With temperature increases of +2 °C and +4 °C, shade selection increased across all orientations for both species (Figure 6.7C). Finally, total water loss exhibited the highest maximum values in the East and South orientations, although the means remained relatively uniform across all aspects (Appendix D Table D4.7). On the other hand, size-corrected water loss was consistent across orientations under current climate conditions, with *L. schreiberi* consistently showing higher values. With temperature increases of +2 °C and +4 °C, size-corrected water loss rates increased primarily for *L. schreiberi* and remained relatively constant for *T. lepidus* across all aspects (Figure 6.7D).

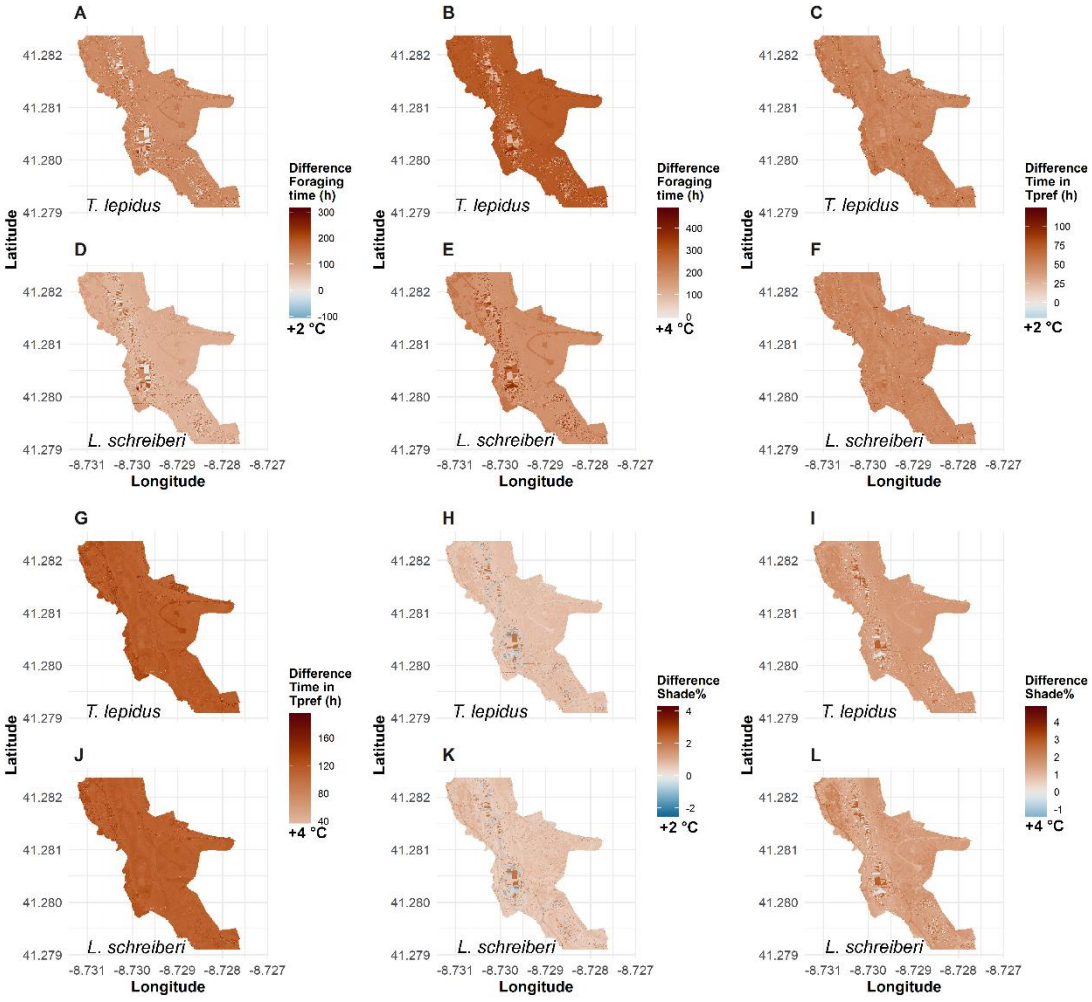

Figure 6.8 Maps of differences on several variables derived from mechanistic niche models for *T. lepidus* (panels A–C and G–I) and *L. schreiberi* (panels D–F and J–L) under different climatic scenarios in Castro São Paio, northern Portugal. Difference in foraging time (h) between scenario +2 °C and current climate (A, D), difference in foraging time (h) between scenario +4 °C and current climate (B, E), time spent at the preferred temperature between scenario +2 °C and current climate (C, F), time spent at the preferred temperature between scenario +4 °C and current climate (G, J), differences in selected shade between scenario +2 °C and current climate (H, K), differences in selected shade between scenario +4 °C and current climate (G, J).

6.4. Discussion

Our study, from a mechanistic perspective, reveals how microhabitats play a crucial role in mediating the impacts of climate in animals both under the current climate and future climate change scenarios. Microhabitats are closely linked to water and thermal dynamics in ectotherms (Kearney and Porter, 2009; Kearney et al., 2014). *Timon lepidus*, being an ecologically more flexible species (Renet et al., 2022), exhibited higher activity levels (foraging and basking) in the current climate and under temperature increase scenarios, particularly in rocky and bare-soil microhabitats. In contrast, although *L. schreiberi* also utilises rocky microhabitats for basking, it does so to a lesser extent. Vegetated microhabitats provide shade availability, a resource selected by this species to a greater level in all climatic scenarios. Water balance is once again confirmed as one of the most distinctive traits between the two species. In absolute terms, *T. lepidus* loses more water due to its larger size, whereas *L. schreiberi* experiences greater water loss when adjusted for body size. Moreover, this physiological rate is projected to be the most sensitive to climate change due to the increase in absolute water loss for both species under climate scenarios. *L. schreiberi* appears to be particularly at risk of hydric stress when considering size-corrected water loss, alongside its higher shade selection demands in all climate scenarios. This contrast suggests that both species adopt distinct strategies to balance thermal and hydric demands, underscoring the importance of microhabitats as regulators of the microclimate required for ectotherms to maintain their essential functions (Kearney et al., 2014) and emphasising the critical role of microhabitats in adapting to climate change (Dobrowski, 2011).

Through mechanistic modelling, we observed that foraging times, basking times, and the time species spend at their preferred temperature are highest for *T. lepidus* under current climatic conditions and contrary to our expectations increase consistently in both climate change scenarios (+2°C and +4°C). These changes are more pronounced in the +4°C scenario for both species. However, these potential increases in activity could come at the expense of greater shade selection and higher water loss due to extended activity periods, especially for *L. schreiberi*, which exhibits higher shade requirements. These trade-offs could limit the actual realisation of these longer activity times. *T. lepidus* exhibits considerably longer foraging and basking times, while the time spent at its preferred temperature shows only slight increases (Table 1, Appendix D Table D4.1). The microhabitat combination in Castro São Paio, dominated mainly by vegetation and rocky substrates (Figure 6.1), provides both shade and solar exposure. These features may favour both species by allowing them to maintain their preferred body temperatures for longer durations during active periods (Kearney and Porter, 2009).

Consequently, the time available for activities such as foraging and basking may increase with a 2 °C or 4 °C increase in ambient temperature. While increased foraging time may meet greater energetic demands, longer periods of basking may signify greater effort required to reach preferred temperatures, which could increase the risk of predation. These dynamics emphasise the trade-offs associated with thermal regulation under changing climatic conditions (Robert and Thompson, 2007). Higher temperatures also elevate metabolic rates (Angilletta Jr., 2009), which, in turn, increase the need to forage to meet higher energetic demands (Kearney and Porter, 2009). These differential patterns are influenced by the availability of microhabitats and the terrain's associated features (Kearney and Porter, 2009; Kearney et al., 2014).

Slope and aspect play a crucial role in shaping organism's activity by influencing temperature stability and access to diverse microhabitats (Kearney and Porter, 2009; Kearney et al., 2014). In the northern hemisphere, eastern and southern orientations provide greater solar exposure, which can enable ectotherms to remain within their thermal range for longer periods (Kearney et al., 2009; Kearney et al., 2021). This interplay between topography, microhabitat diversity, and thermal requirements regulates activity patterns, ensuring an optimal balance between energy expenditure and gain (Kearney and Porter, 2016; Singh, 2018). In our study area, steeper slopes cast more shaded areas that are preferentially selected by *L. schreiberi*, while *T. lepidus* tends to select shaded areas on shallower slopes (Fig. 6.6). However, in both species, steeper slopes are associated with increased absolute water loss, with *L. schreiberi* experiencing relatively higher water loss relative to its body size. (Fig. 6.6, Appendix D Figure D4.7). This may be explained by the fact that shallower slopes tend to have more stable temperatures, less direct solar exposure, deeper soils and greater vegetation cover, which could reduce water loss (Kearney et al., 2013; Singh, 2018). In contrast, steeper slopes often have less vegetation and drier soils (Kearney et al., 2013). The northern and western aspects, on the other hand, show greater selected shade, and also show slightly higher relative water loss for both species. While vegetation patterns were not explicitly modelled, they are significantly influenced by aspect due to fluctuations in temperature and water availability, which may indirectly affect the thermal and hydric conditions experienced by lizards (Singh, 2018). Our mechanistic model-based perspective reveals a consistent increase in shade requirements and water loss under climate change scenarios, underscoring an amplified vulnerability of *L. schreiberi* to increasing environmental temperature. In this context, *L. schreiberi* appears particularly susceptible to the impacts of climate change due to its specific requirements for cool and

shaded microhabitats, as well as its physiological constraints. As noted in previous studies, species with these characteristics are likely to face significant challenges in adapting to warmer conditions (Foden et al., 2018; Pacifici et al., 2015). Our results on water balance and shade selection are congruent with those reported by other authors, particularly regarding water loss and the preference of *L. schreiberi* for more humid and densely vegetated microhabitats (Brito et al., 1998; Llorente et al., 1995; Reyes-Puig et al., 2024). Shade is a key feature of habitats and microhabitats that generates more humid and cooler microclimates, providing refugia that help mitigate temperature extremes (Burraco et al., 2020; Singh, 2018) and allowing ectotherms to behaviourally regulate thermal exposure. The physical configuration of the terrain, determined by slope and aspect, influences the amount of shade available. This feature allows organisms to take shelter, facilitating thermoregulation and minimising water loss (Kearney and Porter, 2016). Orientations with higher solar exposure intensify evaporation processes and thus affect water balance and heat and moisture dynamics (Kearney et al., 2014b).

In *T. lepidus*, the observed longer foraging and basking periods may reflect physiological requirements associated with its larger body size (Meiri, 2010; Reyes-Puig et al., 2024), prey availability could also influence foraging duration. Larger organisms tend to forage at higher metabolic rates and move more to maximise energy return (Nagy et al., 1984). This aligns with previous empirical observations showing that *T. lepidus* is observed in greater proportions in the study area (Reyes-Puig et al., unpubl. data. Chapter 5). Furthermore, larger individuals require extended basking periods to reach their optimal thermal range (Díaz, 1991; Angilletta Jr., 2009). The preference of *T. lepidus* for rocky microhabitats, which provide both shelter and sun exposure, further supports these observations (Fei et al., 2008; Mateo, 2017; Reyes-Puig et al., unpubl. data. Chapter 5). In contrast, *L. schreiberi* restricts its activity to rocky areas and herbaceous vegetation, primarily in south-facing terrain. It has lower activity times compared to *T. lepidus*, which is linked to its smaller body size—approximately 1.6 times smaller than that of *T. lepidus*. Smaller organisms, due to lower thermal inertia, require less time to reach their preferred temperatures (Angilletta Jr., 2009). In addition, *L. schreiberi* experience shorter activity periods with more abrupt fluctuations between minimum and maximum temperature ranges, as evidenced both in laboratory and field studies (Reyes-Puig et al., 2024; Reyes-Puig et al., unpubl. data. Chapter 5). Consequently, vegetation microhabitats become crucial for coping with heat stress (Dobrowski, 2011; Kearney and Porter, 2009). Under climate change scenarios, *T. lepidus* shows the greatest increases in activity, particularly in rocky and bare soil

microhabitats. In contrast, *L. schreiberi* exhibits a more moderate increase in activity and is predicted to frequent vegetated microhabitats oriented towards the east and south (Figures 6.7D, 6.7E), which may experience greater solar exposure (Singh, 2018).

We emphasize the critical role of microhabitats as thermal regulators in the face of climate change impacts. For *T. lepidus*, its reliance on rocky microhabitats provides suitable features for essential activities, such as shelter, hiding, basking or displaying during the breeding period (Renet et al., 2022; Reyes-Puig et al., unpubl. data. Chapter 5). On the other hand, human-created microhabitats, such as walkways, may offer less shelter and shade for species with particular shade and humidity requirements such as L. shreiberi, which significantly increases the risk of heat stress in organisms. This effect is noticeable in both species but has a greater impact on *L. schreiberi*. Our observations are consistent with field data on microhabitat use (Reyes-Puig et al., unpubl. data. Chapter 5), where very few observations of *L. schreiberi* were recorded in these areas compared to *T. lepidus*. This suggests that *L. schreiberi* would tend to avoid these spaces, due the fact that walkways are generally located far from water bodies, making them drier and less suitable for *L. schreiberi*. Human-created structures reflect the potential effects of landscape modification on organism physiology (Sponsel, 2013). As natural habitats are increasingly transformed to remove vegetation, species are likely to face greater challenges in coping with climate change. Herbaceous and vegetated microhabitats, which currently provide cooler and more stable conditions, are essential for mitigating thermal stress and maintaining water balance in *L. schreiberi*. Climate change scenarios predict increased shade requirements mainly for Iberian emerald lizards, which would exacerbate the vulnerability of this species due to its higher relative water loss and physiological requirements. Although *L. schreiberi* shows greater foraging and basking activity in rocky microhabitats these spaces have less available shade (Fig. 3). Therefore, the areas where *L. schreiberi* thermoregulates are usually associated with vegetation and nearby water bodies (Brito et al., 1998; Reyes-Puig, unpubl. data. Chapter 5). In contrast, rocky microhabitats, which are more exposed and thermally variable, allow *T. lepidus* to maintain its activities with greater flexibility (Mateo and Cheylan, 1997; Renet et al.,2022). Therefore, cool and humid microhabitats associated with water bodies are essential to cope with future climate change impacts. Their reduction would directly affect the water balance of more vulnerable species, such as *L. schreiberi*, due to their specific physiological requirements. According to projections from other studies (Habibullah et al., 2022; Ramalho et al., 2023), changes, shifts and reductions in species distributions are likely to intensify due to climate change (Sillero,

2021; Sillero et al., 2022). While both species will likely face these challenges, *L. schreiberi*'s dependence on cooler and more shaded microhabitats makes it particularly susceptible to these impacts

Finally, microhabitats and physical terrain features play a critical role in providing spaces that allow organisms to shelter from extreme environmental conditions (Dobrowski, 2011; Singh, 2018). The impending advance of climate change highlights the need to understand and reveal how organisms will deal with its effects and how these can be mitigated to ensure the survival of their populations. The microclimatic heterogeneity generated by slope and terrain will become key elements in mitigating the impacts of climate change. However, substrates oriented towards the sun, with greater exposure to solar radiation, may intensify heat stress (Dobrowski, 2011; Kearney et al., 2013). In this context, microhabitats with shade and high humidity will be essential to mediate the capacity to buffer the impacts of climate change by individuals (Dobrowski, 2011; Kearney and Porter, 2009; Singh, 2018). Likewise, ectotherms must balance the need to stay within their optimal thermal range —e.g. by engaging in thermoregulatory behaviours—with the energetic demands of foraging. This trade-off is intensified under warming scenarios, where energy resources become more critical due to increased metabolic rates (Kearney et al., 2013). Ecologically more flexible species, such as *T. lepidus*, may adjust their behaviour to exploit a wider variety of microhabitats, allowing them to extend their activity periods. In contrast, more specialised species, such as *L. schreiberi*, may restrict their activity to specific shaded microhabitats. Our observations and projections based on mechanistic models highlight microhabitats as critical drivers for the survival of species. Areas with favourable microclimates (i.e. specific microhabitats) will be essential to buffer the effects of higher temperatures and decreased water availability in the future (Dobrowski, 2011; Singh, 2018).

References

Åkesson, A., Curtsdotter, A., Eklöf, A., Ebenman, B., Norberg, J., and Barabás, G. (2021). The importance of species interactions in eco-evolutionary community dynamics under climate change. *Nature Communications*, 12(1), 4759. https://doi.org/10.1038/s41467-021-24977-x

Angert, A. L., LaDeau, S. L., and Ostfeld, R. S. (2013). Climate change and species interactions: ways forward. *Annals of the New York Academy of Sciences*, 1297(1), 1-7.

Angilletta Jr., M. J. (2009). Thermal adaptation: a theoretical and empirical synthesis. Oxford press. 288Pp.

Barber, B. J., & Crawford Jr, E. C. (1977). A stochastic dual-limit hypothesis for behavioral thermoregulation in lizards. *Physiological Zoology*, 50(1), 53-60. https://doi.org/10.1086/physzool.50.1.30155715

Boukal, D. S., Bideault, A., Carreira, B. M., and Sentis, A. (2019). Species interactions under climate change: connecting kinetic effects of temperature on individuals to community dynamics. *Current opinion in insect science*, 35, 88-95. https://doi.org/10.1016/j.cois.2019.06.014

Brambilla, M., Scridel, D., Bazzi, G., Ilahiane, L., Iemma, A., Pedrini, P., ... and Chamberlain, D. (2020). Species interactions and climate change: How the disruption of species co-occurrence will impact on an avian forest guild. *Global change biology*, 26(3), 1212-1224. https://doi.org/10.1111/gcb.14953

Brito, J. C., Paulo, O. S., and Crespo, E. G. (1998). Distribution and habitats of Schreiber's green lizard (*Lacerta schreiberi*) in Portugal. *Herpetological Journal*, 8(4), 187–194.

Burraco, P., Orizaola, G., Monaghan, P., and Metcalfe, N. B. (2020). Climate change and ageing in ectotherms. *Global Change Biology*, 26(10), 5371-5381. https://doi.org/10.1111/gcb.15305

Campbell, G. S., and Norman, J. M. (1999). *An introduction to environmental biophysics*. Springer Science & Business Media. 306 Pp.

Chown, S. L., and Klok, C. J. (2003). Water-balance characteristics respond to changes in body size in subantarctic weevils. *Physiological and Biochemical Zoology*, 76(5), 634–643. https://doi.org/10.1086/376919

Claunch, N. M., Nix, E., Royal, A. E., Burgos, L. P., Corn, M., DuBois, P. M., ... & Taylor, E. N. (2021). Body size impacts critical thermal maximum measurements in lizards. *Journal of Experimental Zoology Part A: Ecological and Integrative Physiology*, *335*(1), 96–107. https://doi.org/10.1002/jez.2410

Cohen, J. (1960). A coefficient of agreement for nominal scales. *Educational and psychological measurement*, 20(1), 37-46. https://doi.org/10.1177/001316446002000104

Cohen, J. (1968). Weighted kappa: Nominal scale agreement provision for scaled disagreement or partial credit. *Psychological bulletin*, 70(4), 213. https://doi.org/10.1037/h0026256

Environmental Systems Research Institute (ESRI). (2024). ArcGIS Pro (Version 2024). ESRI. https://www.esri.com

Copernicus Climate Change Service (C3S). (2024). Copernicus: June 2024 marks the 12th month with global temperature reaching 1.5°C above pre-industrial levels. Retrieved November 27, 2024, from https://climate.copernicus.eu/copernicus-june-2024-marks-12th-month-global-temperature-reaching-15degc-above-pre-industrial

Diaz, J. A. (1991). Temporal patterns of basking behaviour in a Mediterranean lacertid lizard. *Behaviour*, 118(1-2), 1-14.

Fei, T., Venus, V., Toxopeus, B., Skidmore, A. K., Schlerf, M., Liu, Y., ... and Bian, M. (2008, December). Understanding lizard's microhabitat use based on a mechanistic model of behavioral thermoregulation. In *International Conference on Earth Observation Data Processing and Analysis* (ICEODPA) (Vol. 7285, pp. 83-92). SPIE.

Dobrowski, S. Z. (2011). A climatic basis for microrefugia: the influence of terrain on climate. *Global change biology*, 17(2), 1022-1035. https://doi.org/10.1111/j.1365-2486.2010.02263.x

Enriquez-Urzelai, U., Tingley, R., Kearney, M. R., Sacco, M., Palacio, A. S., Tejedo, M., and Nicieza, A. G. (2020). The roles of acclimation and behaviour in buffering

climate change impacts along elevational gradients. *Journal of Animal Ecology*, 89(7), 1722-1734. https://doi.org/10.1111/1365-2656.13222

Enriquez-Urzelai, U., and Gvoždík, L. (2024). Impacts of behaviour and acclimation of metabolic rate on energetics in sheltered ectotherms: a climate change perspective. *Proceedings of the Royal Society B*, 291(2017), 20232152. https://doi.org/10.1098/rspb.2023.2152

Farouki, O., and Farouki, O. (1981). *Thermal properties of soils* (Vol. 81, No. 1). Hanover, NH: US Army Corps of Engineers, Cold Regions Research and Engineering Laboratory.

Ferreira, C. C., Santos, X., and Carretero, M. A. (2016). Does ecophysiology mediate reptile responses to fire regimes? Evidence from Iberian lizards*. PeerJ*, 4, e2107. https://doi.org/10.7717/peerj.2107

Foden, W. B., Young, B. E., Akçakaya, H. R., Garcia, R. A., Hoffmann, A. A., Stein, B. A., ... and Huntley, B. (2019). Climate change vulnerability assessment of species. *Wiley interdisciplinary reviews: climate change*, 10(1), e551. https://doi.org/10.1002/wcc.551

Gardner, J. L., Peters, A., Kearney, M. R., Joseph, L., and Heinsohn, R. (2011). Declining body size: a third universal response to warming?. *Trends in ecology & evolution*, 26(6), 285-291. https://doi.org/10.1016/j.tree.2011.03.005

Gilman, S. E., Urban, M. C., Tewksbury, J., Gilchrist, G. W., and Holt, R. D. (2010). A framework for community interactions under climate change. *Trends in ecology & evolution*, 25(6), 325-331. https://doi.org/10.1016/j.tree.2010.03.002

Gottlieb, N. D., and Caldwell, W. E. (1967). Magnetic field effects on the compass mechanism and activity level of the snail Helisoma duryi endiscus. *The Journal of Genetic Psychology*, *111*(1), 85–102. https://doi.org/10.1080/00221325.1967.10533750

Grolemund, G., and Wickham, H. (2011). Dates and Times Made Easy with lubridate. In Journal of Statistical Software (Vol. 40, Issue 3, pp. 1–25). https://www.jstatsoft.org/v40/i03/

Gunderson, A. R., and Leal, M. (2016). A conceptual framework for understanding thermal constraints on ectotherm activity with implications for predicting

responses to global change. *Ecology letters*, 19(2), 111-120. https://doi.org/10.1111/ele.12552

Guisan, A., and Hofer, U. (2003). Predicting reptile distributions at the mesoscale: relation to climate and topography. *Journal of Biogeography*, *30*(8), 1233–1243. https://doi.org/10.1046/j.1365-2699.2003.00914.x

Habibullah, M. S., Din, B. H., Tan, S. H., and Zahid, H. (2022). Impact of climate change on biodiversity loss: global evidence. *Environmental Science and Pollution Research*, 29(1), 1073-1086. https://doi.org/10.1007/s11356-021-15702-8

Hijmans R (2024). raster: Geographic Data Analysis and Modeling. R package version 3.6-30, https://rspatial.org/raster

Hillel, D. (2003). *Introduction to environmental soil physics*. Elsevier. 422 Pp.

Hollister J, Shah T, Nowosad J, Robitaille A, Beck M, Johnson M (2023). elevatr: Access Elevation Data from Various APIs. doi:10.5281/zenodo.8335450, R package version 0.99.0, https://github.com/jhollist/elevatr/

Huey, R. B., Kearney, M. R., Krockenberger, A., Holtum, J. A., Jess, M., and Williams, S. E. (2012). Predicting organismal vulnerability to climate warming: roles of behaviour, physiology and adaptation. *Philosophical Transactions of the Royal Society B: Biological Sciences,* 367(1596), 1665-1679. https://doi.org/10.1098/rstb.2012.0005

IPCC, 2023: Sections. In: Climate Change 2023: Synthesis Report. Contribution of Working Groups I, II and III to the Sixth Assessment Report of the Intergovernmental Panel on Climate Change [Core Writing Team, H. Lee and J. Romero (eds.)]. *IPCC,* Geneva, Switzerland, pp. 35-115, doi: 10.59327/IPCC/AR6-9789291691647

ISRIC, F. (1998). World reference base for soil resources. *World soil resources reports*, *84*.

James, D., and Hornik, K. (2020). chron: Chronological Objects which Can Handle Dates and Times. https://CRAN.R-project.org/package=chron

Kearney, M., and Porter, W. (2009). Mechanistic niche modelling: combining physiological and spatial data to predict species' ranges. *Ecology letters*, 12(4), 334-350. https://doi.org/10.1111/j.1461-0248.2008.01277.x

Kearney, M. (2013). Activity restriction and the mechanistic basis for extinctions under climate warming. *Ecology Letters*, 16(12), 1470-1479. https://doi.org/10.1111/ele.12192

Kearney, M. R., Shamakhy, A., Tingley, R., Karoly, D. J., Hoffmann, A. A., Briggs, P. R., and Porter, W. P. (2014). Microclimate modelling at macro scales: a test of a general microclimate model integrated with gridded continental-scale soil and weather data. *Methods in Ecology and Evolution*, 5(3), 273-286. https://doi.org/10.1111/2041-210X.12148

Kearney, M. R., Isaac, A. P., and Porter, W. P. (2014b). microclim: Global estimates of hourly microclimate based on long-term monthly climate averages. *Scientific data*, 1(1), 1-9. https://doi.org/10.1038/sdata.2014.6

Kearney, M. R., and Enriquez-Urzelai, U. (2023). A general framework for jointly modelling thermal and hydric constraints on developing eggs. *Methods in Ecology and Evolution*, 14(2), 583-595. https://doi.org/10.1111/2041-210X.14018

Kearney, M. R., and Porter, W. P. (2017). NicheMapR–an R package for biophysical modelling: the microclimate model. *Ecography*, 40(5), 664-674. https://doi.org/10.1111/ecog.02360

Kearney, M. R., Munns, S. L., Moore, D., Malishev, M., and Bull, C. M. (2018). Field tests of a general ectotherm niche model show how water can limit lizard activity and distribution. *Ecological monographs*, 88(4), 672-693. https://doi.org/10.1002/ecm.1326

Kearney, M. R., and Porter, W. P. (2020). NicheMapR–an R package for biophysical modelling: the ectotherm and dynamic energy budget models. *Ecography*, 43(1), 85-96. https://doi.org/10.1111/ecog.04680

Keppel, G., Anderson, S., Williams, C., Kleindorfer, S., and O'Connell, C. (2017). Microhabitats and canopy cover moderate high summer temperatures in a fragmented Mediterranean landscape. *PLoS One*, 12(8), e0183106. https://doi.org/10.1371/journal.pone.0183106

Kingsolver, J. G., Diamond, S. E., and Buckley, L. B. (2013). Heat stress and the fitness consequences of climate change for terrestrial ectotherms. *Functional Ecology*, 27(6), 1415-1423. https://doi.org/10.1111/1365-2435.12145

Llorente, G. A., Montori, A., Santos, X., and Carretero, M. A. (1995). Atlas de distribució dels Anfibis y Rèptils de Catalunya y Andorra*. El Grau, Figueres*: 192 pp.

Martinez-Meyer, E. (2005). Climate change and biodiversity: some considerations in forecasting shifts in species' potential distributions. *Biodiversity Informatics*, 2. https://doi.org/10.17161/bi.v2i0.8

Mateo, J. A., and Cheylan, M. (1997). *Lacerta* lepida Daudin 1802. SEH & Muséum National d'Histoire Naturelle.

Mateo, J. A. (2017). Lagarto ocelado—*Timon lepidus*. In A. Salvador and A. Marco (Eds.), Enciclopedia Virtual de los Vertebrados Españoles (pp. 1–52). Museo Nacional de Ciencias Naturales.

Meiri, S. (2010). Length–weight allometries in lizards. *Journal of Zoology*, 281(3), 218-226. https://doi.org/10.1111/j.1469-7998.2010.00696.x

Monteith, J. L., Unsworth, M. H., and Webb, A. (1994). Principles of environmental physics. *Quarterly Journal of the Royal Meteorological Society*, *120*(520), 1699.

Nagy, K. A., Huey, R. B., and Bennett, A. F. (1984). Field energetics and foraging mode of Kalahari lacertid lizards. *Ecology*, 65(2), 588-596. https://doi.org/10.2307/1941421

Nunez, S., Arets, E., Alkemade, R., Verwer, C., and Leemans, R. (2019). Assessing the impacts of climate change on biodiversity: is below 2° C enough*?. Climatic Change*, 154, 351-365. https://doi.org/10.1007/s10584-019-02420-x

Ohlberger, J. (2013). Climate warming and ectotherm body size–from individual physiology to community ecology. *Functional Ecology*, 27(4), 991-1001. https://doi.org/10.1111/1365-2435.12098

Paaijmans, K. P., Heinig, R. L., Seliga, R. A., Blanford, J. I., Blanford, S., Murdock, C. C., and Thomas, M. B. (2013). Temperature variation makes ectotherms more sensitive to climate change. *Global change biology*, 19(8), 2373-2380. https://doi.org/10.1111/gcb.12240

Pacifici, M., Foden, W. B., Visconti, P., Watson, J. E., Butchart, S. H., Kovacs, K. M., ... and Rondinini, C. (2015). Assessing species vulnerability to climate change. *Nature climate change*, 5(3), 215-224. https://doi.org/10.1038/NCLIMATE2448

Pirtle, E. I., Tracy, C. R., and Kearney, M. R. (2019). Hydroregulation: A neglected behavioral response of lizards to climate change?. In Behavior of lizards (pp. 343-374). CRC Press.

Ramalho, Q., Vale, M. M., Manes, S., Diniz, P., Malecha, A., and Prevedello, J. A. (2023). Evidence of stronger range shift response to ongoing climate change by ectotherms and high-latitude species. *Biological Conservation*, 279, 109911. https://doi.org/10.1016/j.biocon.2023.109911

Renet, J., Dokhelar, T., Thirion, F., Tatin, L., Pernollet, C. A., and Bourgault, L. (2022). Spatial pattern and shelter distribution of the ocellated lizard (*Timon lepidus*) in two distinct Mediterranean habitats*. Amphibia-Reptilia*, 43(3), 263–276.

Reyes-Puig, C., Enriquez-Urzelai, U., Carretero, M. A., and Kaliontzopoulou, A. (2024). Is it all about size? Dismantling the integrated phenotype to understand species coexistence and niche segregation. *Functional Ecology*, *38*(11), 2350-2368. https://doi.org/10.1111/1365-2435.14646

Robert, K. A., and Thompson, M. B. (2007). Is basking opportunity in the viviparous lizard, *Eulamprus tympanum*, compromised by the presence of a predator scent?. *Journal of Herpetology*, 287–293. https://www.jstor.org/stable/4498586

Rozen-Rechels, D., Dupoué, A., Lourdais, O., Chamaillé-Jammes, S., Meylan, S., Clobert, J., and Le Galliard, J. F. (2019). When water interacts with temperature: Ecological and evolutionary implications of thermo-hydroregulation in terrestrial ectotherms. *Ecology and evolution*, 9(17), 10029-10043. https://doi.org/10.1002/ece3.5440

Rubalcaba, J. G., Gouveia, S. F., Villalobos, F., Olalla-Tárraga, M. Á., and Sunday, J. (2023). Climate drives global functional trait variation in lizards. *Nature Ecology & Evolution*, 7(4), 524-534. https://doi.org/10.1038/s41559-023-02007-x

Salvador, A. (1988). Selección de microhabitat del lagarto verdinegro (*Lacerta schreiberi*) (Sauria: Lacertidae). *Amphibia-Reptilia*, 9(3), 265–275. https://doi.org/10.1163/156853888X00350

Scheffers, B. R., Edwards, D. P., Diesmos, A., Williams, S. E., and Evans, T. A. (2014). Microhabitats reduce animal's exposure to climate extremes. *Global change biology*, 20(2), 495-503. https://doi.org/10.1111/gcb.12439

Sentis, A., Bazin, S., Boukal, D. S., and Stoks, R. (2024). Ecological consequences of body size reduction under warming. *Proceedings B*, 291(2029), 20241250. https://doi.org/10.1098/rspb.2024.1250

Sillero, N., Brito, J. C., Skidmore, A. K., and Toxopeus, A. G. (2009). Biogeographical patterns derived from remote sensing variables: the amphibians and reptiles of the Iberian Peninsula. *Amphibia-Reptilia*, 30(2), 185-206.

Sillero, N. (2021). Climate change in action: local elevational shifts on Iberian amphibians and reptiles. *Regional Environmental Change*, 21(4), 101. https://doi.org/10.1007/s10113-021-01831-w

Sillero, N., Ribeiro-Silva, J., and Arenas-Castro, S. (2022). Shifts in climatic realised niches of Iberian species. *Oikos*, 2022(4), e08505. https://doi.org/10.1111/oik.08505

Singh, S. (2018). Understanding the role of slope aspect in shaping the vegetation attributes and soil properties in Montane ecosystems. *Tropical Ecology*, 59(3), 417-430.

Snyder, W. C., Wan, Z., Zhang, Y., and Feng, Y. Z. (1998). Classification-based emissivity for land surface temperature measurement from space. *International Journal of Remote Sensing*, *19*(14), 2753-2774. https://doi.org/10.1080/014311698214497

Sponsel, L. E. (2013). Human impact on biodiversity, overview. *Encyclopedia of biodiversity*, 4, 137–52.

Wickham, H. (2016). Ggplot2: Elegant graphics for data analysis (2nd ed.) [PDF]. Springer International Publishing.

Woods, H. A., Dillon, M. E., & Pincebourde, S. (2015). The roles of microclimatic diversity and of behavior in mediating the responses of ectotherms to climate change. *Journal of Thermal Biology*, *54*, 86–97. https://doi.org/10.1016/j.jtherbio.2014.10.002

Wu, N. C., Bovo, R. P., Enriquez-Urzelai, U., Clusella-Trullas, S., Kearney, M. R., Navas, C. A., and Kong, J. D. (2024). Global exposure risk of frogs to increasing environmental dryness. *Nature Climate Change*, 1-9. https://doi.org/10.1038/s41558-024-02167-z

Chapter 7

General Discussion

The overarching aim of this thesis was to investigate how body size variation influences phenotypic diversification, species coexistence, and vulnerability to global change. This was achieved through four specific goals: (1) evaluating the role of allometric effects in shaping morphological diversity through the analysis of macroevolutionary patterns of sexual differentiation in green lizards (*Timon* and *Lacerta* genera) (Chapter 3); (2) examining the functional and physiological impacts of body size variation in two green lizard species (*Timon lepidus* and *Lacerta schreiberi*) (Chapter 4); (3) identifying the mechanisms of coexistence and niche segregation in these two species through field and laboratory studies (Chapters 4 and 5); and (4) assessing the vulnerability of these two species to climate change using mechanistic niche models (Chapter 6).

7.1. Key findings

Understanding the mechanisms that shape phenotypic diversity, facilitate species coexistence, and drive their vulnerability to climate change, is essential to advance ecological and evolutionary research. This thesis integrates a multidimensional perspective, including morphological, functional, physiological and ecological traits, to investigate the interplay between body size, niche segregation, and vulnerability to climate change in green lizards. The following sections discuss the main findings of this research, outlining the links between intraspecific and macroevolutionary patterns of sexual dimorphism in body size and other traits, the functional and physiological effects of body size, their relationship to coexistence and niche segregation, and the differential impacts of climate change on ectotherms.

7.1.1. Allometric effects in morphological diversity and sexual differentiation

The linkage between intraspecific allometry (i.e., static allometry) and macroevolutionary patterns (e.g., evolutionary allometry) of sexual dimorphism (SD) is important because it bridges how small-scale processes, such as interspecific variation in trait size relative to body size, can shape broader evolutionary trends. In the context of Rensch's rule (RR), which describes a pattern where sexual size dimorphism (SSD) tends to increase with body size in male-biased species and decrease in female-biased species (Rensch, 1950; Abouheif and Fairbairn, 1997), the relationship between static (intraspecific) and evolutionary allometry remains not fully understood. Mainly regarding how parameters like allometric intercept (reflecting the baseline size of the trait when body size is minimal) and slope (indicating how a trait scales with body size) influence macroevolutionary patterns of sexual dimorphism. Chapter 3 addresses that gap by

investigating not only SD trends in body size but also in other morphological traits, providing new insights into the connection between microevolutionary and macroevolutionary processes. Two key phenotypic patterns underline the contribution of Chapter 3 to the understanding of allometric effects on morphological diversity and sexual differentiation: static and evolutionary allometry in the context of sexual dimorphism. These patterns, fundamental to morphological diversity, have been extensively studied in separate (Mori et al., 2017; Ralls and Mesnick, 2009). Although recent studies have provided a basis for methods to extend phylogenetic regression models to compare within-species patterns across phylogenies (e.g., Adams and Collyer, 2024), research focusing on the simultaneous interplay between static and evolutionary allometry through intercept and slope parameters has been little explored (Voje et al., 2014; Voje et al., 2022). Chapter 3 significantly advances our understanding of the role of allometric intercept and slope in shaping Rensch's rule. To this end, Chapter 3 primarily employed computational simulations that provided a standardised and controlled framework to demonstrate that sexual dimorphism in traits is significantly influenced by variations in static allometric slopes between sexes, while differences in the allometric intercept alone have minimal impact. These findings reveal that Rensch's rule, and its converse can emerge in traits when sexual differentiation in slopes is present, even in the absence of RR in body size. Empirical examples using Mediterranean green lizards corroborated these patterns, showing that traits like head size follow RR in this group, whereas limb traits exhibit its converse, reinforcing the critical role of static allometric slopes in driving macroevolutionary trends.

Specifically, a positive difference in slopes, where the larger sex has steeper slopes, produces classical RR patterns, while a negative difference leads to converse RR (i.e., sexual size dimorphism increases with body size in female-biased species). The results highlighted that those trends could vary depending on the trait in the same organism, some traits may exhibit classical RR, while others converse RR. This suggests that functional and ecological constraints act differently on traits, shaping evolutionary allometries, in line with previous findings on trait-specific selection pressures (Voje et al., 2014; Hansen & Houle, 2008). Some traits may even show no RR pattern at all, which may be due to biomechanical constraints, as hypothesised in studies on functional trait limits (Gould, 1966a, b). These findings challenge the traditional focus on body size alone when assessing macroevolutionary patterns such as RR, stressing the importance of including different morphological traits. By demonstrating that intraspecific allometric parameters influence evolutionary patterns, this work links microevolutionary processes

and macroevolutionary trends (Hansen and Houle, 2008; Voje and Hansen, 2013). For example, sexual selection, as shown in previous research, may favour steeper slopes in traits critical for mating success (Voje et al., 2014; Pélabon et al., 2014). At the macroevolutionary level, the relationship between static and evolutionary allometry reflects how trait-specific constraints and selective pressures shape species diversification over time, guiding the development of sexually dimorphic traits among lineages (Voje and Hansen, 2013; Voje et al., 2014; Pélabon et al., 2014; Voje et al., 2022).

7.1.2. Functional and physiological effects of body size

Chapter 4 confirmed that body size is a forceful trait influencing most phenotypic features. It is crucial to note that most of the trait differences were mainly due to variation in body size, and that only a limited number of traits showed differences once the effect of body size was taken into account. As a key axis of phenotypic variation, body size directly impacted the majority of body parts studied in the model organisms, while also shaping performance and eco-physiological traits. Although this relationship has been extensively studied, and several researchers have explored it in ectotherms (Brown et al., 2004; Irschick, 2002; Mirth et al., 2016), the contribution of Chapter 4 lies in examining multiple traits in two species that differ significantly in body size. This linkage reveals that size-driven relationships extend beyond morphological traits, mediating functional and ecological adaptations. This approach allowed for the integration of dimensions ranging from morphology and performance to eco-physiology into a single framework, extending our understanding of the effects of body size from a comprehensive, multi-dimensional perspective.

Body size is crucial for the locomotor apparatus and trophic anatomical traits and, therefore, for the strategies associated with habitat exploitation (Gomes et al., 2018; Gomes et al., 2020; Huyghe et al., 2005). It exemplifies the biophysical link between muscle mass and strength (Aasa et al., 2003). The results of Chapter 4 highlighted the relationship between body size and manoeuvrability, a trait not frequently explored (Vasilopoulou-Kampitsi, 2020). One key finding derived from this research is that, while body size influenced bite force and maneuverability, it did not affect maximum speeds. This suggests that locomotor performance in terms of sprinting may not scale directly with body size in the model species. Instead, other morphological and ecological factors, such as habitat structure or locomotor strategies, may play a more significant role in determining maximum speeds (Irschick and Losos, 1998; Gomes et al., 2015; Kohlsdorf and Navas, 2012).

Regarding the physiological implications of body size, as shown in biophysical ecology, larger individuals exhibited higher rates of evaporative water loss. However, when body size was taken into account, these rates were proportionally lower in larger than in smaller individuals, which instead had a higher proportion of wet surface area (see Chapter 4). These relationships are explained by the surface-area-to-volume ratio, emphasising the physiological constraints associated with water balance and thermoregulation (Chown and Klok, 2003; Angilletta Jr., 2009; Kearney et al., 2018). The results of the laboratory experiments in chapter 4 underline the fundamental role of water physiology in ecological differentiation and coexistence between the two species. These findings are consistent with the field observations in Chapter 5, where relative humidity was revealed to be a major axis of microhabitat use and segregation. Body temperature preferences showed minimal interspecific differences, yet variance in body temperature did, suggesting adaptations linked to habitat use and constraints imposed by size (larger lizards tend to have greater thermal inertia) (Angilletta Jr., 2009).

Another key finding of Chapter 4 is that particular traits still exhibit differences between species, even after accounting for the effect of body size. This indicates that body size is not the sole force driving trait differentiation, although it remains as a primary driver for specific features. These results suggest that traits may experience selective pressures, such as ecological, sexual, and behavioural pressures, that can overcome the influence of body size (Scales and Butler, 2016). One of the most important contributions of Chapter 4 is the integration of morphological, functional, and physiological traits, illustrating the role of body size in multidimensional space as a central axis of differentiation. Moreover, Chapter 4 findings extend our understanding of phenotypic diversity, offering insights into size-independent traits and how their combination influences ecological adaptations. This work contributes to a broader theoretical framework by exploring the interplay between phenotypic variables influenced by body size and those independent of it, demonstrating how these interactions drive phenotypic diversity and the core role of body size (Woodward et al., 2005).

7.1.3. Mechanisms of coexistence and niche segregation

Niche segregation is a mechanism that facilitates coexistence between different species, reducing competition and optimising resource utilization (Pianka and Huey, 1978; Valladares et al., 2015). In Chapter 4 and Chapter 5, the combination of field and laboratory data provides a comprehensive understanding of how two species of lacertid lizards coexist in Northern Portugal. Chapter 4 and Chapter 5 extend our knowledge about niche differentiation with emphasis on the interplay between morphological,

functional, physiological, behavioural and ecological traits. This research confirms that body size is a primary driver of niche segregation. However, beyond body size, other size-independent traits appear to contribute significantly to species niche segregation.

In the context of laboratory experiments, limb length, variance in preferred temperature and water balance were identified as important morphological and physiological variables for niche segregation between the studied species. These results underscore the importance of conducting standardised experimental protocols to address ecological knowledge gaps that are difficult to investigate in uncontrolled environments. On the other hand, field observations enhance our understanding of coexistence mechanisms by incorporating spatial and temporal data, offering valuable insights into the natural processes driving niche segregation as observed in the field. For instance, *Timon lepidus* predominantly utilises open, rocky spaces, while *Lacerta schreiberi* favours areas with denser vegetation and more humid microhabitats, a pattern consistently observed in both field studies and laboratory experiments. Additionally, temporal segregation proved to be a key factor in understanding the coexistence of both species, suggesting that temporal niche segregation is an adaptive strategy to reduce competition (Navarro et al., 2013; Valladares et al., 2015). Chapter 4 and Chapter 5 findings highlight the importance of integrating laboratory experiments and fieldwork, thereby expanding our understanding of the mechanisms that underlie species coexistence. For the model species, coexistence is driven not only by differences in body size but also by physiological strategies to cope with distinct microhabitat use, as well as spatial and temporal preferences. Although the results of habitat preference align with earlier evidence on the habitat preferences of both species (Llorente et al., 1995; Brito et al., 1998; Ferreira et al. 2016; Renet et al. 2022), no previous studies have comprehensively explored niche segregation between these two species at the level achieved by this research. By integrating multidimensional niche spaces, including morphological, functional, physiological, and field data collected over more than six months of fieldwork, this investigation provides a novel and in-depth understanding of how several traits collectively contribute to niche segregation.

Chapter 4 and Chapter 5 point out that coexistence is not merely a product of body size differences but involves complex interactions across several dimensions of the niche, encompassing phenotypic variation in morphology, physiology, as well as spatial and temporal factors. This multidimensional approach extends the conceptual framework of ecological niche theory and provides a solid foundation for future studies exploring the mechanisms of coexistence in other taxa.

7.1.4. Climate change vulnerability in ectotherms

Ectotherms are particularly vulnerable to climate change due to their dependence on external environmental characteristics (Huey et al., 2012; Woods et al., 2015). Chapter 6 underscores how microhabitat characteristics mediate the physiological responses of ectotherms to external conditions, stressing the role of microhabitats as natural refuges for ectotherms. By integrating field data, laboratory-derived parameters, and a mechanistic modelling approach, this research contributes to the rapidly growing knowledge of how climate change will impact biodiversity.

The two model species provide valuable insights into how the effects of climate change may differ between species of contrasting body sizes. *Lacerta schreiberi*, a smaller species, and *Timon lepidus*, a larger species, illustrate how physiological responses are shaped by body size (Angilletta Jr., 2009; Kearney et al., 2009), as outlined in Chapter 4 and Chapter 5. The findings of this research show the reliance of *L. schreiberi* on humid and shaded microhabitats, which makes it more vulnerable to climate change. Species with higher water loss rates and shade requirements are likely to be more sensitive to extreme temperature increases in the future (Kearney and Porter, 2009; Kearney, 2013). A key finding is that size-corrected water loss in *L. schreiberi* increased significantly with temperature increases, underlining its greater sensitivity to water stress compared to *T. lepidus*. This finding is consistent with previous studies showing that smaller ectotherms are more prone to water loss due to their higher surface area-to-volume ratio (Chown and Klok, 2003; Kearney et al., 2018). The study area where this research was conducted offers several suitable microhabitats that meet the requirements of both species. The combination of exposed rocky microhabitats, typically utilised by *T. lepidus*, and dense vegetation, accessible to *L. schreiberi* due to its smaller size (allowing it to perch on ferns, branches, and grasses) provides suitable thermal and hydric refugia, enabling them to exploit distinct microhabitats. However, in the context of climate change, shade becomes a decisive factor in mitigating its effects on ectotherms (Burraco et al., 2020; Dobrowski, 2011; Kearney, 2013; Singh, 2018). Under climate change scenarios, both species showed a greater dependence on shaded microhabitats, with *L. schreiberi* requiring substantially more than *T. lepidus*. This differentiated dependency on microhabitats reinforces the role of microhabitat availability determining the vulnerability of species to climate change.

Activity trends, including foraging and basking, may also be influenced by climate change, particularly foraging activity, which is closely tied to energy acquisition (Norberg, 1977). Under the climate change scenarios simulations performed in Chapter 6, foraging and basking activity for both model species is expected to increase. However, increased foraging activity could expose lizards to greater heat stress as temperatures rise (Kearney et al., 2013; Kearney et al., 2021). This may force species to adjust their foraging behaviour to other periods of the day, as has been observed in other studies (Jayatilaka et al., 2011). It is well established that activity adjustments, often triggered by or associated with heat stress, can significantly impact energy budgets (Kearney et al., 2021). This effect could be particularly detrimental for *L. schreiberi*, whose microhabitat preferences are strongly constrained by microclimatic conditions such as humidity and shade availability.

Through this mechanistic modelling approach, Chapter 6 findings emphasise the critical role of microhabitats as natural regulators and buffers, enabling ectotherms to cope with environmental extremes (Singh, 2018; Dobrowski, 2011). Microhabitat properties such as slope and terrain play a crucial role at a microscale, providing shade, reducing solar exposure, and mediating water and heat balance. The open, exposed, and rocky habitats preferred by *T. lepidus* have sparse vegetation, with shaded refugia primarily found in holes or crevices, but are characterised by lower microhabitat humidity due to increased solar radiation and evaporation rates. In contrast, the vegetated and humid microhabitats favoured by *L. schreiberi* provide better buffering conditions against external environmental fluctuations. However, these microhabitats are more vulnerable to degradation under warming scenarios (Trew and Maclean, 2021).

This thesis, which integrates parameters collected in both fieldwork and laboratory experiments and combines them into mechanistic models, advances our understanding of how ectotherms might cope with climate change through their use of available microhabitats. By examining the interaction between microhabitat characteristics, body size and physiological traits, this research provides detailed insight into two coexisting species exhibit distinct microspatial responses to climate change. A smaller, more specialised species such as *L. schreiberi*, which prefers humid, vegetated areas with less direct sun exposure to avoid heat and water stress, is expected to be more vulnerable than the larger, more flexible *T. lepidus*. The latter species is better adapted to using rocky and exposed microhabitats with lower relative humidity and lower size-corrected water loss, making *L. schreiberi* more likely to face greater challenges in coping with the effects of climate change. These findings align with broader patterns

observed in ectotherms, where ecological generalists are less affected by climate-induced habitat changes compared to specialists (Foden et al., 2018).

7.2. Concluding remarks and future directions

This thesis provides a comprehensive perspective using several comparative tools to uncover how body size, phenotypic traits (ranging from morphological, functional, physiological to ecological), and microhabitat structure influence phenotypic variation, species coexistence, and responses to climate change in model ectotherm species. With the combination of Chapters 3, 4, 5, and 6, this thesis not only responds to the general question of how body size mediates evolutionary and ecological processes but also sheds light on specific mechanisms that drive ecological interactions, such as species coexistence and vulnerability to climate change in two model lizard species. This thorough work unveils that body size is a determinant factor of phenotypic diversification, influencing the evolution of sexual dimorphism and shaping more complex ecological dynamics such as species coexistence and organisms' responses to external environmental changes. Chapter 3 revealed how intraspecific allometric parameters (slope and allometric intercept) drive macroevolutionary trends such as Rensch's rule, connecting within-species processes with larger-scale evolutionary patterns. Chapters 4 and 5 demonstrated that body size not only dictates functional and physiological traits, but also mediates niche segregation, allowing the coexistence of species with overlapping distribution ranges. For example, the larger-bodied *Timon lepidus* is better adapted to open rocky habitats, while the smaller *Lacerta schreiberi* is better adapted to shaded and humid environments, such as dense vegetation. Coexistence can be maintained by intensifying niche segregation, as the two species not only use different microhabitats but also differ in their spatial and temporal patterns, thus potentially minimising competition. Chapter 6 showed how body size and other physiological traits interact with environmental factors, determining species-specific vulnerability to climate change, mainly associated with water loss processes. The findings of Chapter 4, 5 and 6 suggest that *L. schreiberi* is more vulnerable to global climate change due to its dependence on microhabitats with high humidity and shade, which are likely to be less suitable under future global change scenarios. Climate change will exacerbate existing constraints such as heat and water stress, especially for *L. schreiberi*. In contrast, *T. lepidus* may show greater resilience due to its wider distribution and ecological niche and lower water loss relative to its body size.

By incorporating a model species group with a variety of body sizes (green lizards' clade in Chapter 3) and two green lizard species that differ significantly in body

size (in Chapter 4, 5, and 6), this thesis has explored phenotypic changes triggered by body size as well as those independent of it. Through the integration of experimental and observational data with mechanistic models, this investigation bridges the knowledge gaps between evolutionary and ecological research, primarily to understand the effects of body size across different phenotypic dimensions. This work demonstrates not only the role of body size in shaping traits but also its importance in more complex ecological processes, such as species coexistence through niche segregation and the challenges of ectotherms to future climate change conditions. Most importantly, this research reinforces the idea of considering multiple phenotypic dimensions to understand how traits, both independent of and influenced by body size, contribute to ecological relationships.

While this research has advanced our understanding of phenotypic diversity, species coexistence, ectotherm vulnerability to climate change, and the role of body size in mediating these processes, it has also opened paths for future exploration. For instance, extending these analyses to other species or populations across diverse environmental gradients and microhabitats could provide key broader information into the generality of the obtained results of Chapter 3, 4, 5, and 6. In the context of Chapter 3, future research should examine the interaction between allometric parameters (static intercept and slope) in a simulation setting, as this chapter focused on their effects independently. Investigating how these parameters interact could provide deeper insights into the evolution of sexual body size dimorphism and the emergence of Rensch's rule. Additionally, incorporating long-term monitoring data would allow for validation of the mechanistic future predictions presented in Chapter 6. Similarly, developing transient-state mechanistic models and Dynamic Energy Budget (DEB) models would help capture short-term dynamics, providing a more detailed perspective on how species respond to rapid changes in environmental conditions and their effects on reproduction and growth. These approaches could improve the accuracy of projections and contribute to the formulation of more effective conservation strategies for groups with higher vulnerability to climate change.

In terms of biodiversity conservation, these results underscore the importance of exploring the role of microhabitats as natural refuges. This research places microhabitats as key landscape components for mitigating the effects of climate change, particularly for ectotherms more vulnerable than others, emphasising microhabitat thermal and hydric buffering properties. Finally, this thesis offers a solid framework by integrating multidimensional phenotypic traits and fine-tuned models to understand

macroevolutionary and ecological processes faced by organisms. It lays a basis for future research to explore in greater detail phenotypes, their relationship with coexistence, and the physiological challenges that organisms may face while adapting to a rapidly changing world.

References

Aasa, U., Jaric, S., Barnekow-Bergkvist, M., and Johansson, H. (2003). Muscle strength assessment from functional performance tests: Role of body size. *The Journal of Strength & Conditioning Research*, *17*(4), 664–670. https://doi.org/10.1519/1533-4287(2003)017<0664:msaffp>2.0.co;2

Abouheif, E., and Fairbairn, D. J. (1997). A comparative analysis of allometry for sexual size dimorphism: Assessing Rensch's rule. *The American Naturalist, 149*(3), 540–562. https://doi.org/10.1086/286004

Adams, D. C., and Collyer, M. L. (2024). Extending phylogenetic regression models for comparing within-species patterns across the tree of life. *Methods in Ecology and Evolution*, *15*(12), 2234-2246. https://doi.org/10.1111/2041-210X.14438

Angilletta, M. J., Jr., Steury, T. D., and Sears, M. W. (2004). Temperature, growth rate, and body size in ectotherms: Fitting pieces of a life-history puzzle. *Integrative and Comparative Biology, 44*(6), 498–509. https://doi.org/10.1093/icb/44.6.498

Ás Renet, J., Dokhelar, T., Thirion, F., Tatin, L., Pernollet, C. A., and Bourgault, L. (2022). Spatial pattern and shelter distribution of the ocellated lizard (*Timon lepidus*) in two distinct Mediterranean habitats. *Amphibia-Reptilia, 43*(3), 263–276.

Brito, J. C., Paulo, O. S., and Crespo, E. G. (1998). Distribution and habitats of Schreiber's green lizard (*Lacerta schreiberi*) in Portugal. *Herpetological Journal*, *8*(4), 187–194.

Brown, J. H., Gillooly, J. F., Allen, A. P., Savage, V. M., and West, G. B. (2004). Toward a metabolic theory of ecology. *Ecology*, *85*(7), 1771–1789.

Burraco, P., Orizaola, G., Monaghan, P., and Metcalfe, N. B. (2020). Climate change and ageing in ectotherms. *Global Change Biology*, *26*(10), 5371-5381. https://doi.org/10.1111/gcb.15305

Chown, S. L., and Klok, C. J. (2003). Water-balance characteristics respond to changes in body size in subantarctic weevils. *Physiological and Biochemical Zoology*, *76*(5), 634–643. https://doi.org/10.1086/376919

Dobrowski, S. Z. (2011). A climatic basis for microrefugia: the influence of terrain on climate. *Global change biology*, *17*(2), 1022-1035. https://doi.org/10.1111/j.1365-2486.2010.02263.x

Ferreira, C. C., Santos, X., and Carretero, M. A. (2016). Does ecophysiology mediate reptile responses to fire regimes? Evidence from Iberian lizards. *PeerJ*, *4*, e2107. https://doi.org/10.7717/peerj.2107

Gomes, V., Carretero, M. A., and Kaliontzopoulou, A. (2016). The relevance of morphology for habitat use and locomotion in two species of wall lizards. *Acta Oecologica*, *70*, 87–95. https://doi.org/10.1016/j.actao.2015.12.005

Gomes, V., Carretero, M. A., and Kaliontzopoulou, A. (2018). Run for your life, but bite for your rights? How interactions between natural and sexual selection shape functional morphology across habitats. *The Science of Nature*, *105*, 1–12. https://doi.org/10.1007/s00114-017-1537-6

Gomes, V., Herrel, A., Carretero, M. A., and Kaliontzopoulou, A. (2020). New insights into bite performance: Morphological trade-offs underlying the duration and magnitude of bite force. *Physiological and Biochemical Zoology, 93*(3), 175–184. https://doi.org/10.1086/708248

Gould, S. J. (1966a). Allometry and size in ontogeny and phylogeny. *Biological Reviews*, *41*(4), 587–638. https://doi.org/10.1111/j.1469-185x.1966.tb01624.x

Gould, S. J. (1966b). Allometry in Pleistocene land snails from Bermuda: The influence of size upon shape. *Journal of Paleontology, 40*(5), 1131–1141.

Hansen, T. F., and Houle, D. (2008). Measuring and comparing evolvability and constraint in multivariate characters. *Journal of Evolutionary Biology, 21*(5), 1201–1219. https://doi.org/10.1111/j.1420-9101.2008.01573.x

Huey, R. B., Kearney, M. R., Krockenberger, A., Holtum, J. A., Jess, M., and Williams, S. E. (2012). Predicting organismal vulnerability to climate warming: roles of behaviour, physiology and adaptation. *Philosophical Transactions of the Royal Society B: Biological Sciences*, *367*(1596), 1665-1679. https://doi.org/10.1098/rstb.2012.0005

Huyghe, K., Vanhooydonck, B., Scheers, H., Molina-Borja, M., and Van Damme, R. (2005). Morphology, performance and fighting capacity in male lizards, Gallotia

galloti. *Functional Ecology, 19,* 800–807. https://doi.org/10.1111/j.1365-2435.2005.01038.x

Irschick, D. J. (2002). Evolutionary approaches for studying functional morphology: examples from studies of performance capacity. *Integrative and Comparative Biology*, *42*(2), 278–290. https://doi.org/10.1093/icb/42.2.278

Irschick, D. J., Meyers, J. J., Husak, J. F., and Le Galliard, J. F. (2008). How does selection operate on whole-organism functional performance capacities? A review and synthesis*. Evolutionary Ecology Research, 10*(2), 177–196.

Jayatilaka, P., Narendra, A., Reid, S. F., Cooper, P., and Zeil, J. (2011). Different effects of temperature on foraging activity schedules in sympatric Myrmecia ants. *Journal of Experimental Biology*, *214*(16), 2730-2738. https://doi.org/10.1242/jeb.053710

Kearney, M. (2013). Activity restriction and the mechanistic basis for extinctions under climate warming. *Ecology Letters*, *16*(12), 1470-1479. https://doi.org/10.1111/ele.12192

Kearney, M. R., Munns, S. L., Moore, D., Malishev, M., and Bull, C. M. (2018). Field tests of a general ectotherm niche model show how water can limit lizard activity and distribution. *Ecological monographs*, *88*(4), 672–693. https://doi.org/10.1002/ecm.1326

Kearney, M. R., Porter, W. P., and Huey, R. B. (2021). Modelling the joint effects of body size and microclimate on heat budgets and foraging opportunities of ectotherms. *Methods in Ecology and Evolution*, *12*(3), 458-467. https://doi.org/10.1111/2041-210X.13528

Kearney, M. R., Simpson, S. J., Raubenheimer, D., and Kooijman, S. A. (2013). Balancing heat, water and nutrients under environmental change: a thermodynamic niche framework. *Functional Ecology*, *27*(4), 950-966.

Kearney, M., and Porter, W. (2009). Mechanistic niche modelling: combining physiological and spatial data to predict species' ranges. *Ecology letters*, *12*(4), 334-350. https://doi.org/10.1111/j.1461-0248.2008.01277.x

Kohlsdorf, T., and Navas, C. A. (2006). Ecological constraints on the evolutionary association between field and preferred temperatures in Tropidurinae lizards. *Evolutionary Ecology*, *20*, 549–564. https://doi.org/10.1007/s10682-006-9116-x

Llorente, G. A., Montori, A., Santos, X., and Carretero, M. A. (1995). Atlas de distribució dels Anfibis y Rèptils de Catalunya y Andorra. El Grau, Figueres: 192 pp.

Mirth, C. K., Frankino, W. A., and Shingleton, A. W. (2016). Allometry and size control: what can studies of body size regulation teach us about the evolution of morphological scaling relationships?. *Current opinion in insect science*, *13*, 93–98. https://doi.org/10.1016/j.cois.2016.02.010

Mori, E., Mazza, G., and Lovari, S. (2017). Sexual dimorphism. In J. Vonk, and T. Shakelford (Eds.), Encyclopedia of animal cognition and behavior (pp. 1–7). Springer International Publishing.

Navarro, J., Votier, S. C., Aguzzi, J., Chiesa, J. J., Forero, M. G., and Phillips, R. A. (2013). Ecological segregation in space, time and trophic niche of sympatric planktivorous petrels. *PloS one*, *8*(4), e62897. https://doi.org/10.1371/journal.pone.0062897

Norberg, R. A. (1977). An ecological theory on foraging time and energetics and choice of optimal food-searching method. *The Journal of Animal Ecology*, 511-529. https://doi.org/10.2307/3827

Pelabon, C., Firmat, C., Bolstad, G. H., Voje, K. L., Houle, D., Cassara, J., Rouzic, A. L., and Hansen, T. F. (2014). Evolution of morphological allometry. *Annals of the New York Academy of Sciences*, *1320*(1), 58–75. https://doi.org/10.1111/nyas.12470

Pianka, E. R., and Huey, R. B. (1978). Comparative ecology, resource utilization and niche segregation among gekkonid lizards in the southern Kalahari. *Copeia*, 1978, 691–701. https://doi.org/10.2307/1443698

Ralls, K., and Mesnick, S. (2009). Sexual dimorphism. In J. G. M. Bernd Würsig, and K. K. Thewissen (Eds.), Encyclopedia of marine mammals (pp. 1005–1011). Academic Press.

Rensch, B. (1950). Die Abhängigkeit der relativen Sexualdifferenz von der Körpergrösse. *Bonner Zoologische Beiträge, 1*, 58–69.

Scales, J. A., and Butler, M. A. (2016). Adaptive evolution in locomotor performance: How selective pressures and functional relationships produce diversity. *Evolution*, *70*(1), 48–61. https://doi.org/10.1111/evo.12825

Singh, S. H. I. P. R. A. (2018). Understanding the role of slope aspect in shaping the vegetation attributes and soil properties in Montane ecosystems. *Tropical Ecology*, *59*(3), 417-430.

Trew, B. T., and Maclean, I. M. (2021). Vulnerability of global biodiversity hotspots to climate change. *Global Ecology and Biogeography*, *30*(4), 768-783. https://doi.org/10.1111/geb.13272

Valladares, F., Bastias, C. C., Godoy, O., Granda, E., and Escudero, A. (2015). Species coexistence in a changing world. *Frontiers in plant science*, 6, 866. https://doi.org/10.3389/fpls.2015.00866

Vasilopoulou-Kampitsi, M. (2020). Manoeuvrability and the anotomy of the inner ear in lacertid lizards. An ecological approach. PhD thesis, University of Antwerp.

Voje, K. L., and Hansen, T. F. (2013). Evolution of static allometries: Adaptive change in allometric slopes of eye span in stalk-eyed flies. *Evolution*, *67*(2), 453–467. https://doi.org/10.1111/j.1558-5646.2012.01777.x

Voje, K. L., Bell, M. A., and Stuart, Y. E. (2022). Evolution of static allometry and constraint on evolutionary allometry in a fossil stickleback. *Journal of Evolutionary Biology, 35*(3), 423–438. https://doi.org/10.1111/jeb.13984

Voje, K. L., Hansen, T. F., Egset, C. K., Bolstad, G. H., and Pelabon, C. (2014). Allometric constraints and the evolution of allometry. *Evolution*, *68*(3), 866–885. https://doi.org/10.1111/evo.12312

Woods, H. A., Dillon, M. E., and Pincebourde, S. (2015). The roles of microclimatic diversity and of behavior in mediating the responses of ectotherms to climate change. *Journal of Thermal Biology*, *54*, 86-97. https://doi.org/10.1016/j.jtherbio.2014.10.002

Woodward, G., Ebenman, B., Emmerson, M., Montoya, J. M., Olesen, J. M., Valido, A., and Warren, P. H. (2005). Body size in ecological networks. *Trends in ecology & evolution*, *20*(7), 402–409. https://doi.org/10.1016/j.tree.2005.04.005

Appendix A

Supplementary Material Chapter 3

Supplementary Information for Chapter 3

Rensch's rule: linking intraspecific to evolutionary allometry

List of Supplementary Tables and Figures

Table A1.1 ANOVA table of GLMs used to evaluate static allometry of body traits with body size, and their variation across sexes and lineages of green lizards. Df: degrees of freedom, SS: sum of squares, MS: mean squares, R2: coefficient of determination, F: F value, Z: Z value, and p-values of significance. Significant patterns (using a threshold of a = 0.05) are highlighted with asterisks.

Table A1.2 ANOVA results for the main effects and interactions of variables (logSVL, SEX, and their combinations) on TRL. Df: degrees of freedom, SS: sum of squares, MS: mean squares, Rsq: coefficient of determination, F: F value, Z: Z value, and p-values of significance. The analyses are presented for several green lizard lineages analysed (l)

Table A1.3 ANOVA results for the main effects and interactions of variables (logSVL, SEX, and their combinations) on HS. Df: degrees of freedom, SS: sum of squares, MS: mean squares, Rsq: coefficient of determination, F: F value, Z: Z value, and p-values of significance. The analyses are presented for several *green lizard* lineages analysed (l)

Table A1.4 ANOVA results for the main effects and interactions of variables (logSVL, SEX, and their combinations) on HLL. Df: degrees of freedom, SS: sum of squares, MS: mean squares, Rsq: coefficient of determination, F: F value, Z: Z value, and p-values of significance. The analyses are presented for several *green lizard* lineages analysed (l)

Table A1.5 ANOVA results for the main effects and interactions of variables (logSVL, SEX, and their combinations) on FLL. Df: degrees of freedom, SS: sum of squares, MS: mean squares, Rsq: coefficient of determination, F: F value, Z: Z value, and p-values of significance. The analyses are presented for several *green lizard* lineages analysed (l)

Table A1.6 Statistics of tests for Rensch's Rule with Sexual Dimorphism Ratio (SD Ratio) approach applied to a subsample of 10 individuals per sex per lineage. β1: estimated allometric slope, SE: standard error of the slope estimate, t- and p-value: corresponding t- and p-values of significance testing for slope estimates ($\beta 1 \neq 0$). Significant patterns (using a threshold of $\alpha = 0.05$) are highlighted with asterisks.

Table A1.7 ANOVA table for the linear model used to test for the effect of intersexual differences in static allometric intercept and slope on the trait Rensch's Rule pattern with the SD ratio approach applied to a subsample of 10 individuals per sex per lineage. β1:

estimated allometric slope, β0: estimated allometric intercept. Interaction factors of the model are depicted with an asterisk. F-value and p-values of significance. Significant patterns (using a threshold of α = 0.05) are highlighted with bold asterisks.

Figure A1.1 Simulations of RR in body size tested with different values of SSD. A) mean p-values of RR tested. B) mean slope values of the PGLS used to test RR

Figure A1.2 Simulations of RR in trait tested with different values of static intercept and SSD = 0. A) mean p-values of RR test. B) mean slope values of the PGLS used to test RR.

Figure A1.3 Simulators of RR in trait tested with different values of static slope and SSD= o. A) mean p-values of RR test. B) mean slope values of the PGLS used to test RR.

Figure A1.4 Simulations of RR in trait tested with different values of static intercept and SSD= -0.2. A) mean p-values of RR test. B) mean slope values of the PGLS used to test RR.

Figure A1.5 Simulations of RR in trait tested with different values of static slope and SSD =-0.2. A) mean p-values. B) mean slope values of the PGLS used to test RR.\

Figure A1.6 Simulations of RR in trait tested with different values of static intercept and SSD= 0.2. A) mean p-values of RR test. B) slope values of the PGLS used to test RR.

Figure A1.7 Simulations of RR in trait tested with different values of static slope and SSD= 0.2. A) mean p-values of RR test. B) mean slope values of the PGLS used to test RR.

Figure A1.8 Subsampling simulations to test RR in smaller sample sizes. The subsamples come from original simulations in which we considered 50 individuals per sex, per lineage. Left column, mean p-values of the RR test. Right column, mean slope values of the PGLS.

Figure A1.9 Subsampling simulations to test RR in smaller sample sizes. The subsamples come from original simulations in which we considered 50 individuals per sex, per lineage. Left column, mean p-values of the RR test. Right column, mean slope values of the PGLS.

Figure A1.10 Subsampling simulations to test RR in smaller sample sizes. The subsamples come from original simulations in which we considered 50 individuals per sex, per lineage. Left column, mean p-values of the RR test. Right column, mean slope values of the PGLS.

Figure A1.11 Subsampling simulations to test RR in smaller sample sizes. The subsamples come from original simulations in which we considered 50 individuals per sex, per lineage. Left column, mean p-values of the RR test. Right column, mean slope values of the PGLS.

Figure A1.12 Subsampling simulations to test RR in smaller sample sizes. The subsamples come from original simulations in which we considered 50 individuals per sex, per lineage. Left column, mean p-values of the RR test. Right column, mean slope values of the PGLS.

Figure A1.13 Subsampling simulations to test RR in smaller sample sizes. The subsamples come from original simulations in which we considered 50 individuals per sex, per lineage. Left column, mean p-values of the RR test. Right column, mean slope values of the PGLS.

Table A1.1 ANOVA table of GLMs used to evaluate static allometry of body traits with body size, and their variation across sexes and lineages of green lizards. Df: degrees of freedom, SS: sum of squares, MS: mean squares, R2: coefficient of determination, F: F value, Z: Z value, and p-values of significance. Significant patterns (using a threshold of a = 0.05) are highlighted with asterisks.

			TRL				
	Df	**SS**	**MS**	**R^2**	**F**	**Z**	**Pr(>F)**
Body size	1	23.4	23.401	0.886	10494.996	15.685	**0.001****
Sex	1	1.309	1.309	0.049	587.309	8.19	**0.001****
Lineage	18	0.474	0.026	0.017	11.8	9.631	**0.001****
Body size*sex	1	0.043	0.042	0.001	19.236	3.364	**0.001****
Body size*lineage	18	0.091	0.005	0.003	2.279	3.026	**0.001****
Sex*lineage	18	0.068	0.003	0.002	1.692	1.781	**0.036***
Body size*sex*lineage	18	0.034	0.001	0.001	0.856	-0.32	0.634
Residuals	439	0.979	0.002	0.037			
Total	514	26.399					
			HS				
	Df	**SS**	**MS**	**R^2**	**F**	**Z**	**Pr(>F)**
Body size	1	41.737	41.737	0.884	23421.639	18.848	**0.001****
Sex	1	3.788	3.788	0.08	2125.805	12.391	**0.001****
Lineage	18	0.603	0.033	0.012	18.803	10.39	**0.001****
Body size*sex	1	0.06	0.06	0	33.769	3.684	**0.001****
Body size*lineage	18	0.063	0.003	0	1.975	2.369	**0.008****
Sex*lineage	18	0.095	0.005	0.002	2.966	3.82	**0.001****
Body size*sex*lineage	18	0.037	0.002	0.0007	1.167	0.589	0.285
Residuals	439	0.782	0.001	0.016			
Total	514	47.167					
			FLL				
	Df	**SS**	**MS**	**R^2**	**F**	**Z**	**Pr(>F)**
Body size	1	31.627	31.627	0.884	5388.689	14.411	**0.001****
Sex	1	0.174	0.174	0.004	29.812	4.044	**0.001****
Lineage	18	1.067	0.059	0.029	10.101	8.793	**0.001****
Body size*sex	1	0.01	0.01	0.0002	1.801	0.943	0.176
Body size*lineage	18	0.095	0.005	0.002	0.905	0.302	0.376

Sex*lineage	18	0.101	0.005	0.002	0.956	0.174	0.449
Body size*sex*lineage	18	0.084	0.004	0.002	0.796	0.081	0.454
Residuals	439	2.576	0.005	0.072			
Total	514	35.737					

HLL

	Df	**SS**	**MS**	**R^2**	**F**	**Z**	**Pr(>F)**
Body size	1	35.768	35.768	0.87	13074.838	16.373	**0.001****
Sex	1	0.262	0.262	0.006	95.805	5.978	**0.001****
Lineage	18	3.58	0.1987	0.087	72.705	23.6	**0.001****
Body size*sex	1	0.061	0.061	0.001	22.476	3.359	**0.001****
Body size*lineage	18	0.109	0.006	0.002	2.23	2.642	**0.004***
Sex*lineage	18	0.055	0.003	0.001	1.121	0.411	0.337
Body size*sex*lineage	18	0.046	0.002	0.001	0.939	-0.155	0.569
Residuals	439	1.2	0.002	0.029			
Total	514	41.084					

Table A1.2 ANOVA results for the main effects and interactions of variables (logSVL, SEX, and their combinations) on TRL. Df: degrees of freedom, SS: sum of squares, MS: mean squares, Rsq: coefficient of determination, F: F value, Z: Z value, and p-values of significance. The analyses are presented for several *green lizard* lineages analysed (l).

TRL	Df	SS	MS	Rsq	F	Z	Pr(>F)	l
dt.sub$logSVL	1	0.2872321	0.2872321	0.7021234	134.52522	5.6315977	0.001	adriatic
dt.sub$SEX	1	0.0705397	0.0705397	0.1724305	33.037284	3.7774144	0.001	adriatic
dt.sub$logSVL:dt.sub$SEX	1	7.51E-05	7.51E-05	0.0001836	0.035183	-1.1518891	0.856	adriatic
Residuals	24	0.0512437	0.0021352	0.1252625	NA	NA	NA	adriatic
Total	27	0.4090907	NA	NA	NA	NA	NA	adriatic
dt.sub$logSVL1	1	0.5481845	0.5481845	0.8966275	469.64437	8.7082542	0.001	agilis
dt.sub$SEX1	1	0.0326253	0.0326253	0.0533629	27.95097	3.635498	0.001	agilis
dt.sub$logSVL:dt.sub$SEX1	1	0.000227	0.000227	0.0003713	0.1944831	-0.4592428	0.673	agilis
Residuals1	26	0.0303481	0.0011672	0.0496382	NA	NA	NA	agilis
Total1	29	0.6113849	NA	NA	NA	NA	NA	agilis
dt.sub$logSVL2	1	0.3255875	0.3255875	0.7408313	201.60094	6.6154724	0.001	bilineata
dt.sub$SEX2	1	0.069718	0.069718	0.1586341	43.168768	4.034921	0.001	bilineata
dt.sub$logSVL:dt.sub$SEX2	1	0.0021937	0.0021937	0.0049914	1.3582945	0.7161024	0.254	bilineata
Residuals2	26	0.0419903	0.001615	0.0955433	NA	NA	NA	bilineata
Total2	29	0.4394894	NA	NA	NA	NA	NA	bilineata
dt.sub$logSVL3	1	0.1183529	0.1183529	0.5609291	67.707708	4.9377646	0.001	brevicaudata
dt.sub$SEX3	1	0.0466589	0.0466589	0.2211382	26.692787	3.2710872	0.002	brevicaudata
dt.sub$logSVL:dt.sub$SEX3	1	0.0005346	0.0005346	0.0025339	0.3058581	-0.2057156	0.598	brevicaudata
Residuals3	26	0.0454479	0.001748	0.2153988	NA	NA	NA	brevicaudata
Total3	29	0.2109944	NA	NA	NA	NA	NA	brevicaudata
dt.sub$logSVL4	1	0.0725012	0.0725012	0.6622541	97.326771	4.7014148	0.001	diplochondrodes
dt.sub$SEX4	1	0.0241032	0.0241032	0.2201678	32.356487	3.6837343	0.001	diplochondrodes
dt.sub$logSVL:dt.sub$SEX4	1	0.0024431	0.0024431	0.0223159	3.2796159	1.3164551	0.09	diplochondrodes
Residuals4	14	0.010429	0.0007449	0.0952622	NA	NA	NA	diplochondrodes
Total4	17	0.1094764	NA	NA	NA	NA	NA	diplochondrodes
dt.sub$logSVL5	1	0.0947632	0.0947632	0.4527648	77.09416	4.7795047	0.001	israelica
dt.sub$SEX5	1	0.0818292	0.0818292	0.3909682	66.571794	4.7703258	0.001	israelica
dt.sub$logSVL:dt.sub$SEX5	1	0.0105811	0.0105811	0.0505551	8.6082315	2.2488374	0.008	israelica
Residuals5	18	0.0221254	0.0012292	0.1057119	NA	NA	NA	israelica
Total5	21	0.2092989	NA	NA	NA	NA	NA	israelica
dt.sub$logSVL6	1	0.0654681	0.0654681	0.5502847	20.713283	2.9802188	0.001	kurdistanicus
dt.sub$SEX6	1	0.0087641	0.0087641	0.0736653	2.7728367	1.2026923	0.114	kurdistanicus
dt.sub$logSVL:dt.sub$SEX6	1	0.0036503	0.0036503	0.0306822	1.1549109	0.5451086	0.293	kurdistanicus
Residuals6	13	0.0410889	0.0031607	0.3453678	NA	NA	NA	kurdistanicus
Total6	16	0.1189714	NA	NA	NA	NA	NA	kurdistanicus
dt.sub$logSVL7	1	0.0439478	0.0439478	0.3105934	15.530658	2.8263015	0.002	lepidus
dt.sub$SEX7	1	0.0224241	0.0224241	0.1584783	7.9244206	2.1067747	0.015	lepidus
dt.sub$logSVL:dt.sub$SEX7	1	0.001551	0.001551	0.0109614	0.5481063	0.2082541	0.431	lepidus
Residuals7	26	0.0735734	0.0028297	0.5199669	NA	NA	NA	lepidus

Total7	29	0.1414964	NA	NA	NA	NA	NA	lepidus
dt.sub$logSVL8	1	0.0482485	0.0482485	0.2795112	18.213321	3.0958107	0.001	media
dt.sub$SEX8	1	0.0526056	0.0526056	0.3047524	19.858067	3.0976132	0.001	media
dt.sub$logSVL:dt.sub$SEX8	1	0.0055364	0.0055364	0.0320732	2.0899332	1.0534316	0.136	media
Residuals8	25	0.066227	0.0026491	0.3836632	NA	NA	NA	media
Total8	28	0.1726174	NA	NA	NA	NA	NA	media
dt.sub$logSVL9	1	0.3513242	0.3513242	0.7564473	249.38051	6.7949136	0.001	meridionalis
dt.sub$SEX9	1	0.0723839	0.0723839	0.1558522	51.380307	4.3408014	0.001	meridionalis
dt.sub$logSVL:dt.sub$SEX9	1	0.0041031	0.0041031	0.0088345	2.9125079	1.2506126	0.106	meridionalis
Residuals9	26	0.0366285	0.0014088	0.0788659	NA	NA	NA	meridionalis
Total9	29	0.4644397	NA	NA	NA	NA	NA	meridionalis
dt.sub$logSVL10	1	0.0848646	0.0848646	0.3481512	27.941102	3.6553682	0.001	nevadensis
dt.sub$SEX10	1	0.0742133	0.0742133	0.304455	24.434234	3.6032253	0.001	nevadensis
dt.sub$logSVL:dt.sub$SEX10	1	0.005711	0.005711	0.023429	1.8803082	0.9372618	0.192	nevadensis
Residuals10	26	0.078969	0.0030373	0.3239648	NA	NA	NA	nevadensis
Total10	29	0.2437579	NA	NA	NA	NA	NA	nevadensis
dt.sub$logSVL11	1	0.0353571	0.0353571	0.1844186	8.9452606	2.3089164	0.006	pater
dt.sub$SEX11	1	0.0528766	0.0528766	0.2757986	13.37766	2.6834298	0.001	pater
dt.sub$logSVL:dt.sub$SEX11	1	0.0007204	0.0007204	0.0037576	0.1822649	-0.3711867	0.634	pater
Residuals11	26	0.1027677	0.0039526	0.5360252	NA	NA	NA	pater
Total11	29	0.1917217	NA	NA	NA	NA	NA	pater
dt.sub$logSVL12	1	0.3909805	0.3909805	0.8291461	95.625729	5.5006517	0.001	princeps
dt.sub$SEX12	1	0.0069106	0.0069106	0.0146552	1.6901909	0.8012705	0.225	princeps
dt.sub$logSVL:dt.sub$SEX12	1	5.91E-05	5.91E-05	0.0001253	0.0144499	-1.4134992	0.9	princeps
Residuals12	18	0.0735958	0.0040887	0.1560734	NA	NA	NA	princeps
Total12	21	0.471546	NA	NA	NA	NA	NA	princeps
dt.sub$logSVL13	1	0.3140227	0.3140227	0.6629207	123.59347	5.6430292	0.001	schreiberi
dt.sub$SEX13	1	0.0934947	0.0934947	0.1973729	36.797769	3.7748503	0.001	schreiberi
dt.sub$logSVL:dt.sub$SEX13	1	0.0001183	0.0001183	0.0002497	0.0465619	-1.06744	0.837	schreiberi
Residuals13	26	0.06606	0.0025408	0.1394567	NA	NA	NA	schreiberi
Total13	29	0.4736957	NA	NA	NA	NA	NA	schreiberi
dt.sub$logSVL14	1	0.1828244	0.1828244	0.7017424	102.83246	5.3053168	0.001	schreiberi_I
dt.sub$SEX14	1	0.0361377	0.0361377	0.1387089	20.326223	3.1070278	0.001	schreiberi_I
dt.sub$logSVL:dt.sub$SEX14	1	0.0042315	0.0042315	0.016242	2.3800755	1.113604	0.141	schreiberi_I
Residuals14	21	0.0373356	0.0017779	0.1433068	NA	NA	NA	schreiberi_I
Total14	24	0.2605292	NA	NA	NA	NA	NA	schreiberi_I
dt.sub$logSVL15	1	0.0883739	0.0883739	0.4870775	55.021301	4.3140766	0.001	strigata
dt.sub$SEX15	1	0.0503678	0.0503678	0.2776049	31.358828	3.9021501	0.001	strigata
dt.sub$logSVL:dt.sub$SEX15	1	0.0009347	0.0009347	0.0051519	0.5819706	0.2064976	0.454	strigata
Residuals15	26	0.0417606	0.0016062	0.2301657	NA	NA	NA	strigata
Total15	29	0.181437	NA	NA	NA	NA	NA	strigata
dt.sub$logSVL16	1	0.0110005	0.0110005	0.0783909	5.6696559	1.8403607	0.024	tangitanus
dt.sub$SEX16	1	0.0877554	0.0877554	0.6253571	45.229207	3.9710252	0.001	tangitanus
dt.sub$logSVL:dt.sub$SEX16	1	0.0027678	0.0027678	0.019724	1.426545	0.6803271	0.269	tangitanus
Residuals16	20	0.0388048	0.0019402	0.276528	NA	NA	NA	tangitanus
Total16	23	0.1403285	NA	NA	NA	NA	NA	tangitanus

dt.sub$logSVL17	1	0.1313878	0.1313878	0.5267903	61.309244	4.9921913	0.001	trilineata
dt.sub$SEX17	1	0.0498389	0.0498389	0.1998255	23.256219	3.116598	0.001	trilineata
dt.sub$logSVL:dt.sub$SEX17	1	0.0124664	0.0124664	0.0499831	5.8171643	1.8569337	0.032	trilineata
Residuals17	26	0.0557189	0.002143	0.223401	NA	NA	NA	trilineata
Total17	29	0.2494119	NA	NA	NA	NA	NA	trilineata
dt.sub$logSVL18	1	0.1817798	0.1817798	0.5112877	72.998093	4.9203045	0.001	viridis
dt.sub$SEX18	1	0.1085257	0.1085257	0.3052476	43.581117	4.1589314	0.001	viridis
dt.sub$logSVL:dt.sub$SEX18	1	0.0004826	0.0004826	0.0013575	0.1938124	-0.4077411	0.657	viridis
Residuals18	26	0.0647452	0.0024902	0.1821072	NA	NA	NA	viridis
Total18	29	0.3555332	NA	NA	NA	NA	NA	viridis

Table A1.3 ANOVA results for the main effects and interactions of variables (logSVL, SEX, and their combinations) on HS. Df: degrees of freedom, SS: sum of squares, MS: mean squares, Rsq: coefficient of determination, F: F value, Z: Z value, and p-values of significance. The analyses are presented for several *green lizard* lineages analysed (l).

HS	Df	SS	MS	Rsq	F	Z	Pr(>F)	l
dt.sub$logSVL	1	0.2399949	0.2399949	0.5668862	261.21051	6.5532998	0.001	adriatic
dt.sub$SEX	1	0.1585977	0.1585977	0.3746198	172.61774	6.0687786	0.001	adriatic
dt.sub$logSVL:dt.sub$SEX	1	0.0027131	0.0027131	0.0064085	2.9529346	1.3357786	0.091	adriatic
Residuals	24	0.0220507	0.0009188	0.0520855	NA	NA	NA	adriatic
Total	27	0.4233564	NA	NA	NA	NA	NA	adriatic
dt.sub$logSVL1	1	0.005505	0.005505	0.0290914	3.1930289	1.3783227	0.088	agilis
dt.sub$SEX1	1	0.1384887	0.1384887	0.7318427	80.326108	4.8164492	0.001	agilis
dt.sub$logSVL:dt.sub$SEX1	1	0.000413	0.000413	0.0021826	0.2395647	-0.3339066	0.628	agilis
Residuals1	26	0.0448261	0.0017241	0.2368833	NA	NA	NA	agilis
Total1	29	0.1892329	NA	NA	NA	NA	NA	agilis
dt.sub$logSVL2	1	0.2008553	0.2008553	0.440539	92.245682	5.325778	0.001	bilineata
dt.sub$SEX2	1	0.1941219	0.1941219	0.4257704	89.153256	5.2225716	0.001	bilineata
dt.sub$logSVL:dt.sub$SEX2	1	0.0043414	0.0043414	0.009522	1.9938445	0.9589061	0.178	bilineata
Residuals2	26	0.0566123	0.0021774	0.1241686	NA	NA	NA	bilineata
Total2	29	0.4559308	NA	NA	NA	NA	NA	bilineata
dt.sub$logSVL3	1	0.0943673	0.0943673	0.2546349	38.731315	3.9366799	0.001	brevicaudata
dt.sub$SEX3	1	0.2127558	0.2127558	0.5740871	87.321678	4.8215026	0.001	brevicaudata
dt.sub$logSVL:dt.sub$SEX3	1	0.0001274	0.0001274	0.0003437	0.0522854	-0.923056	0.815	brevicaudata
Residuals3	26	0.063348	0.0024365	0.1709342	NA	NA	NA	brevicaudata
Total3	29	0.3705984	NA	NA	NA	NA	NA	brevicaudata
dt.sub$logSVL4	1	0.1992652	0.1992652	0.6761892	174.02358	5.7552503	0.001	diplochondrodes
dt.sub$SEX4	1	0.0790826	0.0790826	0.26836	69.06493	4.4836577	0.001	diplochondrodes
dt.sub$logSVL:dt.sub$SEX4	1	0.0003101	0.0003101	0.0010521	0.2707758	-0.3443859	0.63	diplochondrodes
Residuals4	14	0.0160307	0.001145	0.0543987	NA	NA	NA	diplochondrodes
Total4	17	0.2946884	NA	NA	NA	NA	NA	diplochondrodes
dt.sub$logSVL5	1	0.0972077	0.0972077	0.2384	46.192697	4.3237988	0.001	israelica
dt.sub$SEX5	1	0.2726633	0.2726633	0.6687012	129.56844	5.3149418	0.001	israelica
dt.sub$logSVL:dt.sub$SEX5	1	3.94E-07	3.94E-07	9.67E-07	0.0001875	-2.2110041	0.991	israelica
Residuals5	18	0.0378791	0.0021044	0.0928978	NA	NA	NA	israelica
Total5	21	0.4077506	NA	NA	NA	NA	NA	israelica
dt.sub$logSVL6	1	0.1046641	0.1046641	0.6889257	110.3659	5.4352965	0.001	kurdistanicus
dt.sub$SEX6	1	0.031838	0.031838	0.2095657	33.572426	3.5630289	0.001	kurdistanicus
dt.sub$logSVL:dt.sub$SEX6	1	0.0030932	0.0030932	0.02036	3.2616687	1.2861624	0.103	kurdistanicus
Residuals6	13	0.0123284	0.0009483	0.0811486	NA	NA	NA	kurdistanicus
Total6	16	0.1519236	NA	NA	NA	NA	NA	kurdistanicus
dt.sub$logSVL7	1	1.4375994	1.4375994	0.9116974	447.00249	8.1629823	0.001	lepidus
dt.sub$SEX7	1	0.0540763	0.0540763	0.0342941	16.814305	3.0026721	0.001	lepidus
dt.sub$logSVL:dt.sub$SEX7	1	0.0015443	0.0015443	0.0009794	0.480173	-0.003131	0.523	lepidus
Residuals7	26	0.0836183	0.0032161	0.0530291	NA	NA	NA	lepidus

Total7	29	1.5768383	NA	NA	NA	NA	NA	lepidus
dt.sub$logSVL8	1	0.3923098	0.3923098	0.7880607	425.06093	8.00247	0.001	media
dt.sub$SEX8	1	0.0817321	0.0817321	0.1641812	88.555356	5.2861877	0.001	media
dt.sub$logSVL:dt.sub$SEX8	1	0.000701	0.000701	0.0014082	0.7595735	0.2906692	0.408	media
Residuals8	25	0.0230737	0.0009229	0.0463499	NA	NA	NA	media
Total8	28	0.4978167	NA	NA	NA	NA	NA	media
dt.sub$logSVL9	1	0.0881006	0.0881006	0.2961356	57.381393	4.4579493	0.001	meridionalis
dt.sub$SEX9	1	0.1647528	0.1647528	0.5537892	107.30624	5.3515139	0.001	meridionalis
dt.sub$logSVL:dt.sub$SEX9	1	0.0047284	0.0047284	0.0158936	3.079668	1.3215962	0.088	meridionalis
Residuals9	26	0.0399191	0.0015354	0.1341816	NA	NA	NA	meridionalis
Total9	29	0.297501	NA	NA	NA	NA	NA	meridionalis
dt.sub$logSVL10	1	0.9891733	0.9891733	0.8071176	752.6902	8.5814692	0.001	nevadensis
dt.sub$SEX10	1	0.1848383	0.1848383	0.1508192	140.64878	5.7177995	0.001	nevadensis
dt.sub$logSVL:dt.sub$SEX10	1	0.0173824	0.0173824	0.0141832	13.226754	2.6371397	0.003	nevadensis
Residuals10	26	0.0341688	0.0013142	0.0278801	NA	NA	NA	nevadensis
Total10	29	1.2255628	NA	NA	NA	NA	NA	nevadensis
dt.sub$logSVL11	1	0.6330972	0.6330972	0.7286416	350.84324	6.9506383	0.001	pater
dt.sub$SEX11	1	0.188002	0.188002	0.2163745	104.18501	5.3242958	0.001	pater
dt.sub$logSVL:dt.sub$SEX11	1	0.0008571	0.0008571	0.0009864	0.4749535	0.0336762	0.511	pater
Residuals11	26	0.046917	0.0018045	0.0539976	NA	NA	NA	pater
Total11	29	0.8688733	NA	NA	NA	NA	NA	pater
dt.sub$logSVL12	1	0.3543804	0.3543804	0.739616	167.8401	6.0946652	0.001	princeps
dt.sub$SEX12	1	0.0775705	0.0775705	0.1618948	36.738582	3.8057651	0.001	princeps
dt.sub$logSVL:dt.sub$SEX12	1	0.0091847	0.0091847	0.0191692	4.3500342	1.5929652	0.046	princeps
Residuals12	18	0.0380055	0.0021114	0.0793201	NA	NA	NA	princeps
Total12	21	0.4791411	NA	NA	NA	NA	NA	princeps
dt.sub$logSVL13	1	0.0550564	0.0550564	0.1501986	22.811336	3.2566525	0.001	schreiberi
dt.sub$SEX13	1	0.2463841	0.2463841	0.672157	102.08352	5.2970726	0.001	schreiberi
dt.sub$logSVL:dt.sub$SEX13	1	0.0023644	0.0023644	0.0064504	0.9796528	0.4707726	0.333	schreiberi
Residuals13	26	0.0627524	0.0024136	0.171194	NA	NA	NA	schreiberi
Total13	29	0.3665574	NA	NA	NA	NA	NA	schreiberi
dt.sub$logSVL14	1	0.087596	0.087596	0.377808	81.583222	4.7507229	0.001	schreiberi_l
dt.sub$SEX14	1	0.1201238	0.1201238	0.5181029	111.87826	5.0476306	0.001	schreiberi_l
dt.sub$logSVL:dt.sub$SEX14	1	0.0015857	0.0015857	0.0068392	1.4768413	0.7693981	0.232	schreiberi_l
Residuals14	21	0.0225477	0.0010737	0.09725	NA	NA	NA	schreiberi_l
Total14	24	0.2318533	NA	NA	NA	NA	NA	schreiberi_l
dt.sub$logSVL15	1	0.0299449	0.0299449	0.1361398	21.615882	3.153219	0.001	strigata
dt.sub$SEX15	1	0.1533556	0.1533556	0.6972068	110.70047	5.6204959	0.001	strigata
dt.sub$logSVL:dt.sub$SEX15	1	0.0006383	0.0006383	0.0029018	0.4607348	-7.82E-05	0.516	strigata
Residuals15	26	0.0360183	0.0013853	0.1637516	NA	NA	NA	strigata
Total15	29	0.2199571	NA	NA	NA	NA	NA	strigata
dt.sub$logSVL16	1	0.3575026	0.3575026	0.6908896	203.46782	6.375864	0.001	tangitanus
dt.sub$SEX16	1	0.1248077	0.1248077	0.2411965	71.032654	4.8273264	0.001	tangitanus
dt.sub$logSVL:dt.sub$SEX16	1	1.30E-06	1.30E-06	2.52E-06	0.0007418	-2.1127947	0.991	tangitanus
Residuals16	20	0.0351409	0.001757	0.0679114	NA	NA	NA	tangitanus
Total16	23	0.5174526	NA	NA	NA	NA	NA	tangitanus

dt.sub$logSVL17	1	0.8582657	0.8582657	0.8193074	459.01286	7.9693834	0.001	trilineata
dt.sub$SEX17	1	0.1404645	0.1404645	0.1340886	75.122446	5.2616126	0.001	trilineata
dt.sub$logSVL:dt.sub$SEX17	1	0.0002051	0.0002051	0.0001958	0.1096852	-0.6040847	0.707	trilineata
Residuals17	26	0.048615	0.0018698	0.0464083	NA	NA	NA	trilineata
Total17	29	1.0475503	NA	NA	NA	NA	NA	trilineata
dt.sub$logSVL18	1	0.0973786	0.0973786	0.2378232	43.320392	4.3074126	0.001	viridis
dt.sub$SEX18	1	0.2536329	0.2536329	0.6194355	112.8325	5.3102006	0.001	viridis
dt.sub$logSVL:dt.sub$SEX18	1	1.97E-06	1.97E-06	4.81E-06	0.0008753	-2.0196041	0.975	viridis
Residuals18	26	0.0584446	0.0022479	0.1427365	NA	NA	NA	viridis
Total18	29	0.4094582	NA	NA	NA	NA	NA	viridis

Table A1.4 ANOVA results for the main effects and interactions of variables (logSVL, SEX, and their combinations) on HLL. Df: degrees of freedom, SS: sum of squares, MS: mean squares, Rsq: coefficient of determination, F: F value, Z: Z value, and p-values of significance. The analyses are presented for several *green lizard* lineages analysed (l).

HLL	Df	SS	MS	Rsq	F	Z	Pr(>F)	l
dt.sub$logSVL	1	0.0160339	0.0160339	0.0086415	0.2320139	-0.3666883	0.624	adriatic
dt.sub$SEX	1	0.1196822	0.1196822	0.0645032	1.7318287	1.026573	0.155	adriatic
dt.sub$logSVL:dt.sub$SEX	1	0.0611514	0.0611514	0.0329578	0.8848754	0.4273704	0.355	adriatic
Residuals	24	1.6585776	0.0691074	0.8938974	NA	NA	NA	adriatic
Total	27	1.8554451	NA	NA	NA	NA	NA	adriatic
dt.sub$logSVL1	1	0.0326934	0.0326934	0.306976	20.299917	3.1282637	0.001	agilis
dt.sub$SEX1	1	0.0279365	0.0279365	0.2623108	17.346268	2.9296394	0.001	agilis
dt.sub$logSVL:dt.sub$SEX1	1	0.0039981	0.0039981	0.0375403	2.4824911	1.1222936	0.144	agilis
Residuals1	26	0.0418734	0.0016105	0.3931729	NA	NA	NA	agilis
Total1	29	0.1065013	NA	NA	NA	NA	NA	agilis
dt.sub$logSVL2	1	0.1720361	0.1720361	0.5612964	42.333851	3.8488742	0.001	bilineata
dt.sub$SEX2	1	0.028803	0.028803	0.0939745	7.0877055	2.0524224	0.014	bilineata
dt.sub$logSVL:dt.sub$SEX2	1	3.84E-08	3.84E-08	1.25E-07	9.46E-06	-2.5732013	0.998	bilineata
Residuals2	26	0.1056587	0.0040638	0.344729	NA	NA	NA	bilineata
Total2	29	0.3064978	NA	NA	NA	NA	NA	bilineata
dt.sub$logSVL3	1	0.0802702	0.0802702	0.4753823	37.141306	3.7449787	0.001	brevicaudata
dt.sub$SEX3	1	0.0314792	0.0314792	0.1864284	14.565528	2.805174	0.001	brevicaudata
dt.sub$logSVL:dt.sub$SEX3	1	0.0009131	0.0009131	0.0054077	0.4225033	-0.0282994	0.511	brevicaudata
Residuals3	26	0.0561915	0.0021612	0.3327815	NA	NA	NA	brevicaudata
Total3	29	0.168854	NA	NA	NA	NA	NA	brevicaudata
dt.sub$logSVL4	1	0.0591481	0.0591481	0.6125762	22.505893	3.0421053	0.002	diplochondrodes
dt.sub$SEX4	1	0.0002565	0.0002565	0.0026564	0.0975958	-0.7425588	0.766	diplochondrodes
dt.sub$logSVL:dt.sub$SEX4	1	0.0003581	0.0003581	0.0037087	0.1362559	-0.622021	0.738	diplochondrodes
Residuals4	14	0.0367936	0.0026281	0.3810587	NA	NA	NA	diplochondrodes
Total4	17	0.0965563	NA	NA	NA	NA	NA	diplochondrodes
dt.sub$logSVL5	1	0.0396693	0.0396693	0.452677	17.66591	2.832629	0.001	israelica
dt.sub$SEX5	1	0.006628	0.006628	0.0756336	2.9516343	1.3194244	0.099	israelica
dt.sub$logSVL:dt.sub$SEX5	1	0.0009159	0.0009159	0.0104516	0.4078801	-0.024427	0.527	israelica
Residuals5	18	0.0404195	0.0022455	0.4612378	NA	NA	NA	israelica
Total5	21	0.0876327	NA	NA	NA	NA	NA	israelica
dt.sub$logSVL6	1	0.0432191	0.0432191	0.4373888	11.020975	2.4256545	0.007	kurdistanicus
dt.sub$SEX6	1	0.001049	0.001049	0.0106158	0.2674891	-0.275538	0.619	kurdistanicus
dt.sub$logSVL:dt.sub$SEX6	1	0.0035637	0.0035637	0.0360652	0.9087413	0.3391061	0.395	kurdistanicus
Residuals6	13	0.0509799	0.0039215	0.5159302	NA	NA	NA	kurdistanicus
Total6	16	0.0988116	NA	NA	NA	NA	NA	kurdistanicus
dt.sub$logSVL7	1	0.2954302	0.2954302	0.8990735	244.82519	7.0466025	0.001	lepidus
dt.sub$SEX7	1	0.0017559	0.0017559	0.0053436	1.4551039	0.776573	0.232	lepidus
dt.sub$logSVL:dt.sub$SEX7	1	3.38E-05	3.38E-05	0.0001029	0.0280286	-1.1203962	0.86	lepidus
Residuals7	26	0.0313742	0.0012067	0.09548	NA	NA	NA	lepidus

Total7	29	0.328594	NA	NA	NA	NA	NA	lepidus
dt.sub$logSVL8	1	0.1515114	0.1515114	0.7273401	76.706559	5.1188775	0.001	media
dt.sub$SEX8	1	0.0070178	0.0070178	0.0336894	3.552946	1.4912225	0.063	media
dt.sub$logSVL:dt.sub$SEX8	1	0.0003995	0.0003995	0.0019178	0.2022504	-0.4257879	0.663	media
Residuals8	25	0.0493802	0.0019752	0.2370528	NA	NA	NA	media
Total8	28	0.2083089	NA	NA	NA	NA	NA	media
dt.sub$logSVL9	1	0.0995538	0.0995538	0.5735059	57.654065	4.4708564	0.001	meridionalis
dt.sub$SEX9	1	0.0290681	0.0290681	0.1674546	16.834073	2.8547598	0.001	meridionalis
dt.sub$logSVL:dt.sub$SEX9	1	7.08E-05	7.08E-05	0.000408	0.0410151	-1.0922615	0.855	meridionalis
Residuals9	26	0.0448953	0.0017267	0.2586314	NA	NA	NA	meridionalis
Total9	29	0.1735881	NA	NA	NA	NA	NA	meridionalis
dt.sub$logSVL10	1	0.1108827	0.1108827	0.6386404	48.837726	4.2467685	0.001	nevadensis
dt.sub$SEX10	1	0.003692	0.003692	0.0212646	1.6261331	0.8182876	0.223	nevadensis
dt.sub$logSVL:dt.sub$SEX10	1	1.71E-05	1.71E-05	9.86E-05	0.0075377	-1.5100469	0.921	nevadensis
Residuals10	26	0.0590312	0.0022704	0.3399964	NA	NA	NA	nevadensis
Total10	29	0.1736231	NA	NA	NA	NA	NA	nevadensis
dt.sub$logSVL11	1	0.1985057	0.1985057	0.7885861	100.45486	5.3343275	0.001	pater
dt.sub$SEX11	1	0.0016166	0.0016166	0.0064221	0.8180906	0.3917126	0.343	pater
dt.sub$logSVL:dt.sub$SEX11	1	0.0002235	0.0002235	0.0008878	0.1130897	-0.6223523	0.714	pater
Residuals11	26	0.0513778	0.0019761	0.204104	NA	NA	NA	pater
Total11	29	0.2517235	NA	NA	NA	NA	NA	pater
dt.sub$logSVL12	1	0.1479871	0.1479871	0.7129746	50.529546	4.1028761	0.001	princeps
dt.sub$SEX12	1	0.0068374	0.0068374	0.0329411	2.3345866	1.0456392	0.155	princeps
dt.sub$logSVL:dt.sub$SEX12	1	2.14E-05	2.14E-05	0.0001033	0.0073196	-1.5773104	0.939	princeps
Residuals12	18	0.052717	0.0029287	0.253981	NA	NA	NA	princeps
Total12	21	0.207563	NA	NA	NA	NA	NA	princeps
dt.sub$logSVL13	1	0.0304512	0.0304512	0.3688935	21.613456	3.1814497	0.001	schreiberi
dt.sub$SEX13	1	0.0073192	0.0073192	0.0886671	5.1950008	1.7089003	0.042	schreiberi
dt.sub$logSVL:dt.sub$SEX13	1	0.0081456	0.0081456	0.0986773	5.7815011	1.8974141	0.024	schreiberi
Residuals13	26	0.0366314	0.0014089	0.4437621	NA	NA	NA	schreiberi
Total13	29	0.0825475	NA	NA	NA	NA	NA	schreiberi
dt.sub$logSVL14	1	0.0505222	0.0505222	0.5785128	34.376401	3.9721822	0.001	schreiberi_I
dt.sub$SEX14	1	0.0035593	0.0035593	0.0407564	2.4218268	1.1257161	0.119	schreiberi_I
dt.sub$logSVL:dt.sub$SEX14	1	0.0023865	0.0023865	0.0273266	1.6238	0.8892665	0.193	schreiberi_I
Residuals14	21	0.0308632	0.0014697	0.3534043	NA	NA	NA	schreiberi_I
Total14	24	0.0873311	NA	NA	NA	NA	NA	schreiberi_I
dt.sub$logSVL15	1	0.0380041	0.0380041	0.3527314	18.489494	2.9721923	0.001	strigata
dt.sub$SEX15	1	0.0154158	0.0154158	0.1430805	7.4999999	2.1922971	0.014	strigata
dt.sub$logSVL:dt.sub$SEX15	1	0.0008809	0.0008809	0.0081757	0.4285552	-0.0472574	0.539	strigata
Residuals15	26	0.0534415	0.0020554	0.4960124	NA	NA	NA	strigata
Total15	29	0.1077422	NA	NA	NA	NA	NA	strigata
dt.sub$logSVL16	1	0.0875831	0.0875831	0.5452359	26.154443	3.6811801	0.001	tangitanus
dt.sub$SEX16	1	0.0031935	0.0031935	0.0198804	0.9536437	0.4142501	0.362	tangitanus
dt.sub$logSVL:dt.sub$SEX16	1	0.0028831	0.0028831	0.0179482	0.8609571	0.3575457	0.365	tangitanus
Residuals16	20	0.0669738	0.0033487	0.4169356	NA	NA	NA	tangitanus
Total16	23	0.1606334	NA	NA	NA	NA	NA	tangitanus

dt.sub$logSVL17	1	0.1196185	0.1196185	0.6604719	60.155751	4.5026393	0.001	trilineata
dt.sub$SEX17	1	0.0029359	0.0029359	0.0162105	1.4764533	0.7570678	0.24	trilineata
dt.sub$logSVL:dt.sub$SEX17	1	0.0068558	0.0068558	0.0378541	3.4477477	1.4009602	0.079	trilineata
Residuals17	26	0.0517005	0.0019885	0.2854635	NA	NA	NA	trilineata
Total17	29	0.1811106	NA	NA	NA	NA	NA	trilineata
dt.sub$logSVL18	1	0.0450953	0.0450953	0.3344236	20.326183	3.2985318	0.001	viridis
dt.sub$SEX18	1	0.0320021	0.0320021	0.2373253	14.42457	2.7193364	0.001	viridis
dt.sub$logSVL:dt.sub$SEX18	1	6.43E-05	6.43E-05	0.0004771	0.0289969	-1.1961182	0.866	viridis
Residuals18	26	0.0576832	0.0022186	0.4277741	NA	NA	NA	viridis
Total18	29	0.134845	NA	NA	NA	NA	NA	viridis

Table A1.5 ANOVA results for the main effects and interactions of variables (logSVL, SEX, and their combinations) on FLL. Df: degrees of freedom, SS: sum of squares, MS: mean squares, Rsq: coefficient of determination, F: F value, Z: Z value, and p-values of significance. The analyses are presented for several *green lizard* lineages analysed (l).

FLL	Df	SS	MS	Rsq	F	Z	Pr(>F)	l
dt.sub$logSVL	1	0.3391013	0.3391013	0.6231482	55.980174	4.3472278	0.001	adriatic
dt.sub$SEX	1	0.0515	0.0515	0.0946388	8.5018245	2.1758067	0.011	adriatic
dt.sub$logSVL:dt.sub$SEX	1	0.0081925	0.0081925	0.0150548	1.3524423	0.7412948	0.238	adriatic
Residuals	24	0.1453806	0.0060575	0.2671581	NA	NA	NA	adriatic
Total	27	0.5441743	NA	NA	NA	NA	NA	adriatic
dt.sub$logSVL1	1	0.0151685	0.0151685	0.1039856	5.9321944	1.8894912	0.024	agilis
dt.sub$SEX1	1	0.0622234	0.0622234	0.4265636	24.334706	3.3125682	0.002	agilis
dt.sub$logSVL:dt.sub$SEX1	1	0.0019979	0.0019979	0.0136962	0.7813466	0.3521043	0.395	agilis
Residuals1	26	0.0664816	0.002557	0.4557546	NA	NA	NA	agilis
Total1	29	0.1458714	NA	NA	NA	NA	NA	agilis
dt.sub$logSVL2	1	0.1990049	0.1990049	0.5556996	61.333907	4.395987	0.001	bilineata
dt.sub$SEX2	1	0.0736958	0.0736958	0.2057874	22.713254	3.2076961	0.001	bilineata
dt.sub$logSVL:dt.sub$SEX2	1	0.0010553	0.0010553	0.0029469	0.3252561	-0.1083615	0.549	bilineata
Residuals2	26	0.08436	0.0032446	0.2355661	NA	NA	NA	bilineata
Total2	29	0.358116	NA	NA	NA	NA	NA	bilineata
dt.sub$logSVL3	1	0.0756593	0.0756593	0.4849906	73.789703	4.9497771	0.001	brevicaudata
dt.sub$SEX3	1	0.0536034	0.0536034	0.3436082	52.278836	4.303247	0.001	brevicaudata
dt.sub$logSVL:dt.sub$SEX3	1	8.01E-05	8.01E-05	0.0005135	0.0781237	-0.8421866	0.786	brevicaudata
Residuals3	26	0.0266588	0.0010253	0.1708877	NA	NA	NA	brevicaudata
Total3	29	0.1560016	NA	NA	NA	NA	NA	brevicaudata
dt.sub$logSVL4	1	0.0570257	0.0570257	0.5025354	14.832641	2.7371844	0.003	diplochondrodes
dt.sub$SEX4	1	7.61E-05	7.61E-05	0.0006709	0.0198013	-1.4035876	0.9	diplochondrodes
dt.sub$logSVL:dt.sub$SEX4	1	0.0025496	0.0025496	0.0224686	0.6631746	0.2018966	0.441	diplochondrodes
Residuals4	14	0.0538245	0.0038446	0.4743252	NA	NA	NA	diplochondrodes
Total4	17	0.1134759	NA	NA	NA	NA	NA	diplochondrodes
dt.sub$logSVL5	1	0.0642749	0.0642749	0.5314486	38.919031	3.950893	0.001	israelica
dt.sub$SEX5	1	0.0247959	0.0247959	0.2050218	15.01415	2.7227422	0.002	israelica
dt.sub$logSVL:dt.sub$SEX5	1	0.002145	0.002145	0.0177353	1.2987914	0.6740226	0.262	israelica
Residuals5	18	0.029727	0.0016515	0.2457943	NA	NA	NA	israelica
Total5	21	0.1209428	NA	NA	NA	NA	NA	israelica
dt.sub$logSVL6	1	0.0313163	0.0313163	0.4637634	14.122641	2.6259221	0.002	kurdistanicus
dt.sub$SEX6	1	0.00715	0.00715	0.1058849	3.2244354	1.2887057	0.104	kurdistanicus
dt.sub$logSVL:dt.sub$SEX6	1	0.0002332	0.0002332	0.003454	0.1051813	-0.7478751	0.773	kurdistanicus
Residuals6	13	0.0288269	0.0022175	0.4268977	NA	NA	NA	kurdistanicus
Total6	16	0.0675264	NA	NA	NA	NA	NA	kurdistanicus
dt.sub$logSVL7	1	0.3261936	0.3261936	0.8513133	156.98786	6.3129157	0.001	lepidus
dt.sub$SEX7	1	0.0027118	0.0027118	0.0070773	1.3050945	0.6674704	0.273	lepidus
dt.sub$logSVL:dt.sub$SEX7	1	0.0002363	0.0002363	0.0006167	0.1137326	-0.6567302	0.731	lepidus
Residuals7	26	0.0540235	0.0020778	0.1409927	NA	NA	NA	lepidus

Total7	29	0.3831652	NA	NA	NA	NA	NA	lepidus
dt.sub$logSVL8	1	0.1339711	0.1339711	0.5567001	36.932383	4.229642	0.001	media
dt.sub$SEX8	1	0.0112381	0.0112381	0.0466986	3.0980593	1.3166744	0.097	media
dt.sub$logSVL:dt.sub$SEX8	1	0.0047563	0.0047563	0.019764	1.3111766	0.6089586	0.301	media
Residuals8	25	0.0906867	0.0036275	0.3768374	NA	NA	NA	media
Total8	28	0.2406522	NA	NA	NA	NA	NA	media
dt.sub$logSVL9	1	0.084084	0.084084	0.3936597	38.658396	3.8489308	0.001	meridionalis
dt.sub$SEX9	1	0.0702591	0.0702591	0.3289352	32.302281	3.5216726	0.001	meridionalis
dt.sub$logSVL:dt.sub$SEX9	1	0.0027012	0.0027012	0.0126463	1.2419037	0.6314495	0.292	meridionalis
Residuals9	26	0.0565513	0.0021751	0.2647588	NA	NA	NA	meridionalis
Total9	29	0.2135957	NA	NA	NA	NA	NA	meridionalis
dt.sub$logSVL10	1	0.0886761	0.0886761	0.5395738	30.538749	3.651085	0.001	nevadensis
dt.sub$SEX10	1	7.66E-05	7.66E-05	0.0004662	0.0263887	-1.2631326	0.874	nevadensis
dt.sub$logSVL:dt.sub$SEX10	1	9.52E-05	9.52E-05	0.000579	0.0327704	-1.1651363	0.865	nevadensis
Residuals10	26	0.0754968	0.0029037	0.4593809	NA	NA	NA	nevadensis
Total10	29	0.1643448	NA	NA	NA	NA	NA	nevadensis
dt.sub$logSVL11	1	0.207423	0.207423	0.6722228	55.69284	4.4630989	0.001	pater
dt.sub$SEX11	1	0.0028491	0.0028491	0.0092333	0.7649687	0.3093858	0.4	pater
dt.sub$logSVL:dt.sub$SEX11	1	0.0014562	0.0014562	0.0047191	0.3909752	0.001238	0.51	pater
Residuals11	26	0.0968347	0.0037244	0.3138248	NA	NA	NA	pater
Total11	29	0.3085629	NA	NA	NA	NA	NA	pater
dt.sub$logSVL12	1	0.132455	0.132455	0.7777464	78.027451	4.5806639	0.001	princeps
dt.sub$SEX12	1	0.0066915	0.0066915	0.039291	3.9418754	1.3820745	0.085	princeps
dt.sub$logSVL:dt.sub$SEX12	1	0.0006039	0.0006039	0.0035457	0.3557249	-0.1499226	0.58	princeps
Residuals12	18	0.0305558	0.0016975	0.1794168	NA	NA	NA	princeps
Total12	21	0.1703061	NA	NA	NA	NA	NA	princeps
dt.sub$logSVL13	1	0.0269535	0.0269535	0.3832804	26.838606	3.3939657	0.001	schreiberi
dt.sub$SEX13	1	0.0141658	0.0141658	0.2014376	14.105348	2.782745	0.002	schreiberi
dt.sub$logSVL:dt.sub$SEX13	1	0.0030927	0.0030927	0.0439777	3.0794672	1.3149759	0.087	schreiberi
Residuals13	26	0.0261113	0.0010043	0.3713043	NA	NA	NA	schreiberi
Total13	29	0.0703233	NA	NA	NA	NA	NA	schreiberi
dt.sub$logSVL14	1	0.0468097	0.0468097	0.4246552	23.162601	3.2035792	0.001	schreiberi_I
dt.sub$SEX14	1	0.0171005	0.0171005	0.1551348	8.4617496	2.1879465	0.008	schreiberi_I
dt.sub$logSVL:dt.sub$SEX14	1	0.0038804	0.0038804	0.0352031	1.920134	0.9693701	0.181	schreiberi_I
Residuals14	21	0.0424392	0.0020209	0.3850068	NA	NA	NA	schreiberi_I
Total14	24	0.1102298	NA	NA	NA	NA	NA	schreiberi_I
dt.sub$logSVL15	1	0.0242815	0.0242815	0.2154588	14.288769	2.7835619	0.001	strigata
dt.sub$SEX15	1	0.0435586	0.0435586	0.3865105	25.632561	3.4881876	0.001	strigata
dt.sub$logSVL:dt.sub$SEX15	1	0.0006739	0.0006739	0.0059796	0.3965544	-0.0133768	0.516	strigata
Residuals15	26	0.044183	0.0016993	0.3920511	NA	NA	NA	strigata
Total15	29	0.112697	NA	NA	NA	NA	NA	strigata
dt.sub$logSVL16	1	0.0797081	0.0797081	0.4055404	18.343431	3.298343	0.001	tangitanus
dt.sub$SEX16	1	0.0180443	0.0180443	0.0918059	4.1525727	1.5420341	0.053	tangitanus
dt.sub$logSVL:dt.sub$SEX16	1	0.0118891	0.0118891	0.0604894	2.7360622	1.2149737	0.104	tangitanus
Residuals16	20	0.0869064	0.0043453	0.4421642	NA	NA	NA	tangitanus
Total16	23	0.1965479	NA	NA	NA	NA	NA	tangitanus

dt.sub$logSVL17	1	0.1335778	0.1335778	0.694788	69.675682	4.9032453	0.001	trilineata
dt.sub$SEX17	1	0.0087028	0.0087028	0.0452663	4.5394542	1.6237052	0.05	trilineata
dt.sub$logSVL:dt.sub$SEX17	1	0.0001308	0.0001308	0.0006805	0.0682393	-0.9085515	0.818	trilineata
Residuals17	26	0.0498456	0.0019171	0.2592653	NA	NA	NA	trilineata
Total17	29	0.192257	NA	NA	NA	NA	NA	trilineata
dt.sub$logSVL18	1	0.0616498	0.0616498	0.3174526	14.303656	2.8061368	0.003	viridis
dt.sub$SEX18	1	0.0199836	0.0199836	0.1029016	4.6364989	1.6357658	0.044	viridis
dt.sub$logSVL:dt.sub$SEX18	1	0.0005063	0.0005063	0.0026068	0.1174576	-0.623555	0.73	viridis
Residuals18	26	0.1120619	0.0043101	0.577039	NA	NA	NA	viridis
Total18	29	0.1942015	NA	NA	NA	NA	NA	viridis

Table A1.6 Statistics of tests for Rensch's Rule with Sexual Dimorphism Ratio (SD Ratio) approach applied to a subsample of 10 individuals per sex per lineage. β1: estimated allometric slope, SE: standard error of the slope estimate, t- and p-value: corresponding t- and p-values of significance testing for slope estimates (β1 ≠ 0). Significant patterns (using a threshold of α = 0.05) are highlighted with asterisks.

Trait	β_1	SE	t-value	p value
SVL	0.32	0.042	7.33	**<0.001****
TRL	-0.101	0.038	-2.659	**0.05***
HS	0.17	0.048	3.555	**<0.05***
FLL	-0.165	0.038	-4.336	**<0.001****
HLL	-18.5	0.043	-4.314	**<0.001****

Table A1.7 ANOVA table for the linear model used to test for the effect of intersexual differences in static allometric intercept and slope on the trait Rensch's Rule pattern with the SD ratio approach applied to a subsample of 10 individuals per sex per lineage. β1: estimated allometric slope, β0: estimated allometric intercept. Interaction factors of the model are depicted with an asterisk. F-value and p-values of significance. Significant patterns (using a threshold of α = 0.05) are highlighted with bold asterisks.

SD ratio	TRL		HS		FLL		HLL	
Source of variation	F-value	p-value	F-value	p-value	F-value	p-value	F-value	p-value
Species size (SVL)	0.511	0.466	27.888	**<0.001*****	56.868	**<0.01***	28.742	**<0.001*****
β_1	0.032	0.64	2.399	0.163	10.82	**<0.01***	1.952	0.183
β_0	79.408	**<0.01****	0.316	0.589	21.995	**<0.01***	5.308	**<0.05***
sp.sz* β_1	29.384	**<0.01****	4.114	**<0.001*****	18.14	**<0.01***	22.652	**<0.001*****
sp.sz* β_0	17.151	**<0.01****	-2.063	0.977	1.398	0.263	1.032	0.345
β_0* β_1	5.86	**<0.05***	0.623	0.408	3.642	**0.088.**	0.18	0.687
sp.sz* β_0* β_1	12.817	**<0.01****	-0.77	0.759	0.048	0.828	0.003	0.955

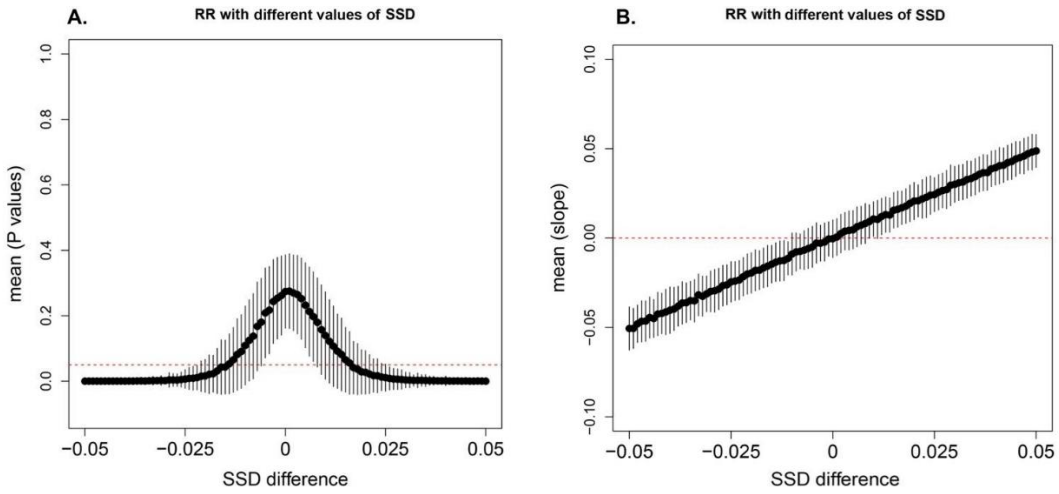

Figure A1.1 Simulations of RR in body size tested with different values of SSD. A) mean p-values of RR tested. B) mean slope values of the PGLS used to test RR

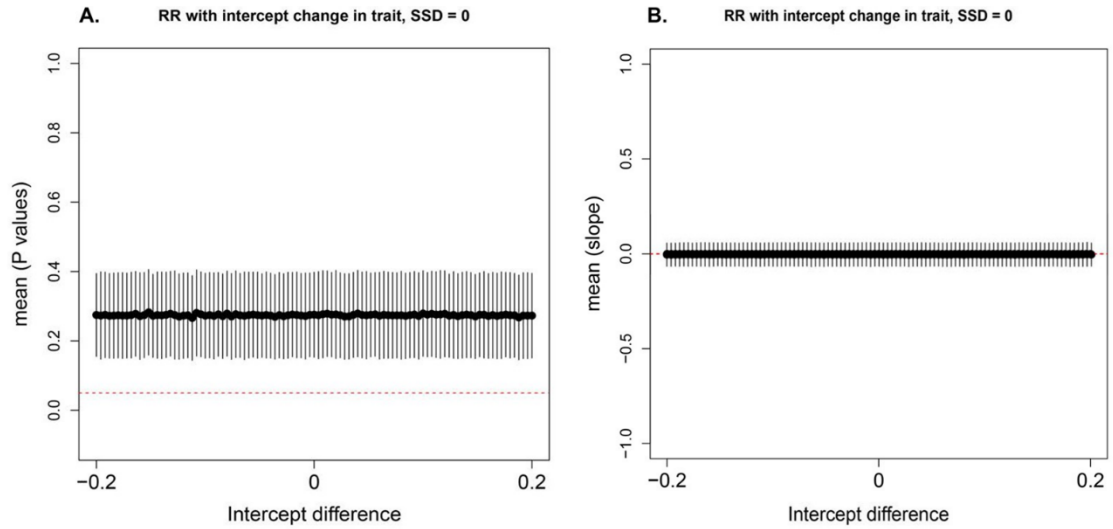

Figure A1.2 Simulations of RR in trait tested with different values of static intercept and SSD = 0. A) mean p-values of RR test. B) mean slope values of the PGLS used to test RR.

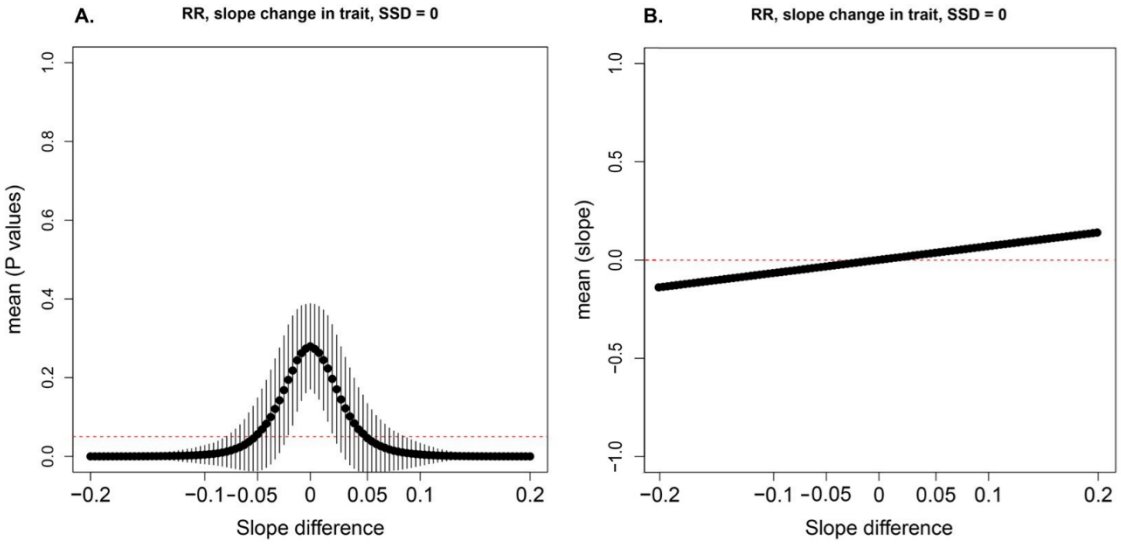

Figure A1.3 Simulators of RR in trait tested with different values of static slope and SSD= o. A) mean p-values of RR test. B) mean slope values of the PGLS used to test RR.

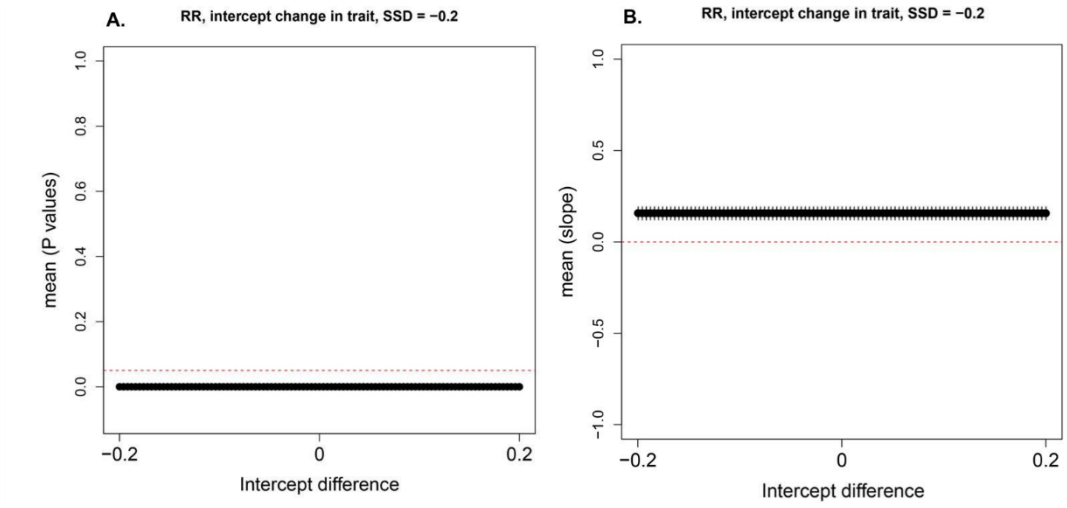

Figure A1.4 Simulations of RR in trait tested with different values of static intercept and SSD= -0.2. A) mean p-values of RR test. B) mean slope values of the PGLS used to test RR.

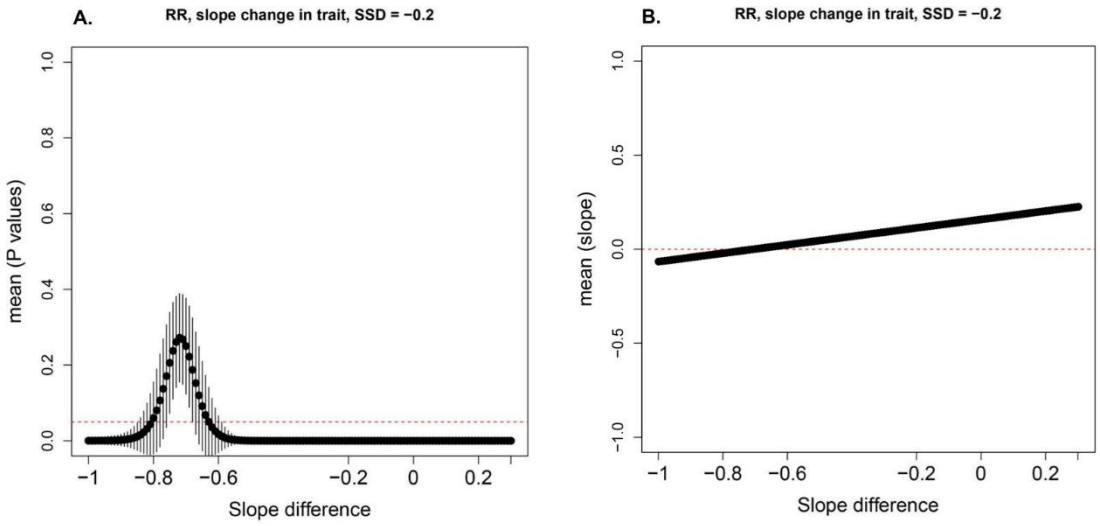

Figure A1.5 Simulations of RR in trait tested with different values of static slope and SSD =-0.2. A) mean p-values. B) mean slope values of the PGLS used to test RR.

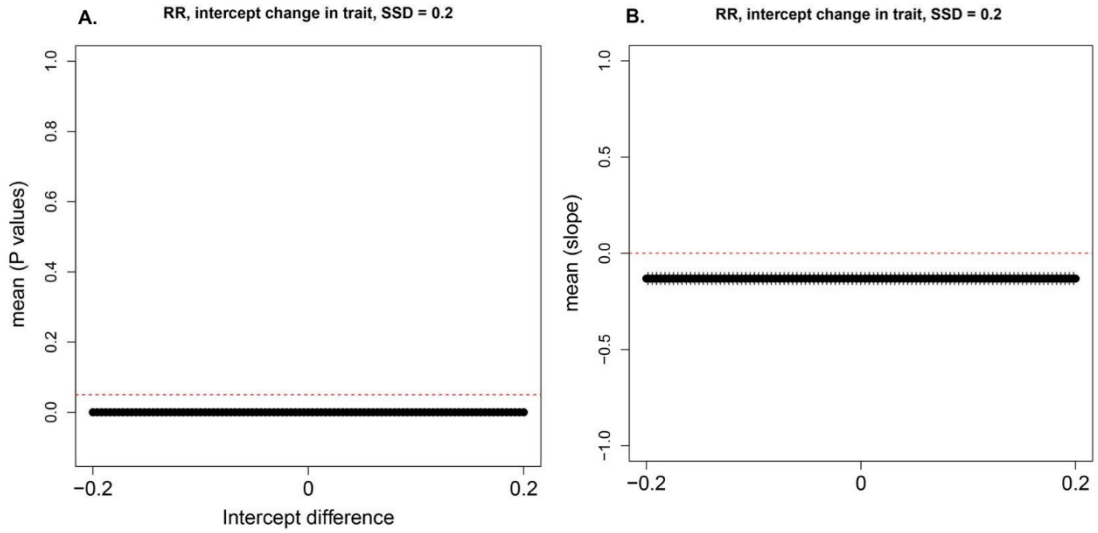

Figure A1.6 Simulations of RR in trait tested with different values of static intercept and SSD= 0.2. A) mean p-values of RR test. B) slope values of the PGLS used to test RR.

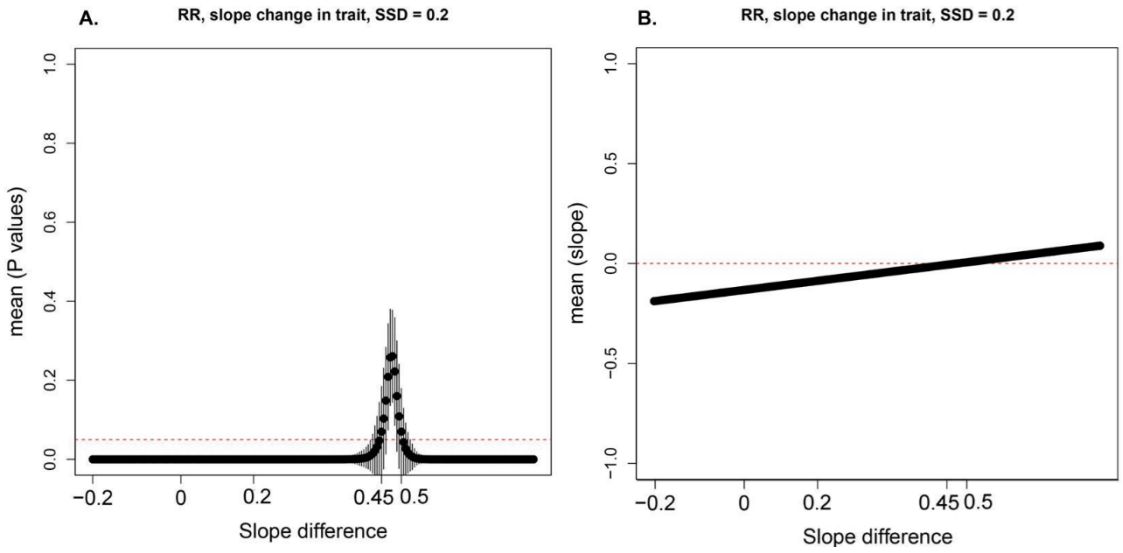

Figure A1.7 Simulations of RR in trait tested with different values of static slope and SSD= 0.2. A) mean p-values of RR test. B) mean slope values of the PGLS used to test RR.

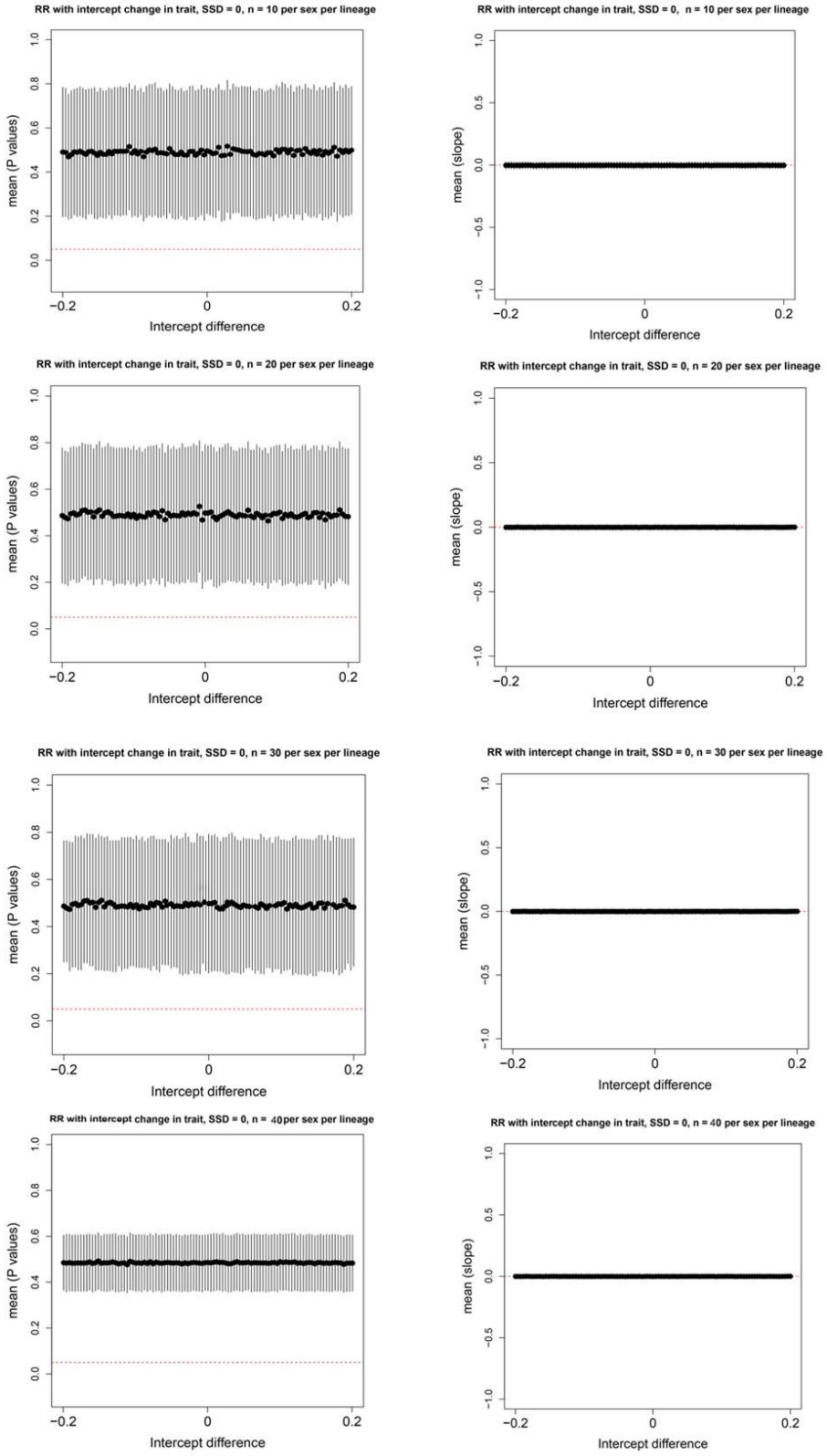

Figure A1.8 Subsampling simulations to test RR in smaller sample sizes. The subsamples come from original simulations in which we considered 50 individuals per sex, per lineage. Left column, mean p-values of the RR test. Right column, mean slope values of the PGLS.

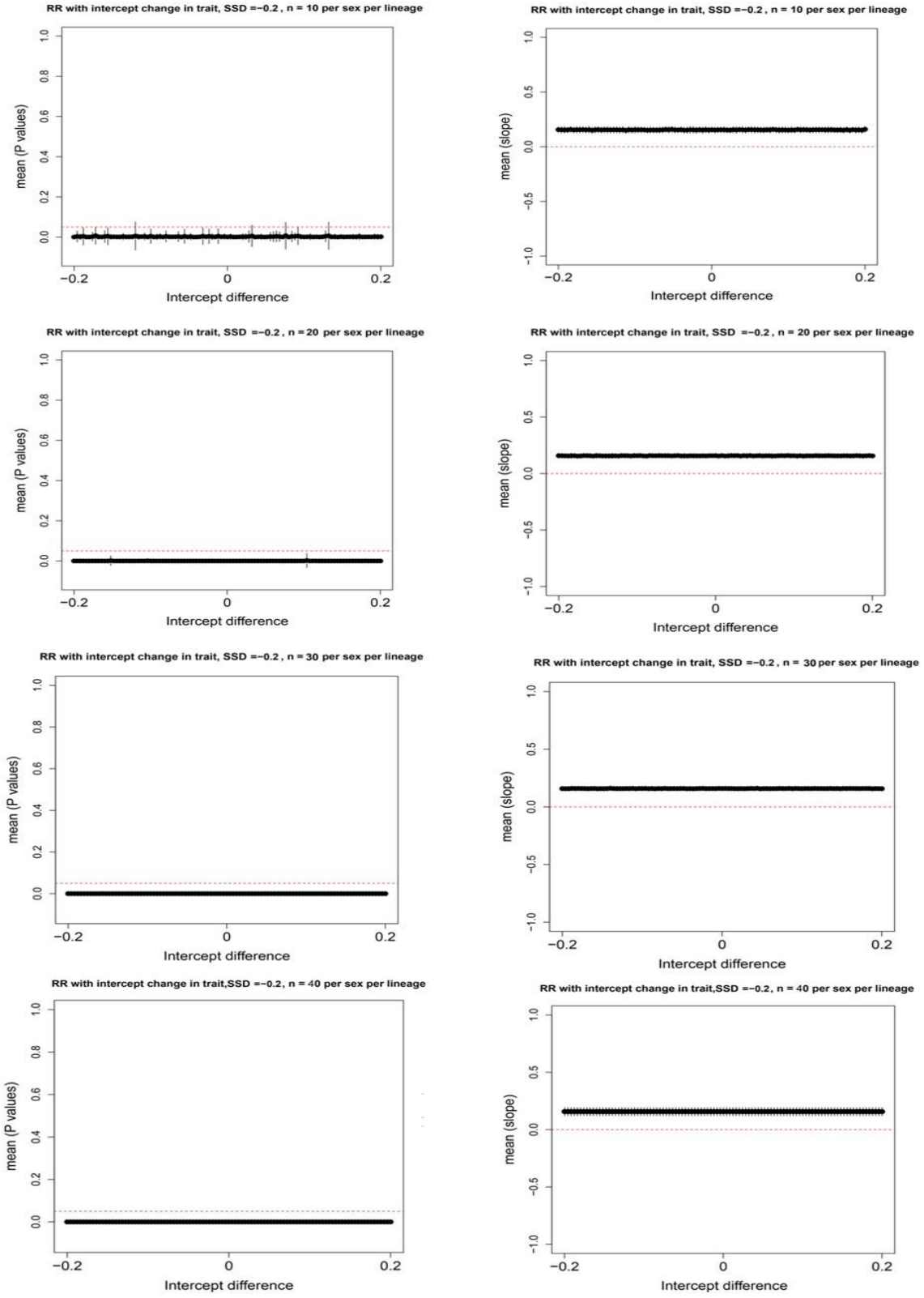

Figure A1.9 Subsampling simulations to test RR in smaller sample sizes. The subsamples come from original simulations in which we considered 50 individuals per sex, per lineage. Left column, mean p-values of the RR test. Right column, mean slope values of the PGLS.

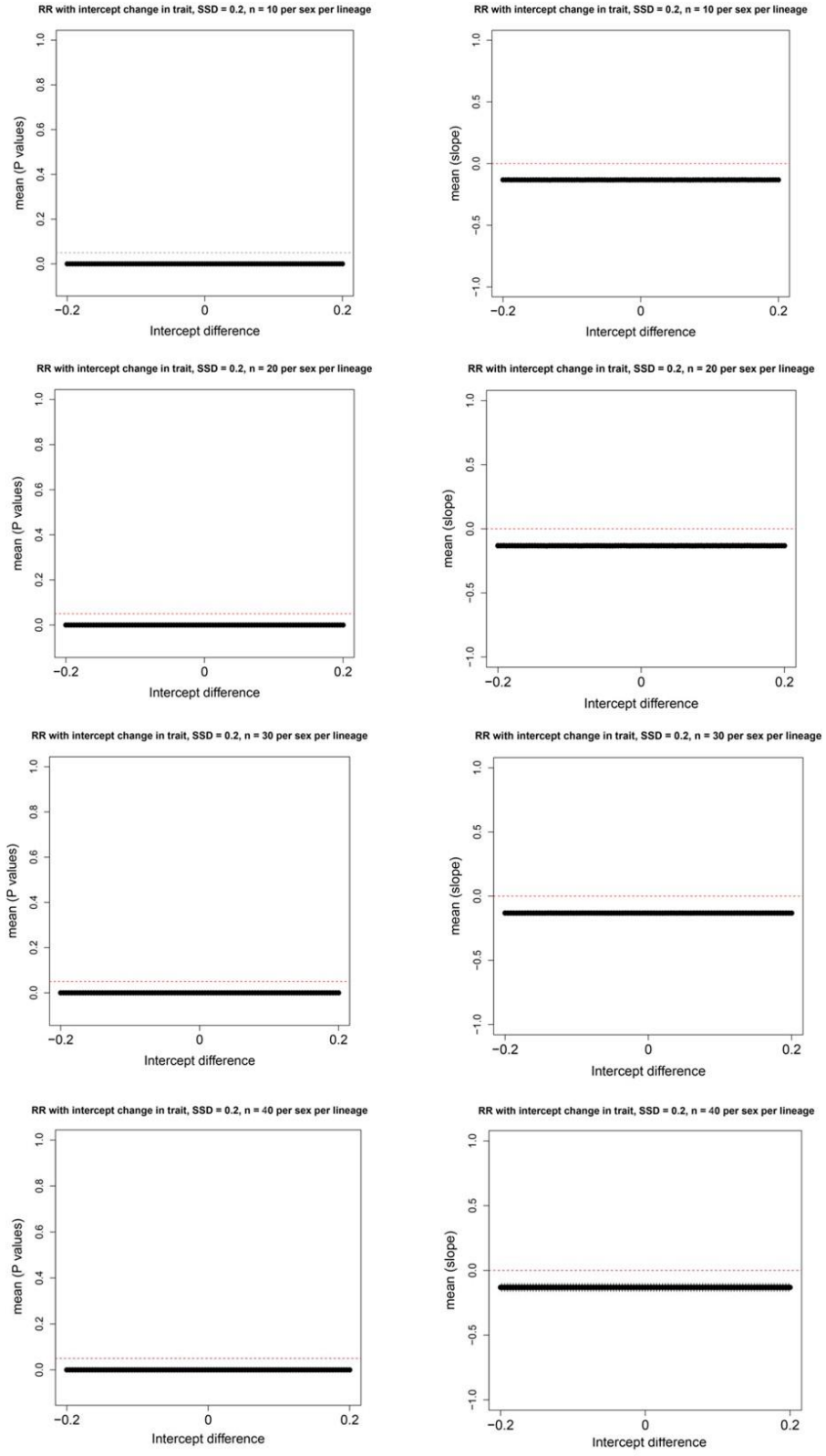

Figure A1.10 Subsampling simulations to test RR in smaller sample sizes. The subsamples come from original simulations in which we considered 50 individuals per sex, per lineage. Left column, mean p-values of the RR test. Right column, mean slope values of the PGLS.

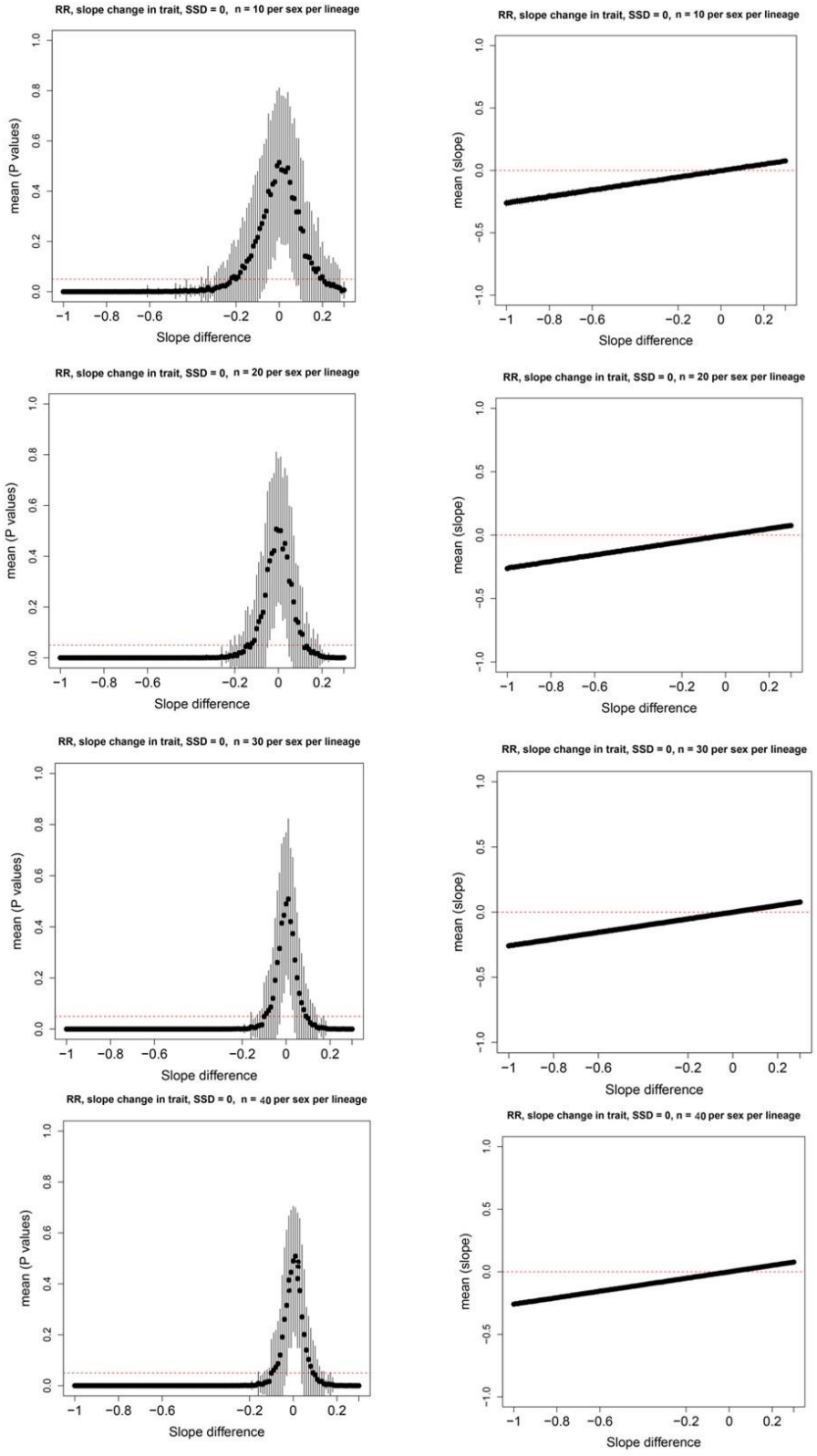

Figure A1.11 Subsampling simulations to test RR in smaller sample sizes. The subsamples come from original simulations in which we considered 50 individuals per sex, per lineage. Left column, mean p-values of the RR test. Right column, mean slope values of the PGLS.

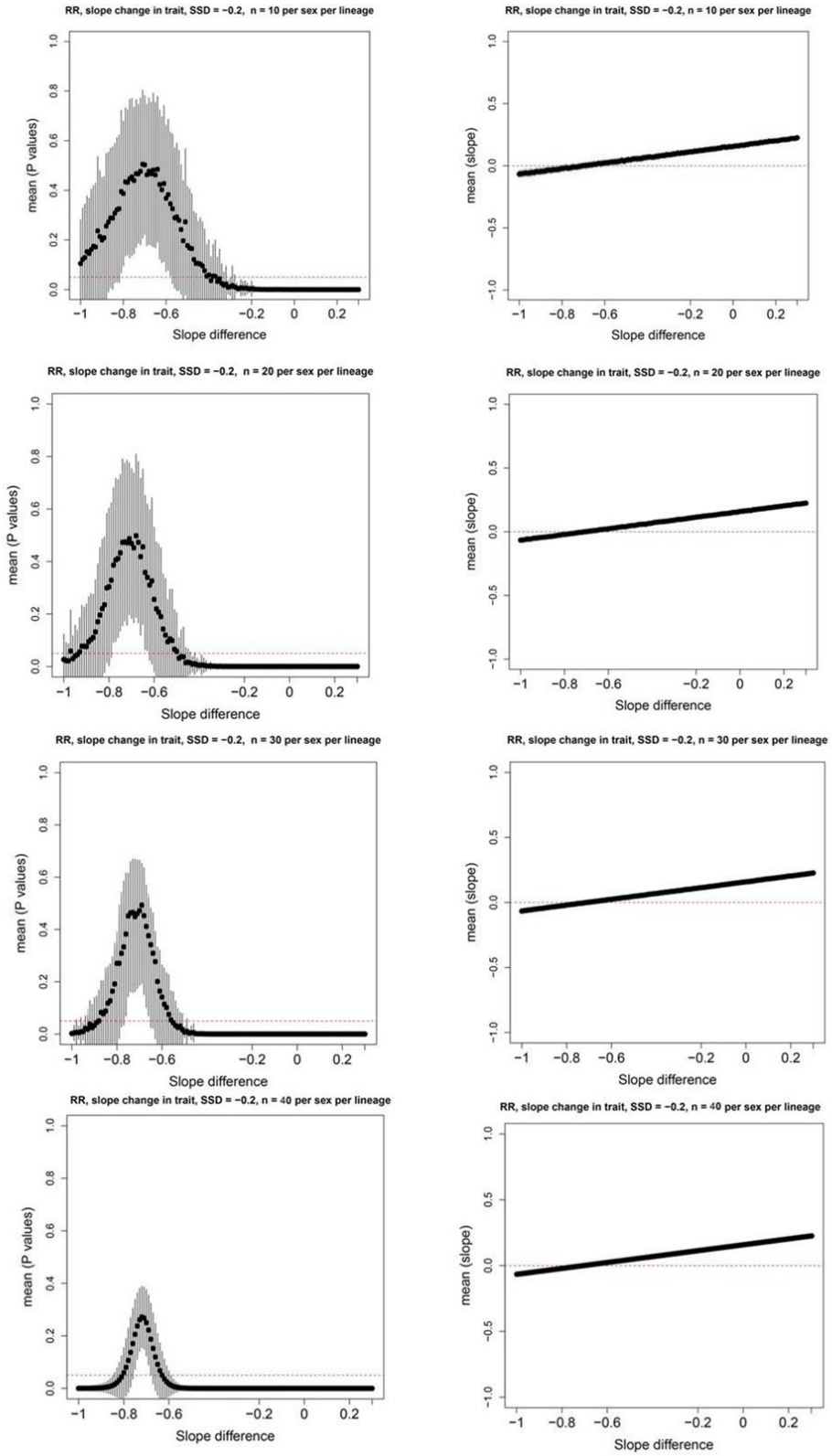

Figure A1.12 Subsampling simulations to test RR in smaller sample sizes. The subsamples come from original simulations in which we considered 50 individuals per sex, per lineage. Left column, mean p-values of the RR test. Right column, mean slope values of the PGLS.

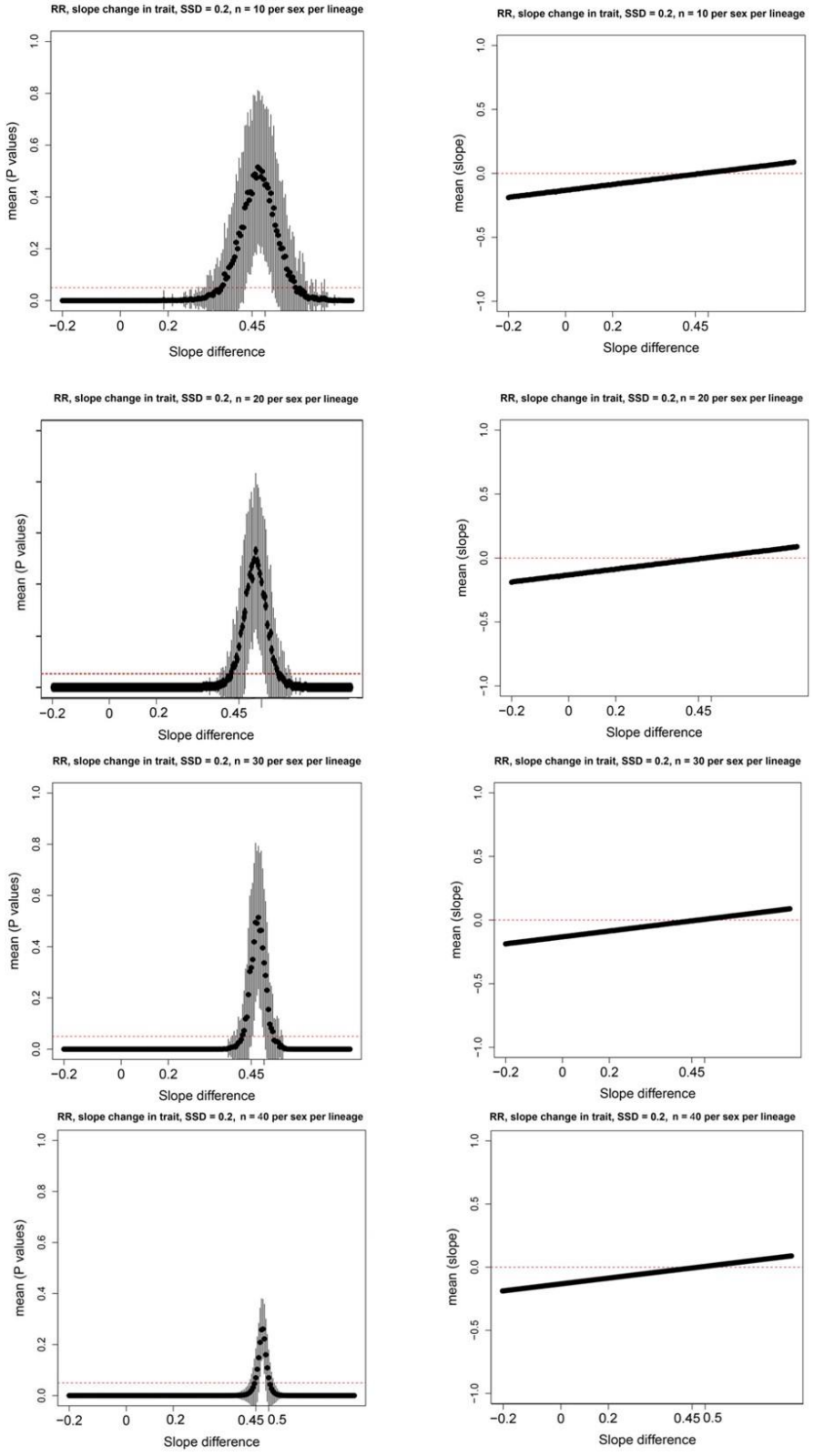

Figure A1.13 Subsampling simulations to test RR in smaller sample sizes. The subsamples come from original simulations in which we considered 50 individuals per sex, per lineage. Left column, mean p-values of the RR test. Right column, mean slope values of the PGLS.

Appendix B

Supplementary Material Chapter 4

Supplementary information for Chapter 4

Is it all about size? Dismantling the integrated phenotype to understand species coexistence and niche segregation

B1. Detailed methodology for experimental procedures and data analysis

Locomotor performance

Before locomotion experiments, individuals were placed in separate thermal chambers at 32°C for *T. lepidus* and 33°C for *L. schreiberi*, based on previously published information of each species' selected temperature (Barroso et al., 2016; Ferreira et al., 2016). Before and in-between all performance trials, lizards were placed again in the thermal chambers for at least 20 minutes.

We examined locomotor performance in two different ecologically relevant settings (Figure 4.1A, B): in a straight, 2.5 meters long and 0.2 m wide corridor, with cork substrate (Vanhooydonck and Van Damme, 2003) to measure maximum sprint speed (MaxSPR); and in a double-L racetrack (i.e. a straight surface of 0.8 m, an angle of 90°, a straight surface of 1 m, a second angle of 90° and a final straight surface of 0.8 m) and cork substrate to quantify maneuverability (MNV), based on Vasilopoulou-Kampitsi (2020). We run each individual three time in each racetrack. To motivate lizards to run, we chased them during the trials in both racetracks. We excluded from analyses all the trials in which the lizards completely stopped or turned to face the researchers.

We filmed all trials with a digital camera (Olympus TG-5) at a filming speed of 30 fps. The trajectory of the lizards in each trial was digitized using Tracker video analyzer software (Open-Source Physics, OSP). We followed standard procedures to calculate MaxSPR (Gomes et al., 2018; Kaliontzopoulou et al., 2013; Massetti et al., 2017) and we calculated the maximum instantaneous speed (evaluated between consecutive frames, Gomes et al., 2018) across all trial repetitions. So, the maximum speed recorded throughout the entire trial within two consecutive frames. The highest speed observed across the three trials was used to estimate the maximum locomotor performance capacity of each animal. For MNV we digitized the trajectory, speed, distance, time, and angles of the turns with the software for 2D motion analysis Kinovea (Puig-Diví et al., 2019). For the trials on the double-L racetrack we focused on the angles of the turns to quantify turning capacity. So, we considered the following variables: maximum trunk angle bending (TA), maximum head angle bending (HA), maximum speed in the double-L racetrack (Max_L), minimum time to complete double-L racetrack (min_T). We counted

the numbers of successful turns, i.e., trials where the lizards turned without colliding against the walls, or where the contact with the walls did not prevent the completion of the turn. We also counted the number of unsuccessful turns, in which the lizards crashed into the walls or where they did not complete the turns. We considered the following variables to describe MNV: i) success of the turn, considering as unsuccessful any turns in which the lizard collided or climbed the walls, ii) maximal speed during the path and turn; iii) maximum bending angle of the trunk and head during a turn; and v) maneuvering strategy (MS). MS were modified from the categories proposed by Vasilopoulou (2020): MS0 trials in which lizards crashed against the walls and therefore, unsuccessful turns; MS1 trials in which lizards completed the turns stopping before the turns; MS2 trials in which the lizards completed the turn without stopping. All data on locomotor performance were log-transformed prior to analyses.

Bite force

We measured bite force (BF) with an isometric Kistler force transducer (type 9203, Kistler, Winterthur, Switzerland) set on a vertical holder and attached to a Kistler charge amplifier (type 5058A). We deliberately provoked the lizards to bite a pair of thin metal plates tied to the force transducer (Herrel et al., 2001). We put two marks on the edge of the plates to delimit where the lizards should bite to ensure an equal distance and thus standardize the point of effort of the bite force. We tested each individual five times to ensure that we quantified the maximal bite force of each lizard. We retained the maximum bite force per lizard and log-transformed the data before statistical analyses.

Preferred body temperatures

Lizards were kept in individual terraria with water *ad libitum* for 48 hours before preferred temperature experiments. Since digestion and selected temperatures are related (Jobling 1997; Stevenson et al., 1985), all individuals were fasted during this period. To acclimate to experimental arenas (1 m long, 0.3 m wide and 0.4 m high), lizards were individually released into experimental terraria with a sand substrate, but without creating the thermal gradient, 24 hours prior to experiments. To estimate preferred temperatures, we exposed lizards to a thermal gradient between 20 and 50 °C created with a 150-W infrared bulb fixed at 25 cm above one end of the open terrarium (Ferreira et al., 2016). We conducted the experiment in a temperature-controlled room with temperature at 18 °C in order to have temperature gradients within the terraria. We conducted all experiments between 9 h and 17:30 h, and we measured body temperatures every half hour, resulting in 19 temperature measurements per individual.

All individuals had water supply along the whole thermal gradient (Figure 4.1C) to avoid hydroregulation from biasing thermoregulation results. To measure body temperatures, we used a FLIR T335 thermal camera (sensitivity: < 0.05 °C; accuracy: ± 2%; IR image resolution: 320×240 pixels; Flir Systems Inc., Wilsonville, Oregon, USA) held at a distance of 10–20 cm from the lizard, depending on its size. This way, we kept images of approximately the same resolution. We recorded temperatures located at the dorsum above the cloaca and from the lizards´ eye, dorsum temperature was used to calculate effective proportion of surface area that is wet (see below), and eye temperatures were used to calculate preferred temperatures (T_{pref} and T_{pref} V). We analyzed the IR photos with the software FLIR Tools 2.1 (Copyright 2014 FLIR Systems, Inc; http://www.flir.com) and setting lizard skin emissivity to 0.96 (Barroso et al., 2016).

Water loss

The experiment was performed at a room temperature of 25 °C. We used a three-channel, open-air circulation system to measure water loss (Figure 4.1D). Air from the room was pumped into the system, subsequently passing through three chambers filled with 2 kg of silica gel to dry the air to a range between 3-8% of relative humidity (RH). Then, the air flow was split into three channels with two chambers each: the first, or animal, chamber contained the lizard and the second, or measurement, chamber contained a data logger to record temperature and humidity HOBO U23 Pro V2. The 'animal chamber' of one of the channels was left empty during each trial as control (Figure 4.1D). The system was connected to a flowmeter to keep the air flow stable between 0.8 and 1 $Lmin^{-1}$. Experiments lasted for 2.5 hours. Once the data were extracted from data loggers, we obtained the minimum RH values from the five most stable periods of data recordings for further analysis.

We evaluated water loss rates by estimating two variables, evaporative water loss (EWL) and effective proportion of surface area that is wet (p_wet), which is a metric that refers to the percentage of a surface that is in contact with moisture at a given time and is important for temperature regulation processes (Kearney and Porter, 2009; Kearney et al., 2018). In order to calculate EWL of each lizard, we first quantified the saturation vapor density (vd), which is the maximum water vapor density at a specific temperature. For this, we used the values extracted from water loss experiments detailed above, and we then calculated the saturation vapor density with the WETAIR function of the NicheMapR package (Kearney and Porter, 2017). We calculated the saturation vapor water density for control chambers and for chambers containing animals, and then water vapor density by multiplying the values of vd by the relative humidity corresponding to

each chamber. Finally, to obtain the total evaporative water loss (EWL), we subtracted the control chambers' vapor water density values from the animal chambers' water density values. We then computed the total EWL per individual and finally mass-specific water loss, calculated as the residual values of EWL on weight (res.EW). We then extracted p_wet from our experimental water loss data. For this we used the get_p_wet function from the package NicheMapR (Kearney and Porter, 2017, Kearney et al., 2018). To calculate p_wet we included the observed total evaporative water loss from the experiments, lizard weight, lizard body and skin temperatures, environmental temperature, relative humidity, and flowmeter flow rate values as indicated on the NicheMapR package.

References

Barroso, F. M., Carretero, M. A., Silva, F., and Sannolo, M. (2016). Assessing the reliability of thermography to infer internal body temperatures of lizards. *Journal of Thermal Biology*, *62*, 90–96. https://doi.org/10.1016/j.jtherbio.2016.10.004

Ferreira, C. C., Santos, X., and Carretero, M. A. (2016). Does ecophysiology mediate reptile responses to fire regimes? Evidence from Iberian lizards. *PeerJ*, *4*, e2107. https://doi.org/doi:10.7717/peerj.2107

Gomes, V., Carretero, M. A., and Kaliontzopoulou, A. (2018). Run for your life, but bite for your rights? How interactions between natural and sexual selection shape functional morphology across habitats. *The Science of Nature*, *105*, 1–12. https://doi.org/10.1007/s00114-017-1537-6

Herrel, A., Damme, R. V., Vanhooydonck, B., and Vree, F. D. (2001). The implications of bite performance for diet in two species of lacertid lizards. *Canadian Journal of Zoology*, *79*(4), 662–670. https://doi.org/10.1139/z01-031

Jobling, M. (1997). Temperature and growth: modulation of growth rate via temperature. In Global warming: implication for freshwater and marine fish. Society for Experimental Biology, Seminar Series, 61, 225–253.

Kaliontzopoulou, A., Bandeira, V., and Carretero, M. A. (2013). Sexual dimorphism in locomotor performance and its relation to morphology in wall lizards (*Podarcis bocagei*). *Journal of Zoology*, *289*(4), 294–302. https://doi.org/10.1111/jzo.12006

Kearney, M. R., Munns, S. L., Moore, D., Malishev, M., and Bull, C. M. (2018). Field tests of a general ectotherm niche model show how water can limit lizard activity and distribution. *Ecological Monographs*, *88*(4), 672–693. https://doi.org/10.1002/ecm.1326

Kearney, M., and Porter, W. (2009). Mechanistic niche modelling: combining physiological and spatial data to predict species' ranges. *Ecology letters*, *12*(4), 334–350. https://doi.org/10.1111/j.1461-0248.2008.01277.x

Kearney, M. R., and Porter, W. P. (2017). NicheMapR–an R package for biophysical modelling: the microclimate model. *Ecography*, *40*(5), 664–674. https://doi.org/10.1111/ecog.04680

Massetti, F., Gomes, V., Perera, A. N. A., Rato, C., and Kaliontzopoulou, A. (2017). Morphological and functional implications of sexual size dimorphism in the

Moorish gecko, Tarentola mauritanica. *Biological Journal of the Linnean Society*, 122(1), 197–209. https://doi.org/10.1093/biolinnean/blx060

Puig-Diví, A., Escalona-Marfil, C., Padullés-Riu, J. M., Busquets, A., Padullés-Chando, X., and Marcos-Ruiz, D. (2019). Validity and reliability of the Kinovea program in obtaining angles and distances using coordinates in 4 perspectives. *PloS one*, *14*(6), e0216448. https://doi.org/doi:10.1371/journal.pone.0216448

Stevenson, R. D., Peterson, C. R., and Tsuji, J. S. (1985). The thermal dependence of locomotion, tongue flicking, digestion, and oxygen consumption in the wandering garter snake. *Physiological Zoology*, *58*(1), 46–57.

Vanhooydonck, B., and Van Damme, R. (2003). Relationships between locomotor performance, microhabitat use and antipredator behaviour in lacertid lizards. *Functional Ecology*, 160–169.

Vasilopoulou-Kampitsi, M. (2020). Manoeuvrability and the anotomy of the inner ear in lacertid lizards. An ecological approach. PhD thesis University of Antwerp.

List of Supplementary Tables

Table B2.1 Results of model selection based on Akaike Information Criterion (AIC) for correcting traits with body size or body weight. Numbers in bold represent values of best fit models (with a difference between the models of at least 4 units from AIC) or equivalent ones. The complete definition of variable abbreviations is shown in methodology section. The abbreviations of the variables are as follows: head size (HS), trunk length (TRL), fore limb length (FLL), hind limb length (HLL), bite force (BF), maximum sprint speed (MaxSPR), maximum trunk angle bending (TA), maximum head angle bending (HA), and minimum time to complete double-L racetrack (min_T), preferred temperature (T_{pref}), preferred temperature variance ($T_{pref}V$), evaporative water loss (EWL), and effective proportion of surface area that is wet (p_wet).

Table B2.2 Results of ANCOVAs performed on morphological traits to test for differences between the two species (Sp) of green lizards (*Timon lepidus* and *Lacerta shreiberi*), considering body size (log(SVL)) as covariate and species as factor. Df: degrees of freedom, SS: Sums of Squares, Rsq: R-squared. The abbreviations of the variables are as follows: snout to vent length (SVL), trunk length (TRL), head size (HS), fore limb length (FLL), and hind limb length (HLL).

Table B2.3 Results of ANCOVAs performed on maximum sprint speed (MaxSPR) and on traits associated with maneuverability to test for differences between two species (Sp) of green lizards (*T. lepidus* and *L. shreiberi*), considering body size (log(SVL)), and size corrected morphological variables. Abbreviations of the variables are as follows: size corrected trunk length (res.TRL), size corrected fore limb length (res.FLL), size corrected hind limb length (res.HLL), maximum trunk angle bending (TA), maximum head angle bending (HA), maximum speed in the double-L racetrack (Max_L), and minimum time to complete double-L racetrack (min_T). Df: degrees of freedom, SS: Sums of Squares, MS: Mean squares, Rsq: R-squared.

Table B2.4 Results of GLMs models performed on performance traits associated with maneuverability to test for differences between the two species (Sp) of green lizards (*Timon lepidus* and *Lacerta shreiberi*), considering body size (log(SVL)), stops before turning (NSBT), maximum speed in the first track (MaxS_I), and maximum speed in the second track (MaxS_II). CODE represents the individual identification of lizards. Df = 1.

Table B2.5 Eigenvalues and variance retained by each principal component in the dataset including all raw variables.

Table B2.6 Correlations scores of the four principal components of the dataset including all raw variables. Correlations >0·5 are highlighted in bold. The abbreviations of the variables are as follows: head size (HS), trunk length (TRL), fore limb length (FLL), hind limb length (HLL), bite force (BF), maximum sprint speed (MaxSPR), maximum trunk angle bending (TA), maximum head angle bending (HA), maximum speed in the double-L racetrack (Max_L), preferred temperature (Tpref), preferred temperature variance (Tpref V), evaporative water loss (EWL), and effective proportion of surface area that is wet (p_wet).

Table B2.7 Eigenvalues and variance retained by each principal component in the dataset including all size-corrected variables.

Table B2.8 Correlations scores of the four principal components of the dataset including all size-corrected variables. Correlations >0·5 are highlighted in bold. The abbreviations of the variables are as follows: size corrected trunk length (res.TRL), size corrected head size (res.HS), size corrected fore limb length (res.FLL), size corrected hind limb length (res.HLL), size corrected bite force (res.BF), size corrected maximum speed in the double-L racetrack (res.max_L), size corrected maximum sprint speed (res.maxSPR), maximum trunk angle bending corrected by size (res.TA), head angle bending corrected by size (res.HA), , preferred temperature corrected by size (res. Tpref), preferred temperature variance corrected by size (res.Tpref V), size corrected evaporative water loss (res.EWL), and effective proportion of surface area that is wet corrected by size (res.p_wet).

Table B2.9 Eigenvalues and variance retained by each principal component in the three different raw variable datasets.

Table B2.10 Correlations scores of the four principal components of the three different raw variable datasets. Correlations >0·5 are highlighted in bold. The abbreviations of the variables are as follows: head size (HS), trunk length (TRL), fore limb length (FLL), hind limb length (HLL), bite force (BF), maximum sprint speed (MaxSPR), maximum trunk angle bending (TA), maximum head angle bending (HA), maximum speed in the double-L racetrack (Max_L), preferred temperature (Tpref), preferred temperature variance (Tpref V), evaporative water loss (EWL), and effective proportion of surface area that is wet (p_wet).

Table B2.11 Eigenvalues and variance retained by each principal component in the three different size-corrected variable datasets.

Table B2.12 Correlations scores of the four principal components of the three different size-corrected variable datasets. Correlations >0·5 are highlighted in bold. The abbreviations of the variables are as follows: size corrected trunk length (res.TRL), size corrected head size (res.HS), size corrected fore limb length (res.FLL), size corrected hind limb length (res.HLL), size corrected bite force (res.BF), size corrected maximum speed in the double-L racetrack (res.max_L), size corrected maximum sprint speed (res.maxSPR), maximum trunk angle bending corrected by size (res.TA), head angle bending corrected by size (res.HA), , preferred temperature corrected by size (res. Tpref), preferred temperature variance corrected by size (res.Tpref V), size corrected evaporative water loss (res.EWL), and effective proportion of surface area that is wet corrected by size (res.p_wet).

Table B2.13 Correlations of flexible discriminant analysis (FDA) scores with phenotypic variables in the different datasets used to discriminate the two species of green lizards (*Timon lepidus* and *Lacerta schreiberi*). Variable abbreviations are shown in the methodology. The first two columns represent FDAs carried out with all phenotypic variables together (before and after size correction), while the last two were performed within each variable subset. The abbreviations of the variables are as follows: head size (HS), trunk length (TRL), fore limb length (FLL), hind limb length (HLL), bite force (BF), maximum sprint speed (MaxSPR), maximum trunk angle bending (TA), maximum head angle bending (HA), maximum speed in the double-L racetrack (Max_L), preferred temperature (Tpref), preferred temperature variance (Tpref V), evaporative water loss (EWL), and effective proportion of surface area that is wet (p_wet). size corrected trunk length (res.TRL), size corrected head size (res.HS), size corrected fore limb length (res.FLL), size corrected hind limb length (res.HLL), size corrected bite force (res.BF), size corrected maximum speed in the double-L racetrack (res.max_L), size corrected maximum sprint speed (res.maxSPR), maximum trunk angle bending corrected by size (res.TA), head angle bending corrected by size (res.HA), , preferred temperature corrected by size (res. Tpref), preferred temperature variance corrected by size (res.Tpref V), size corrected evaporative water loss (res.EWL), and effective proportion of surface area that is wet corrected by size (res.p_wet).

Table B2.1: Results of model selection based on Akaike Information Criterion (AIC) for correcting traits with body size or body weight. Numbers in bold represent values of best fit models (with a difference between the models of at least 4 units from AIC) or equivalent ones. The complete definition of variable abbreviations is shown in methodology section. The abbreviations of the variables are as follows: head size (HS), trunk length (TRL), fore limb length (FLL), hind limb length (HLL), bite force (BF), maximum sprint speed (MaxSPR), maximum trunk angle bending (TA), maximum head angle bending (HA), and minimum time to complete double-L racetrack (min_T), preferred temperature (T_{pref}), preferred temperature variance ($T_{pref}V$), evaporative water loss (EWL), and effective proportion of surface area that is wet (p_wet).

Size correction source	logLik	AIC
Trait: HS		
Body size	72.10985	**-134.2197**
Body weight	67.90428	-125.8086
Trait: TRL		
Body size	54.91706	**-99.83412**
Body weight	51.80282	-93.60563
Trait: FLL		
Body size	70.10991	**-130.2198**
Body weight	69.76327	**-129.5265**
Trait: HLL		
Body size	50.37872	**-90.75744**
Body weight	51.96115	**-93.92229**
Trait: MaxSPR		
Body size	-19.49896	**48.99792**
Body weight	-19.13613	**48.27227**
Trait: BF		
Body weight	39.0681	**-68.13621**
Body size	32.94662	-55.89325
Trait: TA		
Body size	50.87396	**-91.74792**
Body weight	50.74039	**-91.48078**
Trait: max_L		
Body size	7.925437	**-5.850873**
Body weight	9.156607	**-8.313215**
Trait: min_L		
Body size	-24.31098	**58.62196**
Body weight	-24.5567	**59.11341**
Trait: Tpref		
Body size	-48.17555	**106.3511**
Body weight	-47.74423	**105.4885**
Trait: TprefV		
Body size	-91.19583	**192.3917**
Body weight	-91.69732	**193.3946**
Trait: EWL		
Body weight	-49.40007	**108.8001**
Body size	-46.68055	103.3611
Trait: p_wet		
Body size	725.4629	**-1440.926**
Body weight	725.4795	**-1440.959**

Table B2.2 Results of ANCOVAs performed on morphological traits to test for differences between the two species (Sp) of green lizards (*Timon lepidus* and *Lacerta shreiberi*), considering body size (log(SVL)) as covariate and species as factor. Df: degrees of freedom, SS: Sums of Squares, Rsq: R-squared. The abbreviations of the variables are as follows: snout to vent length (SVL), trunk length (TRL), head size (HS), fore limb length (FLL), and hind limb length (HLL).

Model	Source	Df	SS	Rsq	Z	Pr(>F)
TRL ~ SVL*Sp	**log(SVL)**	1	1.947	0.909	7.396	**0.001****
	Sp	1	0.000	0.000	-1.795	0.966
	log(SVL)*Sp	1	0.000	0.000	-1.125	0.849
	Residuals	39	0.196	0.091		
	Total	42	2.143			
HS ~ SVL*Sp	**log(SVL)**	1	2.440	0.963	9.994	**0.001****
	Sp	1	0.002	0.001	0.420	0.359
	log(SVL)*Sp	1	0.004	0.002	0.951	0.184
	Residuals	39	0.088	0.035		
	Total	42	2.534			
FLL ~ SVL*Sp	**log(SVL)**	1	1.082	0.898	8.138	**0.001****
	Sp	1	0.025	0.020	2.469	**0.002***
	log(SVL)*Sp	1	0.002	0.002	0.403	0.354
	Residuals	39	0.097	0.080		
	Total	42	1.205			
HLL ~ SVL*Sp	**log(SVL)**	1	1.955	0.877	7.184	**0.001****
	Sp	1	0.029	0.013	1.684	**0.045***
	log(SVL)*Sp	1	0.003	0.001	0.182	0.431
	Residuals	39	0.242	0.108		
	Total	42	2.230			

Table B2.3 Results of ANCOVAs performed on maximum sprint speed (MaxSPR) and on traits associated with maneuverability to test for differences between two species (Sp) of green lizards (*T. lepidus* and *L. shreiberi*), considering body size (log(SVL)), and size corrected morphological variables. Abbreviations of the variables are as follows: size corrected trunk length (res.TRL), size corrected fore limb length (res.FLL), size corrected hind limb length (res.HLL), maximum trunk angle bending (TA), maximum head angle bending (HA), maximum speed in the double-L racetrack (Max_L), and minimum time to complete double-L racetrack (min_T). Df: degrees of freedom, SS: Sums of Squares, MS: Mean squares, Rsq: R-squared.

Model	Source	Df	SS	Rsq	Z	Pr(>F)
MaxSPR ~ log(SVL)*Sp	**log(SVL)**	1	20122	0.025	0.519	0.318
	Sp	1	3014	0.003	-0.462	0.678
	log(SVL)*Sp	1	240	0.003	-1.491	0.929
	Residuals	39	765259			
	Total	42	788635			
MaxSPR ~ res.TRL*Sp	**res.TRL**	1	0.244	0.038	0.767	0.241
	Sp	1	0.144	0.022	0.482	0.333
	res.TRL *Sp	1	0.040	0.006	-0.242	0.612
	Residuals	39	5.976			
	Total	42	6.405			
MaxSPR ~ res.HLL*Sp	**res.HLL**	1	0.026	0.004	-0.525	0.702
	Sp	1	0.131	0.020	0.386	0.369
	res.HLL*Sp	1	0.116	0.018	0.341	0.383
	Residuals	39	6.131			
	Total	42	6.405			
MaxSPR ~ res.FLL*Sp	**res.FLL**	1	0.022	0.003	-0.530	0.692
	Sp	1	0.166	0.026	0.542	0.319
	res.FLL*Sp	1	0.069	0.010	-0.023	0.538
	Residuals	39	6.147			
	Total	42	6.405			
TA ~ log(SVL)*Sp	**log(SVL)**	1	0.067	0.218	2.586	**0.004****
	Sp	1	0.003	0.0001	-1.588	0.931
	log(SVL)*Sp	1	0.005	0.019	0.492	0.328
	Residuals	39	0.236			
	Total	42	0.309			
HA ~ log(SVL)*Sp	**log(SVL)**	1	0.002	0.015	0.210	0.428
	Sp	1	0.010	0.056	1.159	0.128
	log(SVL)*Sp	1	0.002	0.012	0.071	0.488
	Residuals	39	0.165			
	Total	42	0.180			
Max_L ~ log(SVL)*Sp	**log(SVL)**	1	8×10-5	4×10-5	-1.879	0.973
	Sp	1	0.219	0.111	1.702	**0.043***
	log(SVL)*Sp	1	0.010	0.005	-0.308	0.616
	Residuals	39	1.741			
	Total	42	1.971			
min_T ~ log(SVL)*Sp	**log(SVL)**	1	1.874	0.179	2.382	**0.008***
	Sp	1	0.793	0.075	1.535	**0.059.**
	log(SVL)*Sp	1	0.0002	0.001	-2.022	0.978
	Residuals	39	7.799			
	Total	42	10.467			

Table B2.4 Results of GLMs models performed on performance traits associated with maneuverability to test for differences between the two species (Sp) of green lizards (*Timon lepidus* and *Lacerta shreiberi*), considering body size (log(SVL)), stops before turning (NSBT), maximum speed in the first track (MaxS_I), and maximum speed in the second track (MaxS_II). CODE represents the individual identification of lizards. Df = 1.

Model	Source	SS	F	Pr(>F)
Turn_sucessI ~ log(SVL)*Sp + (1|CODE)	log(SVL)	0.735	0.735	0.359
	Sp	3.690	3.690	0.094.
	log(SVL)* Sp	0.545	0.545	0.332
Turn_sucessI ~ log(SVL) + NSBT*Sp + (1|CODE)	log(SVL)	1.167	1.167	0.169
	NSBT	2.428	2.428	0.062
	Sp	3.623	3.623	0.058
	NSBT* Sp	0.061	0.060	0.798
Turn_sucessI ~ log(SVL) + MaxS_I*Sp + (1|CODE)	log(SVL)	1.445	1.445	0.179
	MaxS_I	2.473	2.473	0.037*
	Sp	4.565	4.565	0.036*
	MaxS_I* Sp	0.262	0.260	0.569
Turn_sucessI ~ log(SVL) + MaxS_I + NSBT*Sp + (1|CODE)	log(SVL)	1.078	1.078	0.144
	MaxS_I	2.327	2.327	0.120
	NSBT	0.969	0.969	0.273
	Sp	4.451	4.451	0.034*
	NSBT* Sp	0.039	0.039	0.845
Turn_sucessII ~ log(SVL)*Sp + (1|CODE)	log(SVL)	0.240	0.240	0.295
	Sp	0.986	0.986	0.357
	log(SVL)* Sp	0.680	0.680	0.409
Turn_sucessII ~ log(SVL) + NSBT* Sp + (1|CODE)	log(SVL)	0.229	0.229	0.315
	NSBT	0.994	0.994	0.353
	Sp	0.129	0.129	0.659
	NSBT* Sp	0.746	0.746	0.388
Turn_sucessII ~ log(SVL) + MaxS_II*Sp + (1|CODE)	log(SVL)	0.285	0.285	0.159
	MaxS_II	3.219	3.219	0.049*
	Sp	1.562	1.562	0.216
	MaxS_II* Sp	0.153	0.1533	0.702
Turn_sucessII ~ log(SVL) + MaxS_II + NSBT*Sp + (1|CODE)	log(SVL)	0.055	0.055	0.026*
	MaxS_II	2.257	2.257	0.006**
	NSBT	1.467	1.467	0.175
	Sp	2.195	2.195	0.161
	NSBT* Sp	4.75	4.75	0.023*

Table B2.5 Eigenvalues and variance retained by each principal component in the dataset including all raw variables.

	eigenvalue	variance percent	cumulative variance percent
PC1	5.813	44.718	44.718
PC2	1.452	11.168	55.886
PC3	1.312	10.094	65.980
PC4	1.176	9.042	75.023
PC5	0.972	7.479	82.502
PC6	0.762	5.860	88.361
PC7	0.509	3.914	92.275
PC8	0.493	3.795	96.071
PC9	0.174	1.339	97.410
PC10	0.160	1.229	98.640
PC11	0.080	0.618	99.258
PC12	0.055	0.426	99.684
PC13	0.041	0.316	100.000

Table B2.6 Correlations scores of the four principal components of the dataset including all raw variables. Correlations >0·5 are highlighted in bold. The abbreviations of the variables are as follows: head size (HS), trunk length (TRL), fore limb length (FLL), hind limb length (HLL), bite force (BF), maximum sprint speed (MaxSPR), maximum trunk angle bending (TA), maximum head angle bending (HA), maximum speed in the double-L racetrack (Max_L), preferred temperature (Tpref), preferred temperature variance (Tpref V), evaporative water loss (EWL), and effective proportion of surface area that is wet (p_wet).

	PC1	PC2	PC3	PC4
TRL	**-0.956**	0.043	-0.065	0.066
FLL	**-0.953**	0.044	-0.079	-0.015
HLL	**-0.954**	-0.011	-0.080	0.013
HS	**-0.960**	0.054	-0.108	-0.063
BF	**-0.909**	0.170	0.034	-0.149
maxSPR	-0.162	0.218	0.072	**0.806**
TA	**0.577**	0.249	-0.443	-0.272
HA	0.198	0.067	-0.718	0.440
max_L	-0.008	0.475	0.178	-0.381
Tpref	-0.059	**-0.697**	0.440	0.139
TprefV	0.465	**0.504**	0.137	0.078
EWL	-0.476	-0.390	**-0.519**	-0.219
p_wet	**0.699**	-0.429	-0.230	-0.099

Table B2.7 Eigenvalues and variance retained by each principal component in the dataset including all size-corrected variables.

	PC1	PC2	PC3	PC4
res.TRL	0.289	-0.451	0.040	-0.195
res.FLL	0.107	-0.267	0.182	**-0.824**
res.HLL	-0.338	-0.128	0.499	-0.111
res.HS	-0.023	**0.619**	0.362	-0.170
res.BF	**0.602**	0.249	0.428	0.026
res.maxSPR	0.145	-0.379	-0.325	0.294
res.TA	-0.064	**0.642**	-0.344	-0.050
res.HA	-0.265	-0.011	**-0.671**	-0.136
res.max_L	0.324	0.472	0.295	0.130
res.Tpref	-0.322	-0.336	0.483	**0.553**
res.TprefV	0.411	0.359	-0.273	0.163
res.EWL	**-0.754**	0.303	-0.022	-0.015
res.p_wet	**-0.814**	0.132	0.134	-0.077

Table B2.8 Correlations scores of the four principal components of the dataset including all size-corrected variables. Correlations >0·5 are highlighted in bold. The abbreviations of the variables are as follows: size corrected trunk length (res.TRL), size corrected head size (res.HS), size corrected fore limb length (res.FLL), size corrected hind limb length (res.HLL), size corrected bite force (res.BF), size corrected maximum speed in the double-L racetrack (res.max_L), size corrected maximum sprint speed (res.maxSPR), maximum trunk angle bending corrected by size (res.TA), head angle bending corrected by size (res.HA), , preferred temperature corrected by size (res. Tpref), preferred temperature variance corrected by size (res.Tpref V), size corrected evaporative water loss (res.EWL), and effective proportion of surface area that is wet corrected by size (res.p_wet).

Dim	eigenvalue	variance percent	cumulative variance percent
PC1	2.278	17.522	17.522
PC2	1.866	14.354	31.875
PC3	1.686	12.968	44.844
PC4	1.221	9.396	54.239
PC5	1.126	8.662	62.901
PC6	1.094	8.418	71.319
PC7	1.008	7.753	79.071
PC8	0.674	5.185	84.256
PC9	0.642	4.942	89.198
PC10	0.477	3.669	92.866
PC11	0.401	3.087	95.953
PC12	0.318	2.448	98.401
PC13	0.208	1.599	100.000

Table B2.9 Eigenvalues and variance retained by each principal component in the three different raw variable datasets.

MORPH dataset			
Dim	**eigenvalue**	**variance percent**	**cumulative variance percent**
PC1	3.750	93.769	93.769
PC2	0.112	2.809	96.579
PC3	0.081	2.046	98.625
PC4	0.054	1.374	100
PERFORM dataset			
	eigenvalue	**variance percent**	**cumulative variance percent**
PC1	1.640	32.818	32.818
PC2	1.163	23.265	56.084
PC3	1.037	20.744	76.829
PC4	0.682	13.656	90.485
PC5	0.475	9.514	100
ECOPHY dataset			
	eigenvalue	**variance percent**	**cumulative variance percent**
PC1	1.413	35.346	35.346
PC2	1.129	28.227	63.574
PC3	0.915	22.890	86.465
PC4	0.541	13.534	100

Table B2.10 Correlations scores of the four principal components of the three different raw variable datasets. Correlations >0·5 are highlighted in bold. The abbreviations of the variables are as follows: head size (HS), trunk length (TRL), fore limb length (FLL), hind limb length (HLL), bite force (BF), maximum sprint speed (MaxSPR), maximum trunk angle bending (TA), maximum head angle bending (HA), maximum speed in the double-L racetrack (Max_L), preferred temperature (Tpref), preferred temperature variance (Tpref V), evaporative water loss (EWL), and effective proportion of surface area that is wet (p_wet).

MORPH dataset				
Trait	**PC1**	**PC2**	**PC3**	**PC4**
TRL	**-0.959**	-0.270	0.051	0.063
FLL	**-0.969**	0.032	-0.245	-0.016
HLL	**-0.968**	0.191	0.088	0.135
HS	**-0.977**	0.045	0.106	-0.180
PERFORM dataset				
Trait	**PC1**	**PC2**	**PC3**	**PC4**
BF	**-0.784**	-0.011	0.130	**0.511**
maxSPR	-0.211	**0.796**	0.374	-0.376
TA	**0.780**	-0.295	0.277	0.005
HA	**0.581**	**0.540**	0.228	0.527
max_L	-0.193	-0.389	**0.867**	-0.055
ECOPHY dataset				
Trait	**PC1**	**PC2**	**PC3**	**PC4**
Tpref	**-0.567**	0.318	-0.713	0.263
TprefV	**0.804**	0.338	0.014	0.489
EWL	**-0.666**	0.207	**0.630**	0.341
p_wet	0.050	**0.933**	0.098	-0.343

Table B2.11 Eigenvalues and variance retained by each principal component in the three different size-corrected variable datasets.

res.MORPH dataset			
Dim	**eigenvalue**	**variance percent**	**cumulative variance percent**
PC1	1.286	32.162	32.162
PC2	1.182	29.559	61.72
PC3	0.847	21.171	82.891
PC4	0.684	17.109	100
res.PERFORM dataset			
	Eigenvalue	**variance percent**	**cumulative variance percent**
PC1	1.603	32.062	32.062
PC2	1.203	24.063	56.124
PC3	1.03	20.605	76.729
PC4	0.63	12.596	89.325
PC5	0.534	10.675	100
res.ECOPHY dataset			
	Eigenvalue	**variance percent**	**cumulative variance percent**
PC1	1.85	46.239	46.239
PC2	1.142	28.552	74.791
PC3	0.753	18.821	93.611
PC4	0.256	6.389	100

Table B2.12 Correlations scores of the four principal components of the three different size-corrected variable datasets. Correlations >0·5 are highlighted in bold. The abbreviations of the variables are as follows: size corrected trunk length (res.TRL), size corrected head size (res.HS), size corrected fore limb length (res.FLL), size corrected hind limb length (res.HLL), size corrected bite force (res.BF), size corrected maximum speed in the double-L racetrack (res.max_L), size corrected maximum sprint speed (res.maxSPR), maximum trunk angle bending corrected by size (res.TA), head angle bending corrected by size (res.HA), , preferred temperature corrected by size (res. Tpref), preferred temperature variance corrected by size (res.Tpref V), size corrected evaporative water loss (res.EWL), and effective proportion of surface area that is wet corrected by size (res.p_wet).

res.MORPH dataset				
Trait	PC1	PC2	PC3	PC4
res.TRL	0.686	-0.468	-0.136	0.541
res.FLL	-0.02	-0.848	-0.257	-0.463
res.HLL	-0.538	-0.492	0.638	0.247
res.HS	-0.726	-0.054	-0.595	0.341
res.PERFORM dataset				
Trait	PC1	PC2	PC3	PC4
res.BF	0.81	-0.045	0.146	0.336
res.maxSPR	-0.38	0.272	0.802	0.354
res.TA	0.04	-0.894	-0.056	0.349
res.HA	-0.663	-0.506	0.223	-0.205
res.max_L	0.601	-0.266	0.559	-0.478
res.ECOPHY dataset				
Trait	PC1	PC2	PC3	PC4
res.Tpref	-0.383	0.688	-0.617	-0.02
res.TprefV	0.388	-0.69	-0.61	0.046
res.EWL	-0.859	-0.372	-0.023	-0.35
res.p_wet	-0.902	-0.233	0.021	0.362

Table B2.13 Correlations of flexible discriminant analysis (FDA) scores with phenotypic variables in the different datasets used to discriminate the two species of green lizards (*Timon lepidus* and *Lacerta schreiberi*). Variable abbreviations are shown in the methodology. The first two columns represent FDAs carried out with all phenotypic variables together (before and after size correction), while the last two were performed within each variable subset. The abbreviations of the variables are as follows: head size (HS), trunk length (TRL), fore limb length (FLL), hind limb length (HLL), bite force (BF), maximum sprint speed (MaxSPR), maximum trunk angle bending (TA), maximum head angle bending (HA), maximum speed in the double-L racetrack (Max_L), preferred temperature (Tpref), preferred temperature variance (Tpref V), evaporative water loss (EWL), and effective proportion of surface area that is wet (p_wet). size corrected trunk length (res.TRL), size corrected head size (res.HS), size corrected fore limb length (res.FLL), size corrected hind limb length (res.HLL), size corrected bite force (res.BF), size corrected maximum speed in the double-L racetrack (res.max_L), size corrected maximum sprint speed (res.maxSPR), maximum trunk angle bending corrected by size (res.TA), head angle bending corrected by size (res.HA), , preferred temperature corrected by size (res. Tpref), preferred temperature variance corrected by size (res.Tpref V), size corrected evaporative water loss (res.EWL), and effective proportion of surface area that is wet corrected by size (res.p_wet).

Raw variable	Correlation score	Residual variable	Correlation score	Dataset	Variable	Correlation score	Dataset	Variable	Correlation score
TRL	**0.885**	**res.TRL**	0.03	**MORPH**	**TRL**	0.883	**res.MORPH**	**res.TRL**	-0.003
HS	**0.895**	**res.HS**	-0.033		**HS**	0.896		**res.HS**	-0.054
FLL	**0.937**	**res.FLL**	0.179		**FLL**	0.931		**res.FLL**	0.162
HLL	**0.925**	**res.HLL**	0.07		**HLL**	0.931		**res.HLL**	0.118
MaxSPR	0.182	**res.MaxSPR**	0.15	**PERFORM**	**MaxSPR**	0.054	**res.PERFORM**	**res.MaxSPR**	0.044
TA	**-0.438**	**res.TA**	0.07		**TA**	-0.507		**res.TA**	0.039
HA	-0.04	**res.HA**	0.032		**HA**	-0.181		**res.HA**	0.112
Max_L	-0.135	**res.Max_L**	$-4.81 \cdot 10^{-6}$		**Max_L**	-0.148		**res.Max_L**	-0.009
BF	**0.785**	**res.BF**	-0.092		**BF**	0.873		**res.BF**	-0.118
Tpref	-0.072	**res.Tpref**	-0.16	**ECOPHY**	**Tpref**	0.014	**res.ECOPHY**	**res.Tpref**	-0.129
TprefV	-0.434	**res.TprefV**	-0.028		**TprefV**	-0.414		**res.TprefV**	-0.002
EWL	**0.447**	**res.EWL**	-0.078		**EWL**	0.448		**res.EWL**	-0.026
p_wet	-0.664	**res.p_wet**	-0.079		**p_wet**	-0.754		**res.p_wet**	-0.095

Appendix C

Supplementary material chapter 5

Supplementary Information for Chapter 5

Niche differentiation in coexisting species: ecological insights into the role of activity patterns, space use and environmental preferences

List of Supplementary Tables

Table C3.1 Results of ANOVAs performed on several variables recorded in the field to test for differences between the two species (Sp) of green lizards (*Timon lepidus* and *Lacerta shreiberi*). Df: degrees of freedom, SS: Sums of Squares, Rsq: R-squared.

Table C3.2 Results of ANOVAs performed on several microhabitat variables recorded in the field to test for differences between the two species (Sp) of green lizards (*Timon lepidus* and *Lacerta shreiberi*) and microhabitat. Df: degrees of freedom, SS: Sums of Squares, Rsq: R-squared.

Table C3.3 Post-hoc pairwise derived from the significant effect of interaction in ANOVA (Illuminance ~ Species * Microhabitat), showing the effect size (d), the 95% upper confidence limit (UCL-95%), the Z-value, and the associated p-value (Pr).

Table C3.4 Post-hoc pairwise derived from the significant effect of interaction in ANOVA (Body temperature ~ Species * Month), showing the effect size (d), the 95% upper confidence limit (UCL-95%), the Z-value, and the associated p-value (Pr). *Ls* (*Lacerta schreiberi*) and *Tl* (*Timon lepidus*).

Table C3.5 Results of ANOVAs performed on several variables recorded in the field to test for differences between the two species (Sp) of green lizards (*Timon lepidus* and *Lacerta shreiberi*) and behaviour. Df: degrees of freedom, SS: Sums of Squares, Rsq: R-squared.

Table C3.6 Post-hoc pairwise derived from the significant effect of interaction in ANOVA (Air temperature ~ Species * Behaviour), showing the effect size (d), the 95% upper confidence limit (UCL-95%), the Z-value, and the associated p-value (Pr). *Ls* (*Lacerta schreiberi*) and *Tl* (*Timon lepidus*).

Table C3.7 Post-hoc pairwise derived from the significant effect of behaviour in ANOVA (Illuminance ~ Species * Behaviour), showing the effect size (d), the 95% upper confidence limit (UCL-95%), the Z-value, and the associated p-value (Pr). *Ls* (*Lacerta schreiberi*) and *Tl* (*Timon lepidus*).

Table C3.8 Post-hoc pairwise derived from the significant effect of behaviour in ANOVA (Body temperature ~ Species * Behaviour), showing the effect size (d), the 95% upper confidence limit (UCL-95%), the Z-value, and the associated p-value (Pr).

Table C3.9 Post-hoc pairwise derived from the significant effect of behaviour in ANOVA (microhabitat substrate temperature ~ Species * Behaviour), showing the effect size (d), the 95% upper confidence limit (UCL-95%), the Z-value, and the associated p-value (Pr).

Table C3.10 Results of ANOVAs performed on several variables recorded in the field to test for differences between the two species (Sp) of green lizards (*Timon lepidus* and *Lacerta shreiberi*) between months. Df: degrees of freedom, SS: Sums of Squares, Rsq: R-squared.

Table C3.11 Post-hoc pairwise derived from the significant effect of months in ANOVA (Air temperature ~ Species * Month), showing the effect size (d), the 95% upper confidence limit (UCL-95%), the Z-value, and the associated p-value (Pr). *Ls* (*Lacerta schreiberi*) and *Tl* (*Timon lepidus*).

Table C3.12 Post-hoc pairwise derived from the significant effect of interaction in ANOVA (Relative humidity ~ Species * Month), showing the effect size (d), the 95% upper confidence limit (UCL-95%), the Z-value, and the associated p-value (Pr). *Ls* (*Lacerta schreiberi*) and *Tl* (*Timon lepidus*).

Table C3.13 Post-hoc pairwise derived from the significant effect of months in ANOVA (Illuminance ~ Species * Month), showing the effect size (d), the 95% upper confidence limit (UCL-95%), the Z-value, and the associated p-value (Pr).

Table C3.14 Model comparison and parameter estimates for several circular models to test differences in time related with body temperature (Tb), environmental temperature (EnT), snout-vent length (SVL), environmental humidity (EH), amount of solar light and species (*L. schreiberi* and *T. lepidus*). The models' performance is evaluated using Deviance Information Criterion (DIC), Watanabe-Akaike Information Criterion (WAIC), and R-hat values, convergence is indicated by values closer to 1 as good convergence. The parameter estimates include the mean (Estimate), standard deviation (SD), and 95% credible intervals (LB, UB). Variable abbreviations as follows: SVL = snout to vent length, AT = air temperature, EH = relative humidity, IL = illuminance.

Table C3.1 Results of ANOVAs performed on several variables recorded in the field to test for differences between the two species (Sp) of green lizards (*Timon lepidus* and *Lacerta shreiberi*). Df: degrees of freedom, SS: Sums of Squares, Rsq: R-squared.

	Df	SS	Rsq	Z	Pr(>F)
Air temperature ~ Species * Sex					
Sp	1	24.03	0.013	1.180	0.123
Sex	1	0.71	4×10^{-4}	-0.837	0.786
Sp*Sex	1	0.83	4.7×10^{-4}	-0.755	0.761
Residuals	186	1759.07	0.985		
Total	189	1784.64			
Relative humidity ~ Species * Sex					
Sp	1	1621.1	0.084	2.925	**0.001****
Sex	1	133.5	0.006	0.501	0.257
Sp*Sex	1	93.7	0.004	0.323	0.359
Residuals	186	19867.6	0.91		
Total	189	21715.9			
Illuminance~ Species * Sex					
Sp	1	188.6	0.015	1.108	0.140
Sex	1	4.5	3.6×10^{-4}	-1.002	0.824
Sp*Sex	1	58.6	0.004	0.215	0.443
Residuals	140	12203.1	0.977		
Total	143	12454.8			
Body temperature ~ Species * Sex					
Sp	1	10.81	0.010	0.569	0.306
Sex	1	0.41	4×10^{-4}	-1.008	0.829
Sp*Sex	1	0.45	4.5×10^{-4}	-0.981	0.821
Residuals	111	1005.75	0.988		
Total	114	1017.43			
Microhabitat substrate temperature ~ Species * Sex					
Sp	1	10.9	0.002	-0.068	0.539
Sex	1	35.0	0.007	0.705	0.250
Sp*Sex	186	6.6	0.001	-0.269	0.624
Residuals	189	4683.7	0.988		
Total		4736.2			

Table C3.2 Results of ANOVAs performed on several microhabitat variables recorded in the field to test for differences between the two species (Sp) of green lizards (*Timon lepidus* and *Lacerta shreiberi*) and microhabitat. Df: degrees of freedom, SS: Sums of Squares, Rsq: R-squared.

	Df	SS	Rsq	Z	Pr(>F)
Air temperature ~ Species * Microhabitat					
Sp	1	35.27	0.057	1.666	0.05.
Microhabitat	3	94.71	0.027	2.182	**0.015***
Sp* Microhabitat	3	45.25	0.89	1.082	0.148
Residuals	177	1482.92			
Total	184	1658.15			
Relative humidity ~ Species * Microhabitat					
Sp	1	1686.1	0.080	3.051	**0.001****
Microhabitat	3	239.5	0.011	-0.118	0.538
Sp* Microhabitat	3	316.2	0.015	0.219	0.415
Residuals	177	18814.0	0.893		
Total	184	21055.8			
Illuminance~ Species * Microhabitat					
Sp	1	9.1	0.0006	-0.713	0.758
Microhabitat	3	284.0	0.020	0.254	0.409
Sp* Microhabitat	3	1022.7	0.075	2.161	**0.015***
Residuals	132	12277.2	0.903		
Total	139	13593.0			
Body temperature ~ Species * Microhabitat					
Sp	1	11.03	0.011	0.677	0.271
Microhabitat	3	18.93	0.020	-0.103	0.544
Sp* Microhabitat	3	10.74	0.114	-0.566	0.700
Residuals	103	895.83	0.956		
Total	110	936.53			
Microhabitat substrate temperature ~ Species * Microhabitat					
Sp	1	16.2	0.003	0.183	0.440
Microhabitat	3	90.4	0.019	0.516	0.302
Sp* Microhabitat	3	72.9	0.016	0.206	0.423
Residuals	169	4345.6	0.960		
Total	176	4525.1			

Table C3.3 Post-hoc pairwise derived from the significant effect of interaction in ANOVA (Illuminance ~ Species * Microhabitat), showing the effect size (d), the 95% upper confidence limit (UCL-95%), the Z-value, and the associated p-value (Pr).

	d	UCL (95%)	Z	Pr > d
Ls.cement/rubble:*Tl*.cement/rubble	12.175	11.909	1.642	**0.042**
Ls.cement/rubble:*Ls*.ground	10.425	16.464	0.788	0.226
Ls.cement/rubble:*Tl*.ground	5.708	18.227	-0.170	0.577
Ls.cement/rubble:*Ls*.herbaceous vegetation	9.419	9.941	1.425	**0.075**
Ls.cement/rubble:*Tl*.herbaceous vegetation	5.534	11.184	0.427	0.372
Ls.cement/rubble:*Ls*.rocky substrate	6.745	14.177	0.476	0.348
Ls.cement/rubble:*Tl*.rocky substrate	10.255	11.102	1.513	**0.069**
Tl.cement/rubble:*Ls*.ground	1.750	14.229	-0.885	0.799
Tl.cement/rubble:*Tl*.ground	17.883	16.163	1.761	**0.027**
Tl.cement/rubble:*Ls*.herbaceous vegetation	2.756	7.708	0.079	0.483
Tl.cement/rubble:*Tl*.herbaceous vegetation	6.641	8.788	1.058	0.163
Tl.cement/rubble:*Ls*.rocky substrate	5.430	12.106	0.308	0.414
Tl.cement/rubble:*Tl*.rocky substrate	1.920	8.423	-0.402	0.652
Ls.ground:*Tl*.ground	16.133	14.237	1.741	**0.032**
Ls.ground:*Ls*.herbaceous vegetation	1.006	14.115	-1.392	0.909
Ls.ground:*Tl*.herbaceous vegetation	4.891	14.287	0.052	0.491
Ls.ground:*Ls*.rocky substrate	3.680	17.293	-0.611	0.734
Ls.ground:*Tl*.rocky substrate	0.170	14.738	-2.203	0.989
Tl.ground:*Ls*.herbaceous vegetation	15.127	16.330	1.492	**0.065**
Tl.ground:*Tl*.herbaceous vegetation	11.242	15.691	0.999	0.170
Tl.ground:*Ls*.rocky substrate	12.453	19.607	0.750	0.249
Tl.ground:*Tl*.rocky substrate	15.964	16.556	1.453	**0.068**
Ls.herbaceous vegetation:*Tl*.herbaceous vegetation	3.885	6.459	0.710	0.248
Ls.herbaceous vegetation:*Ls*.rocky substrate	2.674	9.390	-0.225	0.580

Ls.herbaceous vegetation:*Tl*.rocky substrate	0.836	4.216	-0.557	0.714
Tl.herbaceous vegetation:*Ls*.rocky substrate	1.211	11.415	-1.059	0.835
Tl.herbaceous vegetation:*Tl*.rocky substrate	4.721	7.364	0.834	0.209
Ls.rocky substrate:*Tl*.rocky substrate	3.510	9.500	0.120	0.473

Table C3.4 Post-hoc pairwise derived from the significant effect of interaction in ANOVA (Body temperature ~ Species * Month), showing the effect size (d), the 95% upper confidence limit (UCL-95%), the Z-value, and the associated p-value (Pr). *Ls* (*Lacerta schreiberi*) and *Tl* (*Timon lepidus*).

	d	UCL (95%)	Z	Pr
Ls.May:*Tl*.May	0.877	1.946	0.302	0.402
Ls.May:*Ls*.June	0.399	1.656	-0.391	0.652
Ls.May:*Tl*.June	0.894	1.743	0.522	0.318
Ls.May:*Ls*.July	3.558	3.765	1.479	**0.067.**
Ls.May:*Tl*.July	1.109	4.079	-0.970	0.819
Tl.May:*Ls*.June	1.276	2.029	0.713	0.260
Tl.May:*Tl*.June	0.016	1.661	-2.118	0.986
Tl.May:*Ls*.July	2.681	3.043	1.301	0.107
Tl.May:*Tl*.July	0.232	3.357	-1.725	0.947
Ls.June:*Tl*.June	1.292	1.902	0.933	0.199
Ls.June:*Ls*.July	3.957	3.740	1.661	**0.038***
Ls.June:*Tl*.July	1.508	3.988	-0.788	0.789
Tl.June:*Ls*.July	2.664	3.253	1.189	0.116
Tl.June:*Tl*.July	0.215	3.419	-1.929	0.971
Ls.July:*Tl*.July	2.449	2.773	1.391	**0.084.**

Table C3.5 Results of ANOVAs performed on several variables recorded in the field to test for differences between the two species (Sp) of green lizards (*Timon lepidus* and *Lacerta shreiberi*) and behaviour. Df: degrees of freedom, SS: Sums of Squares, Rsq: R-squared.

	Df	SS	Rsq	Z	Pr(>F)
Air temperature ~ Species * Behaviour					
Sp	1	27.58	0.015	1.395	**0.07.**
Behavior	4	18.13	0.010	-0.544	0.719
Sp*Behavior	4	97.61	0.054	1.786	**0.033***
Residuals	180	1655.59	0.920		
Total	189	1799.01			
Relative humidity ~ Species * Behaviour					
Sp	1	1721.2	0.079	3.088	**0.001****
Behavior	4	754.6	0.034	1.120	0.139
Sp*Behavior	4	834.7	0.038	1.288	0.105
Residuals	180	18462.1	0.847		
Total	189	21772.6			
Illuminance ~ Species * Behaviour					
Sp	1	13.0	0.0009	-0.357	0.649
Behavior	4	3458.6	0.279	5.322	**0.001****
Sp*Behavior	4	257.9	0.018	0.039	0.482
Residuals	134	9742.9	0.707		
Total	143	13772.3			
Body temperature ~ Species * Behaviour					
Sp	1	10.01	0.009	0.681	0.265
Behavior	4	82.20	0.080	1.685	**0.042***
Sp*Behavior	4	53.68	0.052	0.954	0.164
Residuals	105	872.75	0.856		
Total	114	1018.65			
Microhabitat substrate temperature ~ Species * Behaviour					
Sp	1	10.9	0.002	-0.014	0.517
Behavior	4	548.5	0.115	3.332	**0.001****
Sp*Behavior	4	54.1	0.011	-0.530	0.705
Residuals	180	4122.7	0.870		
Total	189	4736.2			

Table C3.6 Post-hoc pairwise derived from the significant effect of interaction in ANOVA (Air temperature ~ Species * Behaviour), showing the effect size (d), the 95% upper confidence limit (UCL-95%), the Z-value, and the associated p-value (Pr). *Ls* (*Lacerta schreiberi*) and *Tl* (*Timon lepidus*).

	d	UCL (95%)	Z	Pr > d
Ls.basking:*Tl*.basking	1.186	1.705	0.766	0.241
Ls.basking:*Ls*.fleeing	0.949	3.172	-0.051	0.534
Ls.basking:*Tl*.fleeing	0.229	2.196	-1.024	0.826
Ls.basking:*Ls*.foraging	0.399	3.036	-0.943	0.813
Ls.basking:*Tl*.foraging	1.727	3.070	0.416	0.376
Ls.basking:*Ls*.mating	2.949	3.695	1.286	0.102
Ls.basking:*Tl*.mating	1.476	2.238	0.914	0.188
Ls.basking:*Ls*.sheltering	0.726	3.193	-0.408	0.651
Ls.basking:*Tl*.sheltering	1.728	2.526	0.756	0.249
Tl.basking:*Ls*.fleeing	0.237	3.909	-1.422	0.920
Tl.basking:*Tl*.fleeing	1.415	2.438	0.718	0.254
Tl.basking:*Ls*.foraging	0.787	2.954	-0.225	0.599
Tl.basking:*Tl*.foraging	0.541	2.243	-0.465	0.672
Tl.basking:*Ls*.mating	1.763	4.407	0.194	0.426
Tl.basking:*Tl*.mating	2.662	2.665	1.581	**0.052.**
Tl.basking:*Ls*.sheltering	1.912	3.322	0.775	0.229
Tl.basking:*Tl*.sheltering	0.542	1.837	-0.150	0.580
Ls.fleeing:*Tl*.fleeing	1.178	3.791	-0.054	0.542
Ls.fleeing:*Ls*.foraging	0.550	4.436	-1.012	0.837
Ls.fleeing:*Tl*.foraging	0.778	4.835	-0.879	0.796
Ls.fleeing:*Ls*.mating	2.000	4.271	0.450	0.344
Ls.fleeing:*Tl*.mating	2.425	3.763	0.890	0.200
Ls.fleeing:*Ls*.sheltering	1.675	4.590	0.143	0.470
Ls.fleeing:*Tl*.sheltering	0.779	4.425	-0.750	0.761
Tl.fleeing:*Ls*.foraging	0.628	3.414	-0.574	0.707
Tl.fleeing:*Tl*.foraging	1.956	3.632	0.562	0.314
Tl.fleeing:*Ls*.mating	3.178	4.345	1.187	0.121
Tl.fleeing:*Tl*.mating	1.247	2.853	0.352	0.381
Tl.fleeing:*Ls*.sheltering	0.497	3.536	-0.896	0.796
Tl.fleeing:*Tl*.sheltering	1.956	2.990	0.807	0.239
Ls.foraging:*Tl*.foraging	1.328	3.863	0.086	0.480
Ls.foraging:*Ls*.mating	2.550	4.831	0.576	0.298
Ls.foraging:*Tl*.mating	1.875	3.649	0.537	0.315
Ls.foraging:*Ls*.sheltering	1.125	4.047	-0.263	0.607
Ls.foraging:*Tl*.sheltering	1.329	3.330	0.261	0.403
Tl.foraging:*Ls*.mating	1.222	5.340	-0.539	0.720

Tl.foraging:*Tl*.mating	3.203	3.686	1.304	**0.093.**
Tl.foraging:*Ls*.sheltering	2.453	4.248	0.749	0.226
Tl.foraging:*Tl*.sheltering	0.001	2.439	-2.641	1.000
Ls.mating:*Tl*.mating	4.425	4.003	1.748	**0.031***
Ls.mating:*Ls*.sheltering	3.675	4.970	1.127	0.132
Ls.mating:*Tl*.sheltering	1.221	4.822	-0.464	0.684
Tl.mating:*Ls*.sheltering	0.750	3.658	-0.536	0.703
Tl.mating:*Tl*.sheltering	3.204	3.384	1.512	**0.064.**
Ls.sheltering:*Tl*.sheltering	2.454	3.834	0.929	0.187

Table C3.7 Post-hoc pairwise derived from the significant effect of behaviour in ANOVA (Illuminance ~ Species * Behaviour), showing the effect size (d), the 95% upper confidence limit (UCL-95%), the Z-value, and the associated p-value (Pr). *Ls* (*Lacerta schreiberi*) and *Tl* (*Timon lepidus*).

	d	UCL-0.95	Z	Pr
basking:fleeing	2.384	7.411	-0.062	0.542
basking:foraging	3.473	8.002	0.060	0.506
basking:mating	8.261	11.978	-0.029	0.519
basking:sheltering	16.926	21.881	0.040	0.493
fleeing:foraging	1.089	7.229	-0.864	0.777
fleeing:mating	10.644	16.548	-0.001	0.503
fleeing:sheltering	14.542	20.999	0.014	0.499
foraging:mating	11.733	17.164	-0.010	0.498
foraging:sheltering	13.453	19.378	0.030	0.486
mating:sheltering	25.187	31.407	0.029	0.470

Table C3.8 Post-hoc pairwise derived from the significant effect of behaviour in ANOVA (Body temperature ~ Species * Behaviour), showing the effect size (d), the 95% upper confidence limit (UCL-95%), the Z-value, and the associated p-value (Pr).

	d	UCL-0.95	Z	Pr
basking:fleeing	0.389	2.637	-0.863	0.798
basking:foraging	1.629	3.200	0.021	0.509
basking:mating	2.644	4.100	-0.009	0.501
basking:sheltering	0.555	2.527	-0.501	0.684
fleeing:foraging	1.240	3.921	-0.133	0.551
fleeing:mating	2.255	4.836	0.068	0.508
fleeing:sheltering	0.166	3.300	-1.417	0.901
foraging:mating	1.015	3.061	-0.068	0.556
foraging:sheltering	1.074	3.577	-0.045	0.527
mating:sheltering	2.089	4.375	0.117	0.488

Table C3.9 Post-hoc pairwise derived from the significant effect of behaviour in ANOVA (microhabitat substrate temperature ~ Species * Behaviour), showing the effect size (d), the 95% upper confidence limit (UCL-95%), the Z-value, and the associated p-value (Pr).

	d	UCL-0.95	Z	Pr
basking:fleeing	5.096	7.687	0.081	0.459
basking:foraging	0.642	3.176	-0.506	0.680
basking:mating	4.057	6.449	0.025	0.482
basking:sheltering	2.424	4.315	0.042	0.516
fleeing:foraging	4.453	8.047	0.093	0.462
fleeing:mating	9.153	12.616	0.077	0.479
fleeing:sheltering	2.672	5.803	0.137	0.476
foraging:mating	4.699	8.008	0.043	0.496
foraging:sheltering	1.781	4.960	0.014	0.516
mating:sheltering	6.481	9.387	-0.005	0.500

Table C3.10 Results of ANOVAs performed on several variables recorded in the field to test for differences between the two species (Sp) of green lizards (*Timon lepidus* and *Lacerta shreiberi*) between months. Df: degrees of freedom, SS: Sums of Squares, Rsq: R-squared.

	Df	SS	Rsq	Z	Pr(>F)
Air temperature ~ Species * Month					
Sp	1	0.48	0.0004	-0.962	0.817
Month	2	95.79	0.085	2.692	**0.004 ****
Sp*Month	2	3.64	0.003	-0.798	0.767
Residuals	135	1020.62	0.91		
Total	140	1120.53			
Relative humidity ~ Species * Month					
Sp	1	381.8	0.046	2.194	**0.001****
Month	2	490.5	0.06	2.431	**0.005****
Sp*Month	2	613.4	0.075	2.765	**0.003****
Residuals	135	6671.6	0.817	0.817	
Total	140	8157.2			
Illuminance~ Species * Month					
Sp	1	0.4	4×10^{-5}	-1.615	0.941
Month	2	3298.4	0.269	5.347	**0.001****
Sp*Month	2	60.2	0.004	-0.409	0.668
Residuals	129	8897.3	0.725		
Total	134	12256.3			
Body temperature ~ Species * Month					
Sp	1	10.81	0.01	0.633	0.283
Month	2	50.03	0.05	1.613	**0.047***
Sp*Month	2	50.61	0.05	1.59	**0.052.**
Residuals	109	905.97	0.89		
Total	114	1017.43			
Microhabitat substrate temperature ~ Species * Month					
Sp	1	28.97	0.009	0.675	0.274
Month	2	68.43	0.228	0.765	0.219
Sp*Month	2	18.94	0.006	-0.421	0.681
Residuals	125	2881.86	0.961		
Total	130	2998.21			

Table C3.11 Post-hoc pairwise derived from the significant effect of months in ANOVA (Air temperature ~ Species * Month), showing the effect size (d), the 95% upper confidence limit (UCL-95%), the Z-value, and the associated p-value (Pr). *Ls* (*Lacerta schreiberi*) and *Tl* (*Timon lepidus*).

	d	UCL-95%	Z	Pr
May:June	0.166	1.192	-0.827	0.776
May:July	1.701	3.031	0.070	0.481
June:July	1.867	3.107	0.041	0.494

Table C3.12 Post-hoc pairwise derived from the significant effect of interaction in ANOVA (Relative humidity ~ Species * Month), showing the effect size (d), the 95% upper confidence limit (UCL-95%), the Z-value, and the associated p-value (Pr). *Ls* (*Lacerta schreiberi*) and *Tl* (*Timon lepidus*).

	d	UCL (95%)	Z	Pr > d
Ls.May:*Tl*.May	8.442	6.656	2.348	**0.005*** **
Ls.May:*Ls*.June	1.000	7.187	-1.695	0.942
Ls.May:*Tl*.June	0.483	3.697	-0.841	0.783
Ls.May:*Ls*.July	2.650	5.774	0.334	0.391
Ls.May:*Tl*.July	4.000	5.994	0.781	0.230
Tl.May:*Ls*.June	7.442	10.552	-0.006	0.490
Tl.May:*Tl*.June	7.959	6.822	2.199	**0.013** **
Tl.May:*Ls*.July	5.792	9.248	0.425	0.367
Tl.May:*Tl*.July	4.442	5.181	1.268	0.114
Ls.June:*Tl*.June	0.517	6.388	-1.896	0.965
Ls.June:*Ls*.July	1.650	7.100	-0.554	0.700
Ls.June:*Tl*.July	3.000	10.233	-1.296	0.901
Tl.June:*Ls*.July	2.167	5.149	0.178	0.446
Tl.June:*Tl*.July	3.517	6.597	0.413	0.373
Ls.July:*Tl*.July	1.350	8.517	-0.991	0.814

Table C3.13 Post-hoc pairwise derived from the significant effect of months in ANOVA (Illuminance ~ Species * Month), showing the effect size (d), the 95% upper confidence limit (UCL-95%), the Z-value, and the associated p-value (Pr).

	d	UCL-95%	Z	Pr
May:June	7.641	10.055	-0.041	0.518
May:July	5.390	8.766	-0.001	0.52
June:July	13.031	16.588	-0.029	0.514

Table C3.14 Model comparison and parameter estimates for several circular models to test differences in time related with body temperature (Tb), environmental temperature (EnT), snout-vent length (SVL), environmental humidity (EH), amount of solar light and species (*L. schreiberi* and *T. lepidus*). The models' performance is evaluated using Deviance Information Criterion (DIC), Watanabe-Akaike Information Criterion (WAIC), and R-hat values, convergence is indicated by values closer to 1 as good convergence. The parameter estimates include the mean (Estimate), standard deviation (SD), and 95% credible intervals (LB, UB). Variable abbreviations as follows: SVL = snout to vent length, AT = air temperature, EH = relative humidity, IL = illuminance.

Model	DIC	WAIC	R-hat	Source	Estimate	SD	LB	UB
Time ~ SVL * AT * Species	166.885	169.21	0.944	Intercept	1.731	0.57	1.077	2.789
				Kappa	3.938	0.58	**2.973**	**5.229**
				SVL	-0.112	0.555	-1.122	1.138
				EnT	0.539	0.369	-0.076	1.34
				SVL:EnT	0.049	0.599	-1.22	1.142
				SVL:Species*T. lepidus*	0.115	0.622	-1.237	1.238
				AT:Species*T. lepidus*	-1.404	0.642	**-2.748**	**-0.235**
				SVL:AT:Species*T. lepidus*	-0.406	0.814	-2.035	1.143
				Species*T. lepidus*	-2.77	0.943	**-4.953**	**-1.487**
Time ~ SVL * AT * EH * Species	165.519	169.569	0.97	Intercept	1.357	0.626	**0.777**	**2.137**
				Kappa	4.059	0.607	**2.966**	**5.333**
				SVL	0.038	0.75	-1.417	1.482
				AT	-0.005	0.645	-1.149	1.381
				EH	-0.744	0.659	-1.984	0.662
				SVL:AT	-0.12	0.753	-1.682	1.334
				SVL:EH	-0.395	0.79	-1.904	1.162
				AT:EH	1.01	0.658	-0.314	2.282
				SVL:Species*T. lepidus*	0.032	0.84	-1.777	1.514
				AT:Species*T. lepidus*	-1.114	0.814	-2.926	0.263
				EH:Species*T. lepidus*	-0.42	0.778	-2.03	1.101
				SVL:AT:EH	0.26	0.755	-1.277	1.729
				SVL:AT:Species*T. lepidus*	-0.493	0.843	-2.264	1.136
				SVL:EH:Species*T. lepidus*	0.223	0.847	-1.624	1.797
				AT:EH:Species*T. lepidus*	-0.536	0.852	-2.301	1.011
				SVL:AT:EH:Species*T. lepidus*	-0.297	0.831	-2.035	1.353
				Species*T. lepidus*	-2.032	0.753	**-3.264**	**-0.325**
Time ~ SVL * Tb * Species	175.28	177.791	0.948	Intercept	-0.486	0.565	-1.697	0.132
				Kappa	3.676	0.533	**2.734**	**4.813**
				SVL	-0.163	0.624	-1.4	1.091
				Eye	0.371	0.315	-0.2	1.043
				SVL:Tb	-0.514	0.66	-1.808	0.834

				SVL:Species*T. lepidus*	1.082	0.826	-0.431	2.698
				Tb:Species*T. lepidus*	0.813	0.791	-0.526	2.533
				SVL: Tb:Species*T. lepidus*	0.912	0.831	-0.582	2.601
				Species*T. lepidus*	1.406	2.015	-5.876	1.387
Time ~ SVL * EH * Species	177.504	179.45	0.936	Intercept	-0.621	0.475	-1.855	0.009
				Kappa	3.683	0.53	**2.685**	**4.74**
				EH	-0.012	0.398	-0.83	0.773
				SVL	-0.163	0.597	-1.278	1.046
				EH:SVL	-0.629	0.66	-2.014	0.469
				EH:Species*T. lepidus*	0.563	0.725	-0.619	2.247
				SVL:Species*T. lepidus*	1.546	0.72	0.161	3.032
				EH:SVL:Species*T. lepidus*	0.389	0.842	-1.105	2.254
				Species*T. lepidus*	1.661	0.943	**-5.738**	**-2.045**
Time ~ SVL * Tb * EH * Species	177.398	178.928	0.974	Intercept	-0.043	0.226	-0.552	0.297
				Kappa	3.662	0.531	**2.726**	**4.794**
				SVL	-0.097	0.839	-1.599	1.61
				Tb	0.361	0.602	-0.754	1.625
				EH	-0.305	0.739	-1.84	1.069
				SVL: Tb	0.063	0.858	-1.544	1.851
				SVL:EH	-0.415	0.809	-2.076	1.092
				Tb:EH	0.055	0.75	-1.454	1.538
				SVL:Species*T. lepidus*	1.08	0.888	-0.678	2.858
				Tb:Species*T. lepidus*	0.901	0.917	-0.863	2.732
				EH:Species*T. lepidus*	0.42	0.896	-1.225	2.199
				SVL:Tb:EH	-0.393	0.814	-1.96	1.3
				SVL:Tb:Species*T. lepidus*	0.829	0.983	-1.14	2.728
				SVL:EH:Species*T. lepidus*	0.52	0.945	-1.334	2.307
				Eye:EH:Species*T. lepidus*	0.481	0.889	-1.224	2.322
				SVL:Tb:EH:Species*T. lepidus*	0.601	0.95	-1.251	2.413
				Species*T. lepidus*	0.635	1.044	-4.478	1.571
Time ~ SVL * IL * Species	178.478	181.17	0.952	Intercept	-0.513	0.498	-1.987	0.093
				Kappa	3.586	0.521	**2.648**	**4.679**
				SVL	-0.274	0.568	-1.411	0.899
				IL	0.001	0.378	-0.864	0.697
				SVL:IL	-0.609	0.654	-1.914	0.734
				SVL:Species*T. lepidus*	1.395	0.695	**0.194**	**2.889**
				IL:Species*T. lepidus*	0.711	0.759	-0.529	2.381
				SVL:IL:SpeciesT.lepidus	0.805	0.771	-0.591	2.384
				Species*T. lepidus*	1.406	2.41	-5.815	1.818

Appendix D

Supplementary material chapter 6

Supplementary Information for Chapter 6

Physiology-microhabitat matching may help organisms cope with the thermal and hydric challenges under climate change: a tale of two lizards

List of Supplementary Tables and Figures

Table D4.1 Summary of the mean, standard deviation, minimum, and maximum difference values for physiological variables between current climate and two climate scenarios: +2°C and +4°C derived from mechanistic models for two species of green lizards, *Timon lepidus* and *Lacerta schreiberi* in different microhabitats. Variables include foraging time, basking time, time spent in the preferred temperature range (Tpref), shade selection, water loss, and size-corrected water loss. Foraging and basking times are in hours, time in Tpref in °C, shade selected in % and water loss metrics are in g/h. CARP: Carpobrotus, GRO/ROCK: rocky and bare soil microhabitats, Wk: walkway, VH: herbaceous vegetation.

Figure D4.1 Maps of the variables obtained from mechanistic niche models for *T. lepidus* (top row: A, B, C) and *L. schreiberi* (bottom row: D, E, F) under current climatic conditions in Castro São Paio, northern Portugal. Panels A and D show the total basking time (in hours); panels B and E represent the difference in basking time between scenario +2 °C and current climate and panels C and F represent the difference in basking time between scenario +4°C and current climate.

Figure D4.2 Total basking time in hours. The facets indicate climatic scenarios: Current climate, Increase in +2 °C, and Increase in +4 °C. The x-axis represents microhabitats: CARP (Carpobrotus microhabitat), GRO/ROCK (rocky and bare soil microhabitat), VH (herbaceous vegetation), and Wk (walkway). The colours correspond to the two species studied: orange for *T. lepidus* and green for *L. schreiberi*. Dots inside the violins represent means with standard error.

Figure D4.3 Water loss in climatic scenarios: Current climate, Increase in +2 °C, and Increase in +4 °C. The x-axis represents microhabitats: CARP (*Carpobrotus* microhabitat), GRO/ROCK (rocky and bare soil microhabitat), VH (herbaceous vegetation), and Wk (walkway). The colours correspond to the two species studied: orange for *T. lepidus* and green *for L. schreiberi*. Dots inside the violins represent means with standard error.

Figure D4.4 Total basking time in hours. The facets indicate slope categories (Low and High), and the colours correspond to the two species studied: orange for *T. lepidus* and green for *L. schreiberi*. Dots inside the violins represent means with standard error**.**

Figure D4.5 Total water loss from mechanistic models in different climatic scenarios. The facets indicate slope categories (Low and High), and the colours correspond to the two species studied: orange for *T. lepidus* and green for *L. schreiberi*. Dots inside the violins represent means with standard error**.**

Figure D4.6 Total basking time in hours from mechanistic models in different climatic scenarios. The facets indicate aspect categories (North, East, South, West), and the colours correspond to the two species studied: orange for *T. lepidus* and green for *L. schreiberi*. Dots inside the violins represent means with standard error**.**

Figure D4.7 Total water loss from mechanistic models in different climatic scenarios. The facets indicate aspect categories (North, East, South, West), and the colours correspond to the two species studied: orange for *T. lepidus* and green for *L. schreiberi*. Dots inside the violins represent means with standard error**.**

Table D4.1 Summary of the mean, standard deviation, minimum, and maximum difference values for physiological variables between current climate and two climate scenarios: +2°C and +4°C derived from mechanistic models for two species of green lizards, *Timon lepidus* and *Lacerta schreiberi* in different microhabitats. Variables include foraging time, basking time, time spent in the preferred temperature range (Tpref), shade selection, water loss, and size-corrected water loss. Foraging and basking times are in hours, time in Tpref in °C, shade selected in % and water loss metrics are in g/h. CARP: *Carpobrotus*, GRO/ROCK: rocky and bare soil microhabitats, Wk: walkway, VH: herbaceous vegetation.

Variable	Scenario	*T. lepidus*	*L. schreiberi*
		CARP	**CARP**
Foraging time	+2°C	**112.126** ± 50.443 (-35-258)	77.661 ± 49.378 (-35-258)
	+4°C	**268.229** ± 75.67 (75-478)	195.65 ± 71.325 (75-478)
Basking time	+2°C	**160.226** ± 64.004 (-31-368)	164.715 ± 63.727 (-34-368)
	+4°C	**319.797** ± 59.221 (158-492)	341.738 ± 60.159 (133-512)
Shade selected	+2°C	0.706 ± 0.639 (-2.192-3.173)	**0.754** ± 0.664 (-1.946-3.493)
	+4°C	1.55 ± 0.656 (-1.381-3.266)	**1.628** ± 0.683 (-0.438-3.653)
Time in Tpref	+2°C	**51.618** ± 6.312 (1-108)	51.058 ± 6.867 (-10-111)
	+4°C	**113.781** ± 6.671 (65-185)	112.213 ± 6.932 (52-187)
Water loss	+2°C	**0.098** ± 0.058 (-0.141-0.374)	0.095 ± 0.054 (-0.253-0.474)
	+4°C	**0.193** ± 0.065 (-0.073-0.493)	0.192 ± 0.06 (-0.079-0.438)
Size-corrected water loss	+2°C	0.001 ± 0.001 (-0.002-0.004)	**0.004** ± 0.002 (-0.012-0.022)
	+4°C	0.002 ± 0.001 (-0.001-0.006)	**0.009** ± 0.003 (-0.004-0.02)
		GRO/ROCK	**GRO/ROCK**
Foraging time	+2°C	**126.257** ± 51.512 (-106-314)	88.707 ± 42.394 (-36-307)
	+4°C	**285.975** ± 64.005 (-5-486)	226.812 ± 55.407 (74-488)
Basking time	+2°C	143.856 ± 51.511 (-8-325)	**145.873** ± 49.462 (-9-325)
	+4°C	282.019 ± 50.606 (140-479)	**302.564** ± 47.523 (138-479)
Shade selected	+2°C	0.564 ± 0.601 (-2.072-3.265)	**0.574** ± 0.634 (-2.459-4.279)
	+4°C	**1.379** ± 0.55 (-1.335-3.971)	1.203 ± 0.58 (-1.32-4.785)
Time in Tpref	+2°C	**55.52** ± 14.221 (-12-122)	49.616 ± 14.274 (-19-124)
	+4°C	**122.634** ± 14.667 (45-188)	117.631 ± 14.088 (42-195)
Water loss	+2°C	**0.065** ± 0.05 (-0.278-0.466)	0.062 ± 0.046 (-0.202-0.387)
	+4°C	0.125 ± 0.054 (-0.228-0.586)	**0.13** ± 0.05 (-0.141-0.512)
Size-corrected water loss	+2°C	0.001 ± 0.001 (-0.003-0.006)	**0.003** ± 0.002 (-0.009-0.018)
	+4°C	0.001 ± 0.001 (-0.003-0.007)	**0.006** ± 0.002 (-0.006-0.023)
		Wk	**Wk**
Foraging time	+2°C	**116.005** ± 25.869 (-27-235)	71.213 ± 23.66 (-106-199)
	+4°C	**283.139** ± 37.759 (76-402)	182.515 ± 38.065 (-1-385)
Basking time	+2°C	170.479 ± 31.057 (-7-332)	**175.052** ± 29.887 (10-316)
	+4°C	312.681 ± 33.002 (173-482)	**365.04** ± 34.684 (189-490)
Shade selected	+2°C	0.897 ± 0.505 (-1.679-3.393)	**1.087** ± 0.647 (-2.537-4.279)

	+4°C	1.933 ± 0.53 (-0.711-4.254)	**2.147** ± 0.681 (-1.421-4.876)
Time in Tpref	+2°C	47.587 ± 10.649 (-16-124)	**50.311** ± 11.326 (-20-123)
	+4°C	108.477 ± 11.436 (47-182)	**112.352** ± 12.394 (37-193)
Water loss	+2°C	**0.131** ± 0.073 (-0.269-0.46)	0.128 ± 0.059 (-0.192-0.381)
	+4°C	0.242 ± 0.084 (-0.228-0.586)	**0.254** ± 0.071 (-0.139-0.517)
Size-corrected water loss	+2°C	0.002 ± 0.001 (-0.003-0.005)	**0.006** ± 0.003 (-0.009-0.017)
	+4°C	0.003 ± 0.001 (-0.003-0.007)	**0.012** ± 0.003 (-0.006-0.024)
		VH	**VH**
Foraging time	+2°C	**117.809** ± 22.38 (-100-310)	71.145 ± 19.58 (-100-316)
	+4°C	**285.231** ± 33.03 (-4-470)	177.932 ± 31.587 (1-491)
Basking time	+2°C	159.346 ± 27.002 (-10-369)	**171.287** ± 24.676 (-6-358)
	+4°C	302.517 ± 28.875 (136-527)	**353.924** ± 27.212 (150-500)
Shade selected	+2°C	**0.665** ± 0.293 (-2.036-3.199)	0.609 ± 0.319 (-1.189-3.258)
	+4°C	**1.516** ± 0.312 (-1.297-3.739)	1.398 ± 0.334 (-0.731-3.888)
Time in Tpref	+2°C	**50.978** ± 7.932 (-10-116)	47.932 ± 7.896 (-17-113)
	+4°C	**112.909** ± 7.698 (52-185)	111.397 ± 7.65 (49-187)
Water loss	+2°C	0.084 ± 0.027 (-0.164-0.372)	**0.085** ± 0.023 (-0.131-0.309)
	+4°C	0.163 ± 0.029 (-0.075-0.493)	**0.171** ± 0.026 (-0.062-0.6)
Size-corrected water loss	+2°C	0.001 ± 0 (-0.002-0.004)	**0.004** ± 0.001 (-0.006-0.014)
	+4°C	0.002 ± 0 (-0.001-0.006)	**0.008** ± 0.001 (-0.003-0.027)

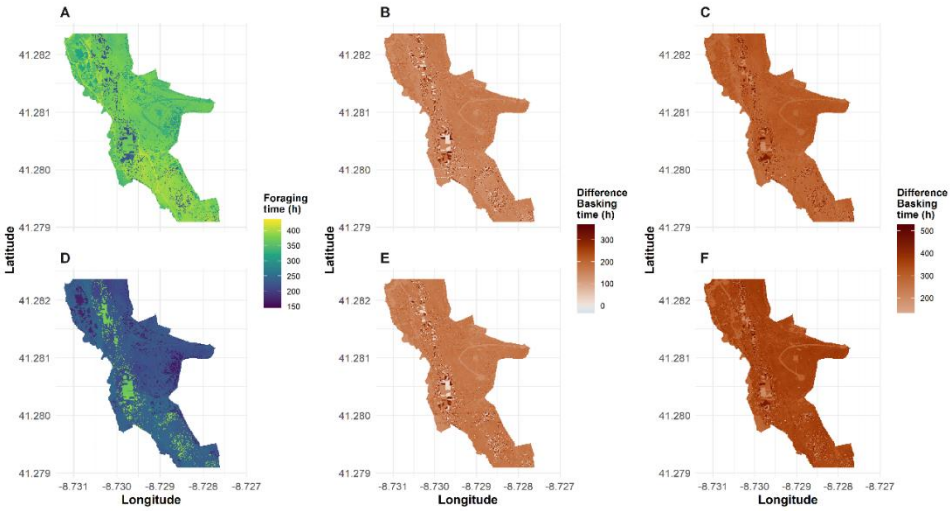

Figure D4.1 Maps of the variables obtained from mechanistic niche models for *T. lepidus* (top row: A, B, C) and *L. schreiberi* (bottom row: D, E, F) under current climatic conditions in Castro São Paio, northern Portugal. Panels A and D show the total basking time (in hours); panels B and E represent the difference in basking time between scenario +2 °C and current climate and panels C and F represent the difference in basking time between scenario +4°C and current climate.

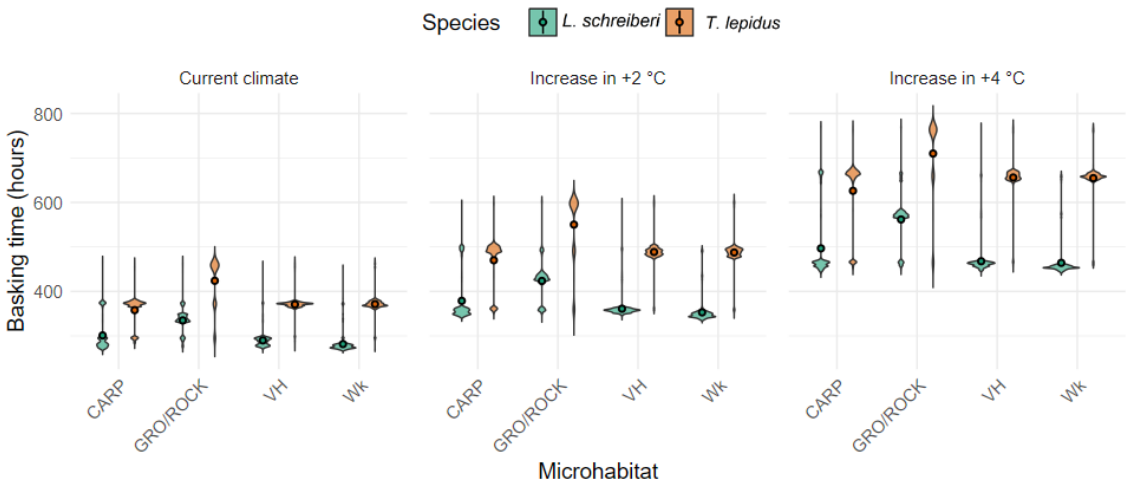

Figure D4.2 Total basking time in hours. The facets indicate climatic scenarios: Current climate, Increase in +2 °C, and Increase in +4 °C. The x-axis represents microhabitats: CARP (Carpobrotus microhabitat), GRO/ROCK (rocky and bare soil microhabitat), VH (herbaceous vegetation), and Wk (walkway). The colours correspond to the two species

studied: orange for *T. lepidus* and green for *L. schreiberi*. Dots inside the violins represent means.

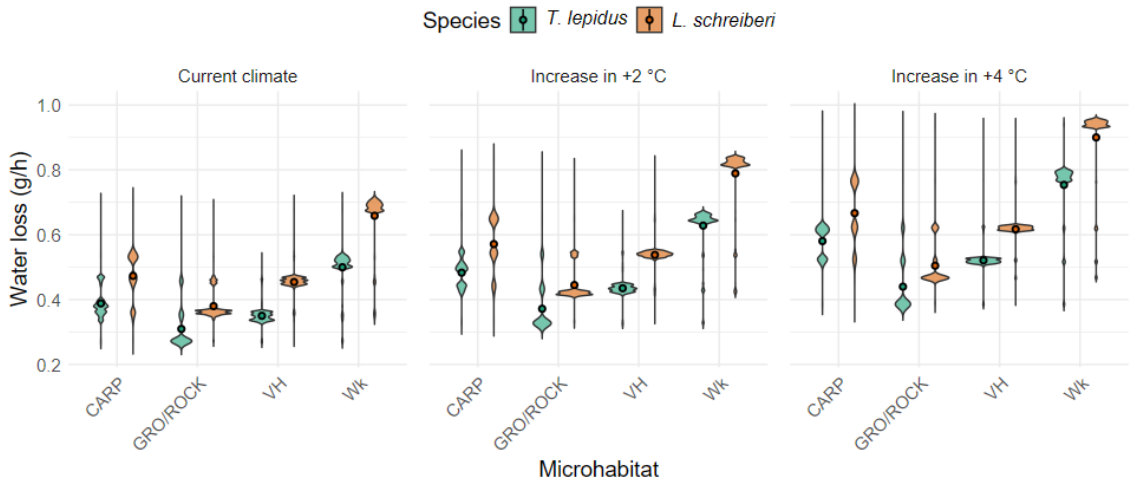

Figure D4.3 Water loss in climatic scenarios: Current climate, Increase in +2 °C, and Increase in +4 °C. The x-axis represents microhabitats: CARP (*Carpobrotus* microhabitat), GRO/ROCK (rocky and bare soil microhabitat), VH (herbaceous vegetation), and Wk (walkway). The colours correspond to the two species studied: orange for *T. lepidus* and green *for L. schreiberi*. Dots inside the violins represent means.

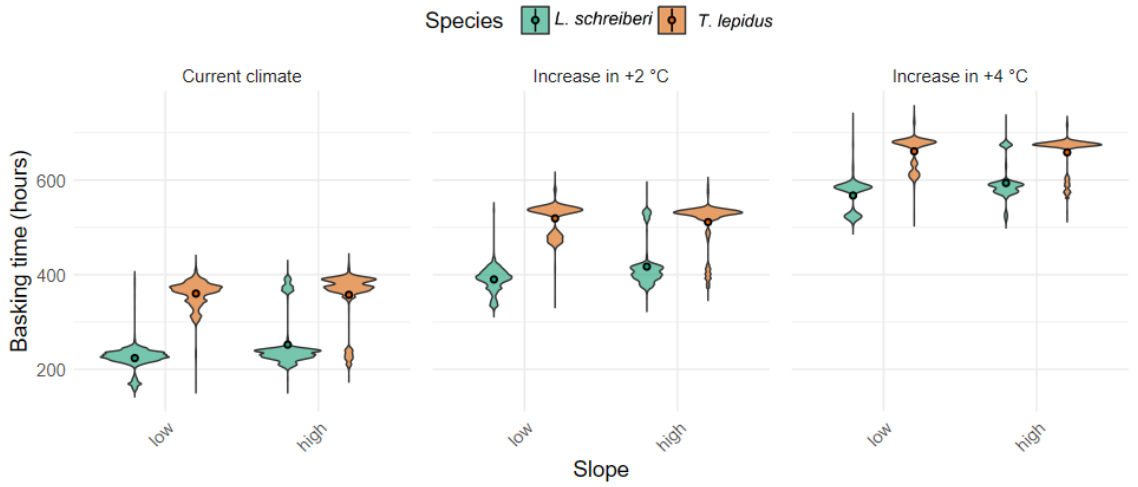

Figure D4.4 Total basking time in hours. The facets indicate slope categories (Low and High), and the colours correspond to the two species studied: orange for *T. lepidus* and green for *L. schreiberi*. Dots inside the violins represent means**.**

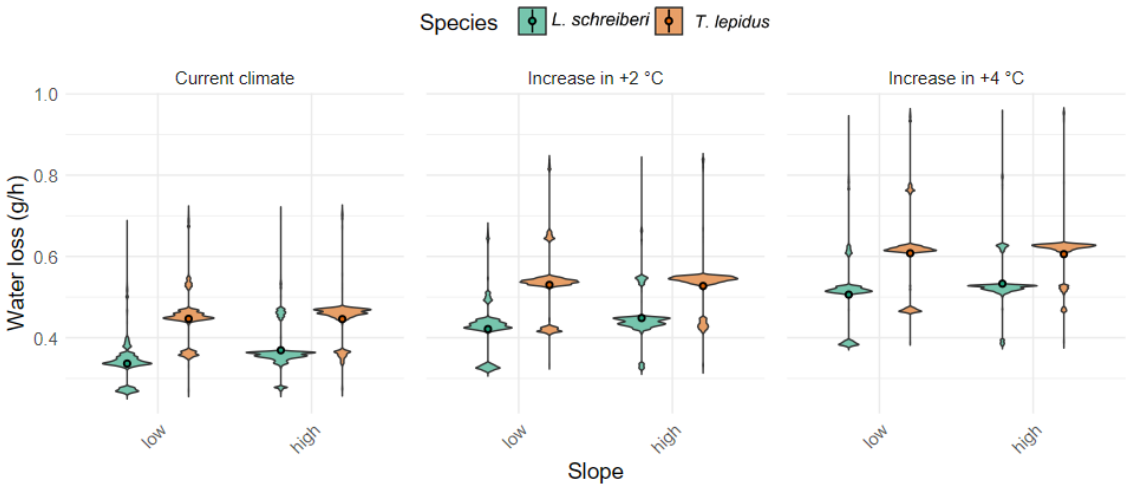

Figure D4.5 Total water loss from mechanistic models in different climatic scenarios. The facets indicate slope categories (Low and High), and the colours correspond to the two species studied: orange for *T. lepidus* and green for *L. schreiberi*. Dots inside the violins represent means**.**

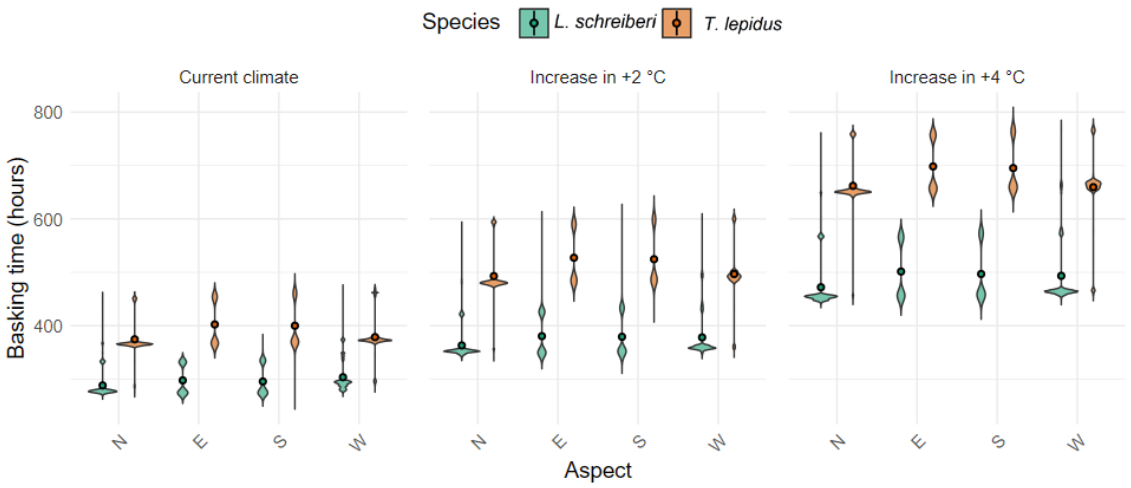

Figure D4.6 Total basking time in hours from mechanistic models in different climatic scenarios. The facets indicate aspect categories (North, East, South, West), and the colours correspond to the two species studied: orange for *T. lepidus* and green for *L. schreiberi*. Dots inside the violins represent means**.**

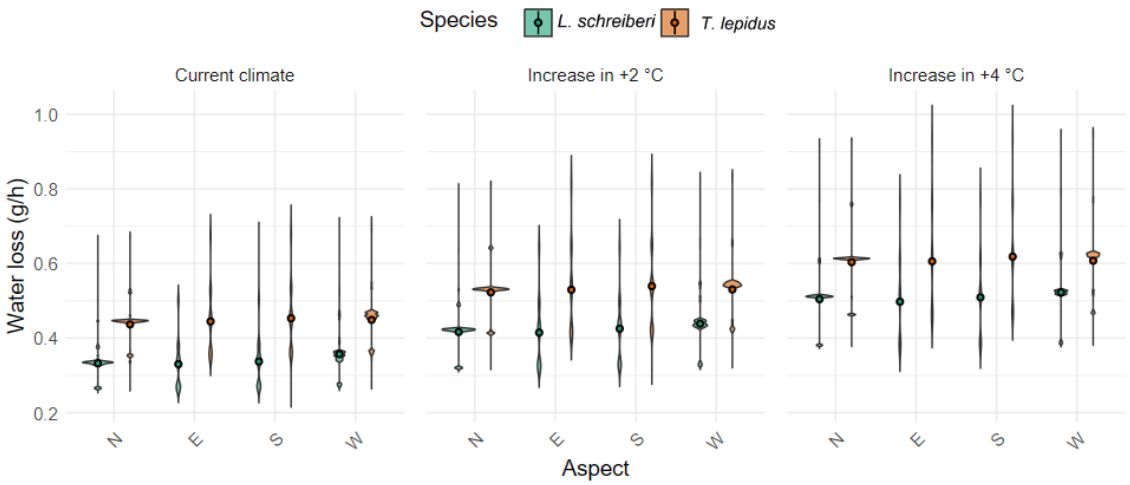

Figure D4.7 Total water loss from mechanistic models in different climatic scenarios. The facets indicate aspect categories (North, East, South, West), and the colours correspond to the two species studied: orange for *T. lepidus* and green for *L. schreiberi*. Dots inside the violins represent means**.**